Megaintegumenta, a seed sized mutant of Arabidopsis thaliana

Schruff, Marie Christine

Award date:
2006

Awarding institution:
University of Bath

MEGAINTEGUMENTA, a seed size mutant of *Arabidopsis thaliana*

~~Volume 4 of 4~~

Marie Christine Schruff
A thesis submitted for the degree of Doctor of Philosophy
University of Bath
Department of Biology and Biochemistry
May 2006

Signed:

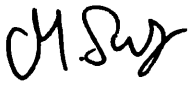

Marie C. Schruff

ProQuest LLC
789 East Eisenhower Parkway
P.O. Box 1346
Ann Arbor, MI 48106-1346

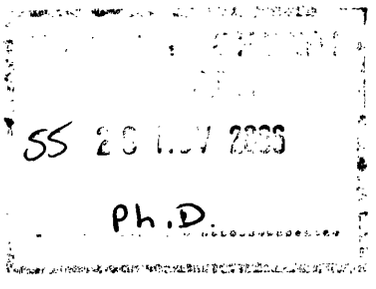
SS 2 0 1.JV 2020
Ph.D.

To Julian

Acknowledgements

I would like to thank Rod Scott my supervisor for inspiration and guidance throughout the work on this Thesis. A big thank you to Melissa Spielman, who managed the project, contributed greatly to most of the work presented here and made sure that work got done and sharp objects were tidied away. A very special thank you to Sushma Tiwari for unending support and guidance, as well as the charitable distribution of Karma points towards successful manipulation of nucleic acid. Sushma and Lucy, your friendship, chitchat, singing and laughter have made this lab a very happy working environment for which I am extremely grateful. Thank you, all past and present members of the plant labs, especially Baoxiou, Ben, Catherine, Jez, Lihua and Sapu for help and pleasant company.

Grateful acknowledgements are also due to Sally Adams who isolated the *mnt* mutant seed, Nick Fenby for his contribution to the mapping and Robert Day for his contribution to the cloning, Rhiannon Hughes for tying up my work, Richard Hooley and James Doughty for helpful discussions, Mike Skinner and Angie Vale for caring for the plants, Ursula Potter for technical support with SEM, Jason Reed for sharing unpublished data and vectors, Michael Mogie and Tamás Székely for help with statistical analysis, Robert Fisher, the ABRC and Bath Janssen for vectors, the Salk Institute and NASC for seed, and Sulis Innovation for generous funding of this project.

Abstract

Important stages of seed development occur before fertilisation during ovule development when the embryo sac and the integuments are formed. This thesis describes the phenotypic and genetic study of a seed size mutant in *Arabidopsis thaliana*, *megaintegumenta* (*mnt*). The size and weight of seed in this mutant are significantly increased due to extra cell division in the integuments surrounding *mnt* mutant ovules. The *mnt* mutation has pleiotropic effects on vegetative and floral development, caused by extra cell divisions and expansion in many organs. Genetic mapping identified the *mnt* as a mutant allele of *AUXIN RESPONSE FACTOR 2* (*ARF2*), a member of a family of transcription factors that mediate gene expression in response to auxin. Detailed studies of the *mnt/arf2* mutant phenotype and *ARF2* gene expression provided evidence that *ARF2* is a repressor of cell division and organ growth throughout the plant. With a view to using the Arabidopsis *mnt/arf2* mutant as a model to investigate methods of seed size enhancement, a number of gene expression studies were conducted, which attempted to gain a deeper understanding of the genetic control of ARF2-led seed size control.

Abbreviations and Acronyms

ACR, acr	*ARABIDOPSIS CRINKLY*
ARF, arf	*AUXIN RESPONSE FACTOR*
ATS, ats	*ABERRANT TESTA SHAPE*
BAC	Bacterial Artificial Chromosome
BDL, bdl	*BODENLOS*
bp, Mbp	base pair(s), Mega base pair(s)
CAPS	Cleaved Amplified Polymorphic Sequences
CTD	C-Terminal Domain
DBD	DNA Binding Domain
DEFRA	Department for Environment Food and Rural Affairs
EMS	Ethyl Methanesulfonate
ETT, ett	*ETTIN*
HI	Harvest Index
IKU, iku	*HEIKU*
INO, ino	*INNER NO OUTER*
MN, mn	*MONOPTEROS*
MNT, mnt	*MEGAINTEGUMENTA*
MR	Middle Region
NPH, nph	*NON-PHOTOTROPIC HYPOCOTYL*
PCR (RT-PCR)	Polymerase Chain Reaction (Reverse Transcription-PCR)
SSLP	Simple Sequence Length Polymorphism
SUP, sup	*SUPERMAN*
TAIR	The Arabidopsis Information Resource
TIR, tir	*TRANSPORT INHIBITOR RESISTANT*

Contents

1 Introduction

1.1 The importance of seed size and yield

The agronomic value of seed crops is great. In 2004, 85% of land reserved for agricultural crops in the UK was cultivated with seed crops including wheat, barley, oilseed rape and pulses (DEFRA, 2006). Despite the existence of over 50,000 food crop species globally, 60% of the world's food energy intake is provided by three seed crops – namely rice, maize and wheat (Loftas, 1995). Yield of seed crop plants is generally estimated by seed weight per unit area in milligram per hectare (Mg/ha), thereby highlighting the important role of seed weight as a determinant of crop productivity. The yield efficiency of a crop plant is expressed as the harvest index (HI), which signifies the weight of harvested product as a percentage of the total plant weight of a crop. Therefore seed weight, as determined by individual seed size and number, is an important determining factor in the production efficiency of a seed crop.

Despite continuous efforts to increase yield of cereals through breeding, and more recently through biotechnology, gains in HI have stagnated for most important grain crops (Peng *et al.*, 2000; Horie 2005; Duvick, 2005). Recent improvements in crop yield have been achieved through improved stress tolerance (Tollenaar and Wu, 1999), pest resistance (Dillehay *et al.*, 2004) and various methods of improved field management but an estimated 40% to 50% increase in rice and wheat production will be needed to meet the demands of a continuously growing world population (Peng and Senadhira 1998; Pfeiffer *et al.*, 2001; Khush, 2005). However, even under optimal field conditions, a crop cannot exceed its maximum yield potential which is defined as the yield of a cultivar that is grown in the absence of environmental stresses with unlimited supplies of nutrients and water (Evans and Fischer, 1999). The maximum yield potential of major cereal crops has been stabilising (Peng and Senadhira 1998; Duvick and Cassman, 1999) and this stagnation has occurred despite a commonly perceived need to target HI in order to continue to improve cereal crop yield (Austin, 1980; Sinclair *et al.*, 2004).

Seed size manipulation presents an important target when aiming to augment the HI in an attempt to affect yield levels without increasing the demands for space, water and nutrients. There is increasing evidence that seeds play an active role in obtaining photo-assimilates from the mother plant and that an increased sink tissue demand can increase plant yield by increasing radiation use efficiency and photosynthetic rate (Patrick and Offler, 1995; Xu *et al.*, 2004; Reynolds *et al.*, 2000 and 2005). It has therefore been suggested that efforts to improve grain size should focus on the capacity of grain filling (Peng and Senadhira, 1998). The potential for improvement of current use of photo-assimilates is suggested by findings showing that the demand for photo assimilates by the developing grain is initially lower than the capacity of leaves to supply them (Austin *et al.*, 1980). Increases in crop yield have been associated with significant increases in seed weight of wheat and barley (Sasahara, 1984) and evidence from a variety of plant species including *Arabidopsis thaliana* shows that increased seed size is positively correlated with a number of fitness gains. These involve germination and survival (Krannitz *et al.*, 1991, Koelewijn and Damme, 2005), early emergence (Winn, 1985; Verdú and Traveset, 2005), and growth rate (Marshall, 1986).

Seed size variations between plant species indicate that there is much genetic potential for the manipulation of seed size: among different plant species, differences in seed weight stretch over a scale of ten orders of magnitude from 0.000002g [orchid, *Goodyera repens*], to 18,000-27,000g [double coconut palm, *Lodoicea maldivica*] (Harper *et al.*, 1970). In grain crops, this potential is expressed by the heterosis of grain size of wheat and triticale hybrids (Pfeiffer *et al.*, 2001). Within a species on the other hand, seed size can show relatively little variability compared to the size variations observed in other plant organs. Seed weight within a species can in fact be so consistent that the seed of the Carob tree (*Ceratonia siliqua*) was once used as a counterweight to gold; a measuring unit now still referred to as 'carat' (Harper *et al.*, 1970) and the seed size and shape of rice is so stable that it can be used for the identification of ecotypes (Sasahara, 1984). In order to enhance maximum yield by increasing the HI, one of the major challenges to breeders and genetic engineers is to overcome seed size stability. This requires a better understanding of the genetic mechanisms that determine final seed size and weight.

1.2 *A. thaliana* as a model species

The plant model species *A. thaliana* is a member of the Brassicaceae family although, unlike its close relative *Brassica napus*, it is not a crop species and therefore has no direct agronomic value. Yet, in order to understand the factors that control and restrict seed size and weight in flowering plants, this model plant provides a potentially useful system in which to study seed size traits due to a number of attributes (Meinke *et al*, 1998). *A. thaliana* is an angiosperm like all major crop species, but it genetically more amenable to plant genetic research as it has a small genome (120Mbp) spread over only 5 chromosomes. The *A. thaliana* genome is less than a third the size of the rice genome (420Mb), a tenth the size of the closely related *B. napus* genome (1200Mbp) and an even smaller fraction the size of maize and hexaploid wheat genomes (2500Mbp and 15900Mbp respectively) (Arumuganathan and Earle, 1991 – see Figure 1.1). Furthermore, the *A. thaliana* genome was fully sequenced in the year 2000 (The Arabidopsis Genome Initiative, 2000) and sequence data is available via the TAIR website (www.arabidopsis.org), which combines a wealth of contributions by and for the Arabidopsis user community including information about genes, markers, polymorphisms, maps, sequences, clones, gene families and proteins as well as access to DNA and seed stocks (Garcia-Hernandez *et al.*, 2002). The Arabidopsis user also benefits from a large number of mutant lines and associated genomic resources from a multinational research community (Scholl *et al.*, 2000). Other advantages include ease of cultivation due to its small size; a rapid life cycle; abundant seed production; and efficient transformation methods utilizing *Agrobacterium tumefaciens* (Gelvin, 2003).

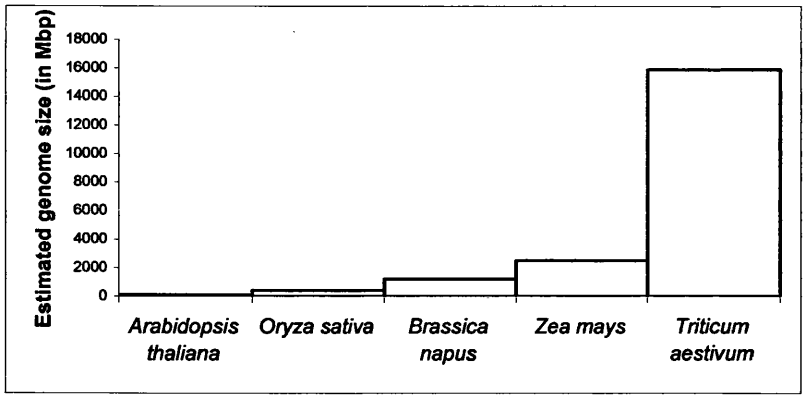

Figure 1.1 Estimated genome sizes of A. thaliana, rice, oilseed rape, maize and wheat as determined by flow cytometry by Arumuganathan and Earle (1991)

In addition to facilitating mapping and identification of mutant genes (Lukowitz *et al.*, 2000, Jander *et al.*, 2002), extensive research into the wild type and mutant phenotypes of the Arabidopsis plant has led to the development of a number of staging systems for whole-plant analysis (Boyes *et al.*, 2001), flower development (Smyth *et al.*, 1990), and ovule development (Schneitz *et al.*, 1995). These systems significantly assist efforts to accurately describe and quantify novel mutant phenotypes.

1.3 Seed development in flowering plants

Seed development in flowering plants (Brink and Cooper 1940; Bhatnagar and Johri, 1972; Esau, 1977; Evenari 1984) and specifically in Arabidopsis (Meinke, 1994) has been described in detail. Important stages of seed development occur in the gynoecium before fertilisation and embryogenesis. Due to the nature of the mutation studied here, special attention will be given to early, pre-fertilisation stages of development, during the development of the ovule.

1.3.1 Seed development before fertilisation: the ovule

Detailed descriptions of ovule development exist for many plant species (Esau, 1977; Bouman, 1984) including *A. thaliana* (Robinson-Beers *et al.*, 1992; Schneitz *et al.*, 1995). The ovule develops within the ovary and although ovule development is closely linked with the development of the flower, it is believed to act as an organ in its own right

(Esau, 1977; Schneitz *et al.*, 1995) and ovule development can therefore be reviewed in isolation of floral development. The ovule can be divided into three discrete regions or pattern elements as defined by Schneitz *et al.* (1995): the chalaza which gives rise to the integuments, the nucellus (megasporangium) which consists of vegetative cells harbouring sporogenous cells and which constitutes the site of megasporogenesis and megagametogenesis, and the funiculus which attaches the ovule to the placenta. Ovules exhibit two polar patterns that are referred to as the proximal-distal and the abaxial-adaxial axes (see Figure 1.2). The proximal-distal axis is characterised by the respective positions of the nucellus, chalaza and funiculus in the young ovule. These regions are described as the micropylar-, central- and the chalazal zone in the mature ovule. The abaxial-adaxial axis can be defined as the 'outside' and 'inside' of the mature ovule. This axis only becomes apparent at the initiation of the outer integument as integument growth on the abaxial side is more pronounced. Subsequent curvature of the maturing ovule around the adaxial pole places the abaxial side on the periphery of the ovule, while the adaxial side is reduced to a fold or groove of integumental tissue, which is termed the adaxial ridge in the mature seed (Schneitz *et al.*, 1995, Balasubramanian and Schneitz, 2002).

The staging system commonly used in the analysis of Arabidopsis ovule development has been developed by Schneitz *et al.*, (1995). The system is based on the observation of distinctive developmental events involving overall ovule growth, integument growth and the development of the embryo sac that can be observed during ovule maturation. A diagram depicting external and internal ovule morphology during different stages of development is shown in Figure 1.2. The following account of ovule development is based on descriptions by Esau (1977) and Schneitz *et al.* (1995).

Ovules first arise as primordial protuberances (stage 1-I) from the placenta, which is located near the central replum at the inside of the ovary. As these ovule primordia elongate (stages 1-II to 2-II), a ring of inner integument is initiated by periclinal divisions around the flank of the chalaza. Shortly thereafter, the outer integument initiates on the abaxial side, proximal to the inner integument (stage 2-III). Both outer and inner integuments follow on to elongate and thus enclose the nucellus in a sleeve-like fashion (stages 2-IV to 2-V). Meanwhile, the megaspore mother cell enlarges (2-I), undergoes a

first meiotic division (2-IV), and a tetrad is subsequently formed in a secondary meiotic division (2-V). Integument growth on the abaxial side becomes more pronounced as the integuments start to completely enclose the nucellus, at the same time the entire ovule continues to enlarge and elongate while starting to bend until a 180° curvature of the mature ovule has placed the funiculus next to the micropyle in an anatropous fashion (stages 3-I to 3-VI). The micropyle is defined as the ridge that is formed between the tips of the inner and outer integuments that meet when the nucellus has been enclosed entirely. As the ovule starts to curve, embryo sac formation is initiated from the chalazal megaspore during tetrad degeneration (3-I). A first mitotic division gives rise to a two-nuclear embryo sac (3-II), the formation of the vacuole can be detected (3-III) and subsequent mitotic divisions give rise to the four-nuclear (3-IV) and eight-nuclear (3-V) embryo sac stage. Maturation of the embryo sac is completed at stage 3-VI, when the antipodal cells degenerate. The mature megagametophyte is thus composed of three antipodal cells located at the chalazal pole, the central cell containing a large vacuole and two polar nuclei near the micropylar pole, and two synergids as well as the egg cell located at the micropylar pole.

In the mature ovule the vegetative nucellar tissue is reduced to a few cells at the chalazal pole (Figure 1.2 blue arrow) as it has been almost completely replaced by the maturing embryo sac. The integuments form five distinct cell layers that have been characterised in detail by Beeckman *et al.*, (2000). The outer integument comprises two layers (oi1 and oi2) and the inner integument comprises three layers (ii1, ii1' and ii2). ii1' is present only along the central zone (arrow, Figure 1.2[B]) and it is positioned between the layers of ii1 and ii2. ii1 is the innermost layer of the integuments and is also known as the pigment layer or endothelium.

The funiculus remains attached to the placenta as a stalk-like structure. It is the only component of the three main ovular structures that does not form part of the seed, as it is detached during seed ripening.

In summary, ovules contain three distinct zones along the proximal-distal axis, which differentiate into three main tissue types, the nucellus, the chalaza and the funiculus. The chalazal zone gives rise to the integuments and the nucellus houses the development of the embryo sac. Differential growth of the integuments and ovule curvature cause the

formation of an abaxial-adaxial axis and the abaxial integument, which grows at a significantly greater rate than the adaxial integument, makes up most of the mature seed coat.

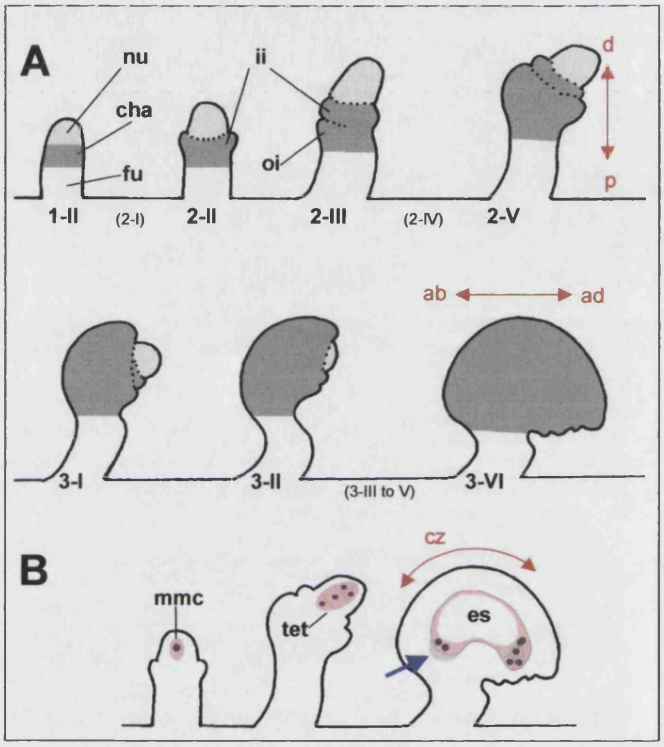

Figure 1.2 Schematic representation of ovule development from initiation(1-II) to maturation (3-VI). External morphology (A) and internal morphology (B) at stages 2-II, 2-V and 3-VI. Stages according to Schneitz *et al.* (2005), omitted stages shown in brackets. The orientations of the proximal-distal axis (p<-->d) and abaxial-adaxial axis (ab<-->ad) apply to all stages depicted here. Abbreviations: cha: chalaza (dark grey); cz: central zone; es: embryo sac; fu: funiculus (white); ii: inner integument; mmc: megaspore mother cell; nu (and blue arrow): nucellus (light grey) oi: outer integument; tet: tetrad.

1.3.2 Seed development after fertilisation

Seeds of flowering plants are a product of a double fertilisation event within the ovule. The following description of seed maturation thus applies to most flowering plants including *A. thaliana.*

Two male gametes are delivered via the pollen tube, one of which fertilises the egg cell and the other fertilises the central cell containing the fused pair of polar nuclei. These two fertilisation events give rise to a seed with two different zygotic products of distinct ploidy and function: a diploid embryo which constitutes the daughter plant, and the triploid endosperm which has a terminal fate and acts as a nutritional sink tissue for the developing embryo or seedling (Lopes and Larkins 1993). The third major component of the seed, the seed coat or testa, is not a product of fertilisation as it is derived entirely from maternal tissue, the integuments.

Successful pollination changes the identity of the ovule to that of a seed and the integuments into seed coat. It also re-defines the gynoecium as a silique (or seed pod), which follows on by elongating as the seeds expand within. Seed developmental progression in Arabidopsis can be categorised into a number of distinctive embryonic growth stages that are defined by changes to the size and the shape of the embryo proper. Embryo morphology thus defines five developmental stages of the seed: globular stage, heart stage, torpedo stage, bent-cotyledon stage and curled cotyledon stage. The developmental progression through these stages occurs before embryo maturation during the first week after pollination. A further week is required for seed maturation and desiccation. (Brink and Cooper, 1940; Evenari, 1984; Meinke, 1994)

Endosperm development and its nutritive role during embryo development have been described in detail (Brink and Cooper, 1947; Bhatnaghar and Sawhney 1981; Lopes and Larkins 1993). The persistent endosperm of monocot species such as maize and wheat makes up the bulk of the mature seed and acts as a storage organ until germination, while endosperm of eudicots such as *A. thaliana* is transient and therefore replaced by the growing embryo which stores reserves within the cotyledons. Endosperm development in *A. thaliana* is initiated by the formation of a syncitium during a rapidly dividing free-nuclear phase, and followed by cellularisation and absorption by the embryo occurring at the heart stage and beyond (Berger, 1999; Vinkenoog *et al.*, 2002). The mature *A. thaliana* seed only contains two layers of residual endosperm: a single layer of peripheral endosperm surrounding the embryo termed the hyaline layer, and a layer of pigmented endosperm termed the aleurone layer, that lines the inside of the seed coat (Beeckman *et al.*, 2000).

Seed coat maturation has been studied in detail by Beeckman *et al.* (2000). The conversion from 'ovular integument' to 'testa' is characterised by vacuolisation as well as starch- and pigment accumulation. No cell division can be observed during seed coat maturation but strong cellular differentiation especially in the outer integument involving mucilage production and cell wall reinforcement (Windsor *et al.*, 2000).

1.4 Seed size genetics

While seed size in monocots like wheat and maize is mostly attributed to endosperm proliferation (Chojecki *et al.*, 1986; Singletary *et al.*, 1994; Jones *et al.*, 1996), it is the embryo which makes up the bulk of eudicot seeds like peas and beans and generally the final size of the seed is only indirectly attributed to endosperm proliferation (Davies, 1977; Lemontey *et al.*, 2000). This must be kept in mind when considering seed size morphology and genetics in model plants and seed crops such as cereals. However, the constituents and the stages of development of seeds in monocotyledonous and dicotyledonous species are nevertheless similar and endosperm proliferation in A. thaliana has been correlated with seed size (Scott *et al.*, 1998; Garcia *et al.*, 2003). The following review will therefore continue to focus mainly on studies of seed size genetics in *A. thaliana.*

Although intraspecific seed size variation is generally quite low, differences in seed size of up to 3.5-fold can be found among closely related accessions within the model plant species *A. thaliana*: while a seed of the Rschew (Rsch) accession weighs only about 10μg (Krannitz, Aarssen and Dow, 1991), that of the Cape Verdi Islands (Cvi), accession can weigh up to 35μg (Alonso-Blanco *et al*, 1999). Due to this significant size variation found within this plant model species, it has been possible to perform QTL mapping using two closely related accessions. Alonso Blanco *et al.* (1999) carried out a seed size QTL analysis as well as a detailed comparison of seed development with respect to size, using the Arabidopsis accessions Cvi and Landsberg *erecta* (L*er*). These accessions differ in the mean seed size (Cvi produces about 180% heavier seed) as well as mean number of seeds produced (Ler produces about 140% more seed). QTL mapping identified 11 putative loci that are responsible for the majority of seed size affecting changes at various

stages throughout seed development including a more rapid and prolonged growth of seed coat and endosperm. Furthermore, the comparison of inbred accessions and hybrid plants revealed that the final seed size is correlated with cell number and cell size in the endosperm and embryo. However, no individual genes relating to seed size modification were identified through this study.

As mentioned above, seed size in monocots is mostly attributed to endosperm proliferation. The role of endosperm as nutritive tissue is discussed by Bhatnagar and Sawhney, (1981) and Lopes and Larkins, (1993). It has been shown in Arabidopsis that disruption of normal development of this tissue can have a strong indirect effect on final seed size. In interploidy crosses where the maternal-to-paternal genome ratio of the seed is changed, the growth rate of the endosperm is affected causing significant effects on seed size (Haig and Westoby, 1991). Seed resulting from crosses where the ploidy of the maternal parent is higher than that of the paternal parent are smaller than seed resulting from crosses between parent plants of equal ploidy. Alternatively, where the ploidy of the paternal parent is higher than that of the maternal parent seed is larger with a significant increase in endosperm proliferation. This parental imbalance observed in interploidy crosses is believed to arise from differential imprinting resulting in the suppression of genes that promote seed size enhancement in the maternally-derived genome, and the suppression of genes that promote seed size reduction in the paternally-derived genome. In support of this theory, the genomic imbalance effect on endosperm proliferation can be phenocopied by ectopic expression of the maternal or paternal alleles of genes which would normally be silenced due to genomic imprinting (Adams *et al.*, 2000). A similar effect of endosperm development on seed size was observed in the seed of the *iku* (*haiku*) mutant where a strong reduction in mitotic division and precocious cellularisation of endosperm is observed which the authors link to the production of small, round seed (Garcia *et al.*, 2003). Another maize mutant that has been used to emphasise the importance of endosperm development on final seed size is the *miniature-1* seed mutant in maize (Miller and Chourey, 1992; Cheng *et al.*, 1996).

Seed size can also be influenced by disrupting seed coat development and a number of genes have been identified that play a role in setting mature seed size through their involvement in integument development.

Arabidopsis mutant plants that give rise to small seed with abnormal shapes include *ats*, *acr4*, *ino*, and *sup* (Leon-Kloosterziel, *et al.*, 1994; Sakai, Medrano and Meyerwoitz, 1995; Gaiser, Robinson-Beers and Gasser, 1995; Baker *et al.*, 1997; Villanueva *et al.*, 1999;). The *ats* (*aberrant testa shape*) mutant yields small, round seed that is affected in integument cell line identity. The inner and outer integuments of this mutant develop as a single structure. The gene responsible for the *ats* mutation has not been identified to date (Leon-Kloosterziel, *et al.*, 1994). *acr4* (*arabidopsis crinkly 4*) integuments lack cell layer identity (Tanaka *et al* 2002; Gifford, Dean and Ingram, 2003). *ACR4* encodes a membrane-localised receptor-like kinase and the *acr4* mutation was shown to interfere with the number and organisation of integumental cell layers with similar effects as observed in *ats* (Tanaka *et al* 2002; Gifford, Dean and Ingram, 2003). *ino* (*inner no outer*) mutant seed is elongated and slim while that of *sup* mutant plants has a variety of shapes and sizes ranging from an oversized wild type-like appearance to small, round forms. Both *ino* and *sup* (*superman*) ovules lack the characteristic anatropous shape which is found in wild type; while the *ino* mutant shape is due to a nearly complete absence of the outer integument, the outer integument of *sup* mutants does develop. However both mutants lack the asymmetric growth pattern which the authors believe to be caused by normal outer integument growth as well as being necessary for ovule curvature. Both the *INO* and the *SUP* genes have been found to encode putative transcription factors, indicating that a number of other genes may be affected in the *ino* and *sup* mutant respectively (Leon-Kloosterziel, *et al.*, 1994; Gaiser, Robinson-Beers and Gasser, 1995; Baker *et al.*, 1997).

A strong reduction in integument development, seed size and shape is observed in *ant* (*aintegumenta*) mutants (Klucher *et al.*, 1996; Elliott *et al.* 1996) and enlarged seed that is affected in size but not shape can be obtained by ectopically expressing the *ANT* gene (Mizukami and Fischer, 2000). *ANT* encodes a transcription factor, which plays a role in the initiation of integuments (Klucher *et al.*, 1996; Elliott *et al.* 1996).

1.5 An Arabidopsis seed size mutant

In order to identify genes that can modify seed size and weight, a sieving screen of EMS mutagenised Arabidopsis seed was employed by Sally Adams (University of Bath) to isolate mutant lines yielding aberrantly sized seed. The sieving screen revealed that there is a linear correlation between average seed weight and seed size as expressed by its ability (or lack of) to pass through a mesh of limited diameter. Mutagenised seed sizes showed greater variation than sizes of wild type seed that do not pass through meshes smaller than 250μm– nor are retained in meshes wider than 300μm in diameter. Seed of the 22.16 mutant line weighing an average of 42μg was recovered from a wide-meshed sieve (355μm diameter). Self-pollination experiments showed that the large-seed phenotype of that line is inherited by subsequent generations and that the mutation in line 22.16 is recessive, derived from a single locus and that it is inherited from the maternal parent. It was also observed that 22.16 mutant plants are of reduced fertility and that the seed shape and the embryo size are affected by the mutation as shown in Figure 1.3. During the course of the study presented here, the mutant line 22.16 was renamed *megaintegumenta* (*mnt*) for reasons described in detail in Chapter 4.

1.6 Aims and objectives of this thesis

This thesis is a detailed study of the Arabidopsis *mnt* mutant. The main aim of this thesis was to investigate how seed yield can be increased by modifying seed development. Using the Arabidopsis *mnt* mutant as a model for creating large seed, we aimed to create a paradigm for seed-size enhancement that can ultimately be applied to agronomically valuable seed crops such as cereals. We therefore set out to understand the following: 1. What causes the large-seed phenotype in *mnt* mutant plants on a phenotypic and genotypic level? 2. How does manipulation of *MNT* gene expression influence seed development in the wild type plant? and 3. How could the large-seed phenotype be replicated in non-mutant plants through genetic engineering?

In order to understand the factors causing the large-seed phenotype in *mnt* mutant plants, two initial objectives were targeted simultaneously: 1) to identify the mutated locus

through positional cloning and 2) to undertake a thorough analysis of mutant plant morphology with a focus on seed development.

Following identification of the *MNT* gene, the aim was to understand how the gene is expressed and how different expression levels of the gene can impact on plant development. The approach was to test gene expression by introducing a number of transgenic constructs into the wild type plant including reporters and enhancers or suppressors of gene function.

In order to formulate a strategy to replicate an *mnt*-like seed phenotype we built on conclusions about gene function and mutant morphology obtained through previous results.

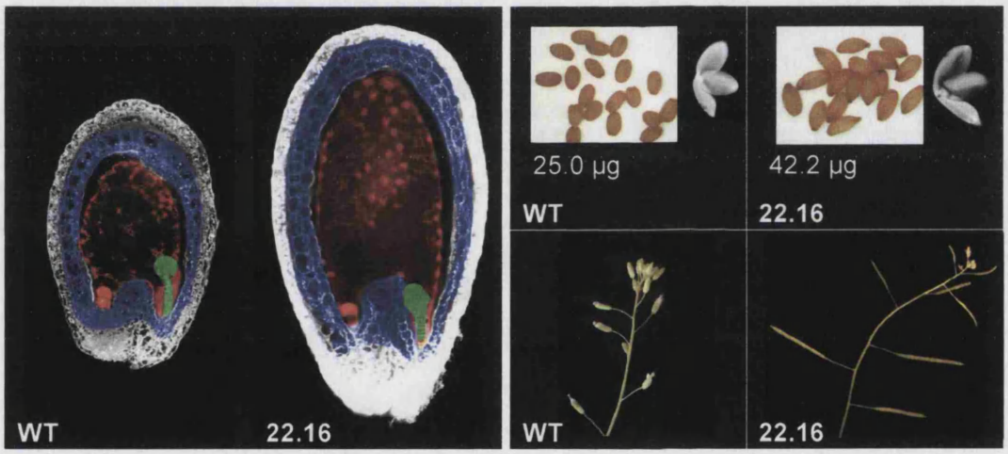

Figure 1.3 The phenotype of mutant line 22.16 – pictures by Sally Adams (University of Bath). Left: Confocal micrograph of wild type and mutant line 22.16 seed taken at the same magnification. The image has been false coloured to indicate the position of the embryo (green), endosperm (red) and the inner region of the seed coat (blue). Right top: Mature seed and their seed weight as well as dark-field illumination of cleared embryos dissected from mature wild type and 22.16 seed. Right-bottom: inflorescences of wild type and 22.16 mutant adult plants.

2 Materials and Methods

2.1 Materials

2.1.1 Plant material

Wild-type Col-3 seeds and Col-3 mutagenized with ethane methyl sulfonate (EMS) were obtained from Lehle Seeds (Round Rock, Texas, USA). Col-0, L*er*, the Salk insertion lines (Alonso *et al.*, 2003) and any mutant lines were obtained from the Nottingham Arabidopsis Stock Centre (NASC, UK).
Seed of *B. napus* Westar was provided courtesy of Biogemma (Cambridge, UK). The Col-0 *pARF2::GUS* line was kindly donated by Thomas Guilfoyle.

2.1.2 Bacterial strains

E. coli strains DH5α ('Subcloning Efficiency' cat#. 18265-017, Invitrogen Ltd, Paisley UK) were used for cloning. For plant transformation the *A. tumefaciens* strain used was GV3101. This strain harbours a non-oncogenic Ti plasmid (pGV3101) (Van Laberecke *et al.*, 1974)

2.1.3 Plasmids

The following plasmids were used for cloning:
pGEM-T vector system (Promega, Southampton, UK).
BJ36 and BJ40, kindly donated by Bart Janssen (Horticultural & Food Research Institute, New Zealand).
MITG10 provided by the ABRC (Arabidopsis Biological Resource Center, Ohio, USA).
GFP and GFP DME NLS (Choi *et al.*, 2002), kindly donated by Robert Fisher (University of California).

2.2 Methods

2.2.1 Plant growth conditions

For the purpose of greenhouse cultivation, seed was stratified and imbibed simultaneously for 3-5 days at 4°C either in a solution of 0.15% agar (n°3, Oxoid Ltd, Basingstoke, UK); in a Petri dish containing a thin layer of Levingtons seedling compost; or directly in trays containing Levingtons L2 compost mixed with approximately 30% perlite. Seed was germinated and plants were grown in a glasshouse at a temperature of 24°C (day) and 17.5°C (night), or in a Sanyo controlled environment room with a day length of 16h, 23°C (day) and 18°C (night). If imbibed/stratified in agar, seed was pipetted onto L2 compost (+ perlite) for germination and cultivation. If imbibed and stratified in a Petri dish, seed was germinated as above and 1-2 week old seedlings were transferred to Levingtons M2 compost for cultivation as above.

Plate-grown seedlings for the purpose of testing for antibiotic resistance and root growth experiments were produced as follows: seeds were surface-sterilized as follows: 5 min in 70% EtOH; 5 min in 50% Bleach with 0.05% Tween 20 followed 6 x washes in sdH2O. After washing, seeds were resuspended in molten sterile 0.5% agar at about 45°C and transferred to Petri dishes containing growth media and antibiotic: Full strength Murashige & Skoog Media with Gamborgs Vitamins (Sigma-Aldrich, Dorset, UK), 1% sucrose, 0.8% Phyto Agar (Duchefa, Haarlem, Netherlands), pH5.7 and antibiotic where necessary. Plates were sealed with parafilm and seed was stratified and germinated as above. Surviving seedlings were transplanted to trays of Levingtons L2 compost.

2.2.2 Seed weight analysis

Mature seeds were collected, dried and stored in 1.5ml eppendorf tubes with pierced lids. Individual seeds were manipulated with a fine paintbrush and weighed in groups of no less than 10 using a Mettler UMT 2 microbalance (Mettler-Toledo, Leicester, UK).

2.2.3 Size measurements

Size measurements of seeds and stems under the Olympus BH-2 microscope were performed using an eyepiece graticule.

All size measurements on digital images were performed using Adobe Photoshop or the Noesis Visilog 5.0.2 software.
Leaf and stem sizes were also obtained using a digital calliper.

2.2.4 Assisted pollination and the mapping cross

Unless left to self-pollinate, unopened flower buds were emasculated using fine tweezers shortly before anther dehiscence and pollinated 2-3 days later for the purposes of crossing and controlled self-pollination.

About 1000 *mnt/mnt* F2 plants which were generated by the mapping cross were used for the fine mapping of the *MNT* locus. An illustration of the mapping cross is shown in Figure 2.1. Generation of the mapping cross involved crossing a homozygous wild type plant of the Landsberg *erecta* background with a homozygous *mnt* mutant plant of the Columbia-3 background. The resulting heterozygous F1 generation was left to self fertilise and the F3 generation was scored for floral phenotype and genetic content.

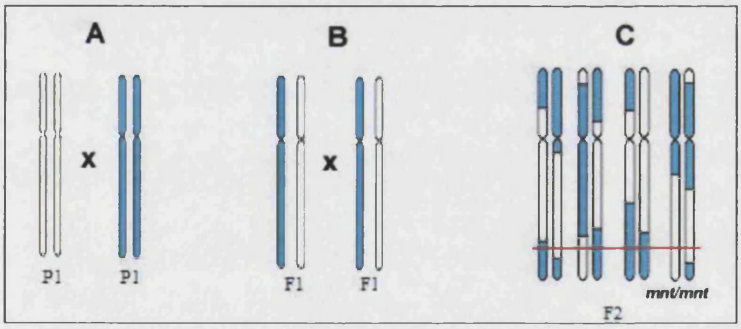

Figure 2.1 Schematic representation of the mapping cross.
A: Homozygous parental (P1) generation, B: heterozygous fist filial (F1) generation, C: segregating second filial (F2) generation; x indicates cross fertilisation; Columbia-3 DNA, containing the *mnt* allele is shown in white, Landsberg *erecta* DNA containing the *MNT* allele is shown in blue. The position of the *MNT* locus is indicated by a horizontal red line. Homozygous F2 *mnt* plants (*mnt/mnt*) were scored for recombination.

2.2.5 Plant DNA extraction

The following protocol was used for the purpose of plant DNA extraction for PCR-based genotyping. It is based on a method by Edwards *et al.*, (1991):
2-3 small leaves and 1 inflorescence were collected and ground in an eppendorf tube containing 350µl EB (100mM Tris pH 8.0, 50mM EDTA pH 8.0, 500mM NaCl, 10mM β-Mercaptoethanol) and a small amount of glass beads (Sigma-Aldrich, Cat# G-9143) using a plastic pestle in a bench top drill. After spinning at 12,000-13,000rpm for 2 minutes, 300µl of supernatant and 300µl of isopropanol were mixed in a fresh tube and left to incubate for 2 minutes. After spinning for 5 minutes as above, the supernatant was removed and the pellet dried in a laminar flow hood for 5-10 minutes until all traces of liquid had evaporated. The pellet was re-suspended in 100µl dH_2O.

2.2.6 Plant RNA extraction

Fresh plant material was transferred to liquid nitrogen. The frozen tissue was ground with a ceramic mortar and pestle and RNA was subsequently isolated using the SV Total RNA Isolation System (cat #: Z3500, Promega, Southampton, UK) according to manufacturers instructions.

2.2.7 Bacterial growth media

LB medium: 10g/l Tryptone, 5g/l yeast extract, 10g/l NaCl, pH 7.5 (+1% agar for solid medium) + appropriate antibiotic.
2YT medium: 16g/l Tryptone, 5g/l Yeast Extract, 5g/l NaCl, pH 7.2 (+1% agar for solid medium) + appropriate antibiotic.
For blue white selection: LB containing 8mg/l X-Gal and 0.01mM IPTG solidified with 1% agar + appropriate antibiotic.

2.2.8 Preparation and transformation of electrocompetent *A. Tumefaciens*

Preparation of electrocompetent *A. tumefaciens* cells was performed according to a modified protocol by the Uppsala Transgenic Arabidopsis Facility. All bacterial growth occurred in 2YT medium and in the presence of gentamycin and rifampicin selection.
Day one: a 10ml starter culture was made from a single colony of freshly streaked *A. tumefaciens* and incubated over night at 28°, 200rpm. Day two: 500ml of 2YT was

inoculated with 4-5ml starter culture and incubated until an OD_{600} of about 0.4-0.8 was reached (early to mid log phase). Bacterial cells were then chilled on ice for 15-30 minutes and harvested by centrifugation at 7500rpm for 15' at 4°C. After removal of all supernatant, the pellet was re-suspended in 500ml chilled 10% glycerol. This process was repeated three times by re-suspending the pellet in 200ml, 10ml and 2ml 10% glycerol respectively. The concentrated re-suspended cells were aliquoted (40µl/tube) into chilled eppendorf tubes, immediately placed on dry ice and stored at –80°C.

For electroporation of *A. tumefaciens*, individual aliquots (1 aliquot per plasmid) were thawed on ice and gently mixed with 1µl of the required plasmid DNA before transfer to a pre-cooled 0.2cm electroporation cuvette. A Gene Pulsar™ and pulse controller unit (Biorad, Hercules, USA) using the Ec2 setting (approx. 12.5kV/cm^2, capacitance of 15µF and resistance of 400Ω) was used to transform the cells. Immediately after transformation, 1ml of pre-warmed 2YT media was added and the cells were incubated at 28°C for at least 2 hours before plating aliquots of 200-800µl on 2YT agar (+selection).

2.2.9 Plant Transformation

Plants were transformed using a 3-day protocol adapted from Bent and Clough (1998) as below:

3-4 pots containing 7-9 plants of the Col-3 or Col-0 background were used per construct. Main bolts were clipped repeatedly to encourage growth of secondary shoots. When ready for transformation, plants contained a mixture of open and closed flowers and were not yet setting seed. Day 1: starter culture of 50ml 2YT containing the appropriate antibiotic was inoculated with a single colony of *A. tumefaciens* and incubated over night at 28°, 200rpm.

Day two: 500ml 2YT (+antibiotics) was inoculated with 10ml starter culture and incubated over night as above. Day three: Bacterial cells were harvested by centrifugation at 7500 rpm for 15' at room temperature and the pellet was resuspended in 500ml infiltration media (fresh solution of 5% sucrose in dH2O with 0.025% Silwett L-77 [cat# VIS-01, Lehle, Roundrock, Texas]). The solution was transferred to a shallow container and plants were dipped, by submerging all floral buds. The plants were

subsequently shaken lightly to remove excess fluid and covered over night before being transferred to the greenhouse.

2.2.10 Plasmid ligation, A-tailing

Ligation of plasmids was performed using T4 DNA Ligase and ligase buffer provided with the pGEM-T vector system (Promega, Southampton, UK) according to manufacturers instructions.

For ligation of fragments amplified by KOD high fidelity polymerase into pGEM-T, the purified fragments were A-tailed as follows: 7µl of concentrated purified DNA fragment, 1µl of Taq DNA polymerase 10x reaction buffer (with $MgCl_2$), 1µl of dATP to a final concentration of 0.2mM and 1µl (5 units) of Taq DNA polymerase were incubated for 15-30 minutes at 70°C.

2.2.11 Transformation of chemically competent bacterial cells

Competent bacterial cells were thawed on ice. 1µl plasmid was added to 50µl and mixed gently. The tube was transferred to ice for 30 minutes, heat shocked at 37°C for 20 seconds and transferred to ice for another 2 minutes. 1ml of warm LB media was added and the tube was incubated at 225rpm for 1 hour prior to plate inoculation using 100-200µl per plate. The plates were incubated over night at 37°C.

2.2.12 DNA purification (cloning)

Plasmid DNA was isolated from overnight cultures using the Wizard Plus Miniprep DNA Purification System (cat#: A7100, Promega, Southampton, UK) according to manufacturers instructions.

Non-plasmid DNA generated for cloning purposes was isolated via gel electrophoresis and recovered from the gel using the Wizard® SV Gel and PCR Clean-Up System (cat#: A9281, Promega, Southampton, UK) according to manufacturers instructions. Eluted non-plasmid DNA was concentrated using Pellet Paint NF Co-Precipitant (cat#: 707483-3) according to manufacturers instructions.

2.2.13 Oligonucleotide synthesis and sequencing services

The gene specific oligonucleotides were synthesized by Invitrogen (Paisley, UK) and Sigma-Genosys (Poole, UK).
Gene sequences were obtained from Lark Technologies (Takeley, UK).

2.2.14 cDNA synthesis

cDNA was synthesised using the Reverse-iT 1st strand Synthesis kit (cat#: AB-0789/a Abgene, Epsom, UK) according to manufacturers instructions.

2.2.15 PCR for genotyping and cloning:

For all purposes other than directly using the amplified PCR product for cloning, Taq SuperPak™ DNA Polymerase with MgCl2 (cat#: D5938-1.5KU, Sigma-Aldrich, Poole, UK) was used according to methods by Innis *et al*, (1990).
For cloning purposes, DNA was amplified using high fidelity KOD HiFi DNA Polymerase (cat#: 71085-3, Novagen/Merck, Darmstadt, Germany) according to manufacturers instructions.
Primer sequences used during the cloning work shown in this thesis are shown in Table 2.1. All primer sequences were checked for compatibility and annealing temperatures using the NetPrimer software downloaded from http://www.premierbiosoft.com/.

2.2.16 Genotyping of insertion lines

To genotype the Salk_108995 T-DNA insertion mutant, primers 108995-R (5'-CAACTGATGCGTCTCTCCAA-3') and left border primer Lba1 (5'-TGGTTCACGTAGTGGGCCATCG-3') were used to identify the T-DNA insertion in the ARF2 gene. Primers 108995-F (5'-GGGCTCACTGTTTTGCTCAT-3') and 108995-R were used to identify the wild-type ARF2 allele in the insertion line. Homozygous insertion mutants were crossed to mnt homozygotes and the F1 progeny were assayed for the mnt mutant phenotype and hemizygosity for the T-DNA insertion.

Table 2.1 Nucleotide sequences of primer pairs and linkers used for work described in Chapters 5 and 6.

Primer name	Primer sequence (5' to 3')	Linker[1]
pMNT_GFP_S	AAAGTCGACACACAAGAAAATAGAAGAGATAAAAA	SalI
pMNT_GFP_X	AAATCTAGACTTAACCAGAGGTAGTCAAAACTCA	XbaI
35S_MNT_X	CTCGAGGAAGGTATGGCGAGT	XhoI
35S_MNT_B	GGATCCTCCAGTCTCCACCAA	BamHI
35S prom	TGGCTAGATATAACAGAAGACG	
35S ARF	AAGGTAGTTCCTACTGAATCTAAG	
AVA prom 1F	ACG ACT CAA TGA CAA GAA GAA AAT	
AVA intron 1F	AGT CCT CCC CTC TTT CTA CCT TC	
pAP1 F	CATATGGACGTACATGTTTAAATTTGGTT	NdeI
pAP1 R	CTGCAGTTTTGATCCTTTTTTAAGAAACTT	PstI
*AP1*F_check	ACGCAAATCCTAAAGAAACCACT	
*MNT*R_check	GAAGTTATCTCCTCCACGATTACC	
*pINO*_RNAi_Eco F	GAATTCCCTGGATTAGTGCAAGGC	
*MNT*R_check	GAAGTTATCTCCTCCACGATTACC	
pINO Eco F	GAATTCCCTGGATTAGTGCAAGGC	EcoRI
pINO Nco R	CCATGGGAGAGTGTGTGTGTACGATG	NcoI
(check)*INO*:*MNT* RNAi F	TTCTCTTGACTTTGCTGTCTCCT	
(check)*INO*:*MNT* RNAi R	ATCTCCTATCATTCATCGTACACAC	
NM2F	TTTTTGAAGGGAGCTTATATATTTT	
NM2R	TTCTTTGTGACTTGTGTTGTTGTGATGGG	

[1]Linker sequences, where present, are underlined in column 2.

2.2.17 Electronic aids for the visualisation and analysis of molecular sequence data

Sequence data obtained from Lark was viewed and compared to other known sequences using the Sequencher 4.5 shareware (GeneCodes Corporatio). The cloning of molecules was planned and visualised using Clone Manager 5 (Sci Ed Central). Sequence alignments and virtual translations into predicted protein sequence were performed using GeneDoc (www.psc.edu/biomed/genedoc).

2.2.18 Microscopic and macroscopic imaging and image processing

Photographs of whole plants, mature seed and inflorescences (including individual floral buds) were obtained using a Nikon Coolpix 4500 digital camera (Nikon, Tokyo, Japan) directly or through a Leica MZ6 dissecting microscope.

All digital images were processed using Adobe Photoshop software. For analysis of stem size and composition, sections were made by hand using a razor blade and stained with 0.1% Toluidine Blue. Sections were photographed under an Olympus BH-2 microscope as above.

2.2.19 Phase contrast microscopy

For analysis of whole-mount seeds, seeds were dissected from siliques and placed in a drop of clearing solution (8 g chloral hydrate, 11 ml water, 1 ml glycerol) for at least 1 hour. Cleared seeds were enclosed under a cover slip and sealed with nail polish. Samples were photographed under a Nikon Eclipse E800 microscope with differential interference contrast optics using a SPOT RT Color camera (Diagnostics Instruments Inc., Michigan, USA).

2.2.20 Confocal laser scanning microscopy

Plant material was dissected on a glass slide in a drop of dH_2O and enclosed under a cover slip sealed with nail polish. Images were obtained using an Axiovert 100M LSM510 laser scanning microscope (Zeiss, Jena, Germany). Confocal flourochrome visualisation was obtained in two channels:
1. GFP - Argon Laser: 488nm (FITC)/BP505-530, 2. Chlorophyll autofluoresence - HeNe1 Laser: 543 nm (rhodamine)/LP585. The objective used to collect images measuring 1024x1024 pixels was a C-Apochromat 63x/1.2 water lens.

2.2.21 Scanning electron microscopy

For scanning electron microscopy (SEM), siliques were slit open and fixed in 3% glutaraldehyde in 0.05 mol/l sodium cacodylate buffer pH 6.8 overnight at 4°C, postfixed in 1% osmium tetroxide in 0.1 mol/l buffer pH 7.0 for 4 hours at RT, rinsed in buffer, dehydrated through an acetone series, and critical point dried. The dried ovules were dissected using a tungsten needle and mounted on conductive carbon adhesive tabs, which were sputter-coated with gold and examined using a JEOL JSM6310 scanning electron microscope (JEOL, Tokyo, Japan).

2.2.22 Histochemical staining for localisation of GUS activity

Plant tissue was dissected on a glass slide in a drop of staining solution (50mM $NaPO_4$ buffer pH7.0, 10mM EDTA, 2mM $K_4Fe(CN)_6.3H_2O$, 2mM $K_3Fe(CN)_6$, 0.1% TritonX-100, 1mg/ml X-GLUC). Dissected tissue was incubated over night in staining solution at 37°C in a microwell plate sealed with prafilm and subsequently cleared in 70% EtOH. For photographic imaging under the dissecting microscope, plant tissue was submerged in a Petri dish containing 70% EtOH.

3 Mapping and Gene Discovery

3.1 Introduction

3.1.1 *Arabidopsis* genetics in the post-genome era

The work presented in this chapter was undertaken two years post publication of the entire sequence of the *A. thaliana* genome. It therefore exemplifies how genetic studies in *A. thaliana* are now benefiting from the genetic tools that are available to us in this post-genome era, including:

1. On-line open access to the entire *A. thaliana* genome sequence via a database that is continuously amended and updated as more information about sequence data, gene function, etc. is obtained.
2. T-DNA insertion lines, which can be used to test the effect of a disruptive insertion in the gene of interest (reverse genetics) as well as providing shortcuts to identify a mutated locus via allelism testing (forward genetics).
3. Expanding databases of other plant species' genomes, including those of *Brassica* and rice, facilitating the application of model plant research to valuable crop species.

Genetic mapping today can be achieved by relying entirely on the published *A. thaliana* genome sequence, which has facilitated the mapping process remarkably (Lukowitz *et al.*, 2000). The markers are PCR-based, either cleaved amplified polymorphic sequence (CAPS) or simple sequence length polymorphic (SSLP) (Bell and Ecker, 1994; Konieczny and Ausubel, 1993) and a comprehensive collection of these markers, which can be found throughout the genome, is available from the *tair* webpages (The Arabidopsis Information Resource, Carnegie Institution, Stanford, CA and National Center for Genome Resources, Santa Fe, NM - https://www.arabidopsis.org).
Using this PCR-based mapping approach, with a mapping cross between two *A. thaliana* ecotypes Columbia (Col) and Landsberg *erecta* (L*er*), it took us about 18 months to locate the *mnt* locus on a single BAC (60kbp region).

At the time of writing (July 2005) the *A. thaliana* genome is predicted to contain around 30,000 genes, only a fraction of which – 20 % in the year 2004 – (MASC Report 2004, http://www.*Arabidopsis*.org/info/2010_projects/MascReport2ndEdition.pdf) have been functionally characterised. In order to understand the role of the remaining genes, a number of programmes have been initiated, aimed at creating a cost effective and efficient tool for verification of gene function. The Salk Institute Genome Analysis Laboratory (SIGnAL) is one of these initiatives which has produced a comprehensive, sequence-indexed library of insertion mutations in the *A. thaliana* genome. The data is publicly available via a web-based graphical interface (http://signal.salk.edu/cgi-bin/tdnaexpress) and the seeds of the T-DNA insertion collection are readily available via the ABRC seed stock collection (*Arabidopsis* Biological Resource Center, Ohio, USA) (Alonso *et al.*, 2003).

3.1.2 Mapping and identifying *MNT*

This chapter describes the genetic mapping and subsequent identification of the *MNT* locus with the help of the above-mentioned methods. The successful identification of *MNT* in the model organism *A. thaliana* prompted the search for an *MNT* homologue in the crop species *Brassica napus* which is also described here. The objective of the mapping procedure was to focus in on the position of the *MNT* locus closely enough to identify a small group of candidate genes. The *mnt* mutation was generated by EMS mutagenesis, which generally causes point mutations. A single base pair mutation was therefore expected to be responsible for the mis-expression of the *MNT* allele. Single base-pair mutations are difficult to detect by restriction digestion and sequencing alone, making it necessary to initiate the identification of the mutated gene by genetic mapping. Previous work by Sally Adams (University of Bath) had shown that the *mnt* mutant allele is stably inherited in a recessive Mendelian fashion and homozygous mutant plants can be scored by their distinct floral phenotype (see Chapter 4 for *mnt* genetics and phenotype). These are the basic parameters that facilitate genetic mapping by chromosome walking (Jander *et al.*, 2002) as employed for the purpose of detecting the *mnt* locus.

3.2 Results

3.2.1 Mapping *mnt*

3.2.1.1 Rough mapping of *mnt* using published markers

The rough mapping analysis was initiated by Dr. Nick Fenby (University of Bath). Using about 100 *mnt/mnt* plants, this study was able to locate the *MNT* locus on the lower arm of Chromosome V, close to the CAPS marker ATTED2 (see Figure 3.1 [A] depicting an electrophoresis gel containing a restriction analysis using this marker). Only one recombination event between ATTED2 and *mnt* was found in about 100 plants (200 chromosomes) implying close proximity of the *MNT* locus.

3.2.1.2 Fine mapping of *mnt* using 10 self-made markers

The DNA of another 900 F2 *mnt/mnt* plants was added to the mapping pool increasing the number of plants tested for recombination to about 1000. Using the published markers LFY3 (CAPS, ~0.4% RF, north of presumed locus) and MBK5 (SSLP, >2% RF, south of presumed locus.), the predicted position of the *MNT* locus was delimited further to a region of about 634kbp.

As no published PCR markers existed for the region between markers LFY3 and MBK5, new markers had to be generated to obtain a more precise position for the *MNT* locus. A list of enzymes which were chosen to test DNA fragments for sequence polymorphisms during marker generation is shown in Table 3.1. A total of 10 markers were generated out of 39 fragments tested, some of which were SSLP that did not require a digestion step. The markers that were generated for the fine mapping process are shown in Table 3.2.

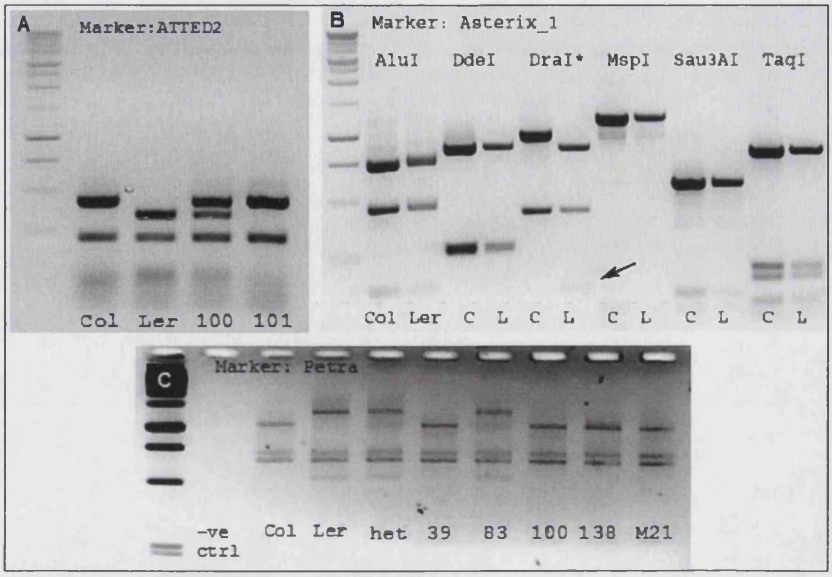

Figure 3.1: DNA electrophoresis gels showing examples of marker analysis and design. A: ATTED2, published marker, restricted by EcoRV, fragment sizes 0.35, 0.23 and 0.08 kb in Ler and 0.43, 0.23 kb in Col-3. Plant 100 is heterozygous (Col-3/Ler) for this marker, plant 101 is homozygous Col-3. B: Making a new marker. Restriction analysis of the Asterix1 fragment, DraI reveals a restriction site polymorphism due to an additional restriction site in Ler (arrow pointing to additional fragment). C: Restriction analysis of 5 plants using Petra, plant 83 is heterozygous for this marker.

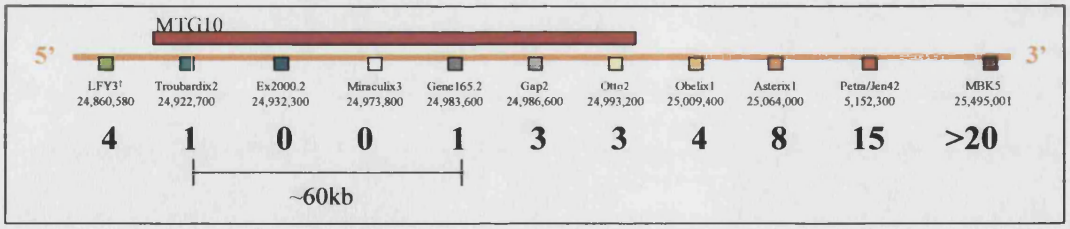

Figure 3.2: Relative positions of markers on Chromosome V (orange) and number of recombination events per 1000 plants (black, bold) found with each marker. The annotation unit/BAC MTG10 is indicated in red.

Table 3.1: Restriction enzymes used for generating fine mapping markers.

AluI	EcoRV	HpaI	NsiI	SphI	XhoI
BamHI	HaeIII	MboI	PstI	TaqI	XmnI
DdeI	HincII	MspI	RsaI	VspI	
DraI	Hind III	NdeI	Sau3AI	VspI	
EcoRI	HinfI	NheI	Sau96I	XbaI	

Table 3.2: Fine mapping markers between LFY3 and MBK5.

Marker name	Primers, 1. = forward, 2. = reverse	Amplicon length	t_{ann}	approx. position on Chromosome[1]	enzyme/ SSLP
Petra[2]	1. gcgccactagtatgccaatgga 2. cgtctgaataaaccgccg	1935bp	63°	25,152,300	AluI
Jen4	1. cggaaaaatacaaggagcca 2. ttcaaaacccgaaagaaacg	1258bp	60°	25,152,901	AluI
Asterix1	1. ccaagggaatgataacggg 2. cgtggcgtgagatgaagtg	1433bp	58°	25,064,000	DraI
Obelix	1. gcatccaactcaaaaagcaa 2. tcggagacatccaaatacca	1136bp	55°	25,009,400	Sau3AI
Otto2	1. cctgcttgttttggcttctt 2. cctctttggctctttcgtct	1364bp	53°	24,993,100	Sau3AI (cannot distinguish *Ler* from het!)
Gap2	1. tccctttggctttcattg 2. atggacccgagacatttacg	1930bp	55°	24,986,600	SSLP
Gene165.2	1. aaaccagcaatcacgactca 2. caaccgacgaaaaacaatca	1631bp	56°	24,983,800	SSLP
Miraculix3	1. aaacgaatcagtgcgagaca 2. tgccaaaacaagaaacagga	1117bp	52°	24,973,800	DraI
Ex2000.2	1. gtgtggagttgtagtcggagg 2. tcccctgaaagtcacgaaag	1128bp	55°	24,932,300	HinfI/ DraI/VspI
Troubardix2	1. gggttttgtttgtttttatttgg 2. cgtgagatttgattggtgga	1084bp	53°	24,922,700	DraI

[1] approximate positions from *tair* are due to change (correct in January 2004);
[2] colour coding of marker names: blue is positioned **south-**, purple is positioned **north** of the *MNT* locus.

3.2.1.3 *MNT* is one of 17 genes in a region of 60kb on the lower arm of Chromosome V

Using the new markers shown in Table 3.2, the gene was fine-mapped to a region of ~60kbp on the annotated BAC clone MTG10 of chromosome 5 between the markers TRB2 (CAPS) and G165.2 (SSLP) (see Table 3.2 and Figure 3.2 for details). This 60kbp region is located on the Annotation Unit MTG10 and contains 17 annotated genes that are listed in Table 3.3.

No assumptions could be made at this point during the mapping process about the identity of the *MNT* gene within the 60kbp region, and as the entire region is too large to be sequenced, Sushma Tiwari (University of Bath) therefore initiated a complementation test using the BAC associated with the Annotation Unit MTG10 (see p 124). In addition, an allelism test using T-DNA insertion lines was undertaken as described in the following section.

Table 3.3: List of genes contained within 60kb fine-mapped region taken from *tair* (Nov. 2003)

GENE NAME	DESCRIPTION	NOTES
AT5G62000.1	auxin response factor - like protein, auxin response factor 9, *Arabidopsis* thaliana, PIR:T08917*	Auxin IAA regulation of transcription, DNA-dependent
AT5G62000.2	auxin response factor - like protein, auxin response factor 9, *Arabidopsis* thaliana, PIR:T08917*	
AT5G62020.1	heat shock transcription factor 6 (HSF6), identical to heat shock transcription factor 6 (HSF6) SP: Q9SCW4 from (*Arabidopsis* thaliana) ;contains Pfam profile: PF00447 HSF-type DNA-binding domain	
AT5G62030.1	expressed protein, predicted proteins, D.melanogaster, C.elegans and yeast	Diphthamide synthase related
AT5G62040.1	Fdr1 Cen - like protein, Fdr1, Oryza sativa, EMBL:AF159883	Fe-deficiency related gene 1- homologous to a trans-Golgi body proteinTFL1. CEN proteins believed to be involved in the maintenance of inflorescence meristem identity
AT5G62050.1	OXA1 protein (OXA1p)	Involved in membrane binding (thylakoids?)
AT5G62060.1	F-box protein family, contains F-box domain Pfam:PF00646	calmodulin binding regions, signalling, F-box
AT5G62070.1	expressed protein, various predicted proteins, *Arabidopsis* thaliana	seems plant specific...(tapetum in *Brassica*), IQ calmodulin-binding region, Protein kinase
AT5G62080.1	protease inhibitor/seed storage/lipid transfer protein (LTP) family, similar to tapetum-specific protein a9 precursor {*Brassica* napus} SP|Q05772; contains Pfam protease inhibitor/seed storage/LTP family domain PF00234; supported by full-length cDNA Ceres:	Tapetum specific in *Brassica*cea Plant lipid transfer/seed storage/trypsin-alpha amylase inhibitor
AT5G62090.1	expressed protein, predicted proteins, *Arabidopsis* thaliana and Oryza sativa	
AT5G62090.2	expressed protein, predicted proteins, *Arabidopsis* thaliana and Oryza sativa	Ubiquitin-related region
AT5G62100.1	BAG domain containing protein, similar to BAG domain containing proteins (At5g07220, At5g52060)	
AT5G62100.2	BAG domain containing protein, similar to BAG domain containing proteins (At5g07220, At5g52060)	Response regulator- related region
AT5G62110.1	hypothetical protein, predicted proteins, Plasmodium falciparum	Very similar to unknown protein in Rice
AT5G62120.1	hypothetical protein, ARR1, *Arabidopsis* thaliana, EMBL:AB016471	hypothetical protein [Prochlorococcus marinus]
AT5G62130.1	expressed protein, predicted proteins, D.melanogaster and S.pombe	Putative dihydrodipicolinate reductase-like protein [Oryza sativa]
AT5G62140.1	hypothetical protein,	
AT5G62150.1	expressed protein, predicted protein, *Arabidopsis* thaliana	
AT5G62160.1	metal transporter, putative (ZIP12), identical to putative metal transporter ZIP12 (*Arabidopsis* thaliana) gi|17385794|gb|AAL38437; similar to zinc transporter protein ZIP1 (Glycine max) gi|15418778|gb|AAK37761; member of the Zinc (Zn2+)-Iron (Fe2+) permea	
AT5G62165.1	MADS-box protein	
AT5G62165.2	MADS-box protein	

* initially annotated as two genes: AT5G62000 and AT5G62010, now annotated as ARF2

3.2.2 Identifying MNT as AT5G62000 via an allelism test

3.2.2.1 17 Salk T-DNA insertion mutants are associated with the list of candidate genes

A list of all Salk lines (available around April-August 2003) that, respectively, carry a T-DNA inserts in one of the 17 candidate genes identified by genetic mapping, is shown in Table 3.4. In April, not all candidate genes (see table Table 3.3) had an associated insertion line. Lines N608995 and N541470 (AT5G6200) only became available several months after all of the other lines had been obtained – a symptom of an actively growing on-line database.

Table 3.4: Available Salk lines from list of putative genes

Candidate gene annotation	SALK insertion mutation lines (NASC stock number alias and position)
AT5G62000.1	N608995 (Exon), N541470 (Exon), N535537 (300UTR3)
AT5G62000.2	
AT5G62020.1	N576690 (promoter), N527578 (300UTR5), N512418 (Exon), N637766 (Exon), N505425 (300UTR3)
AT5G62050.1	N520304 (Exon), N525416 (Exon)
AT5G62060.1	N577484 (exon)
AT5G62070.1	N573090 (intron)
AT5G62090.1	N538662 (Intron), N585761 (Intron), N589954 (exon)
AT5G62090.2	N548809 (1000 -Promoter), N530295
AT5G62100.2	N506711 (Intron), N619497 (300-UTR5)
AT5G62110.1	N539375 (exon), N501606 (Intron), N514463 (Intron) N569053 (Intron), N554073 (1000-Promoter)
AT5G62120.1	N560049 (300-UTR3), N508702 (Exon), N613654 (300-UTR5), N533125 (1000- Promoter)
AT5G62130.1	N573104 (300UTR5)

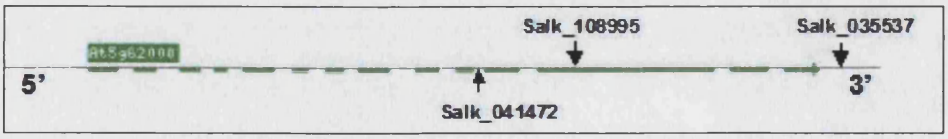

Figure 3.3: Respective positions of 3 Salk T-DNA insertions within the *MNT* gene and its 3'UTR. The exons of AT5G6200 are indicated by the green arrow, gaps indicate the positions of introns.

3.2.2.2 Insertions in the coding region of AT5G62000 cause an *mnt*-like phenotype in 2 out of 3 T-DNA lines

About 20 plants from each line were grown and visually scored for obvious phenotypic traits associated with *mnt* such as lack of flower opening (Figure 3.6) and abnormal seed sizes (Figure 3.4). Out of the 29 lines, one plant belonging to line N608995 (Salk_108995) was found to show *mnt*-like phenotypic traits, which were recognised via the floral phenotype shown in Figure 3.6.

24 plants had been grown from this line, all of which were tested for presence of the T-DNA insert and for insert homozygosity (i.e. lack of wild type genomic sequence devoid of an insertion) as shown in Figure 3.5. Plant M, the only plant that had produced an *mnt*-like phenotype, was also the only plant which tested positive for the T-DNA insert as well as negative for the presence of genomic DNA without insert, thus confirming a homozygous T-DNA insertion. The insertion is situated in the 12th exon of the gene annotated as AT5G62000 (see Figure 3.3 for details). Plant O, which scored heterozygous for the presence of the transgene, had a wild type-like phenotype. The F1 generation of plant O produced 3:1 segregation for the WT:*mnt*-like floral phenotype (data not shown).

The positions of T-DNA insertions in *MNT* associated with three different Salk lines is shown in Figure 3.3. Line N541470 (Salk_041470, T-DNA insertion in the 10th intron) was also found to produce a similar phenotype to *mnt* and N608995 when homozygous for the T-DNA insertion. A homozygous insertion in line N535537 (Salk_035537), which is situated in the 3' untranslated region (3'UTR), did not cause a noticeable disruption of the phenotype. (Data not shown)

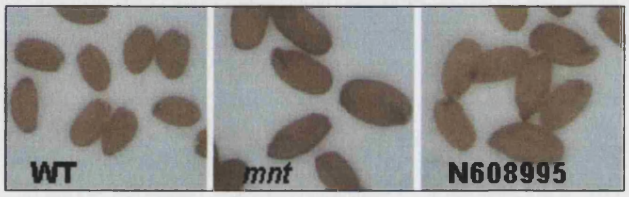

Figure 3.4: Seeds of WT, *mnt* and the Salk_108995 insertion line plants. All images taken at the same magnification.

3.2.2.3 The cross between *mnt* and N608995 confirms the identity of *MNT* as AT5G62000

Plant M was crossed with a plant of the genotype *mnt/mnt* to confirm that the same allele is disrupted in both plant lines. A PCR confirmed heterozygosity for the T-DNA insertion in the F1 plant (Figure 3.5) and the floral phenotype of the progeny plant produced by the cross was *mnt*-like (Figure 3.6). As the *mnt* mutant phenotype was not rescued in the F1 plant by the allele contributed from the insertion line parent, a disruption in the gene annotated as AT5G62000 (*AUXIN RESPONSE FACTOR 2*) was confirmed in *mnt* mutant plants.

ARF2 belongs to a family of 22 transcription factors shown to be involved in plant development via auxin-mediated gene expression (see section 3.3 for details).

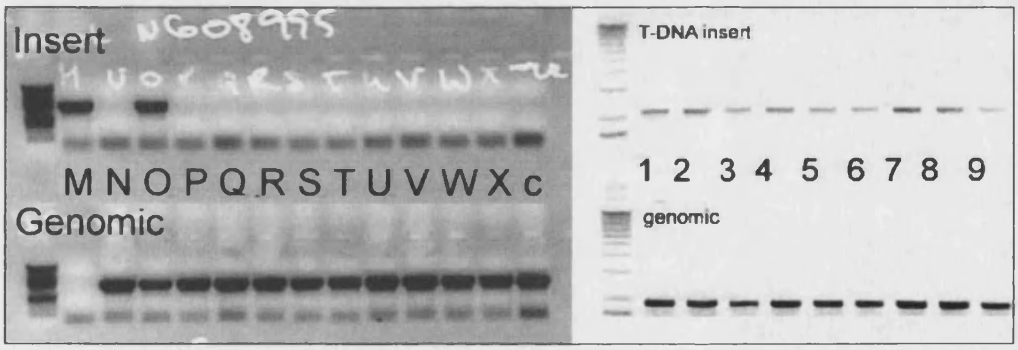

Figure 3.5: Scoring insertion lines

Left: DNA electrophoresis gel showing PCR result scoring for presence of the T-DNA insert 12 in line N608995, plants named M-X. top row: primers used to verify presence of transgene, bottom row: genomic DNA-specific primers, c: WT genomic DNA control

Right: Allelism testing. DNA electrophoresis gel showing PCR result scoring for presence of T-DNA insert in 9 *mnt* x N608995 F1 plants. Top and bottom row as in left gel.

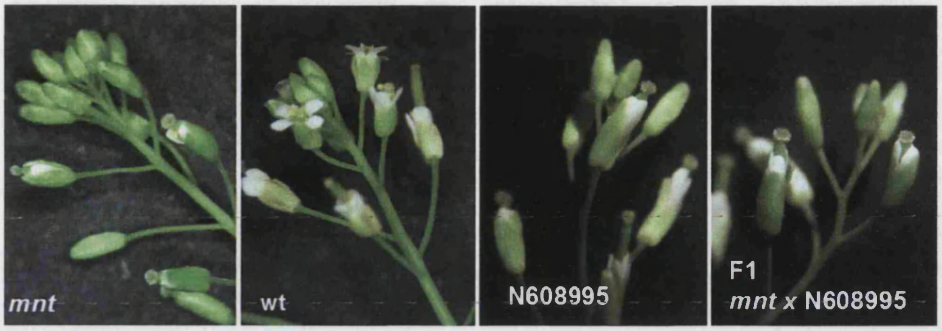

Figure 3.6: Inflorescences of mnt, wt and of Salk_108995 insertion line plants. F1 mnt x N608995 shows the outcome of the allelism test, it is a progeny plant of mnt crossed with the T-DNA insertion mutant with the mnt floral phenotype.

3.2.3 MNT (ARF2) in *Brassica*

3.2.3.1 *A. thaliana*-specific *MNT* primers amplify *Brassica oleracea* genomic DNA

In order to determine whether *MNT/ARF2* is present in the closely related crop species, a PCR using a pair of *Ath-MNT/ARF2*-specific primers (as indicated on Figure 3.8) was performed on *B. oleracea* genomic DNA (kindly provided by Ben Kemp, University of Bath). It was possible to use these *A. thaliana*-specific primers to amplify a fragment of similar size from the *B. oleracea* genomic template. The resulting amplicon, which is similar in size to *Ath-MNT/ARF2* genomic DNA, is shown in Figure 3.7.

The amplified fragment was cloned into pGEM-T and submitted for sequencing. The resulting sequence aligned to some extent with the exons of *Ath-MNT/ARF2* (data not shown). However, due to the presence of intronic sequence it was not possible to create an electronic alignment of the *Brassica* sequence with *Ath-MNT/ARF2* sequence data using the GeneDoc or Sequencher programme, therefore making it difficult to estimate how well the two sequences aligned.

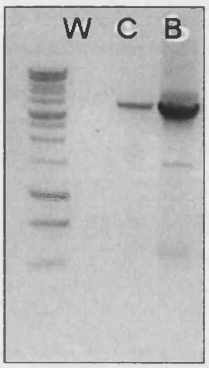

Figure 3.7: Amplification of the *MNT/ARF2* sequence from *Brassica oleracea* genomic DNA. W: water control; C: PCR amplicon using *A. thaliana* Col-3 genomic DNA template; B: PCR amplicon using *Brassica oleracea* genomic DNA template.

3.2.3.2 *MNT/ARF2* is homologous in *A. thaliana* and *B. napus* (cv. Westar)

In order to obtain sequence data from *B. napus* and with the aim of submitting this data to the NCBI, the *MNT/ARF2*-homologous cDNA fragment was generated from RNA extracted of *B. napus* cv. Westar. RNA from whole *B. napus* seedlings was reverse transcribed and subsequently used as a PCR template with the same set of PCR primers as used above. The amplicon was again cloned into pGEM-T and submitted for sequencing.

The resulting reverse transcribed fragment showed a high degree of sequence similarity with *A. thaliana MNT/ARF2* cDNA as shown in the alignment (Figure 3.8). However, the primer pair that had been used to obtain the *Brassica* sequence does not prime for the entire cDNA region in *A. thaliana* (primer sequences are underlined in red in Figure 3.8). The reverse primer sequence of this pair is located about 15bp upstream from the stop codon in *A. thaliana MNT/ARF2* thereby priming for an amplicon, which ends 17 base pairs before the 5' end of the gene. As no stop codon could be identified in the *Brassica* sequence it could be assumed that some sequence data (probably around 17bp) was still missing from the complete *Bn-MNT/ARF2* cDNA sequence. It was however not possible to amplify the complete *Brassica* sequence using an *A. thaliana MNT/ARF2* primer targeted at the 3' end of the gene.

A database of *B. napus* cDNA is available via UK Cropnet (http://ukcrop.net/perl/ace/ncbi_blast/BrassicaDB). In order to complete the *Brassica* sequence, the *Brassica* sequence data obtained thus far was blasted against the BrassicaDB database using UK cropnet. A 429bp 3' overlap with the existing *Brassica* sequence was found with a contig annotated as EM:BH733950. When aligned with the existing *Brassica* sequence, this contig contained a stop codon 15bp from the 3' end of the existing *Brassica* sequence. The two sequences were aligned as shown in Figure 3.8. They were then translated and aligned as shown in Figure 3.9.

In summary, the two sequences compare as follows:

- Length of *A. thaliana* cDNA fragment: 2,580bp
- Length of *Brassica* cDNA fragment: 2,547bp
- Predicted *A. thaliana* protein fragment size: 859aa
- Predicted *Brassica* protein fragment size: 848aa
    - 86% identity (number of residues that match exactly between the two sequences) and 92% similarity (similar residues or conservative substitutions).
    - 96% identity and 98% similarity within the conserved domains (DBD and CTD).

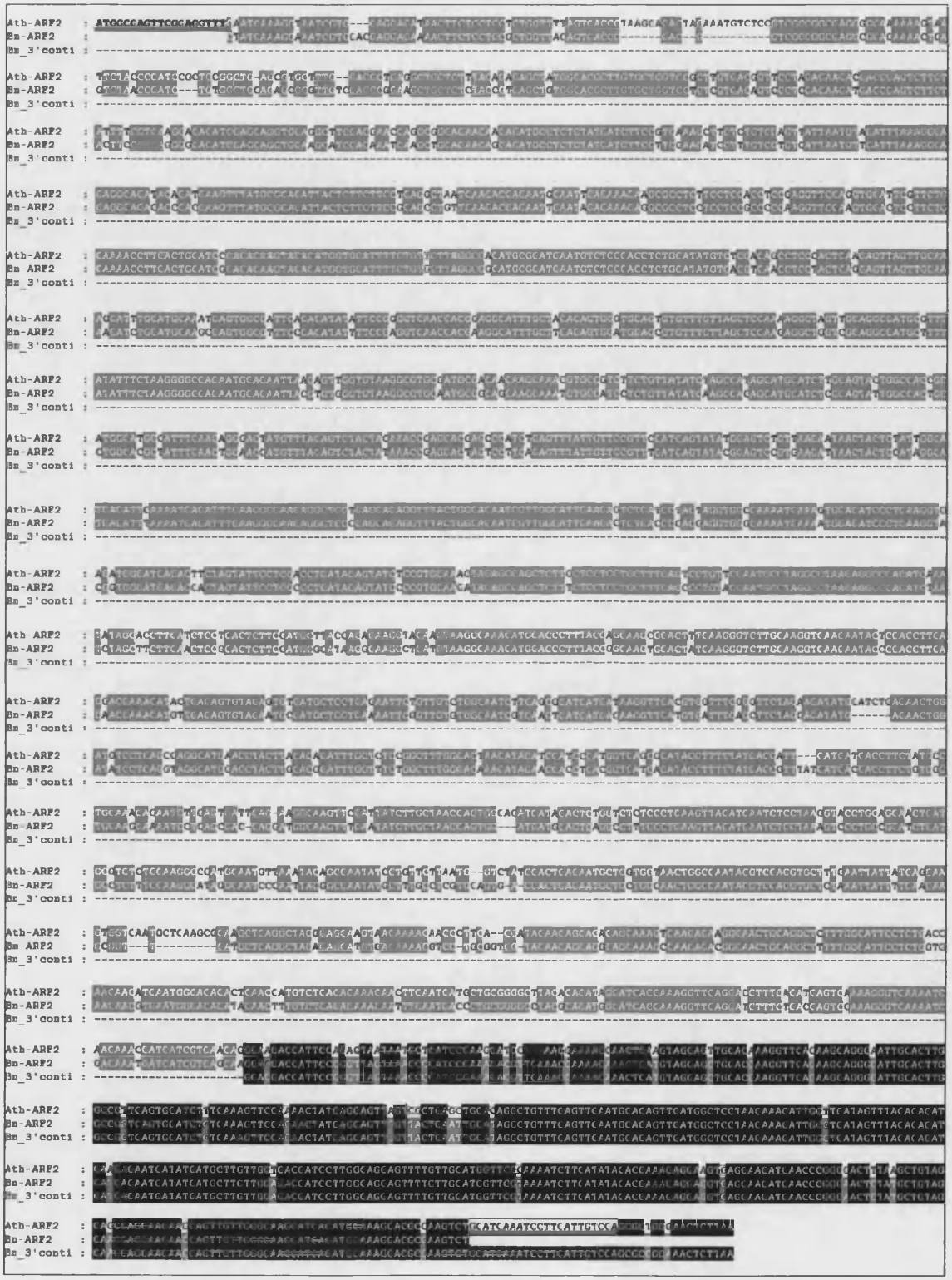

Figure 3.8: cDNA alignment of *MNT* (*ARF2*) in *A. thaliana* and *B. napus*.

3 sequences aligned here are Ath-ARF2 (*A. thaliana MNT* as obtained from *tair*), sequence data obtained from a single clone of Bn-ARF2 cDNA generated by RT-PCR (Brassica *MNT* homologue), Bn_3' contig (EM:BH733950) as obtained from Cropnet. The primer sequences that were used to amplify *MNT* in Brassica are underlined in red. Matching alignments are shaded grey for matches between 2 sequences and black for matches between 3 sequences.

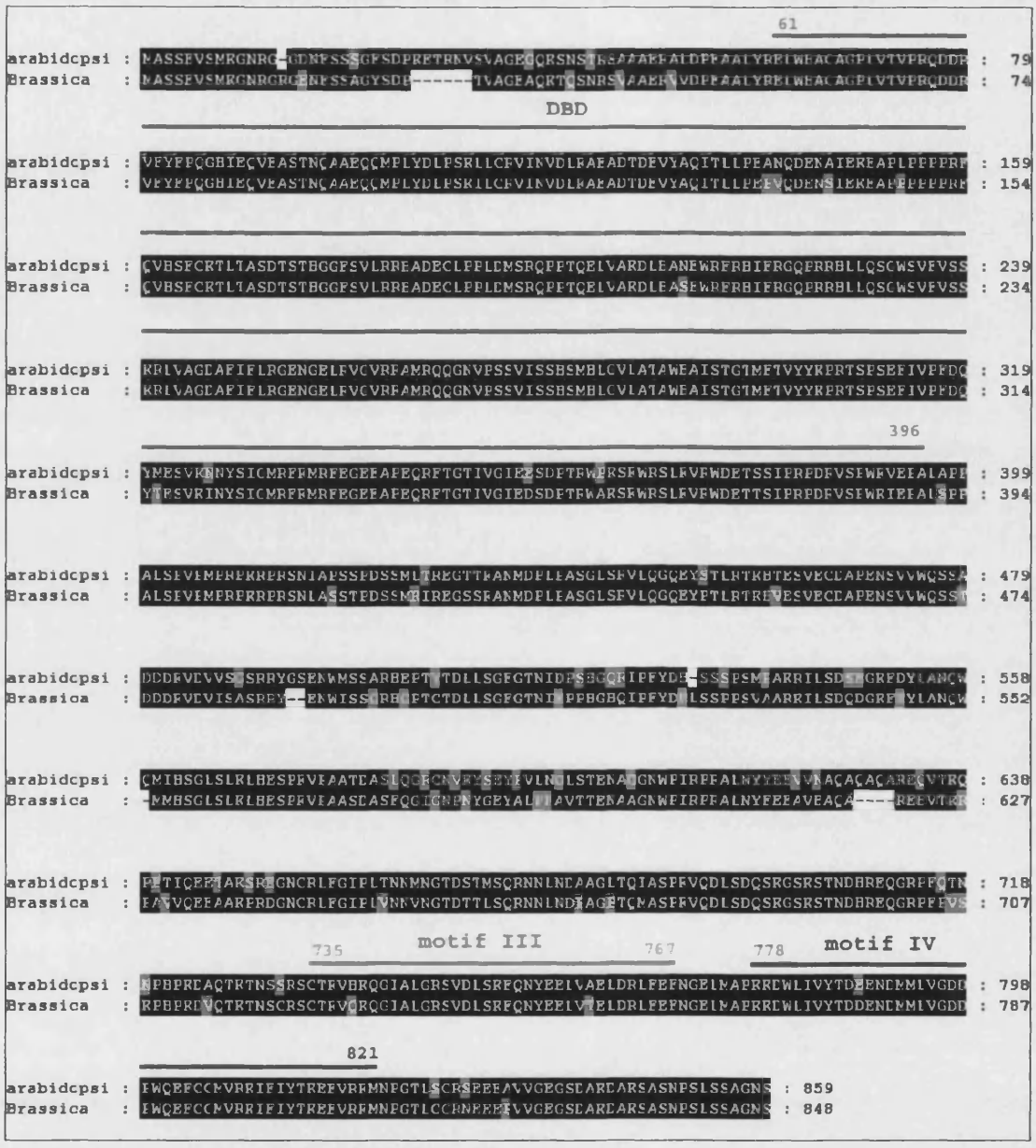

Figure 3.9: (Predicted) protein alignments of MNT (ARF2) in *A. thaliana* and Brassica. The active sites according to Ulmasov, Hagen and Guilfoyle (1999) have been indicated by coloured lines: DBD = DNA Binding Domain; motifs III & IV = C-Terminal Domain (protein-protein interaction).

3.3 Discussion

3.3.1 Helpful tools to identify *MNT* as AT5G62000

With the help of *tair* sequence-based mapping it was possible to pinpoint the *MNT* locus within 18 months of initiating the mapping process. The mutant locus was rough-mapped using a number of published markers also available from the *tair* database and fine mapped with the help of several self-made markers. The two well-studied ecotypes used for the mapping cross (Columbia and Landsberg) contained enough sequence variation in the region of interest to produce CAPS and SSLP markers in a number of positions clustered closely around the presumed (and later confirmed) locus of *mnt*. Recombination events between Columbia and Landsberg DNA detected by these markers permitted the identification of low-frequency recombination events bordering a 60kb region containing the *mnt* locus in the Columbia background. The number of putative genes that the mapping process had narrowed in on was relatively low and all genes were contained on a single annotation unit (BAC, MTG10). Fortunately, most genes within this region were already associated with a T-DNA insertion in *A. thaliana*, which significantly facilitated the identification of the mutated locus.

3.3.2 A secondary confirmation of the *MNT* locus: Complementation and sequencing of *mnt*

Once we had successfully mapped *MNT* to a small region on the lower arm of Chromosome V and confirmed its identity via allelism testing, additional confirmation of the mutated locus was provided by a complementation test and by the identification of a point mutation via sequencing. The last two confirmatory tests had been performed by Dr. Sushma Tiwari (University of Bath).

The complementation test was done using genomic Columbia DNA of the MTG10 BAC obtained from the ABRC (Arabidopsis Biological Resource Centre, Ohio State University, Ohio). Predictably, the wild type phenotype was restored in *mnt*/*mnt* plants that had been transformed with a fragment containing the genomic DNA sequence of AT5G6200.

As expected from a mutation obtained by EMS mutagenesis, the sequencing of *mnt* genomic DNA revealed a single base pair change, from G to A. The base substitution had occurred at the last base at the 3' end of the third intron, 665bp from the translational start codon. The sequence change was predicted to affect the splicing of the third intron by changing the consensus AG sequence to AA. AT5G6200 cDNA was sequenced in *mnt* and wild type Col-3 cDNA which confirmed that the observed sequence change was not due to a difference between Col-0 and Col-3 sequences. It revealed a four base pair deletion at the 5' end of exon 4 in *mnt* cDNA. The predicted protein sequence of *mnt* contains a frame shift and causes a premature stop codon about one fifth into the predicted wild type protein (Figure 3.10).

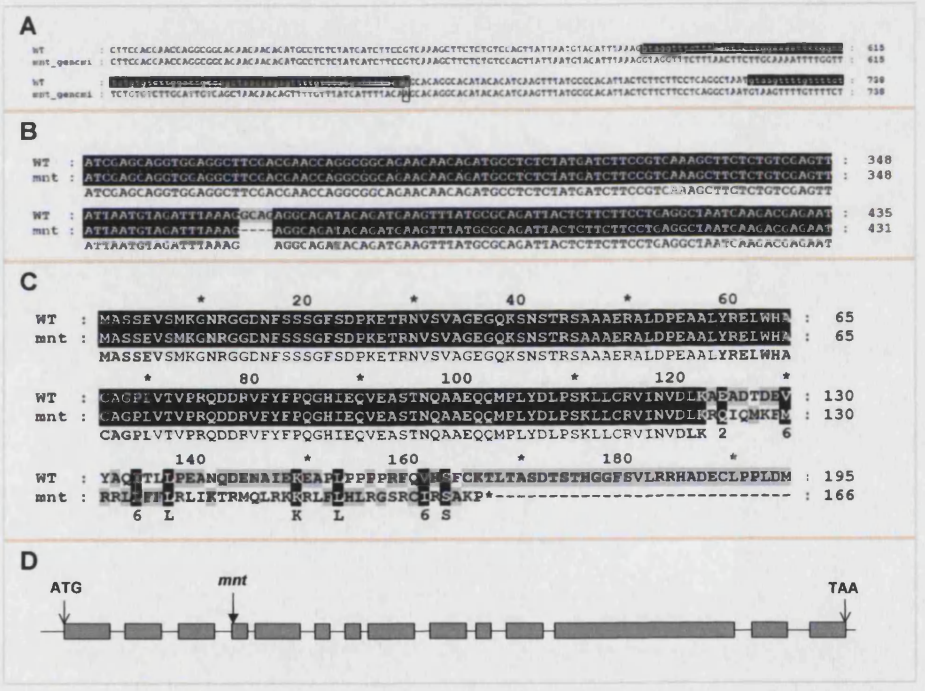

Figure 3.10 DNA and protein alignments showing the single base pair lesion in *MNT/ARF2* and the effects on transcription and translation.

3.3.3 *ARF2* is involved in the signalling of auxin, an important plant hormone.

Auxin is an important phytohormone traditionally known for its critical role in plant growth and development. Auxin has been the subject of a range of studies through its involvement in a number of developmental aspects including the division, turgor, elongation and differentiation of cells leading to regulation of patterning, growth and differential development throughout the plants lifecycle (Woodward and Bartel, 2005). Auxin signalling is therefore believed to regulate many important aspects of plant development, and its role has been implicated not only in root formation but also the maintenance of apical dominance, vascular patterning, tropisms and senescence (Zazimalova and Napier, 2003; Swarup *et al.*, 2002; Berleth and Sachs, 2001).

The most commonly known naturally occurring auxin is indole-3-acetic acid or IAA. It is synthesised in young shoots and shoot meristems of plants and it can be used experimentally to mimic natural hormone stimulation via exogenous application (Woodward and Bartel, 2005).

The large scope of IAA-related developmental processes and a considerable number of genes found to be involved in a signalling cascade peaked by this single hormone makes the study of auxin-based signalling a challenging quest. One signal with so many specific functions appears to require the understanding of a large, interactive signalling network involving processes such as the synthesis, conjugation, transport, reception and catabolism of this hormone as well as auxin dependent gene regulation (Leyser, 2002). A number of proteins have been studied in conjunction with these signalling processes ranging from auxin perception and auxin transport to auxin-led transcription regulation yet our understanding of the auxin signalling network is far from complete (Berleth and Sachs, 2001; Leyser, 2002; Zazimalova and Napier, 2003; Friml and Palme, 2003).

Some of the regulatory properties attributable to the IAA molecule are also believed to depend on interactions with other signals that regulate plant development. Examples include interactions with cytokinin to regulate shoot cell proliferation, with ethylene for apical dominance and apical hook formation, and with gibberellic acid for stem elongation and with light for differential growth (Swarup *et al*, 2002). Figure 3.11 depicts a schematic representation of some of the tightly regulated processes involved in the perception of and the reaction to the IAA signal. The involvement of ARF proteins in the

IAA signalling cascade is believed to occur at the gene regulatory end where ARFs have been shown to play a role in regulating the transcription of developmental genes in reaction to a perceived auxin signal.

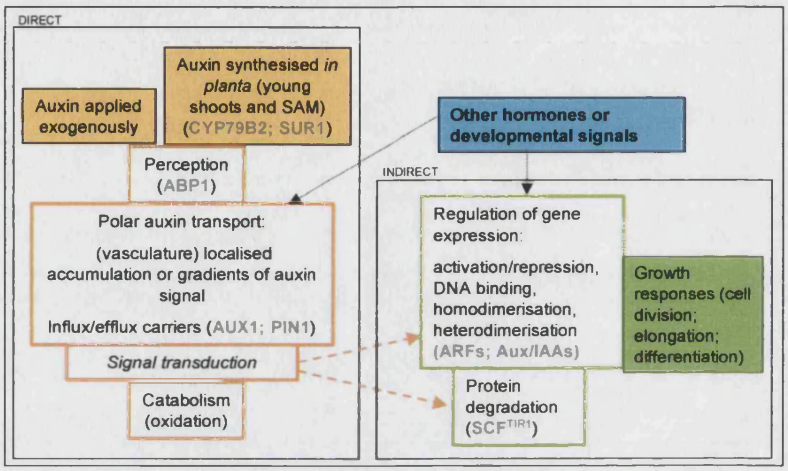

Figure 3.11 Simplified schematic representation of components involved in the signalling of the phytohormone auxin based on reviews by Leyser, 2002 and Zazimalova and Napier, 2003. Processes, structural elements and proteins (examples given in brackets) directly involved with the IAA molecule are shown to the left, indirect involvement of signalling components shown to the right.

3.3.4 The role structure and function of *AUXIN RESPONSE FACTORS* (ARFs) and early auxin response genes (*Aux/IAAs*)

AUXIN RESPONSE FACTOR proteins act in close association with Aux/IAA proteins at the gene regulatory end of the auxin signalling cascade. Their functions and roles are therefore reviewed jointly, starting with the *Aux/IAAs*, which were discovered first.

***Aux/IAAs*:**

Early studies of auxin-regulated gene expression in soybean found that the experimental application of auxin up-regulates the expression of a number of genes, some of which can be detected as early as 3 minutes after exogenous application of IAA (Hagen and Guilfoyle, 1985). This gene expression occurs in the absence of protein synthesis

(implying that their regulation is controlled by factors which are already present) and the genes have been named early- or primary auxin response genes in accordance with their expression patterns. A number of early auxin response genes have been identified and characterised and they are categorised within the early response gene super family, as *Aux/IAAs*, *SAUR*s and *GH3*s (Abel and Theologis, 1996; Guilfoyle *et al.*, 1998; Hagen and Guilfoyle, 2002).

Aux/IAA genes belong to a family containing 29 loci in *A. thaliana* (Liscum and Reed, 2002). They encode short-lived, nuclear localised proteins which share four conserved domains (I, II, III and IV) that are involved in protein stability and dimerisation (Reed 2001; Hagen and Guilfoyle, 2002). A diagram of a typical Aux/IAA protein is shown in Figure 3.12. Aux/IAA proteins act as transcriptional repressors of other auxin-responsive genes (Ulmasov *et al.*, 1997b, Tiwari *et al.* 2001) and this function is mediated by domain I (Tiwari *et al.*, 2004). Protein stability of Aux/IAA proteins is modulated by IAA, increasing levels of which lead to increased protein degradation. This IAA-mediated instability is conferred by domain II via interaction with an ubiquitin ligase complex, SCF^{TIR} (Gray *et al.*, 2001). Accordingly, downstream responses to Aux/IAA protein action are determined by relative abundance of Aux/IAA proteins (Knox *et al.*, 2003). Domains III and IV are involved in protein dimerisation – Aux/IAA proteins have been shown to homodimerise and to heterodimerise with ARF proteins (Kim *et al.*, 1997; Ulmasov *et al.*,1997a, 1997b). The auxin responsiveness of early response gene promoters depends on the presence of a conserved *cis*-acting motif containing the -TGTCTC- sequence element also known as the auxin response element (AuxRE) (Ulmasov *et al.*, 1995). This sequence was originally identified in the promoter of *GH3* in soybean (Hagen *et al.* 1991; Liu *et al.*, 1994) and has been used as bait in a yeast one-hybrid screen to isolate the first known transcription factor of early auxin genes named ARF1 (Ulmasov *et al.*, 1997a).

***ARFs*:**

ARFs are encoded by a family containing 23 loci in *A. thaliana* (22 genes one pseudogene) and 14 loci in rice (Guilfoyle and Hagen, 2001; Remington *et al.*, 2004). The loci of *ARF* genes are scattered throughout the *A. thaliana* genome and at least one *ARF* locus can be detected on every chromosome. ARF proteins have been shown to act

as activators or suppressors by binding to AuxREs, thereby interacting *in trans* with auxin-responsive gene expression of early auxin responsive genes (Tiwari *et al*, 2003). While the transcription of *Aux/IAA* genes and the stability and activity of their proteins are up-regulated by IAA, the transcription of *ARF* genes is not modulated by auxin signalling (Ulmasov *et al.*, 1999b).

The typical protein structure of ARF proteins is shown in Figure 3.12. The proteins generally share 3 domains: a conserved N-terminal DNA binding domain (DBD) which binds to the AuxRE of early auxin gene promoters, a conserved C-terminal dimerisation domain (similar to domains III and IV of the Aux/IAA protein family) and a variable middle region (MR) shown to mediate the regulatory function of the transcription factor (Ulmasov *et al.*, 1999a,b; Tiwari *et al.*, 2003). The composition of the middle regions have been compared and using protoplast transfection assays it has been found that ARFs with glutamine-rich MRs activate auxin response gene expression (Ulmasov *et al.*, 1999a) while ARFs with proline/serine-rich MRs and almost all other MRs compositions tend to act as repressors (Tiwari *et al.*, 2003). The ability to dimerise with other ARF proteins was detected when ARF1 was used as bait in a yeast two-hybrid system which isolated the closely related ARF2 protein (Ulmasov *et al.*, 1997a). ARF activity is likely to be influenced by heterodimerisation with Aux/IAA proteins which can dimerise with ARFs on AuxRE target sites – a dimerisation which has been shown to change ARF-led activation to ARF-Aux/IAA-led repression (Tiwari *et al.*, 2003; Weijers *et al.*, 2005).

3.3.5 Predicted function of proteins encoded by *mnt* and the insertion line allele

The frameshift and premature stop codon in the *mnt* allele occur near the 5' end of the gene and we therefore suggest that the protein is truncated within the DNA binding domain. In order to determine if this lesion causes a complete loss-of-function, further expression studies would need to be undertaken. However, a correlation has previously been made between the positions of mutations on other ARF proteins and the severity of *arf* mutant phenotypes. Weak mutant alleles of *arf3/ett* are caused by mutations near the 3' end of the gene, while strong mutant alleles are caused by lesions proximal to the 5' end of the gene (Sessions and Zambryski, 1995; Sessions *et al.* 1997). This also applies to

mutation sin *arf5/mp* which are only found beyond the DBD (the authors presume that mutations nearer the 5' end of the gene would be embryo lethal) (Hardtke and Berleth, 1998). We suppose that all functional domains are disrupted in the protein that is predicted to be encoded by the *mnt* mutant sequence. Therefore we assume that the *mnt* allele has a complete loss-of-function. Furthermore, despite occurring in different ecotypes and therefore different genetic backgrounds, the phenotypes of *mnt* (Col-3) and the insertion line (Col-0) appear very similar. This implies that *MNT/ARF2* gene function is equally impaired in both lines. The T-DNA insertion in the Salk insertion line is positioned in the third quarter of the gene (around AA550), well beyond the DNA binding domain but similar phenotypes of the insertion line and the EMS line suggest that protein function is disrupted despite a potentially intact DBD in the insertion line.

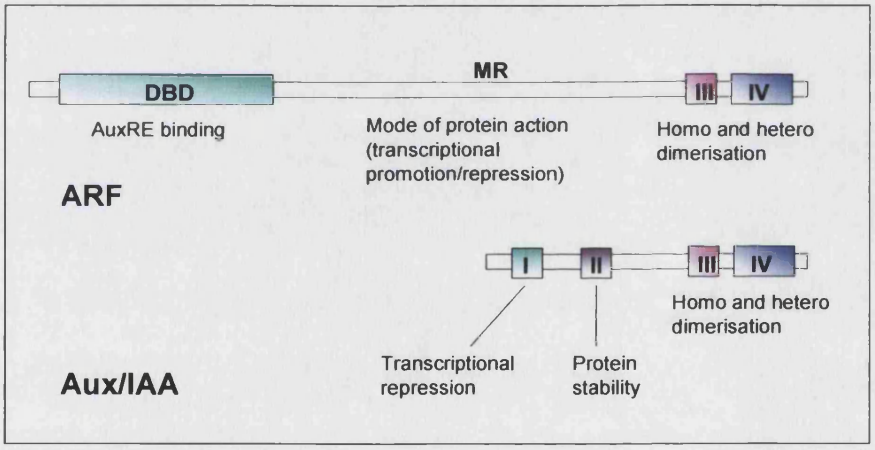

Figure 3.12 Protein structure of typical ARF (top) and Aux/IAA (bottom) proteins (based on Figure by Leyser *et al.*, 2002).

3.3.6 *MNT/ARF2* in Brassica napus and rice

A. thaliana has no genuine value as a crop plant. However, it belongs to the same taxonomic family as the *Brassica* genus, which contains a number of economically important crop species. *A. thaliana* and *Brassica* genes generally share about 85 - 87% sequence identity of homologous genes (Zhang and Wessler, 2004; *Brassica* and UK CropNet, http://ukcrop.net/*Brassica*.html#project) and, despite an obvious difference in overall size, strong phenotypic similarities do exist.

86% identity and 92% similarity of the predicted *B. napus* MNT protein and *AthARF2* suggest functional homology. An active role of the predicted protein in *B. napus* is further implied by the fact that conservation between the two genes is most stringent within the active regions of the gene, i.e. the DNA Binding Domain, and the C-Terminal Domain (Figure 3.9) suggesting increased selective pressure in these regions. However, this does not guarantee that *Bn-ARF2* plays the same role in the *Brassica plant* as *At-ARF2* does in *A. thaliana.* The genomes of *Brassica* species are up to five times the size of the *A. thaliana* genome (Paterson *et al.*, 2001) due to a high level of duplication and redundancy effects, a simple *Bn-arf2* mutation could be masked if it were to be induced in *B. napus*. Yet, it appears as though the *BnARF2* gene might provide a promising target for seed engineering.

An *ARF2* homologue has also been discovered in rice (Moriguchi *et al.*, 2005) and 54% identity and 67% similarity have been found between *Ath-ARF2* and *Os-ARF2* (NP_914881 – alignment not shown). The alignment between the predicted proteins is, as in *Brassica*, most stringent in the DBD and CTD regions. The rice genome contains at least thirteen other *ARF* loci (Remington *et al.*, 2004) implying a regulatory mechanism that is similarly complex to auxin response regulation in *A. thaliana.*

3.3.7 Further work

Protein sequences and protein expression studies including *in situ* analysis of *MNT/ARF2* in *A. thaliana* (*mnt*, *MNT/ARF2* and insertion lines) and in *Brassica* would significantly contribute to the understanding of *MNT/ARF2* gene function and of how the protein is affected by the mutations.

Once a more complete picture of the *Brassica* genome is available, it should be possible to gain an understanding how the *ARF* family is represented in this genus and of how many *ARF2*-related genes are present in this species. This would help to assess whether an *mnt*-like phenotype might be induced in *Brassica.*

A Bn*ARF2*-RNAi construct has already been produced (data not shown). The successful transformation of this construct into *B. napus* may answer whether or not it is possible to recreate an *mnt*-like phenotype by silencing the *Bn-ARF2* gene.

4 Phenotypic analysis of the *mnt* mutant

4.1 Introduction

The *mnt/arf2* mutant was isolated and initially analysed due to the effect of the mutation on seed size. However, a preliminary examination of the *mnt* phenotype shows that the mutation does not only affect seed morphology. The stem, rosette, roots and, most strikingly, the floral phenotype is also affected in the mutant plant with significant consequences on overall appearance and on fertility.

The following section is a review of some of the auxin signalling mutants including other *mnt* mutants studied to date. A review of known auxin mutants in light of the *mnt* mutation studied here serves two purposes: to further our understanding of the involvement of auxin in plant growth and development, thereby gaining some indications as to how the *mnt* phenotype can be explained; and secondly to use existing studies of similar mutants to focus the examination of the *mnt* mutant phenotype with regard to helping our experimental design and data interpretation.

4.1.1 Pleiotropic phenotypes of auxin signalling mutants

Due to the importance of auxin signalling on plant development as highlighted in Chapter 3 (Discussion), the loss of any single component in the auxin-signalling cascade can have severe and pleiotropic effects on plant morphology. Highlighted here are some examples of the phenotypes that are produced when proteins involved in the direct and indirect transmission of the IAA signal are defective or mis-expressed.

At the onset of the auxin-signalling cascade (see Chapter 3, Discussion), ABP1 (AUXIN BINDING PROTEIN1) is characterised as the receptor protein involved in auxin binding. The homozygous *abp1* mutation has been shown to cause a severe effect on early plant development and embryo lethality due to strong defects in cell division and elongation (Chen *et al.*, 2001). Cell numbers and cell size in different organs of *mnt* and wild type plants have been subject to close examination throughout this project.

Mutations in the gene encoding for AUX1 (AUXIN RESISTANT1), a carrier protein involved in polar auxin transport (PAT), cause a root-specific phenotype. Root growth patterns are auxin resistant exhibiting normal root growth in the presence of high levels

of exogenous IAA, they show no ethylene-induced reduction of root growth and root gravitropism is also reduced (Pickett, Wilson and Estelle, 1990). The root phenotype in wild type and *mnt* seedlings is compared in section 4.2.7.

The mutation of another gene involved in polar auxin transport: *PIN1* (*PINOID1*), encoding for a trans-membrane transporter responsible for IAA efflux, causes severe defects in apical patterning. The inflorescence stems of severe *pin1* mutants lack all floral organs (resulting in a pin-like deformation of the inflorescence stem) or have deformed floral organ-like structures. The effect of the *pin1* mutation can be phenocopied by growing wild type plants on medium containing a polar auxin transport inhibitor (Okada *et al.*, 1991). These mutations, which are phenocopied by PAT inhibitors, have two effects: firstly they cause accumulation of auxin in IAA-synthesising tissues and secondly they cause depletion of auxin in tissues that rely on auxin transport from remote sites of IAA synthesis (Mattsson *et al.*, 1999; Sieburth, 1999; Reinhard *et al.*, 2000). The *abp1*, *aux1* and *pin1* mutant phenotypes indicate that defects in auxin perception and transport can have severe and organ specific effects on cell division and elongation.

In addition to auxin sensing and transport, auxin-regulated protein turnover has been shown to play an important role in the regulation of auxin-mediated gene expression. *AXR6* (*AUXIN-RESISTANT6*) encodes for a protein that acts as a subunit in the SCF^{TIR} ubiquitination complex within the auxin signalling cascade and has been implicated in cell cycle-related protein degradation (Leyser *et al.*, 2002). *axr6* seedlings lack roots and hypocotyls and have vascular pattern defects. Like *abp1* embryos, but not as severely, *axr6* embryos are defective in structured cell division (particularly in the suspensor) and the seedling produces a basal stub instead of a root (Hobbie *et al.*, 2000, Hellmann *et al*, 2004). The *axr6* mutation is therefore another example for organ specific defective cell division.

The study of the *axr2* mutation is an example, where authors have implicated tropic growth in the list of defects that are caused by altered auxin signalling. *AXR2* (now known as *IAA7*, Nagpal *et al.*, 2000) was initially identified as a substrate targeted by auxin-regulated protein turnover and *axr2* is therefore a gain-of-function mutation. Mutant seedlings are resistant to auxin, and adult plants produce a dwarfed phenotype defective in shoot and root gravitopism. This lack of tropic growth has been attributed to

altered cell lengths and cell division rates in inflorescence and hypocotyls (Timpte, Wilson and Estelle 1992). The response of wild type and *mnt* seedlings to gravistimulation is examined in section 4.2.7.2.

A number of mutations in the *Aux/IAA* gene family, further downstream in the auxin-signalling cascade, have been reviewed by Liscum and Reed (2002). Some examples are outlined here: Mutants of genes such as *shy1* and *shy2* (*IAA6* and *IAA3* respectively Kim *et al.*, 1996; Tian and Reed, 1999) are insensitive to light signalling and produce agravitropic root growth. Severe alleles of the *bdl* (*bodenlos*) mutation (*IAA12* Hamann *et al.*, 1999) cause a lack of hypocotyls and embryonic root meristem, and reduction in vascular tissue development very similar to *axr1* phenotypes. The *msg2* (*massugu2*) mutation (*IAA19*, Tatematsu *et al.*, 2004) is characterised as an auxin-resistant phenotype showing lack of auxin-induced growth curvature in the hypocotyls, agravitropic and aphototropic hypocotyls, and defects in lateral root formation.
In summary, the auxin-related developmental abnormalities displayed by the *iaa* mutants can be of varying severity and include: Ectopic cell division and lack of organ-specific cell division or elongation leading to stunted growth or overgrowth; defects in root or shoot-specific tropic growth patterns that occur as a result of cell elongation and division; insensitivity to light signalling; and decreased apical dominance. Other characteristic abnormalities such as leaf curling, ectopic organ development and sexual organ deformations also occur.

4.1.2 The phenotypes of other *arf* mutants

The characterisation of T-DNA insertion lines for 18 of the 23 known *ARF* genes by Okushima *et al.* (2005a) has revealed that a large majority of the insertion lines do not show an obvious mutant phenotype. The authors ascribe this lack of mutant phenotypes to functional redundancy among ARF proteins. However, the *auxin response factor* mutants that do display an obvious phenotype, characterised previous to the study by Okushima *et al* (2005a), display a number of distinct phenotypes. These phenotypes are summarised in the following section where four well-studied *arf* mutants *arf3* (*ett*), *arf5*

(*mn*), *arf7* (*nph4*, *tir5* and *msg1*) and *arf8* are described. The mutant phenotype of the fifth well-studied member of the *ARF* gene family, *arf2/mnt*, will be presented in the results section of this chapter and previous work on *arf2* mutant alleles will be reviewed in the Discussion section.

arf3 was first described as *ettin*, a recessive floral patterning mutant which, most prominently, produces irregularities in the patterning of the gynoecium (Sessions and Zambryski, 1995; Sessions *et al.*, 1997). The mutation also affects the size and number of other floral organs as mutant flowers carry increased numbers of petals and sepals and decreased numbers and of the stamens that are also reduced in size (Sessions and Zambryski, 1995). Within the gynoecium, the stigma and all underlying tissue such as the transmitting tract, the style and the ovary show abnormal development affecting size and position of their components. In the stronger mutant alleles this leads to splitting of style and stigma along the medial axis leading to the exposure of ovules. Furthermore, the appearance of ectopic style- and stigma-like outgrowths as well as shortening of the ovary and outgrowth of the transmitting tract have been observed. A detailed analysis of the *mnt* floral phenotype is shown in section 4.2.4.

arf5 mutants were originally detected in a screen for embryonic patterning mutants (Berleth and Jürgens, 1993). *arf5/monopteros* mutants were named according to the frequent occurrence of a single fused cotyledon resulting from patterning and cell differentiation defects including abnormal vascular tissue differentiation. Severe alleles produce mutant embryos that lack all basal structures including hypocotyl, radicle and root formation and the overall phenotype is very similar to that of strong *bdl* (*bodenlos*) mutants (Berleth and Jürgens, 1993; Przemeck *et al.*, 1996; Hardtke and Berleth, 1998). The *mnt* seedling phenotype is examined in section 4.2.7.1.

arf7/non-phototropic hypocotyl4/transport inhibitor-resistant5/massugu1 was first described as the *nph4* allelele which causes failure of phototropic response to blue light stimulation (Liscum and Briggs, 1995 and 1996). The mutation was further identified in two independent studies, once in a screen for seedlings which were resistant to auxin transport inhibition as *tir5* (Ruegger *et al.*, 1997) and again as *msg1* in an analysis of seedlings that did not exhibit a differential growth response to externally applied auxin

(Watahiki and Yamamoto, 1997). All *arf7*-related phenotypes appear to be associated with defects in differential growth. The *arf7* mutants have been found to exhibit several additional differential growth defects, including defects in hypocotyl and stem gravitropism, lack of apical hook (conditional), and abnormal leaf morphology displaying epinasty or hyponasty (Liscum and Briggs, 1996; Watahiki and Yamamoto, 1997; Stowe-Evans *et al.*, 1998; Watahiki *et al.*, 1999; Harper *et al.*, 2000).

The phenotype of the *arf8* mutant is relatively weak compared to the *arf* mutant phenotypes reviewed above. *arf8* mutant hypocotyls are slightly elongated, apical dominance is enhanced and lateral root growth is promoted. Longer inflorescence stems in mature plants have also been observed (Tian *et al.*, 2004). In order to quantify visible yet relatively subtle differences in plant development, numbers of organs were compared in mature *mnt* and wild type plants and the data was analysed statistically where possible.

4.1.3 The focus of *mnt* mutant analysis

Much of the *mnt* phenotypic analysis described in this chapter was undertaken before the mutant gene had been identified and also before any other work on the *arf2* phenotype had been published. Although other aspects of mutant morphology were examined during this study, the main aim of this analysis was to learn how development in *mnt* mutant plants is impacted to allow for the increase in seed size.

Unless otherwise stated *mnt* refers to the homozygous EMS induced allele described in Chapter 3.

4.2 Results

4.2.1 The effect of the *mnt* mutation on mature seed weights

Preliminary data showed that homozygous *mnt* mutant mother plants produce large seed, which can be up to 45% heavier than wild type seed (Figure 4.1). *mnt/mnt* seed weighing 32.4μg (± 1.10) was found on plants grown in the same tray as *MNT/MNT* plants which gave rise to seed weighing 17.92μg (± 0.252). However, seed sizes have been found to vary according to growth conditions of the mother plant.

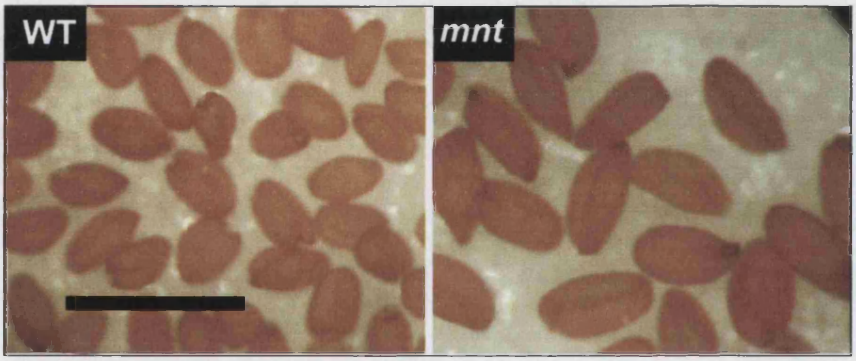

Figure 4.1 Seed of self-pollinated *MNT/MNT* and *mnt/mnt* plants. Pictures taken at the same magnification, bar: 1mm

4.2.1.1 The maternal effect on mnt seed weight

The effect of seed genotype on seed weight was tested under controlled conditions by performing the following manual reciprocal crosses between homozygous *mnt* and *MNT* plants (using manual self-pollinations as controls):

[*MNT* x *mnt*], [*mnt* x *MNT*], [*MNT* x *MNT*] and [*mnt* x *mnt*].

In order to control for possible variation caused by the presence or absence of additional seed pods on the plant only three flowers per stem were pollinated on the primary inflorescence stem. While these three flowers were allowed to set seed, all other flowers (including the remaining primary inflorescence meristem) were removed.

The weight of seed resulting from these crosses is shown in Figure 4.2. Seed phenotypes in all crosses correlated with the phenotype of the mother plant, regardless of seed genotype. A 2-sample t-test confirmed that there is no significant weight difference between the seed of genotypes *mnt/mnt* and *mnt/MNT* (p=0.33) nor between the seed weight of genotypes *MNT/MNT* and *MNT/mnt* (p=0.88), while seed weights of the *mnt* maternal genotype and those of the *MNT* maternal genotype differ significantly.

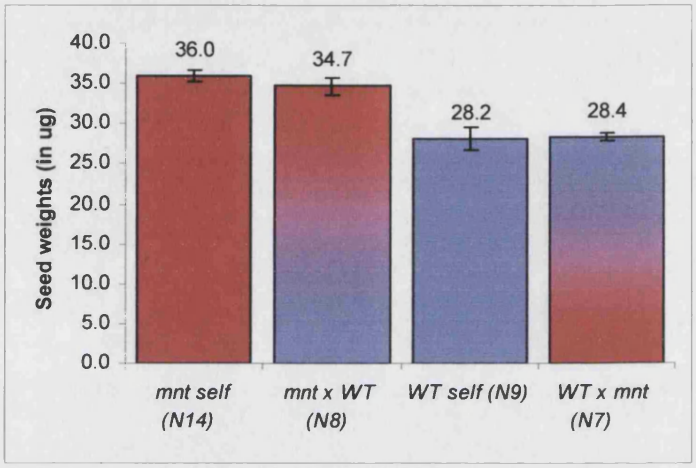

Figure 4.2 Seed weights of *mnt* and WT self- and reciprocal crosses. The crosses that were used to produce the seed weights displayed here are shown below each column. Average seed weights are shown above each column (bars indicate SE mean). The shading of the columns is representative of seed genotype: blue = *MNT*; red = *mnt*.

4.2.1.2 Maternal genotypes and plant growth conditions significantly influence seed weight

Manual pollination and the suppression of further seed set caused an increase in seed weight in wild type plants. A statistically significant increase in weight was observed in manually pollinated and pruned wild type plants from an average of 17.92µg (± 0.252) to an average of 28.2µg (±1.32). Therefore the plants that produced an unrestricted number of seeds gave rise to lighter (smaller) seed.

In order to test the effect of limiting seed set to a small number of pods on the primary inflorescence, the experiment was repeated on a larger scale by Melissa Spielman, who repeated the crosses under two conditions:

1. Manually pollinating 6 flowers on the primary inflorescences of 5 plants, removing all other flowers from this inflorescence ("primary inflorescence only").

2. As above but also removing all secondary inflorescences ("with secondary inflorescences").

This experiment also included seed collected from heterozygous plants produced by the crosses [*MNT/MNT* x *mnt/mnt*] and [*mnt/mnt* x *MNT/MNT*] respectively. Each plant produced between 1 to six seed pods with an average of 46.4 seeds per pod (this is an underestimation as some seed loss occurred when seed pods had shattered prior to seed collection). Average seed weights per pod and per plant were obtained and submitted to a number of statistical tests as shown below. The resulting average seed weights are displayed in Figure 4.3.

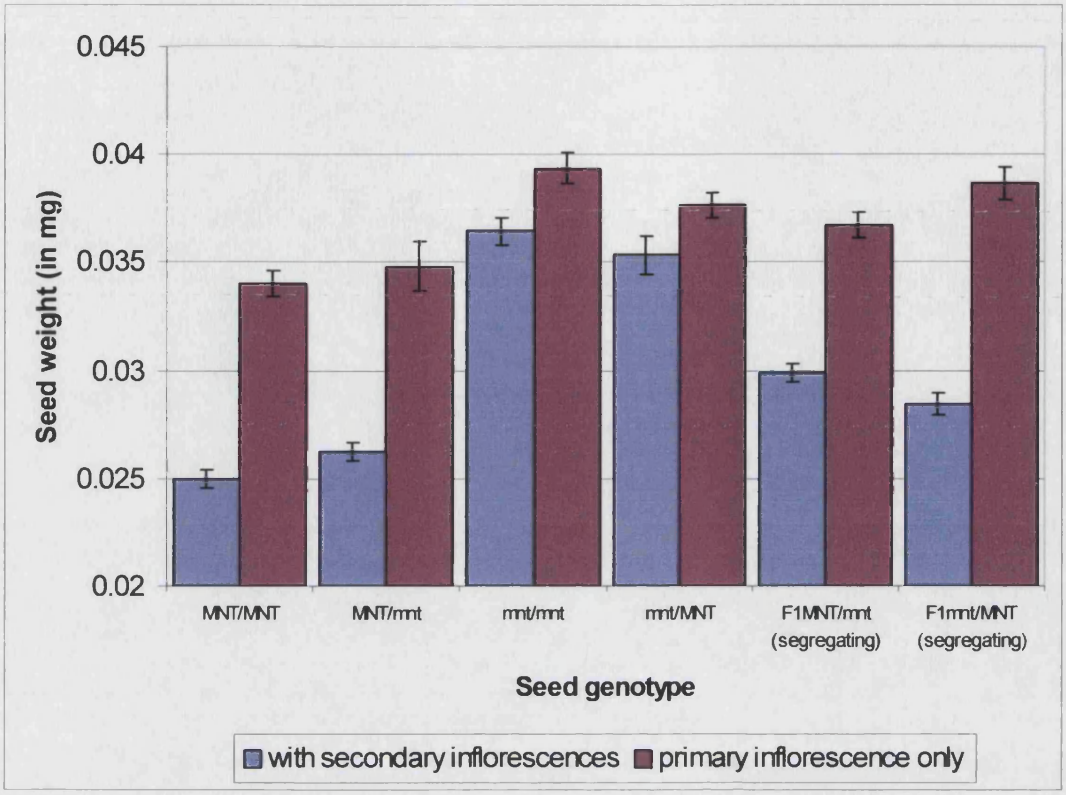

Figure 4.3 Average seed weights of seeds with different genotypes produced by plants under two different growth conditions. Seed weight data of each seed genotype (indicated below each column pair) under both growth conditions has been grouped to contrast the seed weight differences caused by the removal of secondary inflorescences. (N per data point = 5, error bars = S.E. mean)

The following is a summary of the results that can be derived from the data shown in Figure 4.3:

- Removing all secondary inflorescences from the mother plant results in an increase in seed weight produced by all genotypes.
- The increase in seed weight resulting from the removal of secondary inflorescences is most pronounced in seeds of wild type and heterozygous plants.
- Despite an overall increase in seed weight resulting from the removal of secondary inflorescences, seed produced by mother plants of the *mnt* genotype are heavier than those produced by wild type mother plants.

- Heterozygous plants produce larger and heavier seed than wild type plants.
- Seed grown on wild type mother plants without secondary inflorescences is very similar in weight to that grown on *mnt* plants which were allowed to produce secondary inflorescences.

In order to confirm the significance of the above statements, three questions were addressed using statistical analyses:

Q1. Does the seed genotype influence seed weight?

Q2. Does each maternal genotype (i.e. homozygous mutant, wild type or heterozygous) produce a statistically distinct seed phenotype?

Q3. How does the removal of all secondary inflorescences impact on the weight of wild type seed?

1. As in section 4.2.1.1, no significant difference was detected between seeds of different genotypes resulting from mother plants of similar phenotypes. Therefore a maternal effect is observed whereby the phenotype of the seed is determined by the maternal genotype, not the seed genotype. The statistical test results are displayed in Table 4.1. A first round of tests compared the effect of seed genotype on seed phenotype under both growth conditions ("primary inflorescence only" and "with secondary inflorescences"). This also applied to seed produced by heterozygous mother plants and it is consistent under both growth conditions.
Seeds produced by a heterozygous mother plant contain embryos of segregating genotypes. However the segregating genotype of the zygote has no detectable influence on seed phenotype as seed of a heterozygous plant is homogeneous in size.

2. The outcome differed according to growth conditions (pruned or not pruned). Given that seed genotype did not appear to significantly affect seed size (see 1.), size data of seed arising from the same maternal genotype was pooled creating three maternal groups which were compared statistically. Under the "with secondary inflorescences" condition, seed weights from all three maternal groups (*MNT* mother, *mnt* mother and heterozygous mother) differ significantly (25.6μg, 35.9μg and 29.2μg respectively). Under the "with

secondary inflorescences" condition, hetereozygous plants produce seed with a weight that is intermediate between seed weights obtained from *MNT* and *mnt* plants.
When grown under the "primary inflorescence only" condition, the weight of seed produced by the wild type maternal group, as above, differed significantly from that of seed produced by the other two groups. However, there was no statistical difference in seed weight between seed produced by heterozygous plants and that produced by an *mnt* plant (*MNT* mother: 34.4μg, *mnt* mother: 38.52μg, heterozygous mother: 37.69μg).
A heterozygous mother plant therefore significantly impacts on the weight of the seed despite a wild-type like appearance of seed shape produced by these heterozygous plants.

3. There is no statistically significant difference between the weights of seed produced on a wild type plant from which all secondary inflorescences were removed (34.42μg) and of seed produced on an *mnt* plant which was left to produce secondary inflorescences (35.89μg). The removal of all secondary inflorescences causes an increase in wild type seed weight which is similar to the size/weight increase conferred by the homozygous *mnt* allele in plants with secondary inflorescences (this does not apply to shape or other aspects of the seed phenotype).

Table 4.1 Comparing effects of seed genotype and effects of mother plant genotype on seed weight under two different growth conditions.

Seed Genotypes compared (N)	Growth conditions (inflorescences)[3]	Statistical test	p-value	Significant difference?
MNT/MNT (5) and *MNT/mnt* (5)	"with secondary"	2-sample t-test	0.67	no
mnt/mnt (5) and *mnt/MNT* (5)	"with secondary"	2-sample t-test	0.34	no
F1 *MNT/mnt* (5) (segregating) and F1 *mnt/MNT* (5) (segregating)	"with secondary"	2-sample t-test	0.06	no
MNT/MNT (5) and *MNT/mnt* (5)	"primary only"	2-sample t-test	0.56	no
mnt/mnt (5) and *mnt/MNT* (5)	"primary only"	2-sample t-test	0.10	no
F1 *MNT/mnt* (5) (segregating) and F1 *mnt/MNT* (5) (segregating)	"primary only"	2-sample t-test	0.07	no
MNT mother (10) and *mnt* mother (10)	"with secondary"	2-sample t-test	0.00	yes
MNT mother (10)and het mother (10)	"with secondary"	2-sample t-test	0.00	yes
mnt mother(10) and het mother (10)	"with secondary"	2-sample t-test	0.00	yes
MNT mother (10)and *mnt* mother (10)	"primary only"	2-sample t-test	0.00	yes
MNT mother (10)and het mother (10)	"primary only"	2-sample t-test	0.00	yes
mnt mother (10)and het mother (10)	"primary only"	2-sample t-test	0.29	no
1. *MNT* mother (10) and **2.** *mnt* mother (10)	1. "primary inf. only" 2. "with secondary"	2-sample t-test	0.08	no

[3] Refers to the two plant growth conditions, "with secondary inflorescences" and "with primary inflorescences".

4.2.2 The effect of the *mnt* mutation on the size of maturing seed

Having established that mature seed produced by an *mnt/mnt* mother is significantly larger and heavier than seed produced by a wild type mother, the next aim was to determine at which point during seed development this size difference arises.

4.2.2.1 mnt mutant seed is larger from the onset and grows at a faster rate

Immature seeds were dissected from pods of *MNT/MNT* and *mnt/mnt* self-pollinated plants and cleared to reveal internal morphology (Figure 4.4). Seed development was staged according to embryonic growth phases that were grouped as 1. Pre-globular stages; 2. globular stages; 3. heart stages; 4. torpedo stages; 5. bent cotyledon (or walking stick) stages; and 6. curled cotyledon/mature stages. In order to obtain an estimate of seed size with respect to the potential amount of endosperm and the size of the embryo that the seed can contain, we chose to compare the size of the seed cavity in wild type and *mnt* seeds.

Seed cavity size differences in *mnt* and *MNT* seed at different developmental stages are displayed in Figure 4.5, which depicts a developmental progression of post-fertilisation seed enlargement. According to our data which is shown in Figure 4.5, the following two statements can be made about post-fertilisation seed size:

1. *mnt* seed is significantly larger at all stages during seed maturation.
2. The seed size of *mnt* mutant seed increases at a greater rate than wild type seed.

Due to the difference in seed size observed in very young wild type and *mnt* seed we also chose to compare pre-fertilisation seed development (i.e. ovule development) in the mutant and non-mutant backgrounds as described in the following section.

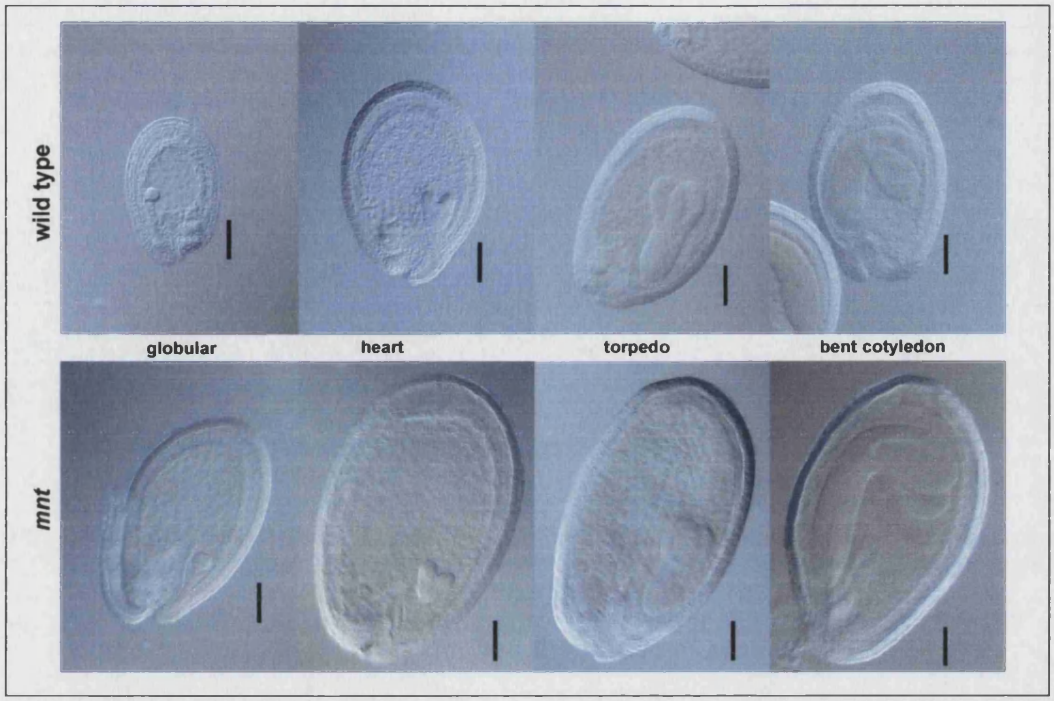

Figure 4.4 Differential interference contrast microscopy images of cleared wild type (top row) and *mnt* (bottom row) seeds at different embryonic growth stages. Bar: 0.1mm

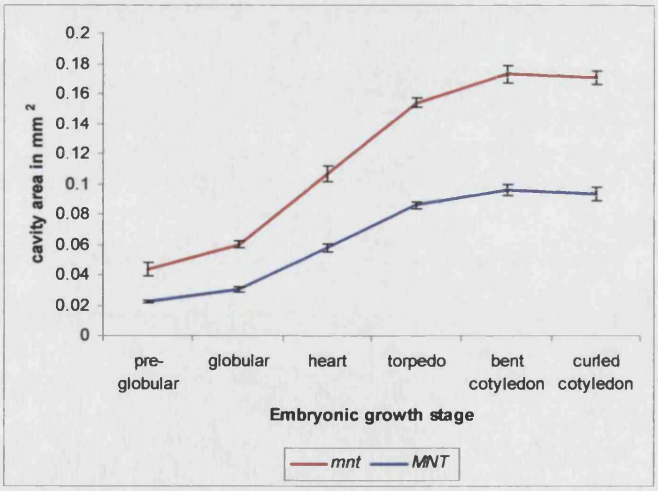

Figure 4.5 Seed cavity area in *mnt* mutant (red) and wild type seeds (blue) at different embryonic growth stages. The seed cavity area displayed here are a representation of an average of 15 seeds per stage per genotype (bars = +/- standard error).

4.2.3 The impact of the mnt mutation on ovule development

4.2.3.1 No external morphological abnormality can be detected in young *mnt* ovules

Earlier studies of seed phenotype using confocal microscopy revealed that *mnt* seeds contain an additional number of cells in the seed coat (see Introduction). However, the results of section 4.2.2 indicated that the differences in seed size are initiated prior to fertilisation, during ovule development. In order to determine if the *mnt* mutation causes a distinct morphological discrepancy from wild type ovule development during these pre-fertilisation developmental stages, the developing ovules of wild type and *mnt* plants were compared using two methods: 1. Scanning electron microscopy (SEM) to compare external ovule morphology and 2. resin-embedded sections to understand the cellular composition of the maturing ovule. The former will be expanded on in this section; the latter was performed by Melissa Spielman and that data will be used to explain some of the results in the Discussion section of this chapter.

Five different developmental stages of wild type and mutant ovules are shown in Figure 4.6. The first four images depict the very early stages from the elongation of the ovular protrusions (1-II) through to the initiation of integuments and the nearly complete envelopment of the ovules by the extending integuments. The shapes and sizes of the young *mnt* ovules appear normal, for example: the integuments develop asymmetrically as previously described and the ovules curve normally. Therefore, no externally visible differences in development was observed in these early stages of development.

4.2.3.2 Mature *mnt* ovules are larger than wild type and differ in shape

A difference in external ovule morphology can be detected between the mature ovules of *mnt* and wild type plants (Figure 4.6 [5]). The ovules are larger and there is a slight difference in the shape which is described in more detail below.
In order to depict the difference in ovule size and shape, the outlines of the mature ovules shown in Figure 4.6 (5) have been superimposed in Figure 4.7 which also contains a schematic representation of the components of the ovule. The region which appears

enlarged or extended in the mutant ovule corresponds to the central-to-chalazal region of the abaxial integument.

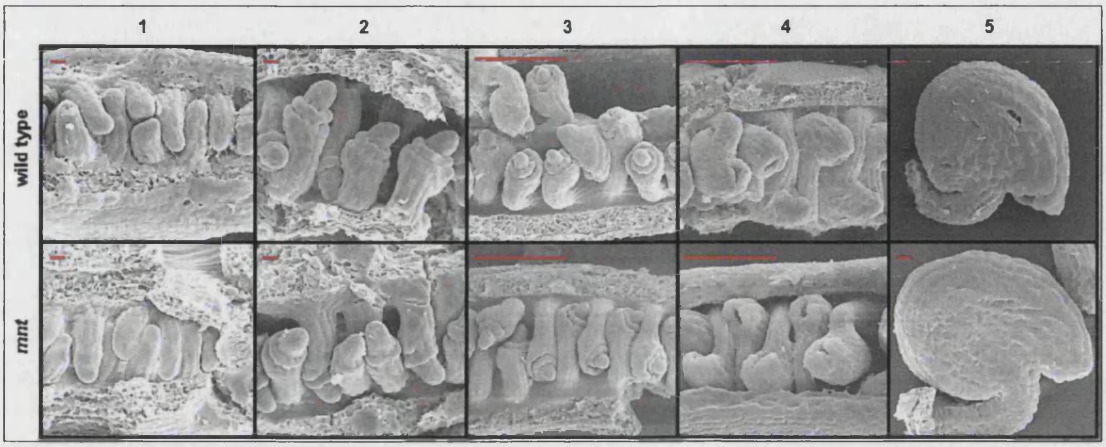

Figure 4.6 Scanning Electron Microscopy Images showing ovule development in wild type and *mnt* flowers. Stages according to Schneitz *et al.*, (1995): 1: stages 1-I to II; 2: stage 2-III; 3: stage 3-I; 4: stage 3-IV; 5: stage 3-VI. Bars: 10µm (1,2,5) and 100µm (3,4)

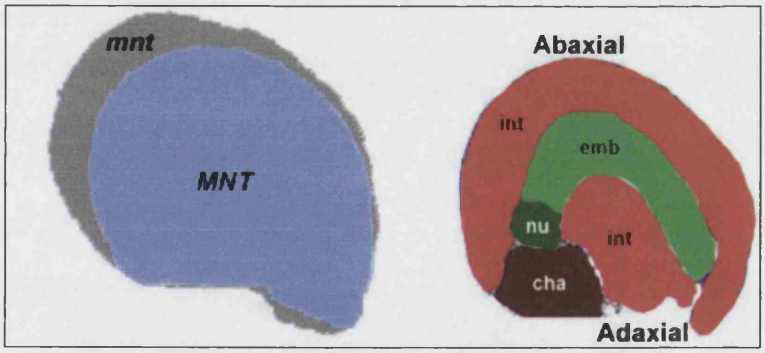

Figure 4.7 Superimposed outlines of wild type and mutant ovules (left) and a schematic representation of ovular components (right). cha = chalazal region, emb = embryo sac, int = integuments, nu = nucellus,

4.2.4 The mnt floral phenotype

Inflorescences of *MNT/MNT* and *mnt/mnt* plants are shown in Figure 4.8. The mutant flowers display two characteristic abnormalities:

1. The flowers do not open at anthesis, and 2. Most of the flowers fail to self fertilise.

4.2.4.1 Genetics of *mnt* floral trait inheritance

The floral phenotype, which co-segregates with the large-seed phenotype (4.2.1), can be used to visually score *mnt/mnt* mutant plants. According to the floral phenotype, the *mnt* mutation is inherited as a single allelic trait in a recessive Mendelian fashion. The 3:1 segregation of the *mnt* floral phenotype was confirmed via a Chi^2 test using the following two crosses:

1 -- *mnt/MNT* x *mnt/MNT*

2 -- *MNT/mnt* x *MNT/mnt*

which gave rise to these phenotypes:

1 -- 32 *MNT*, 12 *mnt* ($\chi^2 = 0.03$, $p<0.05$)

2 -- 30 *MNT* and 11 *mnt* ($\chi^2 = 0.0081$, $p<0.05$)

An inflorescence of a plant that is heterozygous for the *mnt* allele (*MNT/mnt*) is shown in Figure 4.13. No significant difference between *MNT/MNT* flowers and the flowers on a heterozygous plant have been detected.

4.2.4.2 Staging floral development on *mnt* and wild type plants

The inflorescence meristem of *A. thaliana* grows indeterminately and new flower buds are continuously added to the tip of the inflorescence. Therefore, each of the flower buds that are positioned along the inflorescence stem presents a snapshot of the developmental progression of flower maturation. Earlier stages of development are positioned at the top and later stages are found towards the bottom of this developmental timeline which is the inflorescence stem. The floral organ data presented here is based on the developmental

progression displayed by flowers that were dissected from an inflorescence stem in series as shown in Figure 4.9.

Figure 4.8 Inflorescences of wild type Col-3 (left) and *mnt* mutant (right). Photos taken at the same magnification.

Due to the lack of flower opening, the absence of self pollination and other abnormalities found within *mnt* flowers, it was not possible to directly compare the growth and development of *mnt* and wild type flowers. A staging system was therefore developed by Melissa Spielman in order to focus the comparison of developmental progression between two conspicuous developmental events:

A – The transition from bi-nucleate to tri-nucleate pollen

B – The dehiscence of the stigmatic papillae.

On inflorescences of *mnt* plants, more flowers are contained within these two developmental events that delineate the series that are described in detail below. On average there were 7.4 flowers on wild type inflorescences, while an average of 9 flowers could be found within the two developmental markers on *mnt* inflorescences.

Importantly, the actual temporal progression of development within the stages has not been measured. The data could therefore not be used to compare actual growth rates but is has been used to compare growth curves (Figure 4.11) or to contrast the relationship of organ lengths (Figure 4.12 and Figure 4.10).

Figure 4.9 Wild type (bottom) and mnt (top) flowers. Flowers in each set were removed in sequence from the same inflorescence, aligned (respective top row) and dissected (respective bottom row) to reveal internal organs. Arrow: transition from closed to open wild type flowers. Asterisk: crushed stigmatic papillae on an mnt flower. Inset: bent anther filaments depositing pollen on the ovary wall. Bar: 1mm.

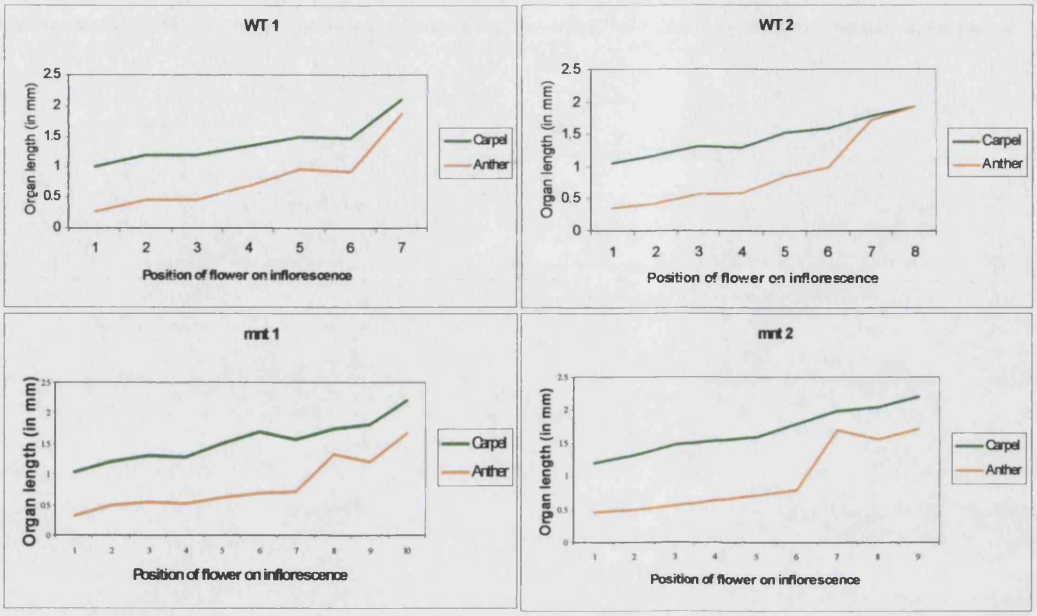

Figure 4.10 Lengths of gynoecia (ovary plus style) and anther filaments in two series of WT (top row) and mnt (bottom row) flowers. Each graph displays length data of flowers on a single inflorescence. Data points of respective anther filament and gynoecium lengths have been connected for ease of interpretation.

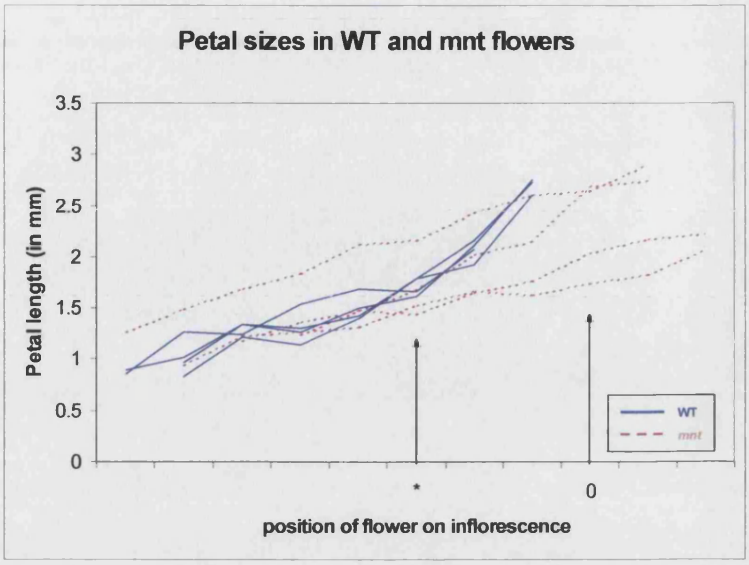

Figure 4.11 Petal elongation of flowers on 4 WT and *mnt* inflorescences. Petal length was recorded from flowers of the respective inflorescences in series (from tri-nucleate pollen stage to stigmatic papillae dessication) and the series of the respective genotypes were aligned at the point of anthesis (pollen release), which is indicated by an asterisk for WT and a 0 for *mnt*.

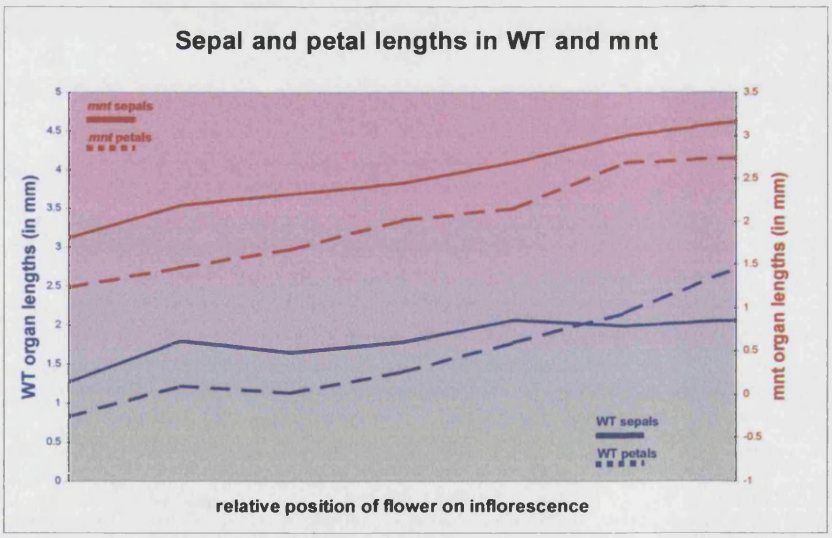

Figure 4.12 Elongation of petals and sepals in flowers on a WT and an *mnt* inflorescences. The wild type curves are plotted against the primary y axis (left) and the *mnt* curve is plotted against the secondary y axis (right). The floral sepal and petal lengths shown here are representative of organ lengths measured in 5 plants of each genotype.

Figure 4.13 Flowers of a heterozygous (*MNT/mnt*) plant removed in sequence from the same inflorescence (top row) and dissected (bottom row) to reveal internal organ morphology. Bar: 1mm

4.2.4.3 The petals of *mnt* flowers fail to reflex at anthesis and do not undergo a distinctive growth surge after anthesis

The failure of *mnt* petals to reflex and of flowers to open at anthesis is depicted in Figure 4.9 (arrow) where the transition from closed to open *MNT* flower is indicated by a white arrow.

In order to detect any abnormalities in petal size and development, the length of petals of four series of *mnt* and wild type flowers respectively was measured and is displayed in Figure 4.11. Petal expansion in wild type flowers displays a distinctive trend, which contains a growth surge after anthesis (Figure 4.11 [*]). Elongation of *mnt* petals was found to occur at a steadier rate and no significant increase in elongation rate could be identified after anthesis (Figure 4.11 [0]). *mnt* petals also show a greater variation in length.

4.2.4.4 The petal:sepal length ratio in *mnt* is lower than in wild type flowers

Although the petals of *mnt* flowers do eventually reach the same length as petals of open WT flowers, the flower buds of *mnt* plants fail to open and the petals and pistils remain

enclosed under the sepals. This observation lead to a more detailed analysis of sepal growth and the relationship between sepal and petal length.

The relationships between sepal and petal lengths in WT and *mnt* flowers respectively are shown in Figure 4.12 (displaying one example of a total of 4 data series for each genotype that display similar trends). While petals in *mnt* flowers were found to remain shorter than sepals throughout the all measured series, the petals of WT flowers were consistently found to outgrow the sepals shortly after anthesis. Therefore the petal:sepal length ratio of wild type flowers changes from <1 to >1 at the point of flower opening, while the length ratio of mutant flowers remains at <1.

This lack of floral opening affects the growth of internal organs in *mnt* flowers as exemplified by the magnified flower in Figure 4.9 (box), where the anther filaments are bent as a result of expansion within the space confined by the unopened sepals. In addition, the stigmatic papillae of this flower are crushed (white asterisk), which is a common occurrence in *mnt* flowers as well as the occurrence of bent gynoecia (not shown here).

4.2.4.5 *mnt* flowers are mostly sterile and there is a greater distance between the stigma and anthers than in wild type flowers

Hand-pollination experiments show that the stigma of an *mnt* plant is equally fertile as a wild type stigma; but without any intervention, the majority of *mnt* flowers fail to set seed. This can be seen in Figure 4.8, where elongating gynoecia and the formation of seed pods on the wild type inflorescence signify successful self-pollination, while no seed pods are developing on the *mnt* inflorescence.

The absence of seed set despite an otherwise healthy stigma suggests that the sterility of *mnt* flowers is caused by a mechanical factor that prevents pollen from reaching the stigma in order to achieve successful self-pollination. That mechanical factor was found to be an increased distance between the stigma and anther in *mnt* flowers:

Figure 4.10 shows the lengths of anther filaments (long anthers) and the length of corresponding gynoecia (from bottom of ovary to top of style) of the same flower which were measured in two series of *MNT/MNT* and *mnt/mnt* inflorescences respectively. The

greatest length difference between the gynoecium and anther filament among the fully fertile WT series is 0.22mm. The shortest length difference between the two organs among the sterile *mnt* series is 0.51mm. Interestingly, *mnt* fertility is rescued in flowers that are produced on secondary inflorescences of old plants (from 6 to 8 weeks). These flowers are often smaller than the first flowers on a young plant and although flower opening does not take place at anthesis, pollination does occur (data not shown).

4.2.5 The effect of the *mnt* mutation on leaf number and size

mnt plants flower about one week later than wild type plants grown under the same conditions as exemplified by the plants shown in Figure 4.14. The extent of delay in flowering time depends on light intensity and day length – flowering time differences are generally more pronounced under long-day conditions (data not shown). Delays in flowering time have been positively correlated with the number of rosette leaves produced (Koornneef *et al.*, 1998). In order to obtain statistically verifiable data to confirm the delay in flowering time observed in *mnt*, leaves were dissected from the rosettes *MNT* and an *mnt* plants as shown in Figure 4.15.

4.2.5.1 *mnt* plants produce more rosette leaves than *MNT* plants

Table 4.2 (set 1) shows the results of Gregory Blackman (University of Bath), who found that rosette leaves of *MNT* and *mnt* plants were produced at a comparable rate to an average of about 13.7 leaves per plant before bolting. However, once the plants have bolted, leaf numbers remain relatively constant in *MNT* plants while *mnt* mutant plants continue to produce new leaves (up to 20 per plant). These findings regarding differences in leaf numbers after bolting were later confirmed with a different set of flowering *MNT* and *mnt* plants (Table 4.2, set 2). Both 'post-bolt' data sets are normally distributed and the size distributions differ significantly (2-sample t-test, p=0.00).

Figure 4.14 The late flowering phenotype. Wild type *MNT* (left) and mutant *mnt* (right) plants grown under the same conditions for 6 weeks at 16h light.

Figure 4.15 Cotyledons and rosette leaves of five-week-old *MNT* and *mnt* plants, dissected and aligned in order of position on the stem. Inflorescence stem height: approx. 2.5 cm. Bar: 1cm

4.2.5.2 No single 'distinguishing leaf' to compare leaf expansion

In order to compare the leaf sizes of two different *A. thaliana* genotypes, Hu, Xie and Chua (2003) compare the size of the 5th rosette leaf to contrast lateral organ expansion in wild type and transgenic Col-0 plants. The correlation of 5th leaf size and overall leaf size were therefore tested in the wild type and *mnt* background.

Although some of the leaves produced by *mnt* plants appeared to be larger, no significant size difference (measured as leaf surface area) between the 5th leaves in *mnt* (average 163.82mm^2 ± 7.89) and *MNT* (average 157.74 mm^2 ± 8.0) could be detected.

Furthermore, no significant difference between *mnt* and *MNT* was found among the 7th, 8th and 10th leaves respectively (data not shown). Leaves 11 and above cannot be used for a 'single distinguishing leaf' comparison as many *MNT* plants do not produce more than 10 leaves.

Table 4.2 (set1&2): Rosette leaf numbers of *MNT* and *mnt* before and after flowering.

	Growth stage[4]	Leaf numbers (± S.E. mean)	
		***MNT* (N=18)**	***mnt* (N=18)**
set 1	3.20- 3.50 (pre-bolt 1)	11.11 (±0.179)	11.67 (±0.162)
	3.70- 3.90 (pre-bolt 2)	13.28 (±0.195)	14.17 (±0.232)
	5.10 - 6.00 (post-bolt)	13.94 (±0.262)	19.28 (±0.266)
set 2		***MNT* (N=13)**	***mnt* (N=14)**
	5.10 - 6.00 (post-bolt)	11.46 (±0.46)	15.07 (±0.40)

4.2.5.3 The rosettes of *mnt* plants produce larger leaves

The largest leaf out of 14 flowering *mnt* plants (approximate plant age: 5-6 weeks – same plants as those used in Table 4.2 [set 2]) has a surface area of 765mm^2. Out of 13 *MNT* plants at comparable stages, the largest leaf produced was found to have a surface area of 524mm^2.

[4] Principal Growth Stages according to Boyes *et al.*, 2001

On average, the largest leaves produced by the 14 *mnt* plants measure 592.8mm^2 (±32); the largest *MNT* leaves are about 26% smaller, measuring an average of 440.2mm^2.
The largest *mnt* leaf is generally found around position 12; the largest *MNT* leaf is generally the 10th leaf that the plant produces. There is a correlation between size of the largest leaf and inflorescence height in *mnt* (78.6%, p= 0.001) and in *MNT* plants (77.3%, p = 0.002).
Heterozygous plants exhibit a wild type-like flowering time and rosettes of heterozygous plants are indistinguishable from wild type rosettes (not shown).

4.2.6 The effect of the *mnt* mutation on the growth of the inflorescence stem

The *mnt* plant shown in Figure 4.16 exhibits the agravitropic stem phenotype that is characteristic for this genotype. The inflorescence stems of *mnt* mutant plants also appear thicker than those that are produced by wild type plants. Furthermore, secondary inflorescence growth is slightly inhibited in *mnt* mutant plants (data not shown).

Figure 4.16 *MNT* and *mnt* plants, flowering. The *mnt* plant is approximately 1 week older than the wild Wild Type plant grown under the same conditions.

4.2.6.1 Inflorescence stems of *mnt* plants are thicker than *MNT* stems

Transverse hand sections that were made of primary inflorescence stems of *mnt* and *MNT* plants between the 1st and 2nd node, were compared in order to estimate the difference in stem thickness (Figure 4.18). We found that there is a strong correlation between inflorescence height and stem diameter in both *mnt* (N=15, 86.4%, p= 0.000) and *MNT* (N=14, 76.1%, p = 0.002) plants. In order to compare stem thickness, between MNT and mnt primary inflorescences, size data from mature stems between 15 and 22cm in length was included in the parametric test as this range contained a similar sample number for both genotypes. Using 11 data points for each set, a significant difference (2-sample t-test, p=0.000) was found between the stem diameters in *MNT* and *mnt* plants.

Table 4.3 Cell numbers and area of different inflorescence stem tissues in mutant and wild type plants.

	Cell numbers				Area in μm^2		
	Xylem	**Cortex/ Epidermis**	**IF**	**Pith**	**Phloem bundle**	**IF cells**	**Pith cells**
WT	45	5-7	5	18	6361	395	2269
mnt	59.5	5-7	5.5	24	9164	284	2388
Significant?	yes	no	no	yes	yes	no	no

IF: Interfascicular fibre. p-values (not shown) were calculated using the Mann-Whitney test. Significance was measured at the p=0.05 level.

4.2.6.2 Cell numbers and tissue size differ in wt and *mnt* inflorescence stems

Figure 4.18 shows transverse sections of toluidine blue stained primary inflorescence stems. Stems of both genotypes were found to contain eight vascular bundles and despite an obvious difference in total surface area, the staining patterns of stem tissue showed no differences in stem composition of wild type and mutant plants. We therefore compared the surface area and cell numbers of stem tissue using transverse hand sections of wild type and mutant stems.

Size and cell number data regarding the different tissues of the inflorescence stem are shown in Table 4.3 and the data was collected as follows: Xylem cell counts were made

of the total number of cells per vascular bundle; cortex/epidermis cell numbers refer to the number of cell layers in the stem periphery; similarly, interfascicular fibre (IF) and pith cells were counted along a bisecting line. Phloem cell numbers or sizes could not be obtained using manual sections; the total surface area of the phloem bundle was recorded instead. Cell sizes of IF and pith cells present an average of all cell sizes of each tissue recorded along a bisecting line.

The following is a summary of the results that can be derived from the data shown in Table 4.3: More cells were found in the xylem and pith of *mnt* mutant stems, however the number of cell layers in the cortex and IF is similar in the two genotypes. The surface area of the phloem (similar to total stem surface area) is larger but no statistically significant difference in cell sizes of IF and pith cells was observed.

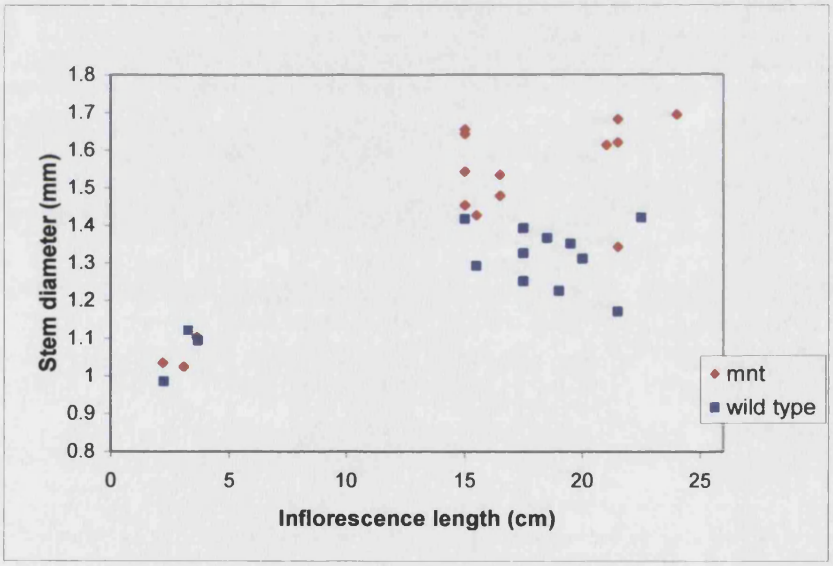

Figure 4.17 Inflorescence stem thickness in *mnt* and wild type. Stem diameter plotted against total stem length of the primary inflorescence of *mnt* (red) and wild type (blue) plants grown under the same conditions.

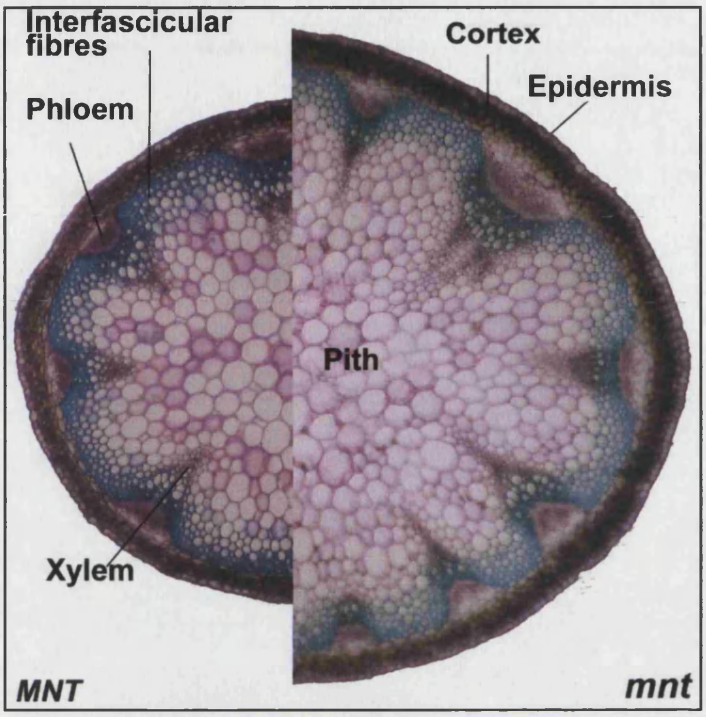

Figure 4.18 Stem sections of *MNT* and *mnt* inflorescence stems. The stems were sectioned by hand, stained with toluidine blue and photographed at the same scale (work undertaken by Gregory Blackman). Cell/tissue types are annotated. Note: a vascular bundle is the area containing xylem and phloem tissue.

4.2.7 Seedlings and seedling root phenotypes of the *mnt* mutant

4.2.7.1 Seedling size and vigor is increased in *mnt* mutant seed

Previous work on *mnt* had shown that mature seed produced by *mnt* plants contains larger embryos (see Introduction). These large embryos were found to become larger and more vigorous seedlings – a size difference which is most obvious shortly after germination (Figure 4.19).

Seedling vigor has not been tested directly however an evaluation of seedling survival under adverse conditions could be made when growing *mnt* and wild type seed on plant medium containing kanamycin for seed selection. After transformation via the floral dip method (see Materials and Methods), the majority of seed does not contain an insert with

the antibiotic resistance. Susceptibility to the antibiotic causes lack of root growth and chlorosis. Susceptible *mnt/mnt* seedlings were observed to grow for about 1 week longer on selective media than susceptible wild type seedlings (data not shown).

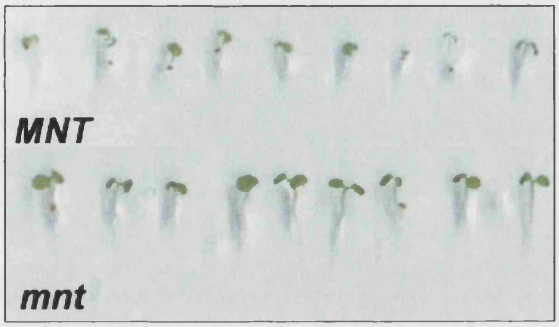

Figure 4.19 4 day old wild type (top row) and *mnt* seedlings (bottom row) grown vertically on phytoagar. Seedlings of both genotypes were photographed at the same magnification.

4.2.7.2 The response to gravistimulation is slightly enhanced in *mnt* seedlings

In order to determine if root development is compromised in *mnt* mutant seedlings, three experiments were undertaken:

1) Seedling growth on plant media containing various amounts of IAA during 13 days of growth (Gregory Blackman).
2) Seedling growth on vertical plates of plain media during 11 days of growth (Melissa Spielman).
3) Seedling growth on vertical plates turned 90° after a period of growth in the dark.

In summary of points 1 and 2, no significant differences in growth pattern were observed between *MNT* and *mnt*. The third experiment was designed to detect subtle differences in growth patterns and some discrepancies were detected.

Two sets of Petri dishes (SET 1 and SET 2) containing *MNT* and *mnt* seedlings (which had been germinated for 24 hours in light) were placed in the dark. After a 48 hour growth

period a photograph was taken from all plates of both sets. The plates were then returned to the dark but those belonging to SET 2 were placed at a 90° angle from their previous orientation. After a further growth period of 24 hours in the dark, all plates were removed and photographed.

The extent of root growth during the last 24 hours of growth in the dark was estimated using the two photos taken from the control plates (SET 1) shown in Figure 4.20. Within 24 hours, the roots of *MNT* seedlings (N=11) had grown by an average of 1.97mm (± 0.13); root length of *mnt* seedlings (N=12) had increased by an average of 2.93mm (± 0.2).

The angle of the root tips belonging to SET 2 (gravistimulated), was measured in order to compare the efficiency of both genotypes to re-adjust the angle of root growth. Roots of both genotypes exhibited a clear change in growth direction towards a 90° angle with respect to their previous growth direction. Figure 4.21 (C) illustrates to which extent the root tips of each genotype had been re-orientated towards a 90° angle after 24 hours of growth. A 2-sample t-test ($p=0.02$) confirms that the level of growth adjustment differs significantly between the two genotypes: After 24h of re-orientation, the roots of wild type seedlings were oriented to about 70.9 degrees (±3.8). The roots of mutant seedlings had re-oriented their growth direction to an average of 83.4 degrees (±3.8).

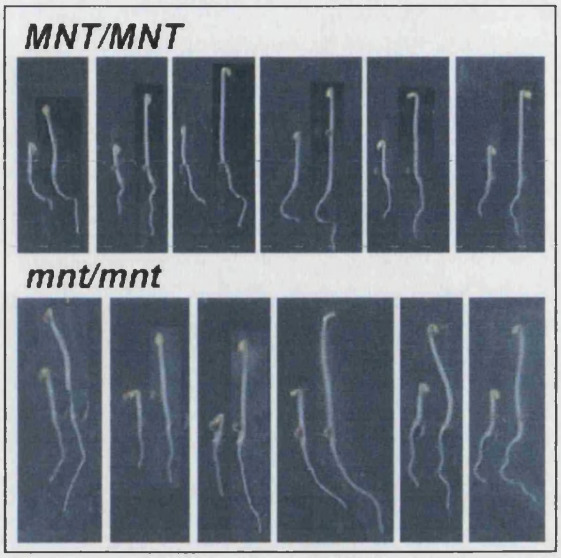

Figure 4.20 Comparison of seedling elongation after 2 and 3 days of growth on vertical plates in the dark. These seedlings belong to SET 1 (non-gravistimulated). Each picture contains two superimposed images of the same seedling taken, respectively, after a growth period of 48 hours (left) and of 72 hours (right).

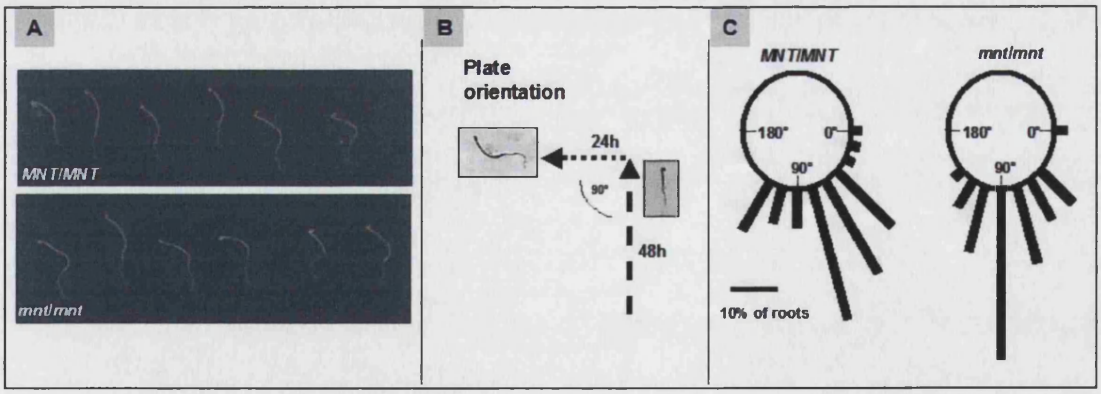

Figure 4.21 Re-orientation of *MNT* and *mnt* seedling roots (SET 2) 24 hours after gravistimulation by turning the plate by 90 degrees. A: Images of plates containing gravistimulated wild type and mutant seedlings. B: Diagram showing orientation of plates to induce gravistimulation for 24 hours after 48 hours of vertical growth. C: Schematic representation of root orientation (modified from Marchant *et al.*, 1999). Each root (N_{MNT}=48, N_{mnt}=41) was assigned to one of ten 15° sectors. The percentage of seedlings showing direction of root growth within each sector is represented by the length of the bar.

4.2.8 mnt, ethylene and gibberellin

4.2.8.1 *mnt* and the ethylene response mutant *ctr1-1*

The recessive *ctr1* (*constitutive triple response1*) mutant constitutively expresses ethylene-regulated genes, the adult *ctr1* plant is dwarfed and flowers early (Kieber *et al*, 1993).

The flowers of *ctr1-1* mutant plants resemble those of the *mnt* mutant grown under the same conditions (Figure 4.22). Young *ctr1-1* mutant flowers are sterile but, as with *mnt*, normal seed set was achieved through manual pollination (data not shown). Dissection of unopened *ctr1-1* floral buds revealed strong morphological similarities with buds dissected from an *mnt* inflorescence.

Figure 4.22 Inflorescences of *mnt* and *ctr1-1* (left) and flowers of a ctr1-1 inflorescence aligned and dissected (right). Inflorescences photographed at the same magnification. bar: 1mm

4.2.8.2 *mnt* treated with gibberellic acid

Research on gibberellin-deficient mutants has shown that the flowers produced by the *ga1-1* plant are completely sterile, do not self pollinate and do not produce seed when pollinated manually. Furthermore, the petals and stamens of *ga1-1* plants fail to develop fully, the sepals are very short and flowers do not open at anthesis. This phenotype can be rescued through exoneous application of GA_3. (Goto and Pharis, 1999)

Results shown in section 4.2.4.3 indicate that the flowers of *mnt* mutants do not open at anthesis due to a lack of petal expansion and the abnormal petal: sepal length ratio (Figure 4.9, Figure 4.12).

Repeated GA_3 treatment of *mnt* inflorescences was found to cause petals to elongate and lead to flower opening, although the petals of these rescued flowers do not reflex as markedly as in wild type flowers (Figure 4.23). A complete rescue of the *mnt* floral phenotype can not be obtained using exogenous gibberrellic acid treatment as it does not restore fertility.

Figure 4.23 *mnt* mutant inflorescences which have been mock-treated (left) and treated with GA_3 (right). Both inflorescences were found on plants grown under the same conditions.

4.3 Discussion:

Certain aspects of the *arf2* mutant phenotype based on the analysis of other EMS and T-DNA insertion alleles have recently been described independently by Li *et al.* (2004) and Okushima *et al.,* (2005b); their findings will be integrated here and in the following chapters in light of our results. Unless otherwise stated *mnt* refers to the homozygous EMS induced allele described in Chapter 3.

4.3.1 *mnt* causes organ specific hyperplasia which is due to extra cell divisions in certain tissues

The *mnt*-induced effect on plant development is pleiotropic and organ specific: Leaves, stems and seeds are abnormally large compared to those of wild type plants and the irregular flower morphology of the homozygous *mnt* mutant is due to size discrepancies which cause abnormal proportions of floral components.
This specificity of growth irregularities exhibited by the *mnt* mutant plant can be detected at different growth stages (temporal specificity) and within different tissues of the same organ (tissular specificity):

Temporal specificity of growth irregularities caused by *mnt* can be observed when comparing flowers and inflorescences. While young wild type and *mnt* flowers are indistinguishable until stage 12 (Floral stages according to Smyth *et al.*, 1990), older *mnt* flowers differ significantly in size and proportion from old wild type flowers. On a smaller scale, ovule development appears wild-type like until late stage 3.
This implies that differences in size or initial growth rates are not present from the onset but occur only at certain developmental stages. It also implies that primordial tissue development is not affected by the *mnt* mutation.

Tissue specific effects of the *mnt* mutation on plant development can be observed when looking at sections that reveal the cellular composition of different plant organs. Longitudinal sections of mature wild type and mutant ovules are shown in Figure 4.24. When comparing numbers and sizes of cells contained within the abaxial (long) integuments of wild type and mutant ovules, it was concluded that the overall size differences of mature ovules are mainly due to differences in cell numbers rather than

differences in cell sizes. Cell sizes and numbers were measured in three layers of the abaxial integuments (oi2, ii1, and ii1' described in the introduction, Beeckman) which are longer in the mutant. Integument length differences were found to arise from additional cell numbers (not size) in all layers except the abaxial micropylar oi2 (red arrow), which contains fewer and longer cells in mnt. No abnormal cell numbers were found in other parts of the ovule including the funiculus. Differences in cell numbers and similarities in cell sizes were also observed when comparing the inflorescence stems of mutant and wild type plants. The latter findings indicate that an overall increase in cell numbers can be found while the cell layer numbers and cell sizes remain unaffected by the mutation. Importantly, despite obvious differences in overall size, the tissue composition of ovules and stems are not altered due to the *mnt* mutation.

Okushima *et al.*, (2005b) reported similar findings regarding the thickness of *arf2* stems. The authors also noticed an intermediate stem phenotype in heterozygous *arf2* plants (see below for details).

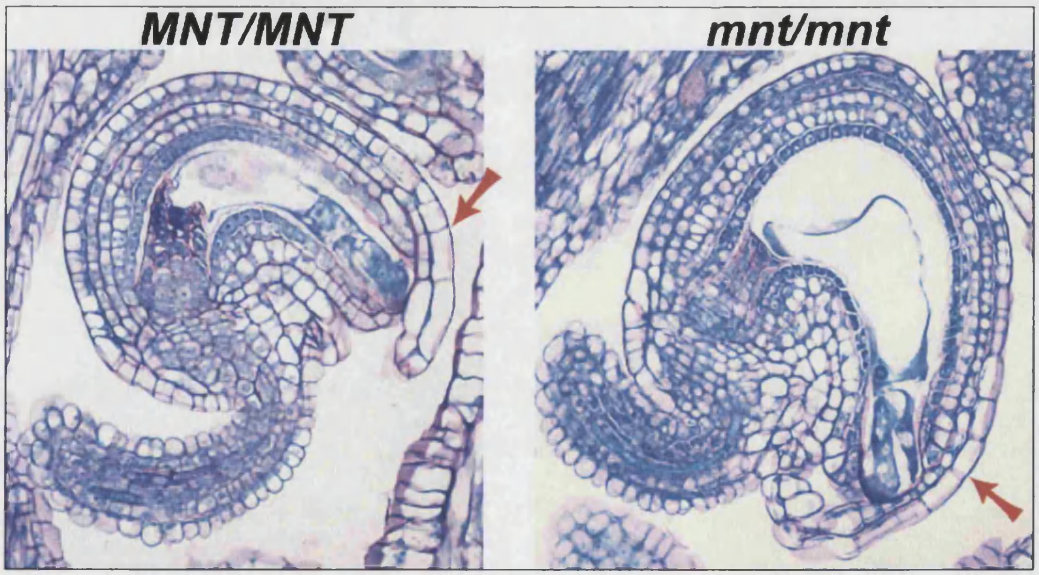

Figure 4.24 Longitudinal sections of mature wild type (left) and mutant (right) ovules at the same magnification. Red arrow = abaxial micropylar oi2. (Resin-embedded sections, images and quantitative data by Melissa Spielman)

Leaf epidermal peels performed by Melissa Spielman indicate that the external leaf cells are slightly larger in the mutant (shown in Figure 4.25). Whether this increase in epidermal cell size is a direct or indirect effect of the *mnt* mutation is unclear. However, it does indicate that the influence of the mutation is tissue specific and that some tissues produce more cells while the cells of other tissues become larger in compensation such as the abaxial micropylar oi2 in the ovule. Additional evidence for abnormal leaf cell numbers in the sub-epidermal layers comes from observations by Li *et al.* (2004) and Ellis *et al.* (personal communication), who observed that *arf2* leaves are dark green compared to the slightly paler wild type leaves. This could suggest an increased number of chlorophyll-containing organelles due to an increased number of sub-epidermal leaf cells such as the palisade cells.

As mentioned previously, the link between auxin signalling and cell cycle regulation can be detected on many levels of the auxin signalling cascade. Interestingly, the auxin signalling pathway and the cell cycle control show some parallels in their regulatory mechanisms such as the involvement of ubiquitin-dependent protein degradation (Jager *et al.*, 2005).
abp1 mutants show aberrant cell division defects, and tobacco tissue culture cells lacking ABP1 divide slowly and form small cells (Chen *et al.*, 2001). Furthermore, genes involved in the ubiquitin-proteasome pathway such as *AXR1,* have been implicated in auxin-regulated G1-to-S phase cell cycle transition (del Pozo *et al.*, 2002). Auxin is known to induce the expression of various mitotic cyclins and cyclin-dependent kinase inhibitors such as *KRP*s (Vanneste *et al.* 2005). The G2-to-M phase transition involves the presence of auxin-regulated genes such as *PRZ1* (Sieberer *et al.*, 2003) or *HBT* (Willemsen *et al.*, 1998; Blilou *et al.*, 2002) and M-phase-specific transcript accumulation of *ARF1* and *Aux/IAA* gene family members has been detected in synchronised tobacco cell suspensions (Breyne *et al.*, 2002), thus linking *ARF* and *Aux/IAA* functions with cell cycle activity. Conversely, the promoters of cell cycle genes such as *CYCD3;1* and *KRP2* – both of which are involved in G1-to-S phase transition – were found to contain several auxin responsive *cis* –acting elements (Richard *et al.*, 2002).

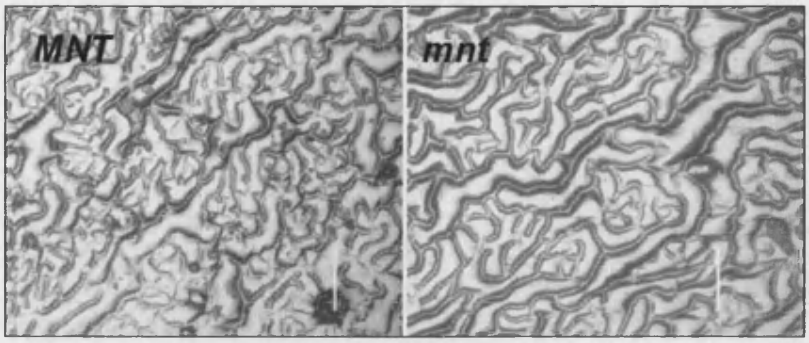

Figure 4.25 Leaf epidermis cells visualised using a nail varnish peel of the largest leaf on a wild type (left) and mutant (right) rosette (Peels and images by Melissa Spielman).

Our findings regarding the phenotype of *mnt* indicate that the pleiotropic effects on mutant morphology are based on defects in auxin-regulated cell cycle control. Based on *mnt/arf2* mutant analysis we can conclude that functional MNT/ARF2 protein acts negatively on cell proliferation and it does so in a tissue specific manner. Our findings indicate that MNT/ARF2 acts during the processes of organ enlargement rather than at organ initiation and that it does so by regulating cell proliferation rather than cell identity.

4.3.2 Sterile flowers complicate the comparison of *arf2* and wild type yield

The inability of *mnt* flowers to self-pollinate appears to arise from discrepancies in floral organ lengths that were identified when comparing the lengths of wild type and mutant sepals/petals and carpels/anthers respectively. In the wild type plant, the onset of flower opening is marked by a rapid increase in petal length, leading to a situation where the petal length exceeds that of the sepal. This appears to cause the covering sepals to be forced apart. In the fully opened flower, petals have not only outgrown the sepals by several millimetres, they have also curved outwards (or reflexed). In the mutant flower, neither the outgrowing of sepals by the petals nor the outward curvature of petals can be observed. As sepal length continues to exceed petal length, it looks as if the petals are not able to generate enough force to push the covering sepals apart. Whether the lack of petal reflexation results from the fact that they remain locked under the sepals or whether it is due to a result of a lack of growth surge is unclear.

Figure 4.9 illustrates most clearly why a length discrepancy between the gynoecium and the anther filament appears to lead to a complete failure of self-pollination. Successful pollination occurs when pollen is deposited onto the stigma that is positioned above the style. While the anther of wild type flowers is level with the stigma in the open wild type flower, dissection of *mnt* flowers with dehisced anthers show that pollen shed occurs on the ovary wall. Interestingly, anther filament and gynoecium length comparisons indicate that the difference in total length discrepancy can be less than half a millimetre (Figure 4.10). However, an increased length discrepancy that was not quantified in these measurements may occur from the bent shape of anther filaments (Figure 4.9 inset), which may significantly lower the position of the anther with respect to the stigma.
The lack of unassisted seed set in *arf2* mutant plants leads to a number of difficulties when attempting to compare seed yield in mutant and wild type plants. Due to the high number of flowers that are produced by an *A. thaliana* plant, the manual pollination of each flower on an *arf2* plant was not deemed realistically feasible for the purpose of this study. Therefore it was decided to minimise possible variation caused by additional (unassisted) seed set on wild type plants by pruning the plants. However, the pruning of both wild type and mutant plants had other unexpected consequences on seed yield as discussed below.

4.3.3 Does *arf2* increase the seed weight capacities of *A. thaliana*?

Seed weights appear to be most constant in species with indeterminate terminal meristems that are not exhausted during flowering (Harper *et al.*, 1970). *A. thaliana* is one example of those species. However, when *A. thaliana* seed set was restricted by hand-pollination experiments, a significant increase in seed weight was observed by Meyer *et al.* (2004 and personal communication) and was observed by us when limiting seed set to a few pods per plant and removing all secondary inflorescences ("primary only"). Limiting seed set by removing the primary inflorescence meristem and all other inflorescences was done in order to control for variations in resource allocation caused by the lack of seed production in non-manually pollinated *mnt* plants. However, the removal of these tissues creates an unnatural growth condition that does not necessarily reflect the

true variation caused by the *mnt* allele on seed size. Furthermore, auxin is synthesised throughout the plant, predominantly in leaf areas exhibiting high rates of cell division (Ljung *et al.*, 2001). Removing all secondary inflorescences may significantly decrease auxin levels in "primary only" plants due to the lack of proliferating tissue such as that of shoot apical meristems and young cauline leaves. This removal of sites of auxin synthesis could have a different impact on wild type plants, where auxin signalling is not disrupted than it has on *mnt* plants. The difference in auxin disruption caused by pruning could thus be displayed by the differences in impact on *mnt* and wild type seed weight.

On the other hand, limiting the possibilities for seed set and seed maturation to a few seeds per plant may reveal another theoretical feature of seed size determination that is revealed by the *mnt* mutation:

Seed size appears to be relatively constant on wild type plants under normal growth conditions. This might be because – given the indeterminate growth pattern of *A. thaliana* inflorescences – potentially an indefinite number of seeds could be produced by each mother plant. The mother plant might therefore produce as much seed as possible and the size of this seed is determined by an ecological optimum and the amount of resources that can be invested into each seed for an indeterminate amount of time. *mnt* seed size might not present the ecological optimum, it could instead present the potential maximum of seed size that the mother plant can produce and invest into. The seed of *mnt* plants can 'demand' this maximal investment because of its physiology: An expanded seed coat (caused by large integuments) could create room for more endosperm tissue and subsequently a larger embryo. When seed set is limited due to the removal of additional inflorescences, seed production is no longer indefinite. Therefore the mother plant might be making a hypothetical switch from an indeterminate investment mode into a maximum investment mode that causes an increased flow of resources into the few developing seeds that remain after pruning. This new investment strategy stretches wild type seed capacity for enlargement to the maximum. Seed produced by a heterozygous mother plant has been bestowed with some extra capacity for enlargement, which is conferred by the *mnt* allele. Therefore, the seed weight of these plants increases to an *mnt*-like weight. Seed produced by an *mnt/mnt* mother plant on the other hand already represents the maximal

investment capacity of the mother plant; therefore the weight of *mnt* seed does not increase significantly upon removal of secondary inflorescences.

The increase in seed weight which is observed upon removal of secondary inflorescences could therefore be explained by two theories: Firstly, the removal of inflorescences removes the sites of auxin synthesis and thereby disrupts normal auxin signalling in wild type plants causing these plants to produce abnormal seed growth. Secondly, *mnt* seeds have an increased size capacity that leads to an increase of investment. This increase in investment can also be caused by mimicking determinate growth.

4.3.4 *MNT/ARF2* plays a role in maintaining stem and root gravitropism

The agravitropic stem phenotype of adult *arf2* plants was also observed by Li *et al.* (2004). This study analysed the *hss1/arf2* (*hss* = *hooklesss suppressor*) mutation in *A. thaliana* seedlings due to its involvement in hypocotyl bending during apical hook formation in light of the *hls1* (*hookless1*) mutation. The mutation of the ethylene-regulated gene *HLS1* leads to an inability to maintain an apical hook. *hss1/arf2* was identified in a mutant screen as the wild type apical hook phenotype is partially restored by the *hss1/arf2* allele in the double mutant background. The ability of the *hss1/arf2* allele to restore apical hook formation in the *hls* background has been attributed to the involvement of *HSS/ARF2* in differential cell elongation. *ARF2/HSS1* was therefore described as a negative regulator of differential growth, which is most apparent in the adult plant (no visible defects in apical hook formation were detected in *arf2/hss1* single mutants) (Li *et al.*, 2004).

We observed that *mnt* roots have a slightly enhanced root gravitropic response. Root gravitropism is influenced by a combination of cell division at the root apical meristem and differential cell expansion at the flanks of elongation zones (Chen *et al.*, 2002). Whether the abnormal stem curvature and the enhanced root gravitropism observed in the *mnt* mutant are due to defects in cell numbers or cell elongation is still unknown. However, both findings regarding stem and root orientation are in agreement with the observation that *ARF2* has a negative effect on differential growth (Li *et al.*, 2004) which is alleviated in the *arf2* mutant.

4.3.5 The genetics of seed and flower morphology conflict in heterozygous plants

According to the floral phenotypes of *MNT/mnt*, and *mnt/MNT* heterozygous plants, the mutant allele appears to play a recessive role in plant development. Similarities between heterozygous and wild type flowers were not investigated in much detail; however, the flowers open, petals reflex and the plants are fully fertile, thereby implying that the phenotype is rescued by a single wild type allele. Furthermore, heterozygous plants do not exhibit the late flowering phenotype.

These findings, which imply a recessive role of the mnt allele, are contradicted by the genetics of seed size. Seed produced by a heterozygous plant (within a wild type-like flower) is significantly heavier than seed of a wild type plant, a discrepancy which is intensified by restricting of seed set to a limited number of seed pods on the primary inflorescence.

Findings reported in a recent paper by Okushima *et al.* (2005b) are in agreement with the partially semi-dominant phenotype observed in the heterozygous plant, confirming that *mnt* (*arf2* T-DNA insertion) alleles are recessive with respect to the floral phenotype, while a semi-dominant effect can be observed regarding length and thickness of the inflorescence stem.

These findings indicate that the effect of *arf2/mnt* on plant development is organ specific in a quantity-dependent manner. In the case of the heterozygous plant, the organ specific influence of the *mnt* allele appears to be weakened by the presence of a functional *MNT* allele. This wild type allele masks the semidominant effect in some situations (flowering time, floral organ development) and not in others (integument development, inflorescence stem development).

4.3.6 *ARF2* and the complex interactions of phytohormones on plant development

Interactions between phytohormones have long been known to play an important role in plant development and growth responses. Studies that examine the interactions between auxin and other plant hormones are exemplified by tobacco callus experiments by Miller and Skoog (1957) which showed that *in vitro* shoot and root differentiation is determined

by the auxin-cytokinin content of the growth medium. Auxin has been shown to increase gibberellic acid production in pea (Ross *et al.*, 2000) and barley (Wolbang *et al.*, 2004) and it has been shown to act together with brassinosteroids to promote root gravitropic curvature in maize (Kim *et al.*, 2000). Jasmonate interacts indirectly with auxin by inhibiting IAA-induced cell elongation (Saniewski *et al.*, 2002). Furthermore, jasmonates and auxin are linked via SCF-mediated ubiquitin ligase (Xu *et al.*, 2002).
Plant cell cycle regulation is known to depend on the integration of numerous independent hormone signals at different levels of the signalling network (del Pozo *et al.*, 2005). Furthermore, regulatory elements that confer inducibility by a number of plant hormones including GA, ethylene and ABA have been found in addition to auxin responsive elements in the promoters of cell cycle genes (Richard *et al.*, 2002).
Pathways by which different hormones act on plant development therefore appear to merge at certain points to control the expression of genes involved in plant growth responses and development.
Ethylene (C_2H_4) is involved in the regulation of a variety of developmental and stress responses which include cell elongation, cell fate, fruit ripening, leaf abscission and flower senescence (Alonso *et al.*, 1999). Interactions between auxin and ethylene have been highlighted by the seedling phenotypes of two *arf* mutants, namely *nph4/arf7* (Harper *et al.*, 2000) and *hss/arf2* (Li *et al.*, 2004). Ethylene treatment of *nph4/arf2* mutants has been shown to suppress the hookless phenotype of mutant seedlings (Harper *et al.*, 2000) while *HSS/ARF2* protein accumulation was found to be negatively regulated by ethylene in a *HLS*-dependent manner (Li *et al.*, 2004).

[C2H4 –> HLS1 –(proteasome-dependent prot. degradation) –I HSS1/ARF2 –I differential cell elongation in apical hookl]

The *ctr1* (*constitutive triple response1*) mutant had been isolated in a screen for mutations that cause constitutive activation of ethylene responses. Mature *ctr1* plants mimic the phenotype of ethylene-treated plants: they are dwarfed, flower late, are partially infertile, and show stunted root growth. Rosette leaves of *ctr1* mutants have also been found to contain smaller epidermal cells. (Kieber *et al.*, 1993) Furthermore, the gynoecium had been shown to protrude through unopened flowers (Kieber *et al.*, 1993; Alonso *et al.*, 1999).

Despite an overall difference in plant morphology, especially regarding rosette and seed sizes, the similarity between *mnt* and *ctr1-1* mutant flower morphology is striking (Figure 4.22). Ethylene treatment reduces ARF2 protein levels (Li *et al.*, 2004) but a reduction in ARF2 protein due to the *arf2* mutation causes an identical phenocopy of ethylene-treated wild type morphology. A reduction in ARF2 levels therefore appears to cause some ethylene-related phenotypes such as abnormal floral organ size ratios and late flowering but it has opposite effects regarding most other aspects of plant development including the large cell size of leaf epidermal cells and even delayed organ senescence (Okushima *et al.*, 2005b). This implies that the pathways of auxin and ethylene signalling share the control over some aspects of plant growth, while other aspects correspond entirely to the influence of each individual hormone. On the other hand, additional defects that are caused by the arf2 mutation might mask the effects caused by abnormal ethylene signalling or vice versa.

4.3.7 Unique features of the *arf2* mutation

The *mnt/arf2* mutant shows us that an observable increase in seed weight and size is linked with increased cell numbers in the seed periphery. We have found that this increase is due to an enhanced cell proliferation during the late stages of ovule development.

The economically appealing seed size morphology exhibited by the *mnt* mutant is coupled with a number of other morphological abnormalities involving many parts of plant development. These abnormalities appear to be caused by tissue-specific increases in cell numbers that affect organ sizes but not tissue identity as observed in *arf3* and *arf5* mutants. Unlike *arf7* and *arf8* mutants that are also defective in differential growth patterns and other auxin-related phenotypes such as tropic responses and apical dominance, *mnt/arf2* has been shown to cause a localised increase in cell division, which is unique to this *AUXIN RESPONSE FACTOR* mutant.

4.3.8 Further work

In order to quantify the effect of a homozygous and heterozygous *mnt* allele on plant development, a more structured and comprehensive analysis of organ size abnormalities is necessary. This may reveal a pattern as to which types of organs are most affected depending on their composition. On a more refined scale, the current observations regarding stem and ovule cell composition should be extended to other organs in order to establish whether certain tissue types are generally more affected than others.

The work presented here is based on the comparison of developmental snapshots which have been scored by using developmental stages such as those of embryonic development, inflorescence stem length, stages of ovule development, the colour of anthers or the dehiscence of stigmatic papillae. Although this has been sufficient to understand how final growth patterns are established in the mutant compared to the wild type, it does not take into account how long it has taken to reach each developmental stage. in addition to an accurate estimation of flowering time differences, time courses of root, shoot, floral and seed development would bolster our understanding of how mutant morphology is achieved.

5 Gene expression studies of *MNT/ARF2*

5.1 Introduction

Past gene expression studies of a number of *ARF* genes including *ARF2* have improved our understanding of *ARF* gene family function by elucidating where the genes are expressed, how this expression may be regulated and how their expression can influence development, directly or indirectly, by affecting the expression of other genes. Studies that focused on the quantification or manipulation of gene expression have been used to answer a number of specific and general questions about the involvement of *ARF* family members in plant development mechanisms. The following section contains a short review of work involving gene expression of members of the ARF family. These studies acted as guidelines for our characterisation of *ARF2* gene expression in a similar fashion as previous phenotypic studies of *arf* mutants guided our work involving the phenotypic analysis of *arf2/mnt.*

5.1.1 Expression studies of *ARF* genes

5.1.1.1 Where are ARFs expressed?

ARF gene expression patterns are usually studied in light of known phenotypes and the link between expression pattern and gene function is often made during expression studies. The expression of *ARF* gene family members can be detected throughout the *A. thaliana* plant. In a whole-organ analysis of general *ARF* mRNA expression, a northern blot analysis of ten *ARFs* (*ARF1-10*) revealed transcript of all genes in mature leaves and flowers. Expression levels were uniformly high in all plant organs with the exception of *ARF5*, which showed lowered expression in the leaves. Transcript levels in siliques were tested for *ARF2,4,6* as well as *ARF8*, and found to be relatively low except for *ARF2* mRNA which is highly abundant in all tissues (Ulmasov *et al.*, 1999). We therefore expected to find high levels of *MNT/ARF2* transcript in all plant tissues that we would choose to examine.

Another general analysis of *ARF* gene expression was performed by Okushima *et al.* (2005b). This study combined expression studies of all *ARF* gene family members (including *ARF1-10*) with the phenotypic analysis of associated T-DNA insertion mutants. Again, *ARF* genes were found to be expressed in seedlings, roots, leaves flowers and stems as previously described for *ARF21-10* (Ulmasov *et al.*, 1999). Interestingly, *ARFs 12-15* and *20-22*, which happen to be clustered on the upper arm of Chromosome I, were undetectable through RNA hybridisation analysis, while RT-PCR analysis was able to detect weak expression of these genes in the seed during embryogenesis (Okushima *et al.*, 2005b). So far, this is the only published study identifying expression patterns of an *ARF* gene that are exclusive to the seed. More detailed transcript expression studies of members of the *ARF* family were carried out on individual genes in conjunction with detailed mutant analysis such as those of *arf3, arf5* and *arf2*.

ettin/arf3 mutants show defects in floral organ shape and numbers. It was therefore concluded that *ETT/ARF3* plays a role in both the initiation and the maturation of floral organs and expression should be found in young floral organs (Sessions and Zambryski, 1995). An *in situ* hybridisation assay confirmed that *ETT/ARF3* transcript is expressed throughout young floral meristems, within petal, stamen and carpel primordial tissue and procambial tissue of maturing flowers (Sessions *et al.*, 1997).

Polar auxin transport is impaired in *monopteros/arf5* mutants with serious effects on embryonic development (Berleth and Jürgens, 1993). This observation lead to the suggestion that the ARF5/MP protein plays a role in regulating genes that are responsible for the correct development of vascular tissue and that transcript should be located to these sites. As expected, *in situ* analysis of MP/ARF5 protein showed high levels of expression in the centre of young organs and the provascular tissue of mature organs (Hardtke and Berleth, 1998).

A detailed analysis of *ARF2* expression in seedlings with respect to the *HOOKLESS* mutation was undertaken by Li *et al.* (2004) who examined the role of *HSS1/ARF2* in apical hook formation. In this study, *hss1* was identified in a screen for mutations that suppress the *hookless1* (*hls1*) phenotype in *A. thaliana* seedlings. It was therefore expected that localised *HSS1/ARF2* expression would be found in the regions of the seedling that are involved in apical hook development and maintenance. Presence of

HSS1/ARF2 mRNA was indeed detected in the apical hook region, as well as the cotyledon and leaf primordia of etiolated and de-etiolated seedlings.

The introduction of reporter constructs for the study of gene expression has two advantages: Firstly that low expression levels can be amplified and therefore easily detected by the reporter signals; and secondly that visualisation is straightforward and does not require much pre-treatment of the plant tissue of interest. The following expression studies of *ARF7,8, 12* and *22* as well as *ARF2* employed promoter::GUS fusions to visualise gene expression in various *A. thaliana* tissues.
ARF7 has been implicated in the regulation of differential growth in response to auxin signalling through light stimulation (Liscum and Briggs, 1995; 1996). A *pARF7::GUS* fusion experiment revealed strong expression of *ARF7* throughout the hypocotyl but expression was also detected in the vascular tissue of the mature primary root, indicating that the role of ARF7 is extended to other organs (Okushima *et al.*, 2005a). Interestingly, the same study by Okushima *et al.* (2005a) revealed that *arf7arf19* double mutants are impaired in lateral root formation and show abnormal gravitropism in hypocotyls and roots.
The *arf8* mutant phenotype can be characterised as a weak phenotype showing slightly elongated hypocotyls, enhanced apical dominance pronounced lateral root growth (Okushima *et al.*, 2005a), leading to the assumption that *ARF8* expression should be found near the root and shoot meristems. Accordingly, *pARF8::GUS* expression analysis has revealed constitutive expression in shoot and root apexes, and light-induced expression in hypocotyls (Tian *et al.*, 2004; Okushima *et al.*, 2005a) .
In accordance with the seed-only expression pattern detected by RT-PCR, *pARF12::GUS* and *pARF22::GUS* expression analysis revealed GUS signal in developing seeds including embryos and seed coat (Okushima *et al.*, 2005a).

5.1.1.2 Studies of potential ARF targets

ARF proteins have been shown to bind *in vitro* to auxin-responsive elements (AuxREs) in the promoters of early auxin-regulated genes; a property which also lead to the

discovery of the ARF protein by Ulmasov *et al.* (1997a). In order to study the effect of individual ARF genes on potential targets, a number of reporter constructs such as *DR5* have been developed to monitor the expression of auxin responsive genes. *DR5* is a synthetic Auxin Response Element (AuxRE), consisting of 7 tandem repeats of an auxin-responsive TGTCTC element that was introduced into a *DR5::GUS* reporter construct driven by a minimal 35S promoter (Ulmasov *et al.*, 1997b). The construct has been used to test the effect of Aux/IAA proteins as well as ARF proteins on AuxRE-dependent transcription. Using effector-reporter co-transfection assays it was found that Aux/IAA proteins act by repressing transcription (Tiwari *et al.*, 2001) while ARFs can have either repressive or activating functions (Tiwari *et al.*, 2003). ARF1-4 and ARF9 were found to limit auxin-stimulated expression of *DR5::GUS*; base-level expression was constantly low and appeared unaffected by the introduction of the effector and reporter constructs. ARF5-8 on the other hand showed a clear enhancement of auxin-stimulated *DR5* expression as well as increased base-level expression of these genes in carrot and *A. thaliana* protoplast suspension cultures (Tiwari *et al.*, 2003).

The *DR5::GUS* reporter construct was also used for the *in situ* analysis of auxin responses in mutant backgrounds including a study of auxin responsive expression in polar auxin transport mutants and *mp/arf5* mutants (Sabatini *et al.*, 1999). When compared to *DR5* reporter expression in wild type plants, expression levels of *DR5* in *mp/arf5* mutant plants were found to be abnormally low in *mp* root primordia.

Auxin signalling rapidly induces the transcription of three gene families: *SAUR*, *GH3* and *Aux/IAA*. Members of these families have been shown to be able to bind directly to ARFs via domains III and IV (Ulmasov *et al,* 1999b). Two studies were performed in order to test the effect of *arf* mutations on base-level and IAA-induced transcription levels of these early auxin response genes. Using an RNA blot assay, Stowe-Evans *et al.* (1998) evaluated transcript levels of *SAUR*, *GH3* and 6 *IAA* genes in seedlings of wild type and *arf7/nph4* mutant backgrounds. According to this assay, the *arf7* mutation negatively affects expression of all early auxin-induced genes tested. These findings were confirmed in a microarray analysis performed by Okushima *et al.* (2005a) which expanded on the effects of *arf7* and *arf19* and double mutants on the expression of various genes that are auxin-related (*ARF4*, *IAA5 GH3*), other phytohormone-related (*ETR2*), cell wall-related,

metabolism-related and development-related (*ARGOS*). The expression of all of these genes was shown to be either up-regulated or down-regulated in response to exogenous auxin stimulation. Again, it was found that the *arf7* mutation impacts negatively on the transcript level in response to auxin stimulation as does the *arf19* mutation although the expression profiles are slightly different in the two mutant backgrounds. The authors also point out that seedlings of the *arf7arf19* double mutant background are nearly completely resistant to IAA treatment, implying that the majority of auxin-regulated gene expression in seedlings is mediated by *ARF7* and *ARF19*.

ARF gene family members have thus been implicated with some evidence as a link between auxin signalling and the expression of a wide range of genes due to their involvement in exerting auxin-regulated growth responses.

5.1.1.3 Ectopic expression studies

Identifying the site as well as the targets of gene expression, as described above, is vital to understand the role of a particular gene in the developmental process. However, if a gene is to be targeted for genetic engineering, another important question to be asked is: which morphological effects can be achieved when a gene is expressed out of its natural context? Ectopic expression of *ANT* for example resulted in a number of interesting effects on plant growth including increased growth of floral organs (Krizek, 1999). This deviation from the natural pattern of gene function is generally achieved by introducing a constitutive over-expression vector with the CaMV promoter *p35S* (Hull, 1983) driving the gene of interest. A number of studies using this over-expression vector have been performed with ARF genes including *ARF5,7* and *ARF8*, all of which have been shown to act as activators of auxin-induced transcription regulation (Tiwari *et al.*, 2003). While the lack of functional *MP/ARF5* as described in the *mp* mutant can lead to fused cotyledons, irregularities in the formation of vascular strands and a lack of basal structures (Berleth and Jürgens, 1993; Hardtke and Berleth, 1998), over-expression of *ARF5* has no obvious effects on plant phenotype in seedlings but an enhanced response to exogenous auxin signal via transcript abundance of *Aux/IAAs* and genes involved in regulation of procambial development (Mattsson *et al.*, 2003). In adult plants, the introduction of

35S::MP caused developmental defects in the inflorescences including fewer and predominantly sterile flowers and terminal meristematic growth leading to the formation of pin-shaped tips (Hardtke *et al.*, 2004). *nph4/arf7* mutant plants are impaired in differential growth responses. Interestingly, the over-expression of *ARF7* using the *35S::ARF7* construct has no obvious effect on plant morphology (Hardtke *et al.*, 2004). Over-expression studies of *ARF8* produced phenotypes that were consistent with *arf8* morphology that appears to enhance apical dominance and shoot growth. *ARF8* over-expressing plants have short hypocotyls, decreased apical dominance and reduced lateral root growth (Tian *et al.*, 2004).

5.1.2 The characterisation of *ARF2* gene expression.

Our mutant analysis of *mnt/arf2* plants indicated that the plants produce large seeds by allowing for additional cell divisions during the maturation of the ovule. We therefore expected that wild type *ARF2* must be expressed in the ovule at a developmental stage that coincides to some extent with the time at which the deviation from wild type phenotype can be observed. Each part of the results section below is introduced by a more specific question relating to the general query as to how *ARF2* is regulated. *ARF2* expression levels were visualised in the ovule and during different stages of development with the help of a GFP reporter. An over-expression vector and an RNA-interference vector were also introduced to wild type plants in order to assess the respective effects of enhancing and reducing *ARF2* gene expression through genetic engineering. Another aim was to determine whether over-expression of *ARF2* can lead to a phenotype that contrasts the *arf2* phenotype by leading to smaller seeds. A *DR5::GUS* expression study examined the impact of the *arf2* mutation on auxin responsive gene expression and finally a short study was dedicated to the effects of transforming an *mnt/arf2* mutant plant with wild type *ARF2* genomic DNA.
Although the seed phenotype was the main focus of the study, general plant morphology was also recorded and expression was therefore examined in all of the floral organs that appear to be affected in different severity. This was done so that we would be able to

correlate conclusions about the effect on *ARF2* on seed development with conclusions about roles of the gene in the development of other organs.

5.2 Results

5.2.1 Using a *pARF2::GFP* reporter to analyse expression in the *A. thaliana* flower

Where is *ARF* expressed and how is this expression modulated?

The *in situ* analysis of *ARF2* expression in the wild type ovule and in other floral organs was based on the expression patterns of the *ARF2* promoter visualised by GFP. A *pARF::GFP* reporter construct was cloned and transformed into wild type (Col-3) plants requiring the following steps:

1. The amplification of the promoter sequence from genomic DNA.
2. The fusion of the promoter sequence with the GFP (DME) NLS reporter construct of the pBI-GFP (S65T) DME NLS binary vector (Choi *et al.*, [2002] kindly provided by Robert Fisher).
3. The production of plant lines expressing the *pARF2::GFP*(NLS) transgene by *A. tumefaciens* mediated transformation.

5.2.1.1 Cloning of the *pARF2::GFP* reporter construct

To amplify the *ARF2* promoter (2,477bp), primers pMNT_GFP_S and pMNT_GFP_X were designed against upstream sequence of the *ARF2* coding region. Restriction site linkers were incorporated into the primers to allow for directional cloning into the pBI-GFP(S65T) DME NLS binary vector.

The *ARF2* promoter PCR fragment was amplified from MITG10 plasmid template using proofreading DNA polymerase. The sequence was ligated into the pGEM-T vector thereby creating *pARF2* pGEM-T (Figure 5.1 A). Sequence identity of the insert was checked by obtaining sequence data from *pARF2* pGEM-T.

The promoter fragment was lifted from pGEM-T by cutting at the SalI and XbaI restriction sites, and ligated into the pBI-GFP(S65T) DME NLS binary vector, thereby creating *pARF2::GFP* (DME) NLS pBI (Figure 5.1 B). The binary vector plasmid, which is based on pBI101 and sGFP(S65T), contains the nuclear localisation signal of the DEMETER gene (At5G04560.1) it contains nptII (kanamycinR) for *in planta* selection.

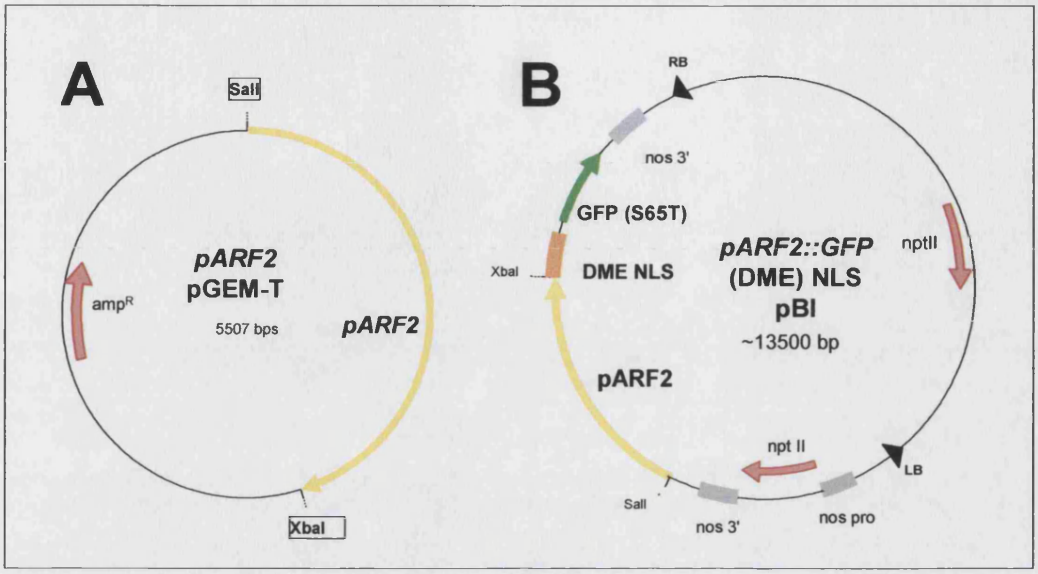

Figure 5.1 Construction of the *pARF2::GFP* binary vector. A: The promoter *pARF2* PCR fragment was ligated into the pGEM-T vector. B: The promoter fragment was removed from pGEM-T using SalI and XbaI and ligated into pBI-GFP (S65T) DME NLS binary vector thereby creating *pARF2::GFP* (DME) NLS pBI.

5.2.1.2 *pARF2::GFP* expression analysis shows strong expression in young ovules and young floral organs

Over 25 lines were positive for kanamycin selection, each line presenting an independent transformation event. To visualise *ARF2* promoter activity in plants that were transformed with *pARF2::GFP* (DME) NLS pBI, the presence of GFP in mature *A. thaliana* plants was examined using confocal microscopy. Five of these lines expressed detectable levels of nuclear localised GFP; three of which (lines 10, 14 and19) showed strong expression of varying levels and were examined in detail as shown in Figure 5.2. All three lines showed strong *ARF2* promoter activity in all tissues of young ovules especially in the nucellar tissue. Column 1 of Figure 5.2 shows young ovules at around stage 2-III (according to Scheitz *et al.*, 2005) where the nucellus is exposed prior to the elongation of the inner and outer integuments. GFP signal, despite being strongest in the nucellar region, was detected in the integuments and the funicular region of the young

ovular protrusions with equal intensity for all three lines. The pictures in column 2 show a nearly mature ovule at around stage 3-III, where the nucellus is completely enveloped but integument growth and ovule curvature have not yet been finalised. At this stage a clear difference between the weaker expression in line 10 and the strong expression in line 19 becomes evident (line 14 shows an intermediate expression level). During ovule maturation, the strength of GFP expression appears to decrease in lines 10 and 14 and to focus on the region that is known to contain nucellar cells at the chalazal pole (see Chapter 3 for details). Line 19 on the other hand still shows strong expression in all parts of the maturing ovule. The pictures in column III show a mature ovule at stage 3-VI just prior to fertilisation. While expression was not detectable in line 10 at this stage, a weak signal was detected in the chalazal region of the ovule in line 14. In the strongly expressing line 19, low levels of expression were seen in the chalazal integuments and the funiculus, however overall expression levels have decreased markedly.

Figure 5.3 shows GFP expression in young and old petals, stamen, gynoecia and sepals of a plant from line 19. Expression in all of these floral organs was strong during the early stages but no signal could be detected at stage 12 or beyond except in the gynoecium, where ample GFP signal was detected throughout all developmental stages. Furthermore, GFP signal was detected in the siliques after fertilisation (not shown). GFP expression was also detected in young stems and leaves, where GFP signal apparently negatively correlated with age and distance from the meristem. Young seed and mature embryos were also examined, revealing no expression in the seed coat or in any other part of the young seed. However, mature embryos that had been dissected from the seed showed strong signal throughout (not shown).

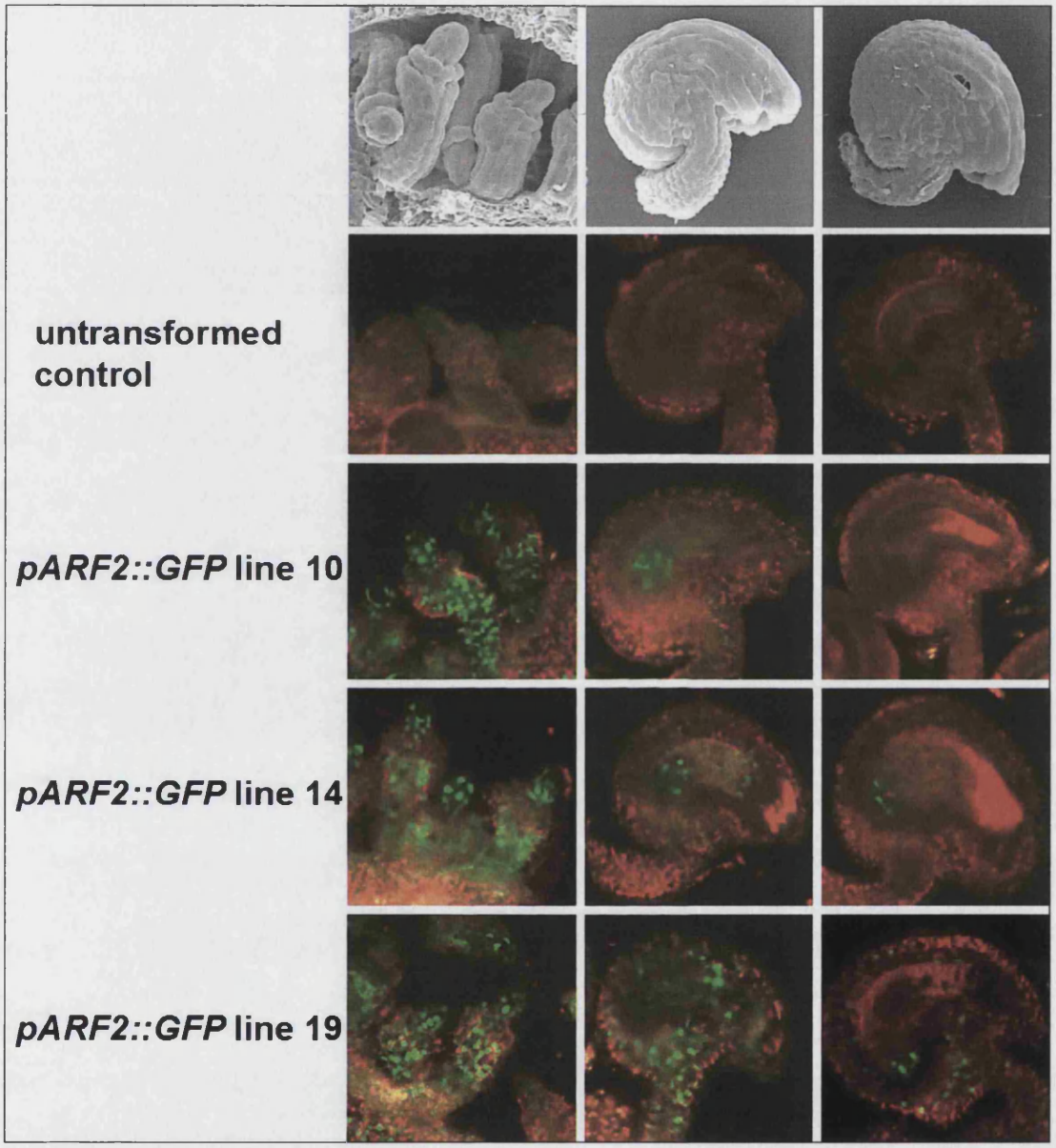

Figure 5.2 *pARF2* promoter activity in ovules. Top row: SEM micrographs of ovules at comparable stages as those shown in confocal micrographs below. Rows 2-5: Confocal images of ovules at around stage 2-III, an ovule at around stage 3-III and a mature ovule at stage 3-VI respectively (from left to right). Stages according to Scheitz *et al.* (2005). Row 2: control, rows 3-5: transformed lines, each line representing an independent insertion event. Confocal images are overlays showing GFP fluorescence (green) recorded by channel 1 and chlorophyll autofluorescence (red) recorded by channel 2.

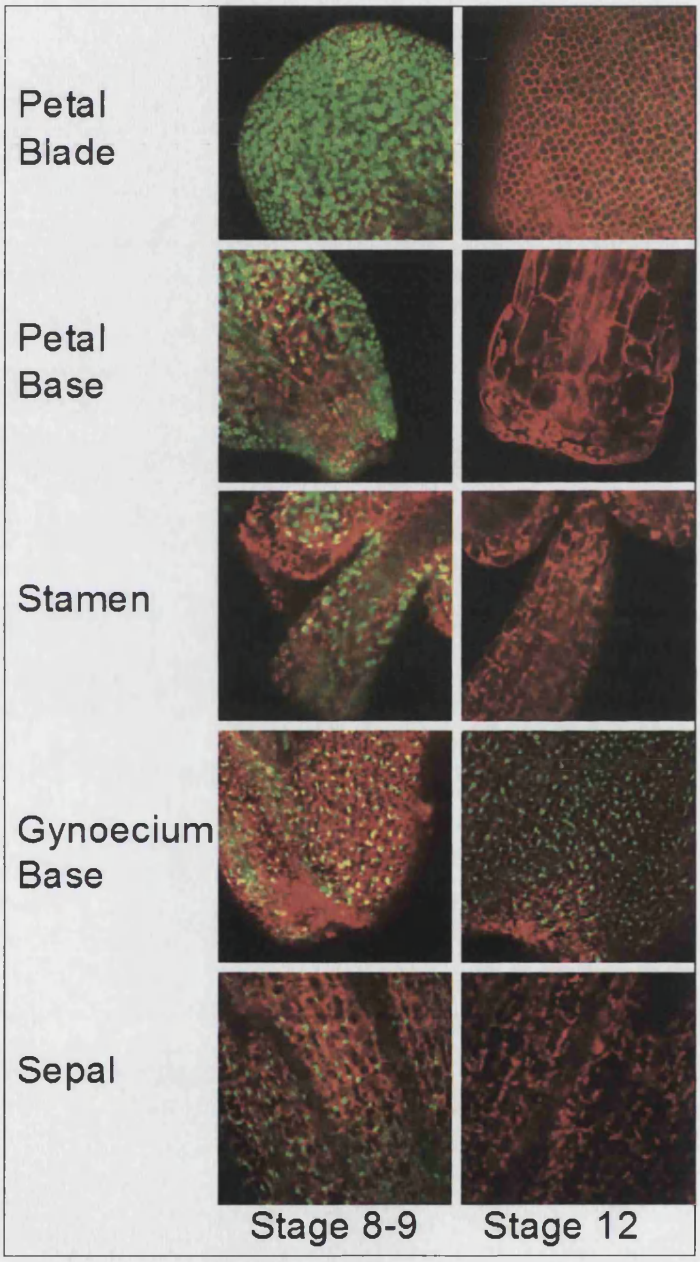

Figure 5.3 *pARF2::GFP* activity in different floral organs at stages 8-9 (left) and 12 (right). Stages according to Smyth *et al.* (1990). Confocal images are overlays showing GFP fluorescence (green) recorded by channel 1 and chlorophyll autofluorescence (red) recorded by channel 2.

5.2.2 The effects of over-expressing *ARF2* in wild type plants using a constitutive promoter

How does vector-driven constitutive expression of *ARF2* affect the phenotype of transformed wild type *A. thaliana* plants?

To test the effects of *ARF2* over-expression *in situ*, *ARF2* cDNA was placed under the control of the CaMV 35S promoter to produce an over-expression vector, which was transformed into wild type (Col-3) plants requiring the following steps.

This required the following steps:

1. The amplification of *ARF2* cDNA from reverse-transcribed mRNA.
2. The fusion of the cDNA fragment into the pART7-35S vector (Gleave, 1992).
3. The production of a binary vector containing the *p35S::ARF2* fusion product using the BJ40 vector (kindly provided by Bart Janssen, Horticultureal & Food Research Institute, New Zealand).
4. The production of plant lines expressing the *p35S::ARF2* transgene by *A. tumefaciens* mediated transformation.

5.2.2.1 Cloning of the *p35S::ARF2* over-expression vector

To amplify *ARF2* cDNA (2,572bp), primers 35S_MNT_X and 35S_MNT_B were designed against the sequence containing the complete *ARF2* coding region. Restriction site linkers were incorporated into the primers to allow for directional cloning into pART7.

The *ARF2* cDNA PCR fragment was amplified as above from cDNA template generated from RNA of mixed plant tissue. The fragment was ligated into the pGEM®-T vector as above thereby creating *ARF2* pGEM-T (Figure 5.4 A). Sequence identity of the insert was checked by obtaining sequence data from *ARF2* pGEM-T using the M13F an M13R universal primers, the two cloning primers and two internal primers (not shown).

The cDNA fragment was lifted from pGEM-T by cutting at the SalI and XbaI restriction sites, and ligated into the multiple cloning site of pART7 vector, thereby creating *ARF2* pART7 (Figure 5.4 B) which now contained the *p35S::ARF2* expression cassette followed by an ocs 3' terminator and bordered by NotI restriction sites . The expression cassette was excised from pART7 using NotI and ligated into BJ40, thereby creating the *p35S::ARF2* BJ40 binary vector. The binary vector plasmid contains nptII (kanamycinR) for *in planta* selection.

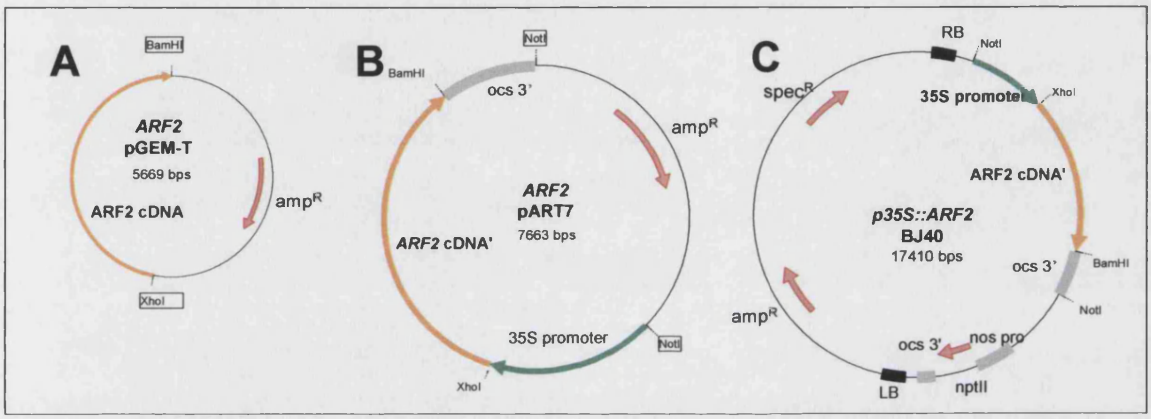

Figure 5.4 Construction of the *p35S::ARF2* binary vector. A: The *ARF2* cDNA fragment was ligated into pGEM-T creating *ARF2* pGEM-T. B: The *ARF2* cDNA fragment was lifted from pGEM-T using BamHI and XhoI and ligated into the multiple cloning site of the pART7 vector creating *ARF2* pART7 . C: The *p35S::ARF2* cassette was lifted from pART7 using NotI and ligated into the BJ40 binary vector thereby creating *p35S::ARF2* BJ40.

5.2.2.2 Verification of successfully transformed plants carrying the *35S::ARF2* transgene

Unlike the GFP reporter construct, the presence of which can be confirmed *in planta* due to the GFP signal, the presence of *p35S::ARF2* transgene could not be verified beyond the molecular level (in the absence of antibiotic selection). Therefore, in order to be confident that any phenotype seen in plants transformed with the *p35S::ARF2* transgene was due to the presence of the correct insert, a PCR reaction using a primer to the 35S promoter fragment as well as a primer to the *ARF2* cDNA fragment was performed. As

the *p35S::ARF2* promoter-gene combination is unique to the insert, a positive result would point to the presence of the correct transgene in the plant of interest. The primers '35S prom' and '35S ARF' were used which amplify a 1.4kbp fragment containing both promoter and cDNA sequence

The presence of the correct insert was confirmed for all plants that were survived under kanamycin selection (Figure 5.5) thereby confirming that the selection had been conferred by *p35S::ARF2* BJ40.

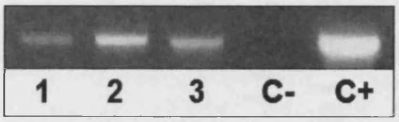

Figure 5.5 PCR checking for presence of *35S::ARF2* transgene in transformed plants using a promoter-specific and an insert-specific primer. Lanes 1-3: genomic DNA plant lines 1-3, C-: genomic DNA untransformed Col-3 control plant, C+: *p35S::ARF2* BJ40 plasmid vector control.

5.2.2.3 *ARF2* over-expression results in an *arf2/mnt* mutant phenotype

After the presence of the *p35S::ARF2* over-expression vector insert in transgenic lines was confirmed as shown above, the phenotype of over 40 transgenic lines was examined. These plants were found to be indistinguishable from that of *arf2/mnt* mutant plants, showing the characteristic *arf2/mnt*-like seed and floral phenotype as seen in Figure 5.6. The adult plants were sterile unless fertilised manually, carpels protruded through unopened flowers and seeds were large and heavy (*p35S::ARF2* = 22.0µg; *arf2/mnt* = 21.3µg) compared to seeds of wild type plants (WT = 14.9µg) grown under the same conditions. Figure 5.7 shows an adult *p35S::ARF2*-expressing plant displaying the typical *arf2/mant* phenotype: agravitropic stem growth leading to bending of the inflorescence stem (plants have been attached to support sticks for display purposes causing artificial straightening of the transformed plant) as well as a complete lack of seed pods.

Figure 5.6 *MNT/ARF2* over-expression line inflorescence and seed compared to *mnt/arf2* and wild type. All seed photographed at the same magnification. Average seed weights below (N=10).

5.2.2.4 *MNT/ARF* transcript levels in *p35S::ARF2* transgenic lines show no suppression at the transcript level.

In order to assess whether the presence of the *p35S::ARF2* transgene negatively affects the transcript levels of *ARF2* in the transgenic line, a semi-quantitative multiplex RT-PCR analysis was carried out. cDNA template was obtained from the reverse transcription of titrated total RNA template of wild type and *35S::ARF2* plants which had been quantified according to optical density.

The PCR product of this analysis was visualised by gel electrophoresis as shown in Figure 5.9. The 1.5kb intron-spanning fragment of *ARF2* cDNA was amplified in the same reaction as a GAP-C control. The PCR shows that *ARF2* transcript is more abundant in *p35S::ARF2* plants than in untransformed control (WT) plants. The assay was repeated using different RNA samples of all three genotypes with identical outcomes (data not shown).

Figure 5.7 Wild type col-3 (left) and transgenic col-3 (right) expressing *p35S::ARF2*. Inflorescence stems are attached to wooden support sticks for display purposes only. Plants were grown at the same time under the same conditions.

5.2.3 Suppression of *ARF2* in wild type plants via RNA interference

Can transgenic interference in wild type *ARF2* gene expression reproduce the *arf2* mutant phenotype?

Transgenic silencing of gene expression is achieved by introducing a short, inverted repeat of homologous cDNA causing targeted disruption of native gene expression in the wild type background (Matthew, 2004). RNA interference has become a popular tool for reverse genetic analysis in plants and a number of RNAi vectors from the Plant Chromatin Database, ChromDB (http://www.chromdb.org/) are distributed via the ABRC (http://www.biosci.ohio-state.edu/~plantbio/Facilities/abrc/abrchome.htm).

In order to assess if the *arf2* phenotype can be obtained by constitutive RNAi-based suppression of the gene in the wild type background, a *p35S::ARF2*-RNAi construct was designed by Robert Day (University of Bath). This construct, based on the ChromDB pFGC5945 vector, contains an inverted repeat of a 570bp *ARF2* cDNA fragment amplified from the 12th exon which is located in the sequence that encodes for the middle region between the DBD and the CTD III. Plants carrying the transgene are basta resistant.

5.2.3.1 Identification of plants carrying the *35S::ARF2*-RNAi transgene

All successfully transformed plants were selected due to resistance to glufosinate (basta). Presence of the correct insert was further confirmed via PCR using primers 'AVA prom 1F' and 'AVA intron 1R'

5.2.3.2 *p35S::ARF2*-RNAi-based suppression of *ARF2* causes an *arf2/mnt*-like phenotype

Over 25 transformed plants carrying the *ARF2*-RNAi transgene were analysed for plant and seed morphology. The phenotype of transgenic plants expressing *p35S::ARF2*-RNAi is nearly indistinguishable from the morphology of *arf2/mnt* mutant although some slight differences were observed. As in *arf2/mnt* mutant plants, the flowers of *ARF2*-RNAi

plants remained closed, carpels protruded from the unopened flower buds and failed to self-pollinate thereby resulting in the absence of maturing seed pods on the adult plant (see Figure 5.10). Furthermore, fertility was compromised. Seeds resulting from manual pollination or seeds found on old plants were large and heavy (Figure 5.8). The large-seed phenotype seen in *mnt/arf2* EMS mutants and T-DNA insertion mutants was thus reproduced using RNAi technology.

Despite the similarity in floral morphology, agravitropic growth patterns and thickness of the inflorescence stem appear less severe in the RNAi transformants. The plants also appeared to flower at the same time as wild type plants. However, due to time constraints these observations were not quantified.

Figure 5.8 Seed of wild type, *mnt* and RNAi transformant plants. Bar: 1mm. All pictures taken at the same magnification, average seed weights shown.

5.2.3.3 The decrease in *ARF2* transcript levels caused by *p35S::ARF2*-RNAi is not detectable by RT-PCR

In order to confirm that the observed phenotype is due to a detectable reduction in *ARF2* transcript, *ARF2* RNA levels of plants transformed with *35S::ARF2*-RNAi were analysed using semi-quantitative multiplex RT-PCR (as shown in Figure 5.9). The cDNA template was obtained from the reverse transcription of titrated total RNA template of wild type and *35S::ARF2*-RNAi plants which had been quantified according to optical density. The PCR product of this analysis was visualised by gel electrophoresis as shown in Figure 5.9. The 1.5kb intron-spanning fragment of *ARF2* cDNA was amplified in the same reaction as a GAP-C control. The PCR shows that *ARF2* transcript is more abundant in *p35S::ARF2* plants than in untransformed control (WT) plants. The reaction

was repeated using different RNA samples of all three genotypes with identical outcomes (data not shown).The resulting PCR using *MNT/ARF2* cDNA-specific primers shows that transcript levels in *p35S::ARF2*-RNAi plants are not obviously lower than in wild type plants.

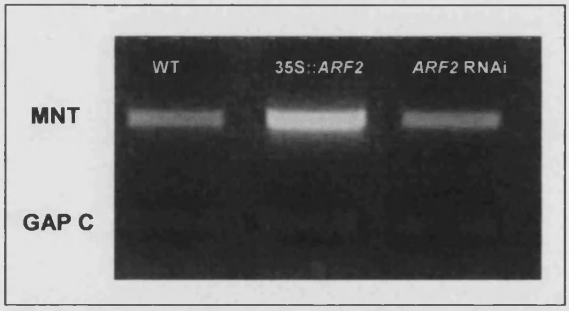

Figure 5.9 RT-PCR showing *ARF2* transcript levels in a wild type plant as well as plants containing the overexpression and RNAi vectors respectively.

Figure 5.10 Wild type Col-0 (left) and a transformed *p35S::ARF2*-RNAi plant (right). Inflorescence stems are attached to wooden support sticks for display purposes only. The plants were grown at the same time under the same conditions.

5.2.4 *DR5::GUS* expression in the wild type and *arf2* mutant background

How does the *mnt/arf2* mutation affect auxin-responsive gene expression? As mentioned above, previous work by Tiwari *et al* . (2003) using the *DR5::GUS* reporter construct indicated that *ARF2* acts as a repressor of auxin-induced gene expression. *MP/ARF5* on the other hand was shown to act as an activator of auxin-responsive gene expression. In an earlier study using the same reporter construct, Sabatini *et al* ., (1999) showed that auxin-responsive gene expression in the *mp/arf5* mutant is reduced in root primordia. Therefore, it was possible to use the *DR5::GUS* reporter to show how an *arf* mutation caused a localised decrease in base-level auxin-responsive expression. The objective of this study was to explore whether the *arf2* mutation can also cause a disruption of base-level auxin-responsive gene expression as reported by the *DR5::GUS* transgene.

5.2.4.1 Combining the *DR5::GUS* transgene with the *arf2* mutation.

A. thaliana seeds of the Col-0 background containing the *DR5::GUS* transgene were kindly donated by Tom Guilfoyle. In order to introduce the *DR5::GUS* vector into *arf2* mutant plants, a vector-containing Col-0 plant was crossed with a homozygous *arf2* mutant Col-3 plant. As a control, the plant was also crossed with a wild-type Col-3 plant. The progeny of both of these crosses were left to self-pollinate. Homozygous *arf2* mutant F2 progeny plants were scored according to floral phenotype. Presence of the *DR5::GUS* vector was verified by histochemical GUS staining of several dissected F2 plants of the control population and of plants carrying the *arf2* genotype.

5.2.4.2 Differences in auxin-responsive gene expression in *arf2* mutant plants can not be detected using the *DR5::GUS* reporter.

In the vector-containing wild type plant, *DR5*-led GUS expression produced clear staining in the chalazal region of the seed and in the funiculus (Figure 5.11). GUS staining was also detected along the edges of leaves, in young pollen and in the xylem of

inflorescence stem sections (not shown). No staining was observed in young flower buds. When compared to these control staining patterns, the *DR5::GUS* response in the *arf2* mutant plant was indistinguishable. Again, staining was observed along the edges of leaves, in the pollen of young flowers and in the xylem. Figure 5.11 shows that the staining pattern in wild type and *mnt/arf2* mutant seed is identical. This was consistent for all organs in several plant lines observed.

Figure 5.11 GUS stained seed pods of wild type (top) and *arf2/mnt* mutant (bottom) plants containing the *DR5::GUS* transgene. Pods have been dissected to reveal seeds. Pods are suspended in 70% EtOH and pictures have been taken at the same magnification.

5.2.5 Introduction of genomic *ARF2* into *arf2* mutant plants.

5.2.5.1 Introducing wild type *ARF2* produces abnormal phenotypes in some *arf2* plants.

The following results are the outcome of a mutant rescue experiment that was undertaken by Sushma Tiwari (University of Bath) in order to identify the *mnt* mutant locus as described in Chapter 3. The work was done after the fine mapping had been completed and before the mutant locus had been identified via the allelism test. It involved the

transformation of *mnt* mutant plants with fragments of genomic DNA from the *mnt*-containing region (as identified by the mapping process). A complete rescue of the MNT phenotype was achieved via introduction of the *ARF2*-containing fragment named SL14.5 (see Chapter 3, Discussion). Any other fragment that did not contain the *ARF2* gene did not affect the mutant morphology of the transgenic mutant plant. However, in addition to restoring the wild type-like plant phenotype, the SL14.5 transgene also produced a number of other morphologies in some of the transformed *mnt* plants, six of which are briefly described here.

5.2.5.2 Certain insertion events of the *ARF2*-containing transgene cause unpredictable phenotypes in the *mnt/arf2* mutant background.

As a general observation, the introduction of the *ARF2*-containing transgene was collectively found to affect all aspects of above-ground plant morphology including stem height, gravitropism, apical dominance (total number of inflorescence stems), rosette size, flower morphology, fertility and seed size. Six examples of extreme morphologies seen in *mnt/arf2* plants transformed with the SL14.5 transgene are shown in Figure 5.12. These plants had grown at the same time in adjoining trays and pictures of the whole adult plant and the inflorescence were taken at the same time. The plants were then left to self-pollinate and seeds were collected after drying.

The morphologies observed in the plants shown in Figure 5.12 are summarised in Table 5.1 as compared to un-transformed *mnt/arf2* and wild type plants.

Table 5.1 Phenotypes of Col-3 plants of *mnt/arf2* mutant background transformed with *ARF2*-containing transgene. Each plant number refers to a different insertion event.

Plant #	Plant (stem) height	Rosette size	Floral phenotype	Fertility	Seed weight
1	dwarfed	very small, few leaves	*mnt*-like although smaller flowers and slight exposure of petals	very poor	13.25µg
2	WT-like	large, many big leaves	WT-like	good	11.22µg
3	tall, *mnt*-like	large, many big leaves	*mnt*-like, no exposure of petals	poor	15.44µg
4	dwarfed	WT-like	WT-like	good	8.44µg
5	tall, *mnt*-like	WT-like	*mnt*-like, some exposure of petals	poor	15.08µg
6	WT-like	WT-like	WT-like	good	14.47µg

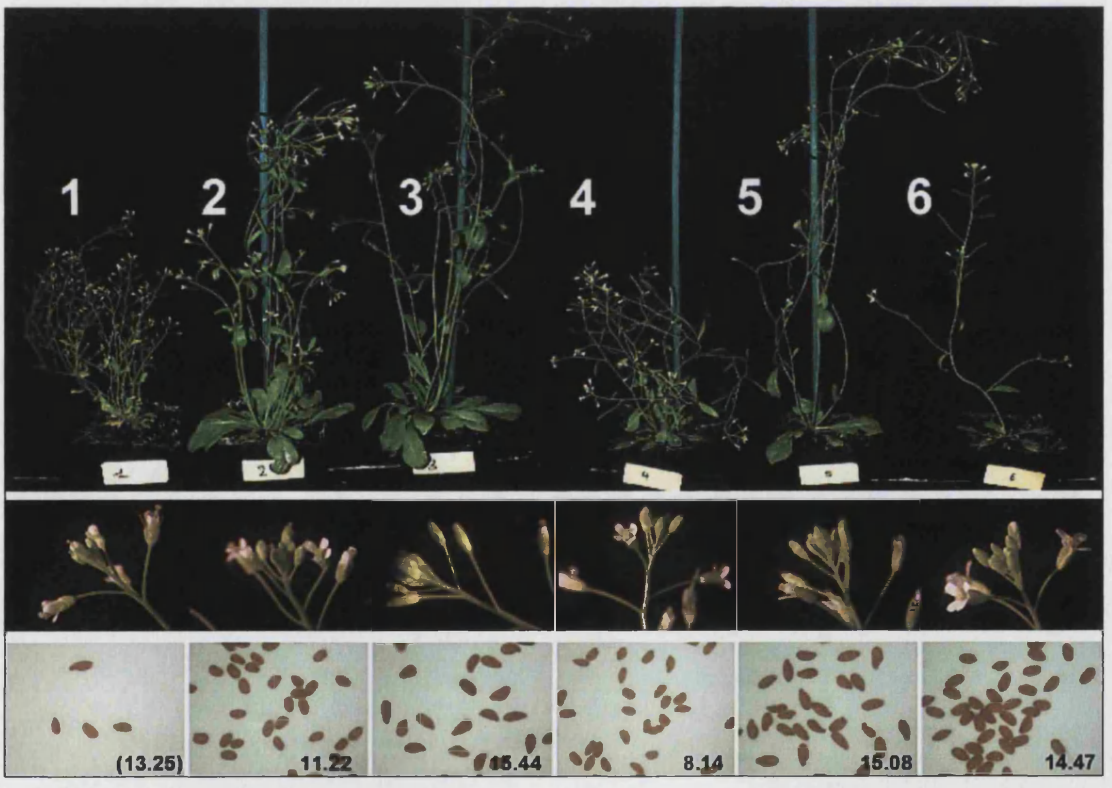

Figure 5.12 Six Col-3 plants of *mnt/arf2* mutant background transformed with wild type genomic *ARF2*. Top row: adult plants, Middle row: respective floral phenotype, Bottom row: respective seed pictures and weights in µg. All images in each respective row taken at the same magnification, plants grown at the same time under the same conditions.

5.3 Discussion

5.3.1 The timing of *pARF2* expression patterns correspond to the predicted role of *ARF2* in organ development.

The *arf2/mnt* mutation was observed to change overall plant morphology by affecting aspects of the development of almost every organ. However, when taking a closer look at organ morphology, we observed that the mutation also acts very specifically as certain cell and tissue types appear to be more directly affected than others. Unlike an overall increase or reduction in organ size, this causes an irregular growth pattern leading to disproportionate organ sizes resulting in defects such as sterility and lack of floral opening. From a genetic point of view, a specific effect on organ size and development suggests that gene expression is either regulated in a very specific manner or that the gene is expressed globally with very specific effects on certain target organs. Previous studies suggested that the gene is indeed uniformly and highly expressed in all plant organs (Ulmasov *et al.*, 1999) and that it acts by suppressing certain auxin-regulated genes (Tiwari *et al.*, 2003). Our results suggest that *ARF2* is highly expressed throughout the plant as suggested previously, as GFP signal was seen in all organs studied. However, during the analysis of *ARF2* expression in floral organs we found that expression is modulated in certain tissue types and during certain stages of development. The *ARF2* promoter appeared to be most active during early organ development such as the early stages of ovule development or in the young petal and stamen. However, the role of *ARF2* does not appear to extend beyond organ maturation. Promoter activity was found to be reduced or even absent in the tissue of maturing organs.

Certain organs, such as the carpel (and later silique) report promoter activity throughout all stages of development. The fact that mature carpels and siliques continue to show strong GFP signal could indicate that carpel maturation is an arbitrary definition which does not correctly describe the growth stage of the organ. Instead, carpel and silique development could be continuous process that is not completed until silique ripening. Therefore, the mature carpel is actually an immature silique and therefore a developing organ. Further evidence for the role of *ARF2* in the early development of young tissues is

gained from observations revealing that *pARF2::GFP* expression is highest in young leaves and stems, especially in proximity of the meristem.
With respect to ovule development and *ARF2* expression, we found that the GFP expression patterns corresponded well with the timing of differences in developmental growth of ovules observed in the *arf2/mnt* mutant described in chapter 4. One of our first observations (using seed clearing and Nomarski optics) was that observable size differences between wild type and *arf2/mnt* seed are initiated before fertilisation. Accordingly, no GFP signal was detected in the seed coat of young seed. Furthermore we found that the mature *arf2/mnt* ovule is larger than the wild type ovule, indicating that the differences in ovule size occur before ovule maturation. Consistent with this, GFP signal in the mature ovule is low or absent while young, growing ovules were found to display high levels of *ARF2* expression. The observed *pARF2* expression patterns thus correlated well with the expected role of *ARF2* during the development of *A. thaliana* ovules.

With respect to the spatial dimension of the observed *ARF2* expression pattern, conclusions about the mode of *ARF2* action in the regulation of seed size were not as easy to draw as originally expected. In a study of *ACR4* by Gifford *et al.* (2003), the authors were able use promoter driven marker gene expression detect a very clear link between gene expression and the *acr4* mutant phenotype, namely the disorganisation of the L1 cell layer resulting in small seeds with a rugged (or crinkly) appearance. The L1 cell layer is defined as the tunica that covers organs such as the shoot apical meristem, the embryo or the ovule, where it corresponds to the outer cell layers including the integuments. As expected, *pACR4*-driven marker expression was clearly and exclusively seen in the peripheral cell layer of *A. thaliana* shoot apical meristem, embryo and the integuments of the mature ovule. Our results regarding *pARF2*-driven marker expression were not as clear-cut. The strong expression of *pARF* in the nucellus and in the funiculus – both of which did not appear to be markedly affected by the mutation in terms of their size or shape – was unexpected. According to our phenotypic observation, a more localised expression in the integuments of young ovules was anticipated. However, our expectations and findings do not necessarily contradict each other since, strong *pARF2* expression is found in the young integuments. On the other hand, the results do indicate

that *ARF2*-mediated regulation of early seed development may not solely be attributed to the increased cell division of integuments. Changes to the development of nucellar and the funicular tissue may play a more important role in the seed size phenotype observed in the *arf2/mnt* mutant than originally assumed.

5.3.2 *pARF2* expression studies confirming additional observed phenotypes

Due to the presumed involvement of *ARF2* in apical hook formation, a *pARF2::GUS::ARF2* reporter fusion was constructed which revealed that expression is strongest in the apical region of the hypocotyl and cotyledons (Li *et al.*, 2004). This reporter also revealed some expression in the roots and increased staining was seen upon exposure to light. These results by Li *et al.* (2004) were later confirmed by Okushima *et al.* (2005b), who examined *pARF2* activity in seedlings and adult plants using a *pARF2::GUS* expression vector. This study was also able to localise GUS expression to seedling root vasculature, especially in lateral root primordia. Okushima *et al.* (2005b) also observed the closed-bud and protruding-carpel floral phenotype of *arf2* that is described in our results in the previous chapter. In the adult plant, *pARF2::GUS* expression was therefore analysed in mature flowers and, in accordance with mutant flower morphology, staining could be found in the sepal, the stamen (especially the apical region), the pistil and the basal region of the gynoecium. GUS staining was also detected in developing seed pods and in the embryo of mature seeds (Okushima *et al.*, 2005b). All of these correspond to our findings although the GUS staining pattern is not as clearly defined as the nuclear localised reporter pattern produced by the *pARF2::GFP* plant. The reporter analyses by Li *et al.* (2004) and Okushima *et al.* (2005b) also confirm that *ARF2* transcript – although found throughout the plant – is not uniformly expressed in all plant tissues and a link to *arf2* mutant morphology can be established due to the specific expression patterns observed with the help of reporter constructs.

5.3.3 Base-level expression of auxin-regulated genes is not significantly affected by the *arf2* mutation.

We were unable to detect a difference in auxin-responsive gene expression between wild type and *arf2* mutant plants transformed by the *DR5::GUS* reporter construct. This confirms the results by Tiwari *et al.* (2003) who did not observe a significant change in base-level *DR5* expression within protoplasts co-transfected by the *ARF2* effector contstruct and the *DR5::GUS* reporter. Our findings regarding *DR5* expression *in vivo* therefore agree with the *in vitro* findings by Tiwari *et al.* (2003), showing that base-level auxin-responsive gene expression is low and does not vary from the control unless stimulated by external auxin. These findings by Tiwari *et al* (2003) lead us to the assumption that the *arf2* mutation causes a decrease of auxin-stimulated gene suppression *in vivo*. However, our results indicate that the effect of the *arf2* mutation cannot be visualised without an artificial auxin stimulus.

5.3.4 Constitutive expression of *ARF2* leads to co-suppression but not at the transcriptional level.

Our work shows that the *p35S::ARF2* vector causes *arf2*-like morphological development in transformed plants. We also showed that this is not due to suppression of *ARF2* transcription, as the levels of *ARF2* cDNA in the transformed plants is higher than in wild type plants.

After our work on the *p35S::ARF2* over-expression vector had been completed, Okushima *et al.* (2005b) showed that the expression of *ARF2* under the *35S* promoter leads to an absence of ARF2 protein in the transformed plant as determined by Western analysis. This confirms our findings regarding the *p35S::ARF2* plant phenotype even though it also shows that our results are incomplete as they lack the protein expression data. However, our RT-PCR data complements the protein expression data in that we now know that suppression happens only at the protein level. Furthermore, the absence of protein product despite abundance of transcript shows that our understanding of *ARF2* gene expression regulation is still open to interpretation: As it appears, the *ARF* pathway – at least with regard to *ARF2* – is susceptible to variations in transcript levels, indicating

the presence of additional feedback control mechanisms. It was therefore not possible to produce seed with a reduced size and weight by over-expressing *ARF2* in the wild type background.

5.3.5 A range of plant morphologies are caused by introducing wild type genomic *ARF2* DNA to the mutant background.

Our findings in paragraph 5.2.5 show that the introduction of wild type *ARF2* genomic DNA (linked to its own upstream genomic DNA presumed to contain the promoter) can lead to the development of a variety of phenotypes. Some of these phenotypes appear to be in direct contrast to the *arf2* phenotype as exemplified by Plant 4 (Figure 5.12). The *arf2* mutant mother plant (T_0) that was used to produce seeds transformed with the wild type gene carried all the characteristic morphological features of the *arf2* mutant: large seeds; long, thick stems; unopening and mostly sterile flowers, large rosette leaves etc. Furthermore, the majority of plants shown to carry the genomic *ARF2* transgene had a wild type-like morphologies. However, a small number of plants resulting from the transformation were seen to produce abnormal morphologies affecting seed size and number, stem thickness, fertility and flower opening in a number of combinations as summarised in Table 5.1.

It was possible to confirm the presence of the correct insert in the 'rescued' *arf2::ARF2* plants using PCR (data not shown), thus confirming that the observed phenotypes can be associated with the *ARF2* transgene. Information about the number of *ARF2* inserts that had been introduced into the *arf2* mutant background was not obtained. However, an answer to the occurrence of abnormal phenotypes among the rescue population could be obtained from existing literature on T-DNA transformation of *A. thaliana*. A number of studies, including the recent work by Radchuk *et al.* (2005) have revealed that *Agrobacterium*-mediated transformation of *A. thaliana* leads to multiple T-DNA insertions in over 30% of transgenic plants. The presence of multiple T-DNA inserts containing the transgene of interest has some implications on the dosage and expression strength of the transgene in transformed T2 progeny. In the case of *arf2* plants

transformed with the wild type *ARF2* transgene, we expected that a single copy of the *ARF2* transgene could rescue the *arf2* mutant phenotype. This expectation was based on the observation that heterozygous *arf2/ARF2* or *ARF2/arf2* plants show a wild type-like phenotype (see chapter 4). As a confirmation we found that the majority of plants of the *arf2* mutant background transformed with the *ARF2* genomic transgene produced a wild type-like phenotype. According to Radchuk *et al.* (2005), over 30% of all transformed progeny plants can be expected to carry more than a single copy of the transgene. Some of the transgenic plants will carry two copies of the transgene, causing them to be indistinguishable from wild type plants. However, a fraction of the transgenic plants can be expected to carry more than the wild type dose of *ARF2* genes, and one can hypothesise that this minority of transformed plants exhibit the effects of slightly raised *ARF2* transcript levels.

5.3.6 RNAi technology can be used reproduce the *mnt/arf2* phenotype

This experiment was undertaken order to test if the big seed phenotype of the *arf2/mnt* mutation can be induced transgenetically by introducing a vector that specifically targets the *ARF2* gene for silencing. Being able to inhibit *ARF2* gene expression using RNA inhibition is especially important in order to achieve controlled variation of *ARF2* expression for seed engineering as described in detail in Chapter 6. Our findings show that the introduction of the RNAi vector caused *arf2*-like morphology in *A. thaliana.* RNAi-based suppression, as well as the *p35S::ARF2*-based suppression of *ARF2* expression described above, was also studied by Okushima *et al.* (2005), who describe the resulting phenotypes as similar to *arf2* mutant plants. Interestingly, we found no significant decrease in *ARF2* transcript levels within plants carrying the *p35S::ARF2*-RNAi construct. There is one possible explanation for the lack of detectable difference in *ARF2* cDNA levels obtained from wild type and the *ARF2*-RNAi plants: the *p35S* promoter – although supposedly constitutively expressed – may not actually be expressed at equal levels in all plant organs. The plant tissue that was collected to obtain RNA for

the RT-PCR reaction contained mostly flower buds but a low level of stem tissue contamination from the tip of the inflorescence meristem was also present. Therefore, a significant amount of stem-based *ARF2* transcript may still have been present in the total plant material that was used to obtain RNA for the RT-PCR reaction. Further indications that the 35S CaMV reporter-driven constitutive expression varies according to tissue types different tissues can be found in the findings of Blumenthal *et al.*, (1999), who measured p35S-driven GFP expression in transgenic tobacco and found that expression varied in certain tissues such as the 7th leaf.

5.3.7 Further work

Before conclusions can be drawn regarding the nature and function of the *ARF2* gene, the *arf2* and wild type plants expressing *DR5::GUS* described in 5.2.4 should be observed under two conditions: with an external auxin stimulus and without. This would uncover the influence of the functional *ARF2* gene with respect to auxin signalling.
Furthermore, a thorough molecular analysis of the rescue plant population shown in section 5.2.5 needs to be undertaken to confirm that the observed phenotypes of *arf2* plants transformed by genomic *ARF2* are due to varying levels of *ARF2* expression. This would require a quantification of *ARF2* expression levels using RT-PCR, as well as segregation analysis to uncover how many T-DNA-containing loci are present in each plant and to see whether the number of insertion correlates with the observed phenotypes.

6 Engineering seed size using the *mnt/arf2* model

6.1 Introduction

The *mnt/arf2* mutant was isolated through a mutant screen and subsequently studied due to the effect of the mutation on the seed size phenotype. The aim of this project was to understand the principle of *arf2*-based seed size enhancement in the model plant *A. thaliana* with a goal to create a model that can be applied to economically valuable crop species such as oilseed rape or even rice, maize or wheat.

Once the lesion responsible for the *mnt* mutation was identified, much of our work on *ARF2* was concerned with how a mutation in *ARF2* affects plant development to result in the production of larger seed. We found that *arf2* causes organ specific hyperplasia due to extra cell divisions in certain tissues such as the integument. The extra divisions occurring in the integuments of the maturing ovule led to the production of an enlarged mature ovule that in turn gave rise to an enlarged seed. The genetics of *ARF2* gene function were subsequently examined and showed that *ARF2* promoter activity coincides with the location and time of early ovule development. We also showed that constitutive expression as well as RNAi-based suppression of *ARF2* lead to an *arf2* mutant phenotype similar to that of the knock-out mutant plant that is described in detail in Chapter 4. However, the *arf2* mutant phenotype is pleiotropic and includes several non-seed traits such as increased stem thickness, delayed flowering, and an abnormal floral phenotype that causes the plant to be partially sterile. Whether a thicker inflorescence stem or a bushier rosette affect seed yield is uncertain. Compromised fertility on the other hand is certainly a highly unfavourable trait given that most seed and grain crop species self-pollinate. Furthermore, a lack of self-pollination leads to a technical problem when attempting to compare the yield of two genotypes under controlled conditions. This problem is highlighted in Chapter 4, where restricting seed set and pruning of wild type plants showed to cause a 57% increase in average seed weight thereby adding another unexpected variable to the comparative evaluation.

Based on our understanding of the role of *ARF2* in seed development, a number of strategies were developed that aimed to achieve adjustment of seed weight whilst removing unwanted side effects such as reduced fertility.

Four of these strategies are presented below and they are summarised as follows:

1. Reinstating flower opening in the *arf2* mutant background by targeted re-introduction of *ARF2* expression.
2. Decreasing seed size by increasing ovule-specific expression of *ARF2*.
3. Increasing seed size through targeted suppression of *ARF2* in wild type ovules.
4. Increasing seed size via targeted expression of *ANT* in wild type ovules.

In order to achieve targeted expression of the gene of interest, the above strategies were implemented by the use of expression cassette vectors. These binary vectors were designed to combine the gene of interest with a promoter that is known to confer targeted expression (or suppression) within the organ of interest.

6.1.1 Reinstating flower opening in the arf2 mutant background

The aim of the first strategy was to restore flower opening while maintaining the large seed phenotype that is caused by the lack of *ARF2* transcript in *arf2* mutant ovules. Flower opening coincides with anthesis and the exposure of stigma and anthers allow for pollen transfer and pollination (van Doorn and van Meeteren, 2003). As shown in Chapter 4, the petals of wild type flowers eventually expand beyond the length of the sepals and flower opening is initiated. An open wild type flower is characterised by expanded and reflexed petals that appear to have forced the flower open and have thereby exposed the stigma and stamens. Flower opening does not take place in *arf2* mutant plants and our data indicates that this occurs because the petals are consistently shorter than the sepals. Therefore the stigma and anthers of *arf2* flowers remain enclosed until dehiscence and abscission occur and successful pollen transfer is prevented. Although the lack of flower opening may not be the sole cause reduced fertility in *arf2* mutant plants (carpel and anther length discrepancies being other possible causes), we reasoned that

restoring the ability of flowers to open at anthesis by allowing petals to expand beyond sepals could substantially improve fertility.

We aimed to restore petal:sepal ratio in *arf2* mutant flowers by re-introducing *arf2* expression in the sepals and petals without affecting the large-seed phenotype. A promoter conveying localised expression in the sepals and petals and not in the gynoecium was therefore needed.

The promoter chosen to drive *ARF2* expression in the sepals and petals of the *arf2* mutant was that of the floral homeotic gene *AP1* (*APETALA1*), which is involved in regulating the transition of the inflorescence meristem to the floral meristem (Mandel *et al, 1992).* RNA expression studies by Mandel *et al.* (1992) showed that *AP1* is expressed throughout the primordial tissue of the young flower becomes restricted to the sepals and petals as flower development progresses. Aside from the pedicel, *AP1* is apparently not expressed anywhere else in the plant. These attributes of *AP1* gene expression suggested that the *pAP1* promoter is a suitable driver of targeted *ARF2* expression in the sepals and petals. The strategy was therefore to place *ARF2* under the control of the *AP1* promoter in an expression cassette that is transformed into an *arf2* mutant plant.

6.1.2 Decreasing and increasing seed size by varying ovule-specific expression of *ARF2.*

Although the general aim of this project was to enhance seed size in order to increase yield, an increase of seed size may not always be desirable for example in situations where the grain must conform to certain consumer preferences such as cooking time and texture. This condition applies in particular to certain food crops such as cooking rice where grain integrity is preserved until consumption. Being able to use our understanding of seed size controlling factors in order to decrease seed size could thus be a benefit in situations where a large-seeded variety is undesirable. Furthermore, the ability to decrease seed size by enhancing *ARF2* expression in the ovule could provide further evidence toward our hypothesis that the wild type *ARF2* gene functions in localised suppression of cell division. The aim of the second strategy was thus to cause a decrease in seed size through localised expression of *ARF2* in the integuments of wild type ovules.

The promoter that was chosen to target *ARF2* expression to the integument is that of the *A. thaliana INNER NO OUTER* (*INO*) gene, which was shown to be essential for formation and asymmetric growth of the ovule outer integument (Baker *et al.*, 1997; Villanueva *et al.*, 1999). *INO* mRNA accumulation was detected on the abaxial side of the chalaza and in the outer integument during the early stages of ovule development. mRNA accumulation was not detected in any other floral structures, making the *INO* promoter a suitable candidate for an integument-targeted gene expression cassette.
The *INO* promoter is also used for the third strategy, which aims to cause localised suppression of *ARF2* in wild type ovules. Our *ARF2*-RNAi study of Chapter 5 has shown that *p35S::ARF2*-RNAi-based suppression of *ARF2* results in an *arf2*-like phenotype of the whole plant. This shows that successful RNAi-based suppression of *ARF2* can be achieved. By using the same vector but replacing the *35S* constitutive promoter with an *INO* promoter, we aim to target *ARF2* expression exclusively to the integument of wild type *A. thaliana.*

6.1.3 Increasing seed size via targeted expression of *ANT* in wild type ovules.

Our final strategy was to increase seed size by modifying ovule development in the wild type background using the principles of *arf2*-led seed size increase. With a view to future applications in seed crop engineering, producing an *arf2* mutant seed crop and re-introducing *ARF2* in non-seed organs was not deemed to be a practical approach. Therefore, the ability to cause an increase in seed size in an otherwise unmodified background was believed to be an important feature.
From our previous analysis of the *arf2* mutant ovule, we deduced that a localised increase of cell division in the integuments of the developing ovule should lead to the development of enlarged seed. We reasoned that it should be possible to achieve an increase of cell division by introducing a suitable gene driven by an integument-specific promoter into the wild type background. The *INO* promoter was again chosen to target gene expression exclusively to the integument of wild type *A. thaliana.* Due to a number of properties outlined below *AINTEGUMENTA* (*ANT*) was chosen as the candidate gene for *INO*-driven modification of ovule development. The *pINO::ANT* expression vector

does not include *ARF2* and can therefore be viewed as an independent trial of the concept of integument-led seed enlargement based on the *arf2* model.

Similar to *ARF2, ANT* is also transcription factor and the gene has a strong link with ovule development as it was shown to be involved in the initiation of integuments (Klucher *et al.*, 1996; Elliott *et al.*, 1996). *ant* mutant plants are female sterile, fail to develop integuments and also produce narrower and fewer floral organs. In the wild type plant, *ANT* is expressed throughout developing ovules and in the primordia of other floral and vegetative organs where it is believed to play an important role in initiation and early growth. Importantly, ectopic expression of *ANT* under a *35S* promoter causes increased growth of shoot organs through increased cell division and expansion (Krizek, 1999; Mizukami and Fisher, 2000). When expressing the *35S::ANT* transgene, abnormal proliferation of chalazal nucellar cells was observed in the *A. thaliana* ovule. Furthermore, both transgenic *A. thaliana* and tobacco were shown to produce large seed (Mizukami and Fisher, 2000). *ANT* is believed to play a role in setting organ size as a positive mediator of growth signal (Mizukami, 2001).

6.2 Results

6.2.1 Localised restoration of *ARF2* expression in the *arf2* mutant sepals and petals

To restore *ARF2* expression in the sepals and petals of the *mnt/arf2* mutant, an *pAP1*::*ARF2* expression cassette was constructed and transformed into *mnt/arf2* mutant (Col-3) plants. This required the following steps:

1. The amplification of the promoter sequence from genomic DNA.
2. The fusion of the promoter sequence with *ARF2* cDNA in the shuttle vector BJ36 (kindly provided by Bart Janssen, Horticultural & Food Research Institute, New Zealand).
3. The production of a binary vector containing the *pAP1*::*ARF2* expression cassette using BJ40.
4. The production of plant lines expressing the *pAP1*::*ARF2* transgene by A. tumefaciens mediated transformation.

6.2.1.1 Cloning the *pAP1*::*ARF2* expression vector

To amplify the *AP1* promoter, primers 'pAP1 F' and 'pAP1 R' were designed against a 1,735bp sequence upstream of the *AP1* coding region (At1G69120). Restriction site linkers were incorporated into the primers to allow for directional cloning into BJ36. Amplifying *pAP1* directly from whole-plant genomic DNA was not possible, therefore the *pAP1* PCR fragment was amplified from genomic DNA template of the F4N2 BAC vector (ABRC). The fragment was ligated into the pGEM®-T vector thereby creating *pAP1* pGEM-T (Figure 6.1 A). The *ARF2* cDNA fragment (*ARF2* pGEM-T) had been created and verified during the production of the p35S::*ARF2* overexpression vector shown in Chapter 5. The *pAP1* promoter fragment was lifted from pGEM-T using NdeI and PstI and ligated into the shuttle vector BJ36, thereby creating pAPI BJ36 (not shown). Subsequently, *ARF2* cDNA was lifted from *ARF2* pGEM-T using BamHI and XhoI and ligated into BJ36, downstream of the promoter fragment, thereby creating *pAP1*::*ARF2* BJ36 (Figure 6.1 B). The *pAP1*::*ARF2* expression cassette and the ocs3'

terminator fragment were lifted from BJ36 using NotI and ligated into the binary vector BJ40, thereby creating *pAP1::ARF2* BJ40 (Figure 6.1C).

6.2.1.2 Verification of plants carrying the *pAP1::ARF2* transgene

The *pAP1::ARF2* transgene is linked to the *NPTII* kanamycin resistance gene which is present in the BJ40 vector. Presence of the correct transgene was also verified in a selection of wild type-like transgenic plants that had grown from seeds that had successfully germinated in the presence of kanamycin selective medium.
Primers 'AP1F_check' and 'MNTR_check' were used to confirm the presence of the *pAP1::ARF2* transgene which amplifies a 347bp fragment containing both promoter and cDNA sequence.
The verification of the transgene was performed by Rhiannon Hughes (University of Bath). It confirmed the presence of the correct transgene in all wild type-like plants which had grown on kanamycin-containing selective medium.

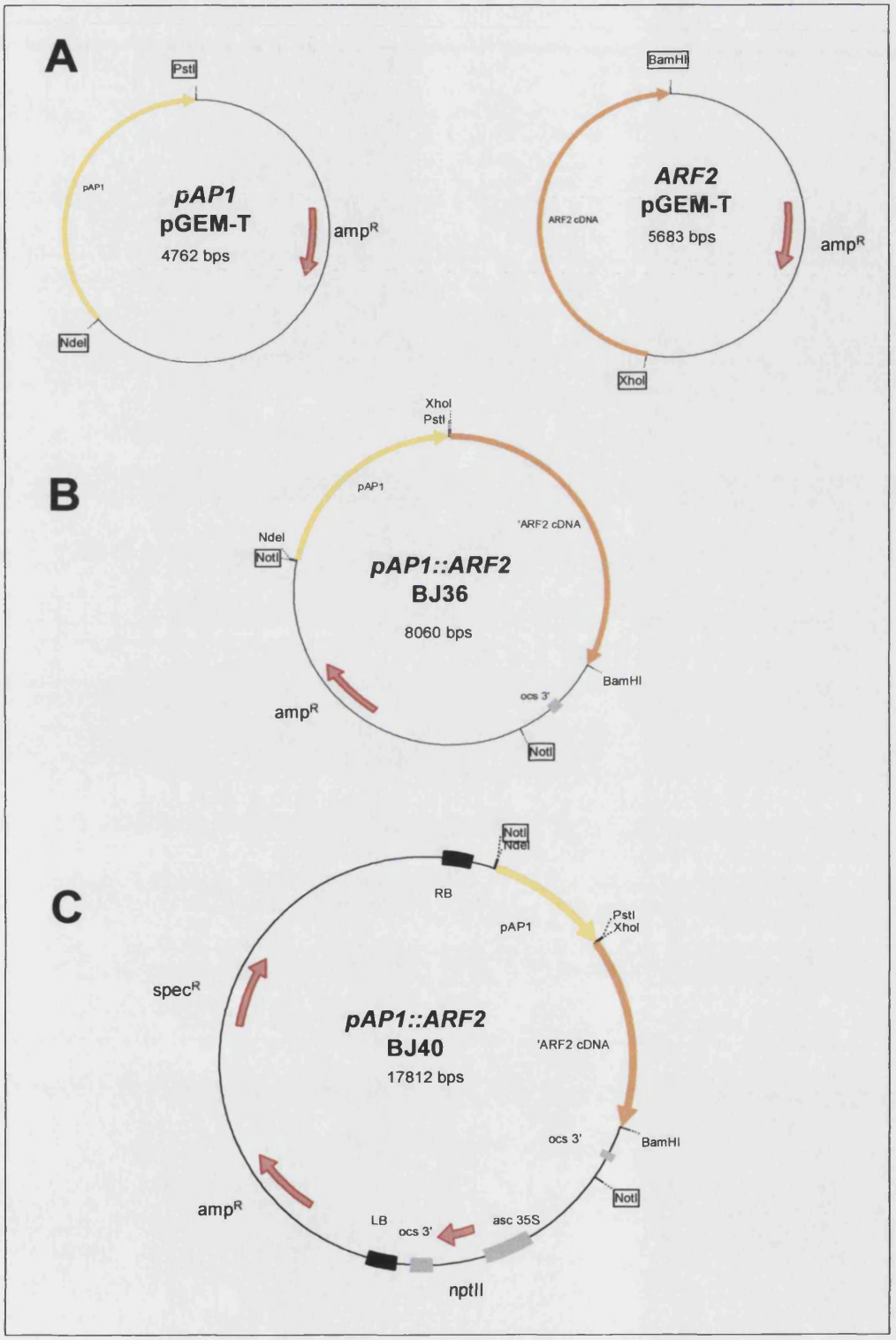
A
PstI
pAP1
pAP1
pGEM-T
4762 bps
ampR
NdeI
BamHI
ARF2
pGEM-T
ARF2 cDNA
5683 bps
ampR
XhoI
B
XhoI
PstI
pAP1
'ARF2 cDNA
NdeI
NotI
pAP1::ARF2
BJ36
8060 bps
BamHI
ocs 3'
ampR
NotI
C
NotI
NdeI
RB
pAP1
PstI
XhoI
specR
pAP1::ARF2
BJ40
17812 bps
'ARF2 cDNA
ocs 3'
BamHI
NotI
ampR
LB
ocs 3'
asc 35S
nptII

Figure 6.1 Construction of the *pAP1*::*ARF2* binary vector. A: The promoter *pAP1* PCR fragment was ligated into the pGEM-T vector creating *pAP1* pGEM-T. *ARF2* pGEM-T had been created for the construction of p35S::*MNT* previous chapter. B: The promoter fragment was removed from pGEM-T using SalI and XbaI and ligated into BJ36; subsequently the cDNA fragment was removed from pGEM-T using BamhI and XhoI and ligated into BJ36 adjacent to the promoter fragment creating *pAP1*::*ARF2* BJ36. C: The *pAP1*::*ARF2* cassette was lifted from BJ36 using NotI and ligated into the binary vector BJ40 thereby creating the vector *pAP1*::*ARF2* BJ40.

6.2.1.3 The *pAP1*::*ARF2* expression cassette rescues flower opening and fertility in *arf2* mutant plants

79 plants of the T_2 generation were examined for floral phenotype. The plants were grouped into 3 categories containing the following distribution of floral phenotypes:

I – *arf2*-like phenotype 54% (45 plants)

II – intermediate phenotype 18% (14 plants)

III – wild type-like phenotype 28% (22 plants)

The *arf2*-like phenotype is characterised by the presence of unopened flowers on the primary inflorescence of young adult plants, with no visible petals and total sterility of young flowers (Figure 6.3, A+B). Plants of the intermediate phenotype contain some open or half-open flowers revealing a limited number of petals, but they are also sterile (Figure 6.3, C). Flowers of the WT-like phenotype show normal opening with expanding petals and these flowers are also fertile (Figure 6.3, D-F). Unlike true wild type flowers, the carpels of flowers in category III appear slightly longer (see Figure 6.3 F). In a preliminary estimation of pod numbers produced on each genotype the fertility of category III plants was compared to the fertility of wild type plants. According to this estimation the fertility of both genotypes is similar (this work was performed by Rhiannon Hughes, University of Bath).

6.2.1.4 The seed weight of wild type-like *arf2* plants rescued by the *pAP1::ARF2* transgene is not negatively affected by the partial rescue of the floral phenotype.

The following seed weights were obtained by Rhiannon Hughes (University of Bath). Despite a WT-like morphology, the seed of plants from the *arf2/arf2* background that were rescued by the *pAP1::ARF2* transgene is about 40% heavier than wild type C-3 seed produced by plants grown under the same conditions. The average seed weight of the transgenic lines (N=10) was found to be 27.7µg, while control seed (N=2) weighed 20.1µg.

Seeds produced by wild type-like transgenic plants are also of similar shape as *arf2* seeds as shown in Figure 6.2.

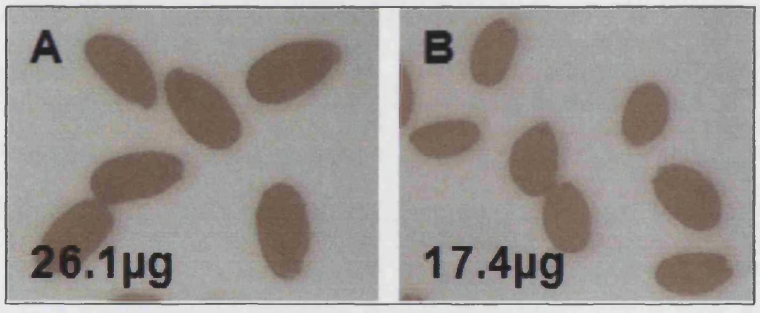

Figure 6.2 *arf2*-like seed shape on mutant plants transformed with the *pAP1::ARF2* transgene. A: *arf2-AP1::ARF2* (wild type like) B: col-3 control pictures taken at same magnification. Average seed weight of batch shown below. Pictures by Rhiannon Hughes.

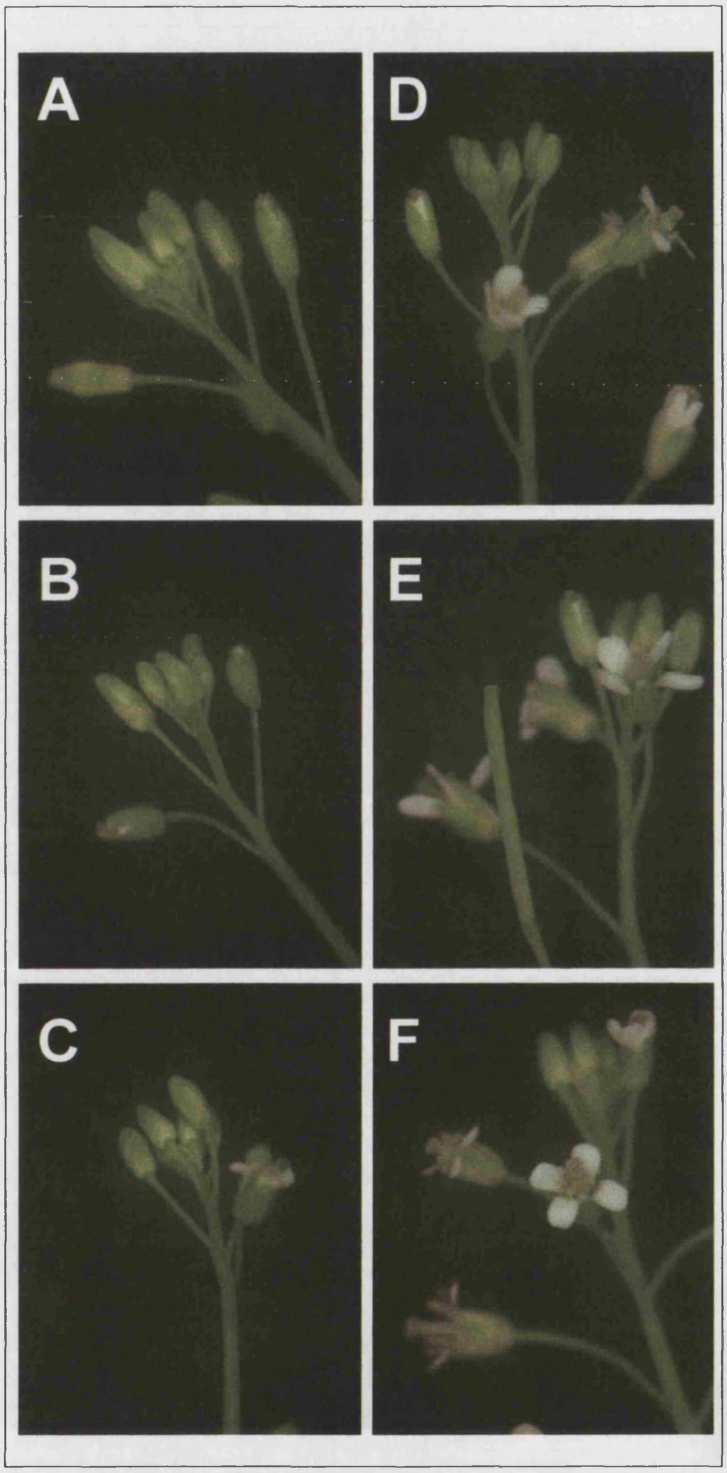

Figure 6.3 Plants of the *arf2/arf2* background transformed with the *pAP1::ARF2* vector. Each inflorescence shown represents an individual insertion event. A+B: category I; C: category II; D-F: category III. All inflorescences photographed at the same magnification. Developing seed pod in E.

6.2.2 Increasing *ARF2* transcript in wild type ovules using the *pINO*::*ARF2* transgene

To assess if a localised increase of *ARF2* transcript in the developing integuments can cause a decrease in seed size, a *pINO*::*ARF2* expression cassette was constructed and transformed into wild type (Col-3) plants. This required the following steps:

1. The ligation of *ARF2* cDNA into the BJ36 shuttle vector containing the *INO* promoter.
2. The production of a binary vector containing the *pINO*::*ARF2* expression cassette in BJ40.
3. The production of plant lines expressing the *pAP1*::*ARF2* transgene by *A. tumefaciens* mediated transformation.

6.2.2.1 Cloning of the *pINO*::*ARF2* expression vector

A 1764bp upstream region of *INO* (AT1G23420) bordered by NdeI and MluI linkers had previously been cloned into BJ36 by Robert Day and the promoter-containing vector was named *pINO* BJ36.

ARF2 cDNA was excised from *ARF2* pGEM-T using BamHI and XhoI and ligated into *pINO* BJ36 thereby creating *pINO*::*ARF2* BJ36. The promoter-cDNA cassette was lifted from BJ36 and ligated into BJ40 at the NotI site, creating *pINO*::*ARF2* BJ40 (Figure 6.4).

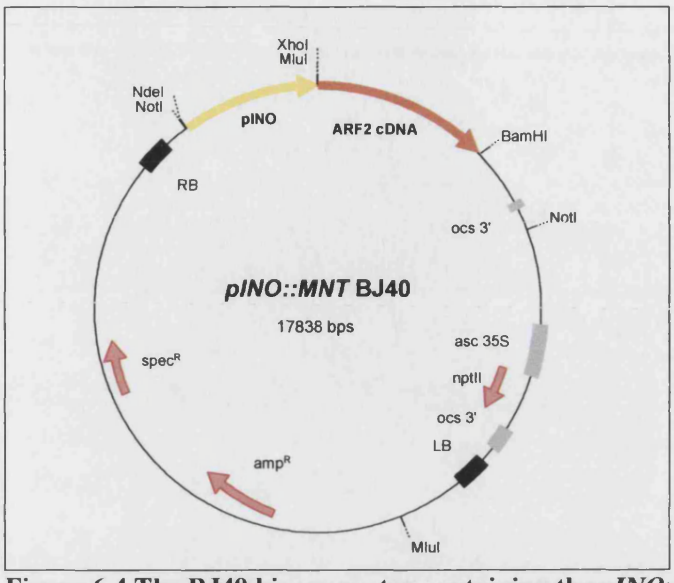

Figure 6.4 The BJ40 binary vector containing the *pINO*::*ARF2* expression cassette.

6.2.2.2 Verification of plants containing the *pINO*::*ARF2* insert

The *pINO*::*ARF2* transgene is linked to the *NPTII* kanamycin resistance gene which is present in the BJ40 vector. Presence of the transgene was verified by germinating seed in the presence of kanamycin in selective medium and scoring for the survival of seedlings. Seed of primary transformant (T_1) plants was again sown on selective medium in order to estimate the number of inserts in each transformed line. A Chi2 test was used to calculate that out of the 9 lines sown on selective medium, 6 lines contained inserts in a single locus, while the segregation pattern of 3 lines contained two or more inserts.

Primers 'pINO_RNAi_EcoF' and 'MNTR_check' were used to confirm the presence of the *pINO*::*ARF2* transgene in plants. These primers amplify a 1.8kbp fragment containing both promoter and cDNA sequence.

The resulting PCR was positive for all plant lines that were verified as exemplified in Figure 6.5.

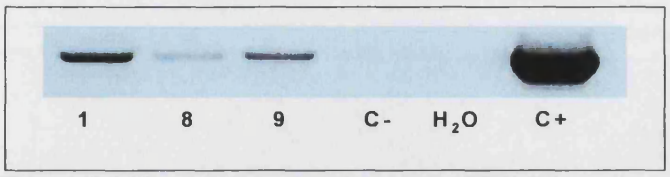

Figure 6.5 Electrophoresis gel loaded with PCR product amplifying a fragment containing *INO* promoter as well as *ARF2* cDNA sequence. Band sizes are approximately 1.8kb confirming presence of *pINO*::*ARF2* insert in lines 1, 8 and 9 of transgenic plants of wild type background using total genomic DNA as template. C-: negative control using wild type col-3 genomic DNA, H2O: water control, C+: positive control using diluted BJ40 plasmid containing the *pINO*::*ARF2* cassette.

6.2.2.3 The *pINO*::*MNT* transgene does not affect seed weight in the wild type background.

The overall morphology of wild type plants transformed with the *pINO*::*MNT* transgene was indistinguishable from wild type control plants. A significant decrease in seed weight of transformed plants was not observed except in the transgenic line #9, the seed of which weighed an average of only 8.9µg in the T_1 generation. In order to test if the low seed weight observed in this generation was linked to this genotype, line #9 and five other lines (the weights of two of which are represented in Figure 6.6) were subsequently grown for another two generations. Three lines were chosen for their abnormally low seed weight (line 9) and the confirmed presence of a single insert (as lines 1 and 8). Seed weights of subsequent generations showed that the low seed weight phenotype was not inherited in line #9 as the seed weight of subsequent generations (T_2-T_3) did not differ significantly from seed weight produced by wild type plants grown under the same conditions (15.2µg) therefore indicating that the initial change in seed size was an artefact.

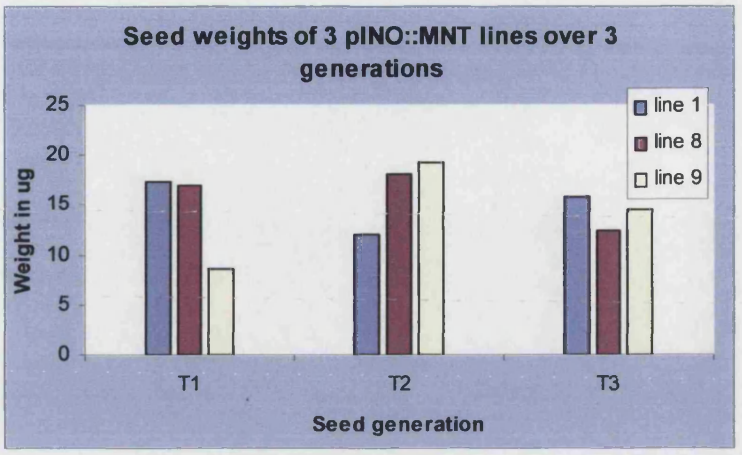

Figure 6.6 Average seed weight over 3 generations (T_1-T_3) of 3 transgenic lines (lines 1,8 and 9) transformed with *pINO::MNT*. Lines 1 and 8 were shown to contain a single copy of the *pINO::MNT* insert, while line 9 contains multiple inserts (segregation patterns as verified by a Chi2-test). Average seed weight of untransformed control: 15.2µg.

6.2.3 Selective suppression of *ARF2* in wild type ovules using RNA interference

To suppress *ARF2* expression specifically in the integuments of wild type ovules, an *ARF2*-RNAi construct driven by the *INO* promoter was cloned and transformed into wild type (Col-3) plants requiring the following steps:

1. The amplification of the *INO* promoter sequence from genomic DNA.
2. Replacing the 35S CaMV constitutive promoter of the pFGC5941 ChromDB vector (http://www.chromdb.org/) with the *INO* promoter.
3. The introduction of the inverted *ARF2* cDNA fragments.
4. The production of plant lines expressing the *pINO::ARF2* RNAi transgene by *A. tumefaciens* mediated transformation.

6.2.3.1 Cloning the *pINO::ARF2* RNAi expression vector

To amplify the *INO* promoter with EcoRI and NcoI linkers, primers 'pINO Eco F' and 'pINO Nco R' were designed against a sequence of 1,770bp upstream of the INO coding region.

The *pINO* PCR fragment was amplified from genomic DNA template and ligated into the pGEM®-T vector thereby creating *pINO* pGEM-T (Figure 6.7A). The 570bp *ARF2* cDNA fragment was obtained by digestion of the p35S::*ARF2* RNAi vector shown in Chapter 5.

The 35S promoter was removed from pFGC5941 using the EcoRI and NcoI restriction sites (Figure 6.7B) and replaced with the *pINO* fragment, which had been lifted from pGEM-T, thus creating *pINO* pFGC5941 (Figure 6.7C). Next, the *ARF2* cDNA fragment bordered by AscI and SwaI was removed from p35S::*ARF2* RNAi (see Chapter 5) and ligated into the SwaI/AscI site adjacent to the *INO* promoter, thereby creating *pINO*::*ARF2* pGFC5941 Step1 (Figure 6.7D). Finally, the *ARF2* cDNA fragment, bordered by BamHI and XbaI, was excised from p35S::*ARF2* RNAi and ligated into *pINO*::*ARF2* pFGC5941 between the chs intron and ocs3' (Figure 6.7E) which completed the cloning (Step 2) of *pINO*::*ARF2* pFGC5941, a binary vector with basta in planta selection.

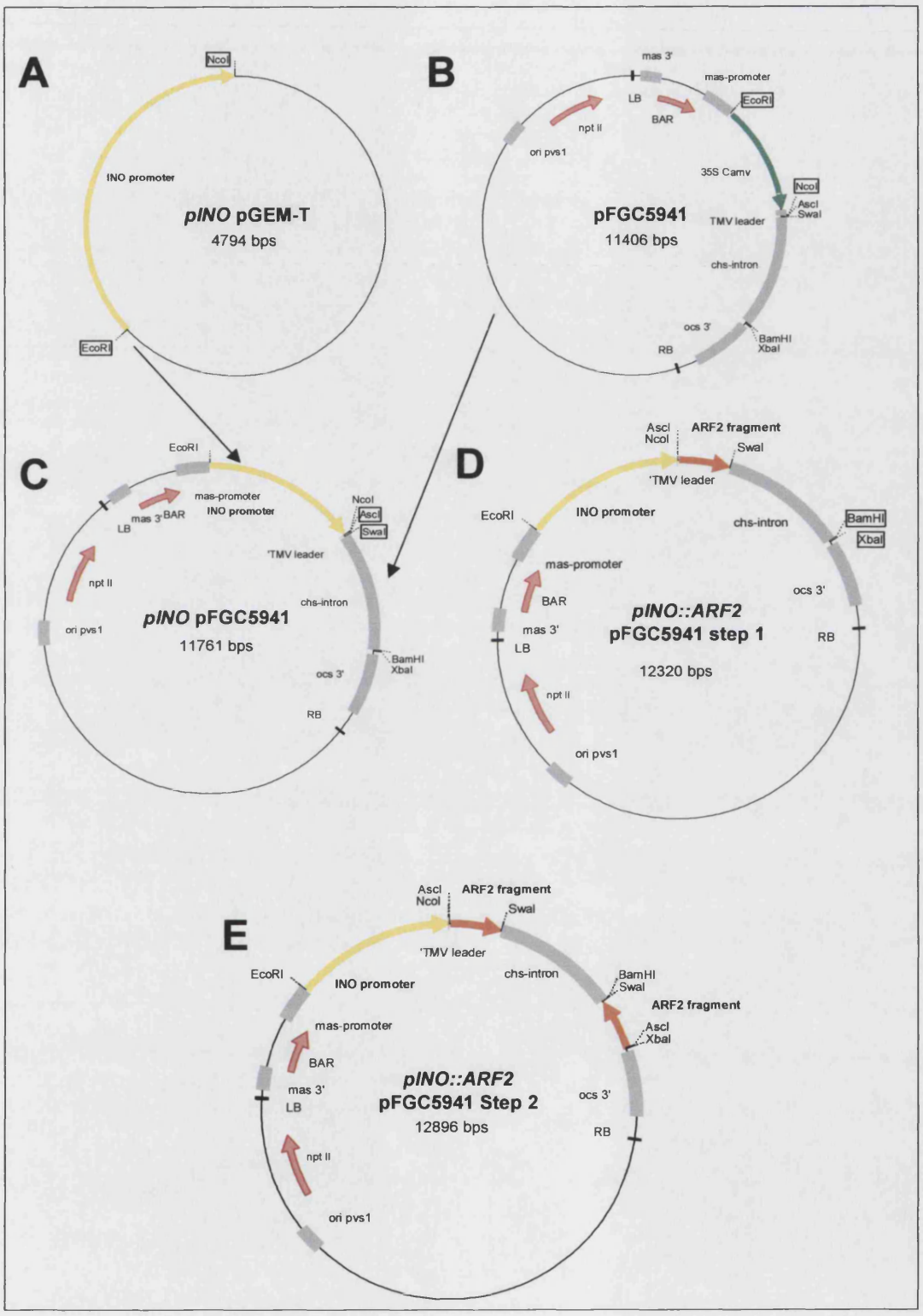
A
NcoI
INO promoter
pINO pGEM-T
4794 bps
EcoRI
B
mas 3'
mas-promoter
LB
BAR
EcoRI
npt II
ori pvs1
35S Camv
NcoI
AscI
SwaI
pFGC5941
11406 bps
TMV leader
chs-intron
ocs 3'
BamHI
XbaI
RB
C
EcoRI
mas-promoter
mas 3'
BAR
LB
INO promoter
NcoI
AscI
SwaI
'TMV leader
npt II
chs-intron
pINO pFGC5941
11761 bps
ori pvs1
BamHI
XbaI
ocs 3'
RB
D
AscI
NcoI
ARF2 fragment
SwaI
'TMV leader
EcoRI
INO promoter
chs-intron
BamHI
XbaI
mas-promoter
ocs 3'
BAR
pINO::ARF2
pFGC5941 step 1
mas 3'
LB
RB
12320 bps
npt II
ori pvs1
E
AscI
NcoI
ARF2 fragment
SwaI
'TMV leader
EcoRI
INO promoter
chs-intron
BamHI
SwaI
ARF2 fragment
mas-promoter
AscI
XbaI
BAR
mas 3'
pINO::ARF2
pFGC5941 Step 2
ocs 3'
LB
12896 bps
RB
npt II
ori pvs1

Figure 6.7 Construction of the *pINO*::*ARF2* RNAi vector. A: The *pINO* PCR amplicon was cloned into pGEM-T. B: The 35S promoter was removed from pFGC5941 using NcoI and EcoRI. C: *pINO* was ligated into the promoterless RNAi vector. D: The *ARF2* forward fragment was ligated into *pINO* pFGC5941 using the SwaI and NcoI sites thereby completing Step 1. E: The same *ARF2* cDNA fragment in the reverse orientation was ligated into the BamHI and XbaI sites, thereby completing the cloning (Step 2) of *pINO*::*ARF2* pFGC5941.

6.2.3.2 Verification of plants carrying the *pINO*::*ARF2* transgene

The *pINO*::*ARF2*-RNAi transgene is coupled with the BAR gene, which confers in planta resistance to glufosinate (basta) selection. Seedlings that tested positive for the presence of the BAR transgene were re-tested by PCR for the presence of the *pINO::ARF2-RNAi* transgene using primers '(check)INO:MNT RNAi F' and '(check)INO:MNT RNAi R' that amplify a fragment of 520bp:

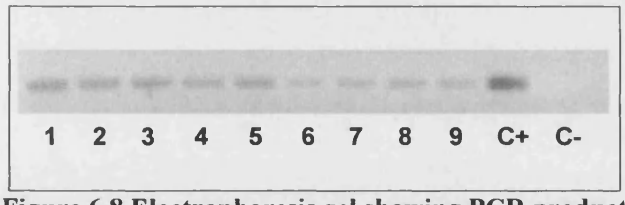

Figure 6.8 Electrophoresis gel showing PCR product amplified from *ARF2* genomic DNA and the pFGC5941 vector in 9 transgenic lines. 1-9: transgenic T_1 lines using total genomic DNA as template. C+: positive control using plasmid DNA of *pINO*::*ARF2* pFGC5941 as template. C-: negative control, H2O template. A negative control using genomic DNA of an untransformed line has also been included to validate this reaction (not shown).

6.2.3.3 The pINO::MNT-RNAi transgene does not significantly affect seed weight.

The following seed weights were obtained by Rhiannon Hughes (University of Bath) from plants of the T_1 generation. With no obvious changes to seed shape and size and an

average of 22.2µg (N=6), and lower, no significant increase in seed weight was observed in plant lines transformed by the *pINO*::*ARF2*-RNAi transgene.

6.2.4 Affecting cell division in the integuments using the p*INO*::ANT expression cassette

6.2.4.1 Confirming presence of the p*INO*::ANT insert in transgenic plants

The *pINO*::ANT expression cassette was designed and cloned into the BJ40 binary vector by Robert Day (University of Bath). The expression cassette contains a fragment of about 1.76bp genomic sequence directly upstream of the *INO* gene (AT1G23420) and a 1.8kbp sequence containing all of the ANT cDNA (AT4G37750) as well as 110bp of 5'UTR. Plants containing the p*INO*::ANT transgene were selected using kanamycin-containing medium.

The presence of the correct insert in plants that grew on selective medium was again confirmed using PCR as shown in Figure 6.9. Primers to a 913bp fragment overlapping both *INO* promoter and ANT cDNA sequence (named NM2F and NM2R) were designed by Nancy Mendoza (University of Bath).

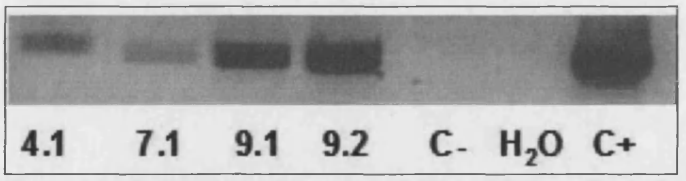

Figure 6.9 Electrophoresis gel showing PCR product amplified from a fragment containing *INO* promoter and ANT cDNA sequence of approximately 913bp. Lanes 1-4: transgenic lines; lane 5: negative control using untransformed col-3 genomic DNA; lane 6: H2O control; lane 7: diluted p*INO*::ANT BJ40 vector plasmid control.

6.2.4.2 The p*INO*::*ANT* expression cassette affects seed size and shape in wild type *A. thaliana*

Ten transformed lines containing the p*INO*::*ANT* insert were grown and analysed for heritable seed size-affecting traits. The average weight seed produced by the T_1 generation was 24.7μg (N=10) compared to the control weight of 22.9μg of the wild type control. Two abnormal seed weights were observed in line 2 (8.3μg) and line 5 (35.2μg). However, neither line showed inheritance of this seed weight phenotype in subsequent generations. Seeds produced by plants of line 9 weighed an average of 25.1μg in the T_1 generation. However, plants of this line containing the transgene in subsequent generations showed an abnormal seed shape phenotype as shown in Figure 6.10. Seed produced by plants of p*INO*::ANT transgenic line 9 were of irregular shape and size. Seed shape, although highly varied, could be described as elongated with a rough surface. Furthermore, seed of the same pod generally did not separate unless manually teased apart and therefore the seeds appeared clumped and fused. When observed under the dissecting microscope as shown in Figure 6.10, it was possible to identify the shape and position of the green embryo which is visible through the seed coat of transgenic seed under the dissecting microscope. As represented in Figure 6.10C, the overall shape of mature wild type seed (left) appear round and it contains a curled embryo of which the cotyledons are positioned in parallel next to the radicle. However, the majority of transgenic seed (right) did not show the characteristic curvature. Although the overall size of the transgenic embryo appeared to be similar to the size of a wild type embryo, it was generally not curved at all or shows only a slight curvature comparable to an early walking stick stage.

The shape of seed produced by this line in generation T_2 was also observed in subsequent generations. Work on this line was continued by Melissa Spielman, University of Bath.

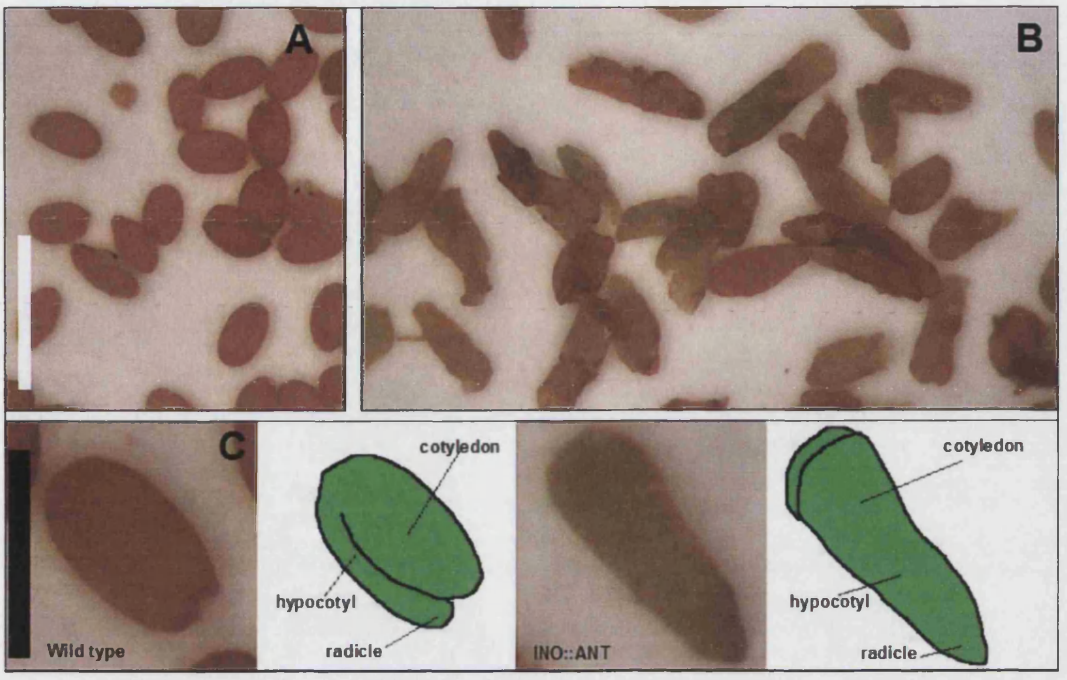

Figure 6.10 The effect of the p*INO*::ANT expression cassette on the shape of wild type seed in plants of line 9, generation T_2. A: wild type untransformed control (white bar = 1mm); B: p*INO*::ANT line 9.1 (same magnification as A); C- from left to right: magnified wild type seed (black bar: 0.5mm), schematic of embryo, magnified seed of line 9.1 (same magnification as wild type), schematic of line 9.1 embryo.

6.3 Discussion

6.3.1 Rescuing of flower opening as well as fertility with *pAP1::ARF2*

When driven by the floral homeotic gene promoter *pAP1*, re-introduction of *ARF2* into plants of the *arf2* mutant background was able to cause restoration of the flower opening phenotype. The fertility of the rescued flowers was also improved while maintaining the large-seed phenotype characteristic of the *arf2* mutant. This is an important result with respect to our aim to improve seed yield by improving seed size, as the *arf2::pAP1::ARF2* mutant plants combines the large seed phenotype with what appears to be ordinary levels of seed set.

The sepal:petal and carpel:anther length ratio data presented in Chapter 4 suggests that the sterility of *arf2* mutant flowers is due to a combination of non-opening flowers as well as a prohibitive length discrepancy between the stigma and anthers. However, the *arf2* lines rescued by the *pAP1::ARF2* transgene suggest otherwise. RNA expression studies showed that *AP1* expression is confined to the petal and sepal primordia (Mandel *et al.*, 1992). The conserved seed phenotype and otherwise *arf2*-like appearance of the transformed lines (category III) lead us to assume that transgenic *ARF2* is not found in regions other than the two outer whorls. Therefore it is possible to conclude that the changed sepal:petal ratio is the main factor impacting on *arf2* plant sterility. However, if deemed necessary, a *pAP1::GFP* reporter could be used to confirm the exact timing and location of expression exerted by the *pAP1* promoter fragment that was used for the *pAP1::ARF2* expression cassette. The *pAP1::GFP* reporter construct has been created and transformed into wild type *A. thaliana* (data not shown). However, no expression analysis of the *pAP1::GFP* transgenic lines has been undertaken so far.

Due to the improved fertility of plant lines created using the *pAP1::ARF2* expression cassette we have been able to create a useful tool to test whether the large-seed phenotype caused by the *arf2* mutation leads to a significant increase in yield. The transgenic lines can be used to test the effectiveness of *arf2*-led seed size increase and other *arf2*-led

phenotype without disturbing normal plant growth and seed set through pruning and manual pollination.

6.3.2 *pINO*-driven expression or suppression of *ARF2* does not have a significant impact on seed development

Neither the *pINO::ARF2* nor the *pINO::ARF2*-RNAi expression cassettes caused a heritable alteration of size in transgenic plants. Therefore we conclude that *pINO*-led increase or decrease of *ARF2* transcript in wild type integuments does not result in a significant modification of seed size. *INO* is known to be involved in the initiation of the outer integument, which fails to develop in *ino* mutant plants. However, despite the known involvement of *INO* during early ovule development, *ARF2* expression was not modified sufficiently by the promoter of this gene in order to disrupt normal integument development in the transgenic plant. A model for interactions among genes regulating ovule development was developed by Baker *et al.*, (1997). The model is based on the presumed function of six known genes in the chalazal developmental process (*ANT, BEL1, ATS, INO, SIN1* and *SUP*) and the involvement of each gene is derived from the studies of mutant phenotypes. According to previous studies *INO* expression occurs into the later stage of integument initiation, where the outer integument initiates after the inner integument has already started to extend (Baker *et al.*, 1997; Villanueva *et al.*, 1999). A modified version of a model by Baker *et al*, (1997) is shown in Figure 6.11. This model includes three possible points of *ARF2* involvement as indicated by numbers in brackets. In contrast to the other genes shown here, the involvement of *ARF2* is believed to be indirect because a mutation in *arf2* does not cause a complete disruption of the developmental process while mutations in any of the other genes terminates or severely disrupts development at the respective stage.

According to our phenotypic analysis of *arf2* presented in Chapter 4, the main involvement of *ARF2* during ovule maturation appears to occur during the process of inner- and outer integument development. This is due to the fact that differences in wild type and *arf2* mutant ovule development become visible only at the later stages of ovule maturation, when both integuments have started to elongate.

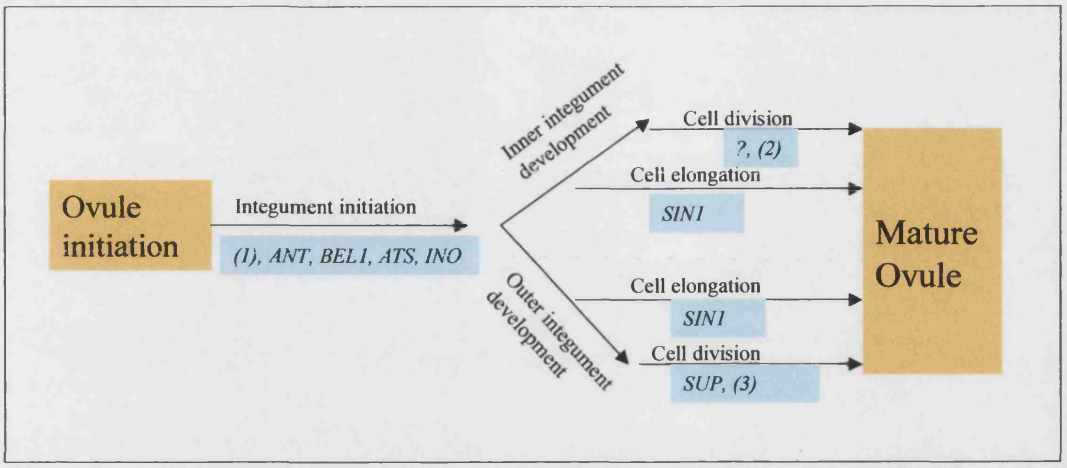

Figure 6.11 Model for the genetic control of integument development, modified from Baker *et al.*, (1999). The model shows chalazal development from ovule initiation to mature ovule. The pathway has been divided into inner- and outer integument development. Arrows are labelled by the processes which they represent and genes that are believed to be involved in each process are shown below the arrow and highlighted in light blue. Possible points of involvement by *ARF2* are indicated by numbers in brackets.

In the model shown in Figure 6.11 this would place *ARF2* involvement at the positions (2) and (3). However, gene expression studies using the *pARF2::GFP* reporter construct (Chapter 5) indicate that *ARF2* expression is strongest during the early stages of ovule development, placing the involvement of *ARF2* at position (1), much closer to the point of action of *INO*.

We have shown that the *arf2* mutation causes a pleiotropic phenotype and *ARF2* is known to be more widely expressed than *INO*. Furthermore, our expression analysis has shown that *ARF2* is expressed throughout both integuments of young ovules and *pARF2* expression is not just limited to the young ovules as expression can also be detected in the nucellus and in the funiculus. *INO* expression on the other hand is limited only to the primordium and the elongating tissue of the outer integument on the abaxial side of the chalaza. Neither the nucellus nor the funiculus are known as sites of *INO* mRNA expression as shown by Villanueva *et al.* (1999).

Compared to *INO,* it is more difficult to say at which point exactly *ARF2* exerts its influence over cell division in wild type integuments. However, the fact that *pINO*-driven expression (or suppression) of *ARF2* is not sufficient to affect integument development in the wild type background indicates that *ARF2* expression needs to be modified for a different duration or in more tissues in order to affect seed size.

6.3.3 *pINO*-driven expression of *ANT* just creates another *ino* mutant.

The introduction of the *pINO::ANT* expression cassette to the wild type plant has a strong impact on seed development as exhibited by transgenic line 9. The severe deformation of seed shape shown in Figure 6.10 could be interpreted as an overgrowth of integuments accompanied by a lack of ovule curvature leading to elongated seeds of irregular shape and size. However, the *pINO::ANT* expression cassette was designed with the objective to create an increase in cell division and expansion in the outer integument, thereby leading to an increase of overall seed size. This size increase was expected to be similar to the size increase seen in the *arf2* mutant.

ant mutant plants fail to initiate both integuments while *35S::ANT* expressing plants produce enlarged ovules that show signs of increased cell division and expansion ((Krizek, 1999; Mizukami and Fisher, 2000). These findings indicate a dual role of *ANT* which is to initiate integument development and to negatively influence cell division and expansion. (Mizukami, 2001) However, the *35S::ANT* phenotype is pleiotropic, causing a general increase in plant size. By placing *ANT* under control of *pINO* we expected to create a localised increase in cell division without affecting other aspects of plant morphology. We find that general plant morphology is indeed unaffected in *pINO::ANT* transgenic plants that exhibit changes in seed morphology. However, the impact on seed development is unexpected as it causes seed to develop an abnormal shape.

Asymmetric development of abaxial and adaxial integuments in the wild type seed causes the ovule to curve from stage 2-III (see Chapter 4, Introduction). The assymetric growth is believed to be influenced by the development of the outer integument as *ino* mutant ovules lack the characteristic curvature in addition to lacking an outer integument. However, it has also been hypothesised that *ANT* controls the expansion of the expression zone of *INO,* as *ant* mutant plants show accumulation of *INO* mRNA outside of the

abaxial size of the chalaza. (Villanueva *et al.*, 1999). The phenotype of *pINO::ANT* transgenic seed shows that transgenic alteration of plant morphology requires a very thorough understanding of the gene interactions that balance plant development. It appears as though the over-expression of *ANT* in the outer integument has indeed caused an increase in cell division within the integument. However, in addition to *ANT*-led hyperplasia of the integument, the expression of *ANT* in the region where *INO* is normally expressed had a detrimental effect on *INO* expression. It appears as though Villanueva *et al.*, (1999) were correct in their assumption that *ANT* negatively regulates *INO* expression and therefore the *pINO::ANT* transgenic plant is in fact just another *ino* mutant. *ino* mutants have been described as exhibiting complete female sterility (Baker *et al* ., 1997). The deformed seed of *pINO::ANT* transgenic plants on the other hand does give rise to viable seedlings and plants. This suggests that the suppression of *INO* in the transgenic line is not as severe as disruption of *INO* displayed by the *ino* mutants.

6.3.4 Further work

Successful transformation of the *35S::*Bn*ARF2*-RNAi vector into *B. napus* is an important step towards the application of the *mnt/arf2* study to increase seed yield in a crop species. Work on B.napus transformation has already been initiated as an RNAi vector was created for this purpose (not shown). The vector is suitable for *A. tumefaciens*-mediated transformation using *B. napus* tissue culture as recommended by the transformation protocol from Biotechnology Resources for Arable Crop Transformation (BRACT) website (http://www.bract.org/).

Further analysis of the phenotype of wild-type like *arf2* mutants rescued by the *pAP1:ARF2* transgene will be necessary to produce interesting data for two purposes. Firstly, a complete rescue of plant fertility must be achieved before the transformed lines can be used to establish whether an increase in seed yield can be obtained by the *arf2* mutation. Secondly, a comprehensive analysis of petal, sepal, anther and carpel lengths similar to the analysis of *arf2* in chapter 4 should be undertaken. This would contribute to our understanding of the true importance of flower opening with respect to plant fertility.

7 Discussion

We have set out to understand the mechanism behind *mnt*-led seed size change and to use the *mnt* model to create a paradigm for seed-size enhancement with possible applications to plant species other than the *A.thaliana* model plant. We have since gained detailed knowledge about the causes for seed size change on a phenotypic level by comparing *mnt* mutant and wild type plant morphology and we have gained a deeper understanding of *MNT/ARF2* gene expression with the help of expression vectors. This study has shown us how the wild type plant phenotype of *A. thaliana* can be changed in response to variation in *MNT/ARF2* levels that could be induced with the help of different transgenes. Finally - and again through the introduction of transgenes - we were able to test a number of theories about how the mutant phenotype could be induced and modulated in the mutant and wild type background.

7.1 Integument development in A. thaliana and other angiosperms

As detailed in Chapter 4 we learned that a significant increase in seed size and weight is achieved by a mother plant that is homozygous for the *mnt/arf2* mutation and that this increase is linked to changes to integument development. Our expression studies (Chapter 5) have provided additional evidence that mutant development is directly affected by *ARF2* expression, which is found throughout the young wild type ovule as well as other young organs. The *mnt/arf2* mutant has therefore been a useful model to demonstrate how seed development is modified to increase seed size. There are, however, still a number of important issues that could lead to question the validity of our *A. thaliana* model with respect to other plant species. Some of these issues are addressed here.
In order to integrate our findings into a worldwide effort to improve the seed yield of valuable crop species (Wollenweber *et al.*, 2005), we must first explore whether there is theoretical potential for applying our model to other angiosperm species. As our model predicts that the integument plays a leading role in setting seed size, we need to ensure that the basis for integument-led seed size manipulation exists not only in *A. thaliana* and closely related *Brassica* species but also in more distant relatives such as for example the rice plant.

Most plants appear to form integuments, which envelop the ovules as observed in *A. thaliana* (Bhatnagar and Johri, 1972). A few ategmic species that are devoid of recognisable integuments exist; however, these do not appear to occur among families of monocotyledenous plants (Bouman, 1984; Howell and Prakash, 1990). This is important, as rice – one of the most important crop plants of the world (Loftas, 1995) – is indeed a monocotyledonous species. Ovules with integuments can either be bitegmic with two discernable integuments, as for example in *A. thaliana*, or unitegmic with only a single integument as for example in certain *Petunia* species (Bouman, 1984; Fahn, 1990). The latter type is believed to have evolved from the bitegmic condition that represents the primitive form (Fahn, 1990; Bhatnagar and Johri, 1972).

A detailed study of integument development in *Oryza sativa* (rice) was performed by Lopez Dee *et al.* (1999). A schematic representation of the rice ovule compared to the ovule of *A. thaliana* based on this study is shown in Figure 7.1. When the development of the bitegmic rice ovule is compared to ovule development in *A. thaliana* a number of differences as well as similarities can be detected as outlined below.

As in *A. thaliana*, integument primordia of both the inner and outer integument in rice initiate on both sides at the base of the ovule primordium. (For a summary of *A. thaliana* ovule development see Chapter 1.) However, integument initiation occurs slightly earlier in rice with respect to megaspore mother cell development, as rice integuments can already be detected during the development of the archespore before differentiation into the megaspore mother cell. Three cell layers have been identified in the inner integument of *A. thaliana*, while the outer integument is made up of at least two cell layers (Beekman *et al.*, 2000). Conversely, the inner integument of rice appears to be comprised of two cell layers, while the outer integument is made up of three cell layers. While the inner integument is initiated first in *A. thaliana*, it is the outer integument that can be observed to differentiate before the inner integument in rice. Furthermore, growth of the outer integument in rice does not keep up with ovule curvature and although the mature ovule is entirely enclosed by inner integument, the outer integument encloses only the basal portion of the mature rice ovule. In addition to being surrounded by inner integument, the mature rice ovule is enclosed by the ovary wall. The mature *A. thaliana* ovule on the

other hand is not physically attached to the ovary wall except via the funiculus at the chalazal pole.

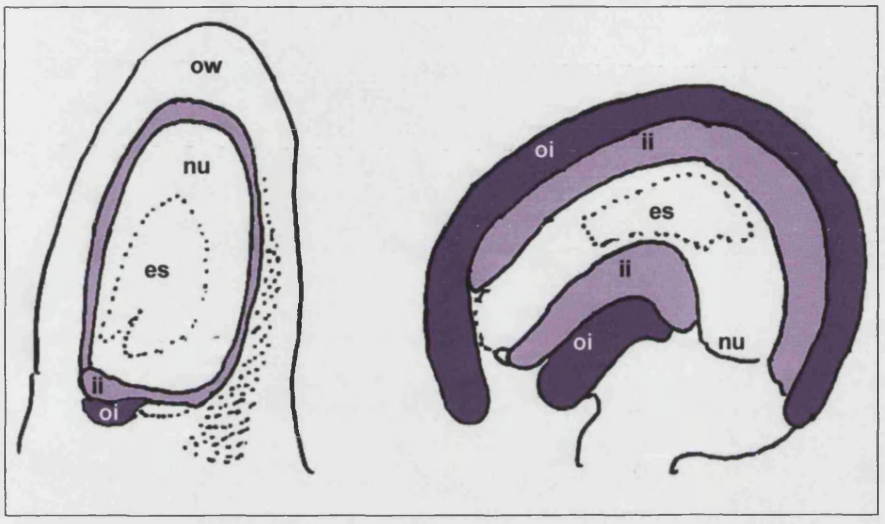

Figure 7.1 Schematic representations of mature ovules of rice (left) and *A. thaliana* (right) highlighting the position of the integuments. es: embryo sac, ii: inner integument, nu: nucellus, oi: outer integument, ow: ovary wall. Ovule sizes are not to scale.

The presence of integuments within most angiosperm families suggests that the role and function of the integument is conserved and therefore of significant importance. In addition, the discovery of *Ath-ARF2* homologues in *B. napus* (Chapter 3) and rice could suggest that the control of organ size is conserved among these plant species. Unfortunately, despite a wealth of information regarding the role and function of integuments in *A. thaliana*, nothing appears to be known of integument mutations that impact on seed production in other plant species. We can speculate that seed size is open to manipulation in species such as *O. sativa* by modifying the growth of the inner integument because the integument envelops the mature ovule in a manner comparable to *A. thaliana.* However, the difficulties encountered during our studies when trying to re-create integument-led seed size enhancement in a non-*ARF2*-led manner have already indicated that more work is required to improve our understanding of integument development (see Chapter 6).

7.2 Sterility and other seed-unrelated changes to *mnt/arf2* mutant morphology

Our analysis of *mnt/arf2*-induced plant morphology beyond the seed uncovered a multitude of other quantifiable changes to wild type growth and development. These changes, also detailed in Chapter 4, include altered petal:sepal ratios leading to mechanical sterility, increased rosette leaf number and sizes, delayed flowering time, a thicker and agravitropic inflorescence stem and slightly enhanced seedling root gravitropy.

The most negative pleiotropic effect of the *mnt/arf2* mutation on *A. thaliana* seed yield is the strongly reduced fertility of mutant plants. Consequently, much work has been dedicated to understand, quantify and counteract this feature of mutant morphology. The rescue of floral sterility using *pAP1*-driven re-introduction of *ARF2* detailed in Chapter 6 shows that we were able to successfully counteract the defective sterility while maintaining increased seed size. The hand-pollinated *mnt/arf2* mutant is fully fertile and the *mnt/arf2* mutant which has been rescued by an *AP1::ARF2* transgene exhibits complete reinstatement of successful self-fertilisation. We therefore have strong evidence to indicate that the sterility observed in the *mnt/arf2* mutant is not caused by abnormal ovule development and that this effect can be overcome through localised introduction of *ARF2* in mutant petals and sepals.

Interestingly, the *mnt/arf2* mutation appears to be the first *A. thaliana* integument mutant described to date in which altered integument development does not lead to female sterility. Well studied *A. thaliana* mutations that lead to female sterility caused by aberrant ovule development include *ino, ant, sup, bel, sin* (Robinson-Beers, Pruitt and Gasser, 1992; Gaiser, Robinson-Beers and Gasser, 1995; Klucher *et al.*, 1996; Elliott *et al.*, 1996; Baker *et al.*, 1997) and a number of other ovule mutants described by Schneitz *et al.*, (1997). These mutants are not only affected in seed size and shape but also exhibit complete or partial sterility, which cannot be overcome by manual pollination.

In light of our findings regarding mutant stem, leaf and seedling morphology we have concluded that a number of plant-wide abnormalities are caused by localised changes in cell size and number – the same changes that were observed in the integuments during ovule development. We have not been able to suppress these additional phenotypic

abnormalities while maintaining the large seed phenotype in a transgenic *mnt/arf2* plant. Re-creating the *mnt* phenotype by use of *pINO*-driven expression or suppression of *ARF2* and *ANT* has not been successful (Chapter 6). However, Rhiannon Hughes (University of Bath) is continuing the analysis of the *pINO::MNT::RNAi* line, which, in contrast to previous findings, may have a measurable impact on seed size without any associated negative consequences.

7.3 Potential applications of other *mnt/arf2*-led changes to plant morphology

Whether the changes to plant morphology observed in the *mnt/arf2* mutant model would translate to negative or positive effects on crop species from an agronomic point of view is not always obvious. As an example, the modification of leaf size could be seen as a negative effect, as it most likely requires a greater investment by the plant into a non-seed organ and also correlates with a modification in flowering time and harvest time. On the other hand, the larger leaf area caused by an increase in rosette leaf numbers translate into increased use of available light for photosynthesis by the individual plant, thereby positively impacting on total yield. Previous work done on photosynthesis rate and leaf exposure indicates that the capacity for light absorption is an important target for plant breeding and genetic engineering (Byzova *et al.*, 2004). In a study involving *A.thaliana* as an applied model for *B.napus,* petals, Byzova *et al.* (2004) successfully transformed into sepaloid organs in order to reduce a yield penalty implemented by the reflection and absorption of light caused by *B.napus* petals. Although it is important to keep in mind that increasing leaf surface area was not the primary aim of our study and that we do not intend to increase seed size by increasing leaf surface as well, it is interesting to see that there could be more uses for information gained from the *arf2/mnt* mutation that previously anticipated.

On the other hand, it is possible to imagine that the increased leaf number could translate into increased biomass in crop plants grown for leaf including forage crops or vegetables like cabbage.

7.4 Improving seed yield in the future, the fruits of a combined effort

The true effect of integument-led seed size enhancement on total yield and its ability to overcome the seed size versus number trade-off has yet to be fully explored. Although we cannot yet show the true effect of integument-led seed size enhancement on overall yield, our work has created a number of insights and tools such as the fertile *arf2:pAP1:ARF2* transgenic mutant that will be able to support future work on seed size enhancement and yield improvement. The next important target will be to create an expression cassette that can induce integument-led seed size enhancement in a crop which has the capacity to maintain the number of seeds produced by meeting the need to invest more resources into a larger seed sink size.

However, even if larger seed does not directly mean more yield under current plant growing practices, the capacity to produce larger seed will have other uses such as bestowing a new flexibility to plant breeders. As highlighted by Wollenweber *et al.*, (2005), future advances in yield improvement will probably need to come from a number of disciplines including plant genomics, plant physiology and agronomy as well as advanced modelling techniques.

Our understanding of plant structure, function and development is constantly being enriched by contributions such as the information gained form the work presented in this thesis. In the future, plant breeders may be able to use this information to create tool boxes of expression cassettes for any given crop species that, like add-ons for computer software, allow for the targeted manipulation of any given combination of parameters such as seed size, seed composition, stem length, stem thickness, leaf surface area, leaf number, root size, nitrogen use efficiency and so on. With minimal investment, a useful expression cassette could thus improve an existing variety with minimal impact on other developmental processes, thereby improving local plant varieties that are already adjusted to local climate, consumer demands or agricultural practices.

8 References

Abel S., and Theologis A. (1996). Early genes and auxin action. *Plant Physiology*, **111**, 9-17.

Adams S., Vinkenoog R., Spielman M., Dickinson H.G., and Scott R.J. (2000) Parent-of-origin effects on seed development in Arabidopsis thaliana require DNA methylation, *Development*, **127**, 2493-2502

Alexander H.M., and Wulff R.D. (1985) Experimental ecological genetics in Plantago X. The effects of maternal temperature on seed and seedling characters in P. lanceolata. *Journal of Ecology*, **73**, 271-282

Alonso J.M., Hirayama T., Roman G., Nourizadeh S., Ecker J.R., (1999) EIN2, a bifunctional transducer of ethylene and stress responses in *Arabidopsis*, *Science*, **284**, 2148-2152

Alonso J.M., Stepanova A.N., Leisse T.J., *et al.* (2003) Genome-wide Insertional mutagenesis of Arabidopsis thaliana, *Science*, **301**, 653-657

Alonso-Blanco C., Blankestijn-De Vries H., Hanhart C.J., and Kornneef M. (1999) *Proceedings of the National Academy of Sciences of the United States of America*, **96**, 4710-4717

Anderson P. (1995) Mutagenesis, *Methods in Cell biology*, **48**, 31-58

Arumuganathan K., and Earle E.D. (1991). Nuclear DNA Content of Some Important Plant Species. *Plant Molecular Biology Reporter*, **9**, 211-215

Austin R.B. (1980) Physiological limitations to cereal yields and ways of rescuing them by breeding. In *Opportunities for increasing crop yields* (eds R.G. Hurd, P.V.Biscoe and C. Dennis) pp3-20, Pitman, London

Austin R.B., Bingham J., Blackwell R.R., Evans L.T., Ford M.A., Morgan C.L., Taylor M. (1980) Genetic improvements in winter-wheat yields since 1900 and associated physiological-changes, *Journal of Agricultural Science*, **94**, 675-689

Baker S.C., Robinson-Beers K., Villanueva J.M., Gaiser J.C. and Gasser C.S, (1997) Interactions Among Genes Regulating Ovule Development in *Arabidopsis thaliana, Genetics*, **145**, 1109-1124

Balasubramanian S., and Schneitz K. (2002) *NOZZLE* links proximal-distal and adaxial-abaxial pattern formation during ovule development in *Arabidopsis thaliana. Development*, **129**, 4291-4300

Beeckman T., De Rycke R., Viane R. and Inzé D. (2000). Histological study of seed coat development in *Arabidopsis thaliana. Journal of Plant Research*, **113**, 139-148.

Bell C.J., and Ecker J.R. (1994) Assignment of 30 microsatellite loci to the linkage map of *Arabidopsis*, *Genomics*, **19**, 137-144

Berger F., (1999) Endosperm development, *Current Opinion in Plant Biology*, 2, 1-70

Berleth T., and Jürgens G. (1993). The role of the *monopteros* gene in organising the basal body region of the *Arabidopsis* embryo. *Development* **118**, 575-587.

Berleth T., Sachs T. (2001) Plant morphogenesis: long-distance coordination and local patterning, Current Opinion in Plant Biology, **4**, 57-62

Bhatnagar S.P. and Johri B.M. (1972) Development of Angiosperm Seeds, *In: Seed Biology*, Edited by Kozlowski T.T., Academic Press, New York

Bhatnagar S.P. and Sawhney V. (1981). Endosperm, its morphology, ultrastructure, and histochemistry. *International Review of Cytology*, **73**, 55-102

Blilou I., Frugier F., Folmer S., Serralbo O., Willemsen V., Wolkenfelt H., Eloy N.B., Ferreira P.C.G., Weisbeek P., Scheres B. (2002) The Arabidopsis HOBBIT gene encodes a CDC27 homolog that links the plant cell cycle to progression of cell differentiation, *Genes & Development*, **16**, 2566-2575

Blumenthal A., Kuznetzova L., Edelbaum O., Raskin V., Levy M., Sela I. (1999) Measurement of green fluorescence protein in plants: quantification, correlation to expression, rapid screening and differential gene expression, *Plant Science*, **142**, 93-99

Bouman F. (1984) The ovule. In *Embryology of angiosperms* (ed. B.M. Johri) pp. 123-157, Springer, Berlin

Boyes D.C., Zayed A.M., Ascenzi R., McCaskill A.J., Hoffman N.E., Davis K.R. and Görlach J., 2001, Growth Stage-Based Phenotypic Analysis of Arabidopsis: A Model for High Throughput Functional Genomics in Plants, *Plant Cell*, **13**, 1499-1510

Breyne P., Dreesen R., Vandepoele K., De Veylder L., Van Breusegem F., Callewaert L., Rombauts S., Raes J., Cannoot B., Engler G., Inze D., Zabeau M. (2002) Transcriptome analysis during cell division in plants, *Proceedings of the National Academy of Sciences of the United States of America*, **99**, 14825-14830

Brink R.A, and Cooper D.C. (1940). Double fertilization and development of seed in angiosperms. Botanical Gazette, **102**, 1–25

Brocklehurst P.A. (1977) Factors controlling grain weight in wheat, *Nature*, **266**, 348-349

Bushell C., Spielman M., Scott R.J. (2003) The Basis of Natural and Artificial Postzygotic Hybridization Barriers in *Arabidopsis* Species, *The Plant Cell*, **15**, 1430-1442

Byzova M., Verduyn C., and De Brouwer D. (2004) Transforming petals into sepaloid organs in Arabidopsis and oilseed rape: implementation of the hairpin RNA-mediated gene silencing technology in an organ-specific manner, *Planta*, **218**, 379-387

Chen J.G., Shimomura S., Sitbon F., Sandberg G., Jones A.M. (2001) The role of auxin-binding protein 1 in the expansion of tobacco leaf cells, *Plant Journal*, **28**, 607-617

Chen R, Guan CH, Boonsirichai K, Masson PH (2002) Complex physiological and molecular processes underlying root gravitropism, *Plant Molecular Biology*, **49**, 305-317

Cheng, W.-H., Taliercio, E. W. and Chourey, P. S. (1996). The *Miniature1* seed locus of maize encodes a cell wall invertase required for normal development of endosperm and maternal cells in the pedicel. *Plant Cell,* **8**, 971-983.

Chevalier D, Batoux M, Fulton L, Pfister K, Yadav RK, Schellenberg M, Schneitz K (2005) STRUBBELIG defines a receptor kinase-mediated signaling pathway regulating organ development in Arabidopsis, *Proceedings of the National Academy of Sciences of The United States of America*, **102**, 9074-9079

Choi Y., Gehring M., Johnson L., Hannon M., Harada J. J., Goldberg R. B., Jacobsen S. E. and Fischer R. L. (2002). *DEMETER*, a DNA glycosylase domain protein, is required for endosperm gene imprinting and seed viability in *Arabidopsis. Cell,* **110**, 33-42.

Chojecki A.J.S., Bayliss M.W. and Gale M.D.,(1986), Cell Production and DNA Accumulation in the wheat endosperm,and their association with grain weight, *Annals of Botany*, **58**, 809-817

Clough S. J. and Bent A. F. (1998). Floral dip: a simplified method for *Agrobacterium*-mediated transformation of *Arabidopsis thaliana. Plant J.* **16**, 735-743.

Cui K.H., Peng S.B., Xing Y.Z., Yu S.B. and Xu C.G. (2002). Molecular dissection of relationship between seedling characteristics and seed size in rice. *Acta Botanica Sinica* **44**, 702-707.

Davies D. R. (1975). Studies of seed development in *Pisum sativum.* I. Seed size in reciprocal crosses. *Planta,* **124**, 303-309.

Davies D.R., (1977) DNA Contents and Cell number in Relation to seed size in the genus Vicia, *Heredity*, **39**, 153-163

Debeaujon I., Léon-Kloosterziel K. M. and Koornneef M. (2000). Influence of the testa on seed dormancy, germination, and longevity in Arabidopsis. *Plant Physiology.* **122**, 403-413.

DEFRA, Agricultural Quick Statistics (2006), URL: http://statistics.defra.gov.uk/esg/quick/agri.asp, *Viewed March 2006.*

Dehio C., and Schell J. (1994) Identification of plant genetic loci involved in a post transcriptional mechanism for meiotically reversible transgene silencing. *Proceedings of the National Academy of Sciences of the United States of America*, **91**, 5538-5542

del Pozo JC, Dharmasiri J, Hellmann H, Walker L, Gray WM and Estelle M (2002) AXR1-ECR1–Dependent Conjugation of RUB1 to the Arabidopsis Cullin AtCUL1 Is Required for Auxin Response, *The Plant Cell*, **14**, 421-433

Desfeux C., Clough J and Bent A F (2000) Female reproductive tissues are the primary target of *Agrobacterium*-Mediated transformation by the Arabidopsis floral-dip method, Plant physiology, **123**, 895-904

Dillehay BL, Roth GW and Calvin DD, (2004) Performance of Bt corn hybrids, their near isolines, and leading corn hybrids in Pennsylvania and Maryland, *Agronomy Journal*, **96**, 818-824

Doganlar S., Frary A., and Tanksley S.D. (2000) The genetic basis of seed-weight variation: tomato as a model system, *Theoretical and Applied Genetics*, **100**, 1267-1273

Duvick D.N. (2005) The contribution of breeding to yield advances in maize (Zea mays L.), *Advances is Agronomy*, **86**, 83-145

Duvick D.N., Cassman K.G., (1999) Post-green revolution trends in yield potential of temperate maize in the north-central United States, *Crop Science*, **39**, 1622-1630

Elliott R. C., Betzner A. S., Huttner E., Oakes M. P., Tucker W.Q.J., Gerentes D., Perez P., and Smyth D. R.. (1996) *AINTEGUMENTA*, an *APETALA2*-like Gene of Arabidopsis with Pleiotropic Roles in Ovule Development and Floral Organ Growth, *Plant Cell*, **8**, 155-168.

Elliott R.C., Betzner A.S., Huttner E., Oakes M.P., Tucker W.Q.J., Gerentes D., Perez P., and Smyth D.R., (1996) *AINTEGUMENTA*, and *APETALA2*-like Gene of Arabidopsis with Pleitropic Roles in Ovule Development and Floral Organ Growth, *The Plant Cell*, **8**, 155-168

Ellis C. M., Nagpal P., Young J. C., Hagen G., Guilfoyle T. J. and Reed J. W. (2005). *AXIN RESPONSE FACTOR1* and *AXIN RESPONSE FACTOR2* regulate senescence and floral abscission in *Arabidopsis thaliana. Development*, **132**, 4563-4574.

Esau K. (1977) *Anatomy of Seed Plants*, 2nd ed. New York: Wiley.

Evans L.T. and Fischer R.A.(1999) Yield potential: Its definition, measurement, and significance, Crop Science, **39**, 1544-1551

Evenari M. (1984) Seed Physiology – From Ovule to Maturing Seed, *Botanical Review*, **50**, 143-170

Fahn, A. (1990). *Reproductive organs*. In Plant Anatomy, A. Fahn, ed (Oxford, UK: Pergamon Press), pp. 411–488

Friml J., and Palme K. (2002) Polar Auxin Transport – old questions and new concepts? *Plant Molecular Biology*, **49**, 273-284

G Howell and N Prakash (1990) Embryology and Reproductive Ecology of the Darling Lily, *Crinum flaccidum* Herbert. *Australian Journal of Botany*, **38**, 433 – 444

Gaiser J.C., Robinson-Beers K., and Gasser C.S., (1995) The Arabidopsis *SUPERMAN* Gene Mediates Asymmetric Growth of the Outer Integument of Ovules, *The Plant Cell*, **7**, 333-345

Garcia D., Fitz Gerald J. N. and Berger F. (2005). Maternal control of integument cell elongation and zygotic control of endosperm growth are coordinated to determine seed size in Arabidopsis. *Plant Cell*, **17**, 52-60.

Garcia D., Saingery V., Chambrier P., Mayer U., Jürgens G., and Berger F. (2003) Arabidopsis haiku Mutants Reveal New Controls of Seed Size by Endosperm, *Plant Physiology*, **131**, 1661-1670

Garcia-Hernandez M., and Reiser L (2002) *Using Information From Public Arabidopsis Databases to Aid Research*. In: Methods in Molecular Biology, vol. 323: Arabidopsis Protocols, Second Edition, J. Salinas and J. J. Sanchez-Serrano © Humana Press Inc., Totowa, NJ

Gelvin, S.B. (2003). Agrobacterium-mediated plant transformation: The biology behind the "gene-jockeying" tool. *Microbiology and Molecular Biology Reviews*. **67**, 16–37

Gifford, M.L., Dean S., and Ingram G.C. (2003) The Arabidopsis ACR4 gene plays a role in cell layer organisation during ovule integument and sepal margin development, *Development*, **130**, 4249-4258

Gleave A.P. (1992) A versatile binary vector system with a T-DNA organizational-structure conductive to efficient integration of cloned DNA into the plant genome, *Plant Molecular Biology*, **20**, 1203-1207

Goto N., and Pharis R.P. (1999) Role of gibberellins in the development of floral organs of the gibberellin-deficient mutant, *ga1-1*, of *Arabidopsis thaliana*, *Canadian Journal of Botany*, **77**, 944-954

Gray W.M., Kepinski S., Rouse D., Leyser O., Estelle M. (2001) Auxin regulates SCFTIR1-dependent degradation of AUX/IAA proteins, *Nature*, **414**, 271-276

Guberac V., Martinic J. and Maric S. (1998) Influence of seed size on germinability, germ length, root length and grain yield in spring oat. *Bodenkultur*, **49**, 13-18

Guilfoyle T., Hagen G., Ulmasov T., Murfett J., (1998) How does auxin turn on genes? Plant *Physiology*, **118**, 341-347

Hagen G., Guilfoyle T. (2002) Auxin-responsive gene expression: genes, promoters and regulatory factors, *Plant Molecular Biology*, **49**, 373

Hagen G., Guilfoyle T.J. (1985) Rapid Induction of Selective transcription by Auxins, *Molecular and Cellular Biology.*, **5**, 1197-1203

Hagen G., Martin G., Li Y., Guilfoyle T.J. (1991) Auxin-induced expression of the soybean GH3 promoter in transgenic tobacco plants, *Plant Molecular Biology*, **17**, 567-579

Haig D, Westoby M (1991) Seed size, pollination costs and angiosperm success, Evolutionary Ecology, **5**, 231-247

Hamann T., Mayer U., Jurgens G. (1999) The auxin-insensitive bodenlos mutation affects primary root formation and apical-basal patterning in the Arabidopsis embryo *Development*, **126**, 1387-1395

Hardtke, C. S. and Berleth, T. (1998). The *Arabidopsis* gene *MONOPTEROS* encodes a transcription factor mediating embryo axis formation and vascular development. *EMBO Journal.* **19**, 4997-5006.

Harper R. M., Stowe-Evans E. L., Luesse D. R., Muto H., Tatematsu K., Watahiki M. K., Yamamoto K. and Liscum E. (2000). The *NPH4* locus encodes the auxin response factor ARF7, a conditional regulator of differential growth in aerial Arabidopsis tissue. *Plant Cell*, **12**, 757-770.

Harper, J. L., Lovell, P. H. and Moore, K. G. (1970). The shapes and sizes of seeds, *Annual Review of Ecology and Systematics*, **1**, 327-356

Heyer, Arnd G., Raap, Maik, Schroeer, Birgit, Marty, Bruno & Willmitzer, Lothar (2004) Cell wall invertase expression at the apical meristem alters floral, architectural, and reproductive traits in *Arabidopsis thaliana*, *The Plant Journal* **39**, 161-169.

Hobbie L, McGovern M, Hurwitz LR, Pierro A, Liu NY, Bandyopadhyay A, Estelle M (2000) The axr6 mutants of Arabidopsis thaliana define a gene involved in auxin response and early development, *Development*, **127**, 23-32

Hooley R.(1998) Auxin Signaling: Homing in with Targeted Genetics, *Plant Cell*, **10**, 1581-1584

Horie T., Shiraiwa T. and Homma K. (2005) Can yields of lowland rice resume the increases that they showed in the 1980s?, *Plant Production Science*, **8**, 259-274

Hu Y., Xie Q., and Chua N.-H., (2003) The Arabidopsis auxin-inducible gene *ARGOS* controls lateral organ size, *Plant Cell*, **15**, 1951-1961

Hull R. (1983). The current status of plant viruses as potential RNA/DNA vector systems. *In Plant Biotechnology. Society for Experimental Biology Seminar Series 18. Eds. S.H. Mantell and H. Smith. Cambridge University Press.* pp 299-312

Hyten D. L., Pantalone V. R., Sams C. E., Saxton A. M., Landau-Ellis D., Stefaniak T. R. and Schmidt M. E. (2004). Seed quality QTL in a prominent soybean population. *Theoetical and Appied Genetics*, **109**, 552-561.

Jager CE, Symons GM and Ross JJ (2005) The brassinosteroid growth response in pea is not mediated by changes in gibberellin content, *Planta*, **221**, 141-148

Jander G., Baerson S.R., Hudak J.A., Gonzalez K.A., Gruys K.J., Last R.L. (2003) Ethylmethanesulfonate saturation mutagenesis in Arabidopsis to determine frequency of herbicide resistance, Plant Physiology, **131**, 139-146

Jefferson R.A., Kavanagh T.A., and Bevan M.W., (1987) GUS fusions: beta-glucuronidase as a sensitive and versatile gene fusion marker in higher plants, *The EMBO Journal*, **6**, 3901-3907

Key J.L., (1969), Hormones and nucleic Acid metabolism., *Annual Review of Plant Physiology*, **20**, 449-474

Khush G.S. (2005) What it will take to Feed 5.0 Billion Rice consumers in 2030?, *Plant Molecular Biology*, **59**, 1-6

Kieber J.J, Rothenberg M., Roman G., Feldmann K.A., and Ecker J., (1993) *CTR1*, a Negative Regulator of the Ethylene Response Pathway in Arabidopsis, Encodes a Member of the Raf Family of Protein Kinases, *Cell*, **72**, 427-441

Kim BC, Soh MS, Kang BJ, Furuya M, Nam HG (1996) Two dominant photomorphogenic mutations of Arabidopsis thaliana identified as suppressor mutations of hy2, *Plant Journal*, **9**, 441-456

Kim J, Harter K, Theologis A (1997) Protein-protein interactions among the Aux/IAA proteins, *Proceedings of the National Academy of Sciences of the United States of America*, **94**, 11786-11791

Kim SK, Chang SC, Lee EJ, Chung WS, Kim YS, Hwang S, Lee JS (2000) Involvement of brassinosteroids in the gravitropic response of primary root of maize, *Plant Physiology*, **123**, 997-1004

Klucher K. M., Chow H., Reiser L., and Fischer R. L.(1996) The *AINTEGUMENTA* Gene of Arabidopsis Required for Ovule and Female Gametophyte Development Is Related to the Floral Homeotic Gene *APETALA2*, *Plant Cell*, **8**, 137-153

Klucher K.M., Chow H., Reiser L. and Fisher B. (1996) The *AINTEGUMENTA* Gene of Arabidopsis Required for Ovule and Female Gametophyte Development Is Related to the Floral Homeotic Gene *APETALA2*, *The Plant Cell*, **8**, 137-153

Knox K., Grierson C.S., Leyser O. (2003)*AXR3* and *SHY2* interact to regulate root hair development, Development, **130**, 5769-5777

Koelewijn H.P. and van Damme J.M.M. (2005) Effects of seed size, inbreeding and maternal sex on offspring fitness in gynodioecious Plantago coronopus, *Journal of Ecology* **93** , 373–383

Konieczny A., and Ausubel F.M. (1993) A procedure for mapping *Arabidopsis* mutations using codominant ecotype-specific PCR-based markers. *Plant Journal*, **4**, 403-410

Koornneef M., Alonso-Blamco C., de Vries H.B., Hanhrt C.J. and Peeters A.J.M. (1998) Genetic interactions Among late-flowering mutants of Arabiodpsis, *Genetics*, **148**, 885-892

Krannitz P.G., Aarssen L.W., and Dow J.M., (1991) The effect of genetically based differences in seed size on seedling survival in Arabidopsis thaliana (Brassicaceae), *American Jounral of Botany*, **78**, 446-450

Krizek B.A. (1999) Ectopic expression of *AINTEGUMENTA* in Arabidopsis plants results in increased growth of floral organs, **25**, 224-36

Krizek BA (1999) Ectopic expression AINTEGUMENTA in Arabidopsis plants results in increased growth of floral organs, *Developmental Genetics,* **25**, 224-236

Lemontey C., Mousset-Déclas, Munier-Jolain N., and Boutin J.-P. (2000) Maternal genotype influences pea seed size by controlling both mitotic activity dirung early embryogenesis and final endoreplication level/cotyledon cell size in mature seed. *Journal of Experimental Botany*, **51**, 167-175

Léon-Kloosterziel K.M., Keijzer C.J., and Koornneef M.(1994) A Seed Shape Mutant of Arabidopsis That Is Affected in Integument Development, *Plant Cell*, **6**, 385-392

Leyser O. (2002). Molecular genetics of auxin signaling. *Annual Review of Plant Biology*, **53**, 377-398.

Li H., Johnson P., Stepanova A., Alonso J. M. and Ecker J. R. (2004). Convergence of signaling pathways in the control of differential cell growth in *Arabidopsis. Developmental Cell*, **7**, 193-204.

Liscum E., and Briggs W. E. (1996). Mutations of Arabidopsis in potential transduction and response components of the phototropic signaling pathway. *Plant Physiol.* **112**, 291-296.

Liscum E., and Reed J. W. (2002). Genetics of Aux/IAA and ARF action in plant growth and development. *Plant Molecular Biology*, **49**, 387-400.

Liu Z.B., Ulmasov T., Shi X.Y., Hagen G., Guilfoyle T.J. (1994) Soybean GH3 Promoter Ccontains Multiple Aauxin-Inducible Elements, *Plant Cell*, **6**, 645-657

Ljung K., Bhalerao RP, and Sandberg G. (2001) Sites and homeostatic control of auxin biosynthesis in Arabidopsis during vegetative growth, *The Plant Journal*, **28**, 465-474

Loftas T. (1995) Dimensions of need – In: *An atlas of food and agriculture, FAO* http://www.fao.org/documents/

Lopes M. A. and Larkins B. A. (1993). Endosperm origin, development, and function. *Plant Cell* **5**, 1383-1399.

Lopez-Dee ZP, Wittich P, Pe ME, Rigola D, Del Buono I, Gorla MS, Kater MM, Colombo L (1999) OsMADS13, a novel rice MADS-box gene expressed during ovule development, *Developmental Genetics*, **25**, 237-244

Lukowitz W., Gillmor C.S. and Scheible W.R. (2000) Positional cloning in *Arabidopsis*. Why it feels good to have a genome initiative working for you. *Plant Physiology*. **123**, 795-805

Mandel A.M., Gustafon-Brown C., Savidge B., and Yanofsky M.F (1992) Molecular Characterization of the Arabidopsis floral omeotic gene *APETALA1*, *Nature*, **360**, 273-277

Manga and Yadav (1995) Effect of Seed size on developmental traits and ability to tolerate drought in pearl-millet. *Journal of Arid Environments*, **29**, 169-172

Marchant A, Kargul J, May ST, Muller P, Delbarre A, Perrot-Rechenmann C, Bennett MJ (1999) AUX1 regulates root gravitropism in Arabidopsis by facilitating auxin uptake within root apical tissues, *EMBO Journal*, **18** , 2066-2073

Marshall D.L. (1986) Effect of seed size on seedling success in three species of Sesbania (Fabaceae). *American Journal of Botany*, **73**, 457-464

Matthew L. (2004) RNAi for plant functional genomics, *Comparative and functional genomics*, **5**, 240-244

Mattsson J, Ckurshumova W, Berleth T (2003) Auxin signaling in Arabidopsis leaf vascular development, *Plant Physiology*, **131**, 1327-1339

Mattsson J, Sung ZR, Berleth T (1999) Responses of plant vascular systems to auxin transport inhibition, Development, **126**, 2979-2991

Meinke D.W. (1994) Seed Development in *Arabidopsis thaliana* In: *Arabidopsis, Cold Spring Harbour Laboratory Press*

Meinke D.W., Cherry JM, Dean M, Rounsley SD, Koornneef M (1998) *Arabidopsis thaliana*: a model plant for genome analysis. Science, **282**, 662–682

Meister R.J., Kotow L.M., and Gasser C.G. (2002) SUPERMAN attenuates positive INNER NO OUTER autoregulation to maintain polar development of Arabidopsis ovule outer integuments, *Development*, **129**, 4281-4289

Meyer R. C., Törjék O., Becher M. and Altmann T. (2004). Heterosis of biomass production in Arabidopsis. Establishment during early development. *Plant Physiology* **134**, 1813-1823.

Miller M.E., and Chourey P.S. (1992) The Maize Invertase-Deficient *miniature-1* Seed Mutation Is Associated with Aberrant Pedicel and Endosperm Development, *Plant Cell*, **4**, 297-305

Mizukami Y. (2001) A Matter of siza: developmental control of orghan size in plants, *Current Opinion in Plant Biology*, **4**, 533-539

Mizukami Y., and Fischer R.L. (2000) Plant organ size control: *AINTEGUMENTA* regulates growth and cell numbers during organogenesis, *Proceedings of the National Academy of Sciences*, **97**, 942-947

Moriguchi K.,Suzuki T., ItoY., YamazakiY., NiwaY. and Kurata N. (2005) Functional isolation of novel nuclear proteins showing a variety of subnuclear localizations, *Plant Cell*, **17**, 389-403

Nagpal P, Walker LM, Young JC, Sonawala A, Timpte C, Estelle M, Reed JW (2000) AXR2 encodes a member of the Aux/IAA protein family, *Plant Physiology*, **123**, 563-573

Nagpal P., Ellis C. M., Weber H., Ploense S. E., Barkawi L. S., Guilfoyle T. J., Hagen G., Alonso J. M., Cohen J. D., Farmer E. E. *et al.* (2005). Auxin response factors ARF6 and ARF8 promote jasmonic acid production and flower maturation. *Development*, **132**, 4107-4118.

Nakagawa H., Ferrario S., Angenent G.C., Kobayashi A. and Takatsuji H. (2004) The Petunia Ortholog of Arabidopsis SUPERMAN Plays a Distinct Role in Floral Organ Morphogenesis, *Plant Cell*, **16**, 920–932

Ohto, M., Fischer, R. L., Goldberg, R. B., Nakamura, K. and Harada, J. J. (2005). Control of seed mass by *APETALA2. Proceedings of the National Academy of Sciences, of the United States of America*, **102**, 3123-3128.

Okada K., Ueda J., Komaki MK., Bell CJ., Shimura Y (1991) Requirement of the auxin polar transport-system in early stages of Arabiodpsis floral bud formation, *Plant Cell*, **3**, 677-684

Okushima Y., Overvoorde P. J., Arima K., Alonso J. M., Chan A., Chang C., Ecker J. R., Hughes B., Lui A., Nguyen D. *et al.* (2005a). Functional genomic analysis of the *AUXIN RESPONSE FACTOR* gene family members in *Arabidopsis thaliana*: unique and overlapping functions of *ARF7* and *ARF19. Plant Cell*, **17**, 444-463.

Okushima Y., Mitina I., Quach H.L., and Theologis A. (2005b) AUXIN RESPONSE FACTOR 2 (ARF2): a pleiotropic developmental regulator, *The Plant Journal*, **43**, 29–46

Patrick J.W., Offler C.E.,(1995) Post sieve-element transport of sucrose in developing seeds, *Australian Journal of Plant Physiology*, **22**, 681-702

Paul M.J. and Foyer C.H. (2001) Sink regulation of photosynthesis. *Journal of Experimental Botany*, **52**, 1381-1400

Peng S., and Senadhira S. (1998) Genetic Enhancement of Rice Yield, In: *Sustainability of rice in the global food system*, IRRI & Pacific Basin Study Center, Manila

Peng S., Laza R.C., Visperas R.M., Sanico A.L., Cassman A.G. and Khush G.S. (2000) Grain Yield of Rice Cultivars and Lines Developed in the Philippines since 1966, *Crop Science*, **40**, 307-314

Perin A., Araújo A. P and Teixeira M.G. (2002) Efeito do tamanho da semente na acumulação de biomassa e nutrientes e na produtividade do feijoeiro, *Brazilian Journal of Plant Physiology*, **37**, 1711-1718

Pfeiffer W.H., Sayre K.D., and Payne T.S. (2001) Increasing Durum Wheat Yield Potential and Yield Stability, In: *Research Highlights of the CIMMYT Wheat Program, 1999-2000.* Mexico, D.F.

Pickett FB. Wilson AK, and Estelle M (1990) The AUX1 Mutation of Arabidopsis confers both auxin and ethylene resistance, *Plant Physiology*, **94**, 1462-1466

Przemeck G. K. H., Mattsson J., Hardtke C. S., Sung Z. R. and Berleth T. (1996). Studies on the role of the *Arabidopsis* gene *MONOPTEROS* in vascular development and plant cell axialization. *Planta*, **200**, 229-237.

Radchuk VV, Van DT, Klocke E (2005) Multiple gene co-integration in Arabidopsis thaliana predominantly occurs in the same genetic locus after simultaneous in planta transformation with distinct Agrobacterium tumefaciens strains, *Plant Science*, **168**, 1515-1523

Reddy V. M. and Daynard T. B. (1983). Endosperm characteristics associated with rate of grain filling and kernel size in corn. *Maydica*, **28**, 339-355.

Reed J.W. (2001)Roles and activities of Aux/IAA proteins in Arabidopsis, *Trends in Plant Science*, **6**, 420-425

Reinhardt D, Mandel T, Kuhlemeier C (2000) Auxin regulates the initiation and radial position of plant lateral organs, *Plant Cell*, **12**, 507-518

Remington D.L., Vision T.J., Guilfoyle T.J., Reed J.W. (2004) Contrasting modes of diversification in the Aux/IAA and ARF gene families, *Plant Physiology*, **135**, 1738-1752

Reynolds M.P., Pellegrineschi A., Skovmand B. (2005) Sink-limitation to yield and biomass: a summary of some investigations in spring wheat, *Annals of Applied Biology*, **146**, 39-49

Reynolds M.P., van Ginkel M., Ribaut J.M. (2000) Avenues for genetic modification of radiation use efficiency in wheat, *Journal of Experimental Botany*, **51**, 459-473

Richard C, Lescot M, Inze D, De Veylder L (2002) Effect of auxin, cytokinin, and sucrose on cell cycle gene expression in Arabidopsis thaliana cell suspension cultures, *Plant Cell Tissue and Organ Culture*, **69**, 167-176

Robinson-Beers K., Pruitt R.E., and Gasser C.S. (1992) Ovule Development in Wild-Type Arabidopsis and Two Female-Sterile Mutants, *The Plant Cell*, **4**, 1237-1249

Ross JJ, O'Neill DP, Smith JJ, Kerckhoffs LHJ, Elliott RC (2000) Evidence that auxin promotes gibberellin A(1) biosynthesis in pea, *Plant Journal*, **21**, 547-552

Ruegger M, Dewey E, Hobbie L, Brown D, Bernasconi P, Turner J, Muday G (1997) Reduced naphthylphthalamic acid binding in the tir3 mutant of Arabidopsis is associated with a reduction in polar auxin transport and diverse morphological defects, *Plant Cell*, **9**, 745-757

Sabatini S, Beis D, Wolkenfelt H, Murfett J, Guilfoyle T, Malamy J, Benfey P, Leyser O, Bechtold N, Weisbeek P, Scheres B (1999) An auxin-dependent distal organizer of pattern and polarity in the Arabidopsis root, *Cell*, **99**, 463-472

Sakai H., Medrano L.J., Meyerowitz E.M., (1995) Role of *SUPERMAN* in maintaining *Arabidopsis* floral whorl boundaries, *Nature*, **378**, 199-203

Saniewski M, Ueda J, Miyamoto K (2002) Relationships between jasmonates and auxin in regulation of some physiological processes in higher plants, *Acta Physiologiae Plantarum*, **24**, 211-220

Sasahara (1984) Panicle Properties and Ripening, In: *Biology of Rice*, Elsevier, Amsterdam pp 173-184

Schaal B.A. (1980) Reproductive capacity and seed size in Lupinus texensis. *American Journal of Botany*, **67**, 703-709

Schneitz K., Hülskamp M. and Pruitt R. E. (1995). Wild-type ovule development in *Arabidopsis thaliana*: a light microscope study of cleared whole-mount tissue. *Plant Journal*, **7**, 731-749.

Schneitz K., Hülskamp M., and Pruitt R.E. (1995) Wilt-type ovule development in Arabidopsis thaliana: a light microscope study of cleared whole-mount tissue, *The Plant Journal*, **77**, 731-749

Schneitz K., Hülskamp M., Kopczak S.D. and Pruitt R.E. (1997) Dissection of sexual organ ontogenesis: a genetic analysis of ovule development in *Arabidopsis thaliana*, *Development*, **124**, 1367-1376

Scholl R.L., May S.T., and Ware D.H. (2000)Seed and Molecular Resources for Arabidopsis, *Plant Physiology*, **124**, 1477-1480

Scott R.J., Spielman M., Bailey J., and Dickinson H.G. (1998) Parent-of-origin effects on seed development in Arabidopsis thaliana, Development, **125**, 3329-3341

Sessions A., Nemhauser J. L., McCall A., Roe J. L., Feldmann K. A. and Zambryski P. C. (1997). *ETTIN* patterns the *Arabidopsis* floral meristem and reproductive organs. *Development*, **124**, 4481-4491.

Sessions R. A. and Zambryski P. C. (1995). *Arabidopsis* gynoecium structure in the wild type and in *ettin* mutants. *Development*, **121**, 1519-1532.

Sieberer T., Hauser M.T., Seifert G.J. and Luschnig C. (2003) *PROPORZ1*, a putative Arabidopsis transcriptional adaptor protein, mediates auxin and cytokinin signals in the control of cell proliferation, Current Biology, **13**, 837-842

Sieburth LE (1999)Auxin is required for leaf vein pattern in Arabidopsis, *Plant Physiology*, **121**, 1179-1190

Sinclair T.R., Purcell L.C. and Sneller C.H. (2004) Crop transformation and the challenge to increase yield potential, *Trends in Plant Science*, **9**, 70-75

Singletary GW, Banisadr R, Keeling PL, (1994), heat-stress during grain filling in maize – effects on carbohydrate storage and metabolism, *Australian Jounrnal of plant physiology* **21**, 829-841

Skinner D. J., Hill T. A. and Gasser C. S. (2004). Regulation of ovule development. *Plant Cell* **16**, S32-S45.

Skoog F., Miller C.O. (1957) Chemical regulation of growth and organ formation in plant tissues cultured in vitro. *Symposia of the Society for Experimental Biology*, **54**, 118-130

Smith and Fretwell, (1974), The optimal Balance between size and number of offspring, *The American Naturalist*, **108**, 499-506

Smyth D.R., Bowman J.L. and Meyerowitz E.M. (1990) Early Flower development in Arabidopsis, *The Plant Cell*, **2**, 755-767

Stowe-Evans E. L., Harper R. M., Motchoulski A. V. and Liscum E. (1998). NPH4, a conditional modulator of auxin-dependent differential growth responses in Arabidopsis. *Plant Physiology*, **118**, 1265-1275.

Swarup R., Parry G., Graham N., Allen T., Bennett M. (2002) Auxin cross-talk: integration of signalling pathways to control plant development, *Plant Molecular Biology*, **49**, 411-426

Tanaka H., Watanabe M., Watanabe D., Tanaka T., Machida C., Machida Y., (2002) *ACR4*, a Putative Receptor Kinase Gene of Arabidopsis thaliana, that is Expressed in the Outer Cell Layers of Embryos and Plants, is Involved in Proper Embryogenesis. *Plant Cell Physioly.* **43**, 419-428

Tatematsu K, Kumagai S, Muto H, Sato A, Watahiki MK, Harper RM, Liscum E, Yamamoto KT (2004) MASSUGU2 encodes Aux/IAA19, an auxin-regulated protein that functions together with the transcriptional activator NPH4/ARF7 to regulate differential growth responses of hypocotyl and formation of lateral roots in Arabidopsis thaliana, *Plant Cell*, **16**, 379-393

The Arabidopsis Genome Initiative (2000) Analysis of the genome sequence of the flowering plant Arabidopsis thaliana, *Nature*, **408**, 796-815

Tian C., Muto H., Higuchi K., Matamura T., Tatematsu K., Koshiba T. and Yamamoto K. T. (2004). Disruption and overexpression of *auxin response factor 8* gene of *Arabidopsis* affect hypocotyl elongation and root growth habit, indicating its possible involvement in auxin homeostasis in light condition. *Plant Journal*, **40**, 333-343.

Tian Q, Reed JW (1999) Control of auxin-regulated root development by the Arabidopsis thaliana SHY2/IAA3 gene, *Development*, **126**, 711-721

Timpte CS, Wilson AK, and Estelle M (1992) Effects of the AXR2 mutation of Arabidopsis on cell-shape in hypocotyl and inflorescence, *Planta*, **188**, 271-278

Tiwari S.B., Hagen G., Guilfoyle T. (2003) The roles of auxin response factor domains in auxin-responsive transcription, *Plant Cell*, **15**, 533-543

Tiwari S.B., Wang X.J., Hagen G., Guilfoyle T.J. (2001) AUX/IAA proteins are active repressors, and their stability and activity are modulated by auxin, *Plant Cell*, **13**, 2809-2822

Tiwari SB, Hagen G, Guilfoyle TJ (2004) Aux/IAA proteins contain a potent transcriptional repression domain, *Plant Cell*, **16**, 533-543

Tollenaar M.M., and Wu J. (1999)Yield Improvement in Temperate Maize is Attributable to Greater Stress Tolerance, *Crop Science*, **39**,1597-1604

Ulmasov T., Hagen G. and Guilfoyle T. (1997a). *ARF1*, a transcription factor that binds to auxin response elements. *Science* **276**, 1865-1868.

Ulmasov T., Hagen G. and Guilfoyle T. (1999a). Activation and repression of transcription by auxin-response factors. *Proceedings of the National Academy of Sciences of the United States of America*, **96**, 5844-5849.

Ulmasov T., Hagen G. and Guilfoyle T. (1999b). Dimerization and DNA binding of auxin response factors. *Plant Journal*, **19**, 309-319

Ulmasov T., Liu Z.B., Hagen G., Guilfoyle T.J. (1995) Composite Structure of Auxin Response Elements, *Plant Cell*, **7**, 1611-1623

Ulmasov T., Murfett J., Hagen G., Guilfoyle T.J. (1997b) Aux/IAA proteins repress expression of reporter genes containing natural and highly active synthetic auxin response elements, *Plant Cell*, **9**, 1963-1971

van Doorn W.G., and van Meeteren U. (2003) Flower opening and closure: a review, *Journal of Experimental Biology*, **54**, 1802-1812

Vandenbussche F., and Van Der Straeten D. (2004). Shaping the shoot: a circuitry that integrates multiple signals. *Trends in Plant Science*, **9**, 499-506.

Wolbang CM, Chandler PM, Smith JJ, Ross JJ (2004)Auxin from the developing inflorescence is required for the biosynthesis of active gibberellins in barley stems, *Plant Physiology,* **134** , 769-776

Wollenweber B., Porter J.R. and Lübberstedt T. (2005) Need for multidisciplinary research towards a second green revolution, *Current Opinion in Plant Biology*, **8**, 337-341

Woodward A.W., Bartel B. (2005) Auxin: Regulation, action, and interaction. *Annals of Botany*, **95**, 707-735

Xu J.L., Yu S.B.,, Luo L.J., Zhong D.B., Mei H.W.,and Li Z.K., (2004) Molecular dissection of the primary sink size and its related traits in rice, *Plant Breeding*, **123**, 43-50

Xu LH, Liu FQ, Lechner E, Genschik P, Crosby WL, Ma H, Peng W, Huang DF, Xie DX (2002) The SCFCOl1 ubiquitin-ligase complexes are required for jasmonate response in Arabidopsis, *Plant Cell*, **14**, 1919-1935

Yoshida S. (1983) Rice, In: *Potential Productivity of Field Crops under Different Environments* , International Rice Research Institute, IRRI, Philippines

Zazimalova E., Napier R.M. (2003) Points of regulation for auxin action, *Plant Cell Reports*, **21,** 625-634

Vanneste S, Maes L, De Smet I, Himanen K, Naudts M, Inze D, Beeckman T (2005) Auxin regulation of cell cycle and its role during lateral root initiation, *Physiologia Plantarum*, **123**, 139-146

Venable D.L., (1992), Size-number trade-offs and the variation of seed size with plant resource status, *American Naturalist*, **140**, 287-304

Verdú M. and Traveset A. (2005) Early emergence enhances plant fitness: A phylogenetically controlled meta-analysis, *Ecology*, **86**, 1385-1394

Villanueva J.M., Broadhvest J., Hauser B.A., Meister R.J., Schneitz K., and Gasser C.S. (1999) *INNER NO OUTER* regulates abaxial-adaxial patterning in *Arabidopsis* ovules, *Genes and Development*, **13**, 3160-3169

Vinkenoog R., Spielman M., Adams S., Dickinson H.G. and Scott R.J. (2002) Genomic Imprinting in Plants, *In: Methods in Molecular Biology vol. 181* Edited by A. Ward, Humana Press, Totowa, NJ

Wang J.-W., Wang L.-J., Mao Y.-B., Cai W.-J., Xue H.-W. and Chen X.-Y. (2005). Control of root cap formation by microRNA-targeted auxin response factors in Arabidopsis. *Plant Cell* **17**, 2204-2216.

Watahiki M. K. and Yamamoto K. T. (1997). The *massugu1* mutation of Arabidopsis identified with failure of auxin-induced growth curvature of hypocotyl confers auxin insensitivity to hypocotyl and leaf. *Plant Physiology*, **115**, 419-426.

Watahiki MK, Tatematsu K, Fujihira K, Yamamoto M, Yamamoto KT (1999) The MSG1 and AXR1 genes of Arabidopsis are likely to act independently in growth-curvature responses of hypocotyls, *Planta*, **207**, 362-369

Weber H., Borisjuk L. and Wobus U. (1996). Controlling seed development and seed size in *Vicia faba*: a role for seed coat-associated invertases and carbohydrate state. *Plant Journal*, **10**, 823-834.

Weijers D., Benkova E., Jager K.E., Schlereth A., Hamann T., Kientz M., Wilmoth J.C., Reed J.W., Jurgens G. (2005) Maintenance of embryonic auxin distribution for apical-basal patterning by PIN-FORMED-dependent auxin transport in Arabidopsis, *Plant Cell*, **17**, 2517-2526

Westoby M., Jurado E., and Leishman M. (1992) Comparative Evolutionary Ecology of Seed Size, *TREE*, **7**, 368-372

Westoby M., Leishman M., and Lord J. (1996) Comparative ecology of seed size and dispersal, *Philosophical Transactions of the Royal Society of London Series B*, **351:** 1309-1318

Willemsen V, Wolkenfelt H, de Vrieze G, Weisbeek P, Scheres B (1998) The *HOBBIT* gene is required for formation of the root meristem in the Arabidopsis embryo, *Development*, **125**, 521-531

Wilmoth J.C., Wang S., Tiwari S.B., Joshi A.D., Hagen G., Guilfoyle T. J., Alonso J. M., Ecker J.R., and Reed J.W. (2005). NPH4/ARF7 and ARF19 promote leaf expansion and auxin-induced lateral root formation. *Plant Journal*, **43**, 118-130.

Windsor J.B., Symonds V.V., Mendenhall J., and Lloyd A.M. (2000) *Arabidopsis* seed coat development: morphological differentiation of the outer integument, *Plant Journal*, **22**, 483-493

Winn A.A., (1985) Effects of seed size and microsite on seedling emergence of Prunella vulgaris in four habitats. *Journal of Ecology*, **73**, 831-840

Development 133, 251-261 doi:10.1242/dev.02194

The *AUXIN RESPONSE FACTOR 2* gene of *Arabidopsis* links auxin signalling, cell division, and the size of seeds and other organs

Marie C. Schruff[1], Melissa Spielman[1], Sushma Tiwari[1], Sally Adams[2], Nick Fenby[1] and Rod J. Scott[1,*]

Control of seed size involves complex interactions among the zygotic embryo and endosperm, the maternally derived seed coat, and the parent plant. Here we describe a mutant in *Arabidopsis, megaintegumenta* (*mnt*), in which seed size and weight are dramatically increased. One factor in this is extra cell division in the integuments surrounding *mnt* mutant ovules, leading to the formation of enlarged seed coats. Unusually for integument mutants, *mnt* does not impair female fertility. The *mnt* lesion also has pleiotropic effects on vegetative and floral development, causing extra cell division and expansion in many organs. *mnt* was identified as a mutant allele of *AUXIN RESPONSE FACTOR 2* (*ARF2*), a member of a family of transcription factors that mediate gene expression in response to auxin. The mutant phenotype and gene expression studies described here provide evidence that *MNT/ARF2* is a repressor of cell division and organ growth. The mutant phenotype also illustrates the importance of growth of the ovule before fertilization in determining final size of the seed.

KEY WORDS: ***MEGAINTEGUMENTA, AUXIN RESPONSE FACTOR 2, Arabidopsis,*** **Integuments, Ovule, Seed size**

INTRODUCTION

Despite the importance of seeds, little is known about the genetic mechanisms that determine their final size and weight. Seed development in flowering plants involves a double fertilization that generates two zygotic products: the embryo, which gives rise to the daughter plant, and the endosperm, which transmits nutrients from the seed parent to the embryo during embryogenesis or germination (Lopes and Larkins, 1993). The third major component of the seed, the seed coat or testa, differentiates after fertilization from maternally derived tissues including the integuments, which enclose the embryo sac. In most monocot species a persistent endosperm forms the bulk of the mature seed, while in most eudicots the endosperm is transient and is replaced by the growing embryo. Therefore, while seed size in monocots such as maize and wheat is often attributable to the extent of endosperm growth (Reddy and Daynard, 1983; Chojecki et al., 1986), in eudicot seeds such as peas and beans, cotyledon cell number has been directly linked to final seed size (Davies, 1975; Davies, 1977). However, in pea, the extent of mitosis in cotyledons is correlated with the extent of invertase activity in the seed coat (Weber et al., 1996), and in the model eudicot *Arabidopsis thaliana*, endosperm proliferation is correlated with seed weight and embryo size, although the mature seed contains only a single layer of endosperm cells (Scott et al., 1998; Garcia et al., 2003). Therefore, in eudicots as well as monocots, the embryo is not the only factor in determining seed size.

The genetic regulation of seed size has been investigated in plants including tomato, soybean, maize, and rice using quantitative trait loci (QTL) mapping. Relatively few loci show significant effects on seed weight in these experiments, and so far none of the corresponding genes have been cloned (Doganlar et al., 2000; Cui et al., 2002; Hyten et al., 2004). In *A. thaliana*, seed weight can vary up to 3.5-fold among accessions (Krannitz et al., 1991), providing an opportunity for QTL analysis of seed size in this species. Alonso-Blanco et al. (Alonso-Blanco et al., 1999) identified 11 loci affecting seed weight and/or length in crosses between the accessions *Ler* and Cvi, with the larger size of Cvi seeds attributed mainly to faster and prolonged growth of the seed coat and endosperm.

Mutations and misexpression experiments have revealed few genes affecting seed size. *miniature1* mutants of maize produce small endosperms, and consequently small seeds, due to lesions in a gene encoding a cell wall invertase involved in sugar transport (Cheng et al., 1996). In *Arabidopsis*, the small seed size of *haiku* mutants is correlated with premature arrest of endosperm proliferation; inhibited cell division in the embryo and cell expansion in the seed coat were considered to be indirect effects (Garcia et al., 2003). Mutations in some *TRANSPARENT TESTA* loci, which affect flavonoid pigmentation in the seed coat, also alter seed growth, usually reducing seed weight (Debeaujon et al., 2000). Large seeds in *Arabidopsis* can be generated by mutation of the *APETALA2* (*AP2*) transcription factor (Jofuku et al., 2005; Ohto et al., 2005) or by expression of an antisense DNA methyltransferase gene in the seed parent resulting in DNA hypomethylation (Adams et al., 2000). The size of many organs, including seeds, is increased by ectopic expression of the *AINTEGUMENTA* (*ANT*) transcription factor (Krizek, 1999; Mizukami and Fischer, 2000).

To improve our understanding of the processes controlling seed size, we screened a population of mutagenized *Arabidopsis* for large seeds. We recovered a mutation, now termed *megaintegumenta* (*mnt*), which increases seed size as well as affecting growth of other aerial organs. The earliest difference we detected in *mnt* compared with wild-type seed development was the presence of extra cells in the integuments before fertilization. Many mutants affecting integuments have been identified in *Arabidopsis*, but these usually reduce female fertility (reviewed by Skinner et al., 2004); by contrast, *mnt* mutants are female fertile. Ectopic cell division and/or expansion were also observed in leaves, stems and some floral organs of *mnt* mutants. Cloning of the *MNT* locus showed it to

[1]Department of Biology and Biochemistry, University of Bath, Claverton Down, Bath BA2 7AY, UK. [2]Department of Biology, University of Leicester, University Road, Leicester LE1 7RH, UK.

*Author for correspondence (e-mail: bssrjs@bath.ac.uk)

Accepted 1 November 2005

encode AUXIN RESPONSE FACTOR 2 (ARF2), one of a family of transcription factors that bind to auxin-responsive elements (AuxREs) in the promoters of auxin-regulated genes (Ulmasov et al., 1997; Ulmasov et al., 1999a; Ulmasov et al., 1999b; Liscum and Reed, 2002; Hagen and Guilfoyle, 2002) and possibly other genes (Okushima et al., 2005a; Ellis et al., 2005). Recent studies of *arf2* mutants have reported a pleiotropic phenotype, including: restoration of differential cell elongation and apical hook formation in *hookless1* mutant seedlings; increased growth of aerial organs; inhibition of floral bud opening; and delays in flowering, leaf senescence, floral organ abscission and silique ripening and dehiscence (Li et al., 2004; Okushima et al., 2005b; Ellis et al., 2005). Here we present the first evidence that an ARF is a general repressor of cell division, one of many processes regulated by auxin. The *mnt/arf2* mutant phenotype also illustrates the importance of growth of the ovule before fertilization in determining final size of the seed.

MATERIALS AND METHODS

Plant growth and stocks

Seeds were stratified for 3-5 days at 4°C in 0.15% agar and germinated on Levingtons F2 compost. Plants were grown in a glasshouse at a temperature of 24°C (day) and 17.5°C (night), or in a Sanyo controlled environment room with a daylength of 16 hours, 23°C (day) and 18°C (night). To test for kanamycin resistance, seeds were surface-sterilized and plated on full-strength M+S with Gamborgs Vitamins (Sigma-Aldrich, Dorset, UK), 1% sucrose, 0.8% Phyto Agar (Duchefa, Haarlem, Netherlands), 50 μg/ml kanamycin. Wild-type Col-3 seeds and Col-3 mutagenized with ethane methyl sulfonate (EMS) were obtained from Lehle Seeds (Round Rock, Texas, US). Col-0, L*er*, and Salk_108995 (http://signal.salk.edu/cgi-bin/tdnaexpress) (Alonso et al., 2003) were obtained from the Nottingham *Arabidopsis* Stock Centre (NASC), UK. *mnt* mutants were outcrossed three times to Col-3 before phenotypic analysis.

Pollinations and seed weights

For cross-pollinations, flowers were emasculated before anther dehiscence and pollinated 2-3 days later. For manually pollinated *arf2* mutants, buds were opened early in development to avoid crushing of the stigmatic papillae due to the elongated gynoecium. Seeds were weighed with a Mettler UMT2 microbalance (Mettler-Toledo, Leicester, UK). Statistical analysis was performed with Minitab 12.2 software (State College, Pennsylvania, USA).

Sample preparation and microscopy

For analysis of whole-mount seeds, seeds were dissected from siliques and placed in a drop of clearing solution (8 g chloral hydrate, 11 ml water, 1 ml glycerol). Samples were photographed under a Nikon Eclipse E800 microscope with differential interference contrast optics using a SPOT RT Color camera (Diagnostics Instruments Inc., Michigan, USA). Digital images were processed using Adobe Photoshop software and measurements were taken with Visilog 5.0.2 software (Noesis, Les Ulis, France).

For sections, plant material was fixed overnight at RT in 4% paraformaldehyde, 25 mmol/l $KHPO_4$ buffer pH 7.0, 0.1% Tween-20, washed in buffer, dehydrated through a graded ethanol series to 95% ethanol, and embedded in JB-4 glycol methacrylate resin (Polysciences, Warrington, PA, USA), or dehydrated to 100% ethanol and embedded in Technovit 7100 resin (Heraeus Kulzer, Germany). Five-micrometre sections were cut in ribbons using glass knives made from microscope slides on a Leica RM2145 microtome, according to Ruzin (Ruzin, 1999). Samples were stained in 0.1% Toluidine Blue in 25 mmol/l $KHPO_4$ buffer pH 5.5, mounted under coverslips in DPX (Agar Scientific, Stansted, UK), and photographed under an Olympus BH-2 microscope with a Nikon Coolpix 4500 digital camera. Digital images were processed using Adobe Photoshop software and measurements were taken with Scion Image 4.0.2 software (Scion Corp., Maryland, USA).

For scanning electron microscopy (SEM), siliques were slit open and fixed in 3% glutaraldehyde in 0.05 mol/l sodium cacodylate buffer pH 6.8 overnight at 4°C, postfixed in 1% osmium tetroxide in 0.1 mol/l buffer pH 7.0 for 4 hours at RT, rinsed in buffer, dehydrated through an acetone series, and critical point dried. Ovules were sputter-coated with gold and examined using a JEOL JSM6310 scanning electron microscope (JEOL, Tokyo, Japan).

For confocal laser scanning microscopy (CLSM), Feulgen-stained seeds were processed and imaged as in Bushell et al. (Bushell et al., 2003). GFP fluorescence and chlorophyll autofluorescence were detected in water-mounted samples using an argon ion laser at 488 nm excitation, 505-530 nm emission, and a HeNe543 laser at 543 nm excitation, ≥585 nm emission, respectively.

For analysis of floral organs, floral buds were photographed under a Leica MZ6 dissecting microscope with a Nikon Coolpix 4500 digital camera. Floral organs were measured using a graticule eyepiece. For analysis of epidermal cells, casts were made of floral organs in clear nail varnish on a microscope slide, and photographed under an Olympus BH-2 microscope as above. Measurements were taken on digital images using Visilog 5.0.2 software.

Statistical analysis was performed with Minitab 12.2 software.

Mapping and sequencing

A recombinant mapping population was generated by crossing *mnt* homozygotes in the Col-3 background with wild-type L*er*. Seven hundred and eighty nine plants with the mutant floral phenotype were selected from the F2 generation and their genomic DNA was scored for published CAPS and SSLP markers (http://www.arabidopsis.org) and for CAPS markers generated in our laboratory (available on request). Genomic and cDNA for sequencing was PCR amplified using proofreading KOD Hi-fi Polymerase (Merck, Nottingham, UK) and cloned into the pGEMT vector (Promega, Southampton, UK). Two independent PCR products were sequenced using internal primers on both sense and antisense strands. Sequences were aligned using Genedoc 2.6.02 software (http://www.psc.edu/biomed/genedoc).

Complementation and allelism test

The region of BAC MTG10 identified by fine mapping as containing the *MNT* locus was restricted with appropriate enzymes to isolate each of the 16 annotated genes. The gel-purified fragments were cloned into shuttle vector ST36 (a modified form of BJ36 in which an *XbaI-SpeI* fragment spanning the OCS terminator was removed) and subcloned into the *NotI* sites of binary vector BJ40 (BJ36 and BJ40 were gifts of Bart Janssen, Hort+Research New Zealand). The shuttle vector was transformed into *Agrobacterium tumefaciens* GV3101. *mnt* mutants were transformed via the floral dip method (Clough and Bent, 1998) and T1 seeds were selected on kanamycin as above.

To genotype the Salk_108995 T-DNA insertion mutant, primers 108995-R (5′-CAACTGATGCGTCTCTCCAA-3′) and left border primer Lba1 (5′-TGGTTCACGTAGTGGGCCATCG-3′) were used to identify the T-DNA insertion in the *ARF2* gene. Primers 108995-F (5′-GGGCTCACTGTTTTGCTCAT-3′) and 108995-R were used to identify the wild-type *ARF2* allele in the insertion line. Homozygous insertion mutants were crossed to *mnt* homozygotes and the F1 progeny were assayed for the *mnt* mutant phenotype and hemizygosity for the T-DNA insertion.

pARF2::GFP

A 2.5 kb region of genomic DNA 5′ to the *ARF2* coding region was amplified by PCR using the primers pARF2-F (5′-AAAGTCGAC-ACACAAGAAAATAGAAGAG-3′) and pARF2-R (5′-TCTAGAC-TTAACCAGAGGTAGTCAAAACTC-3′), and cloned into the *SalI* and *XbaI* sites of the plasmid GFP_DME_NLS (Choi et al., 2002).

Expression analysis

'Young' and 'mature' rosette leaves were harvested from wild-type Col-3, *arf2-8*, and *mnt/arf2-9* plants at 16 and 39 days after germination (dag), respectively. For 'young' stem, primary inflorescence stems were harvested when they reached 5 cm, approximately 29 dag for wild type and up to 32 dag for *arf2* mutants. 'Mature' stem was harvested from plants at 39 dag (wild type) or 43 dag (mutants). For the mature stem base, 10 cm was

measured from the rosette, and for the apex, 10 cm was measured from the cluster of buds at the apex of the inflorescence. All flowers, siliques and axillary shoots were removed from primary inflorescence stems. Total RNA was extracted using TRIZOL (Invitrogen, Paisley, UK).

Five hundred nanograms of total RNA was used for semiquantitative RT-PCR using a Reverse-iT kit (Abgene, Epsom, UK) following the manufacturer's instructions. GapC was used as an internal control. Primers and PCR conditions were: ARGOS (At3g59900), forward 5′-ATCC-TCTGTTTCTGAATCGTGGG-3′ and reverse 5′-ATGCCGTTAGACCA-ACCAATAGG-3′ (26 cycles, annealing temperature 62°C); ANT (At4g37750), forward 5′-ATGAAGTCTTTTTGTGATAATGATG-3′ and reverse 5′-TTGTGTTGTTGTGATGGGTCC-3′ (26 cycles, annealing temperature 55°C); CYCD3;1 (At4g34160), forward 5′-CAAGATT-TGTTCTGGGAAGATG-3′ and reverse 5′-CAATGGAGGTTGTTGCTGC-3′ (27 cycles, annealing temperature 56°C); GAPC (At3g04120), forward 5′-CACTTGAAGGGTGGTGCCAAG-3′ and reverse 5′-CCTGTTGTCG-CCAACGAAGTC-3′ (22-24 cycles, annealing temperature 62°C).

RESULTS

Identification of the *mnt* mutant

In a screen for mutations affecting seed size, approximately 77,000 M2 seeds from an EMS mutagenized population in the Col-3 accession were sieved through a gradient of wire meshes with different apertures (S. A. Adams, PhD Thesis, University of Bath, 2002). Seeds from wild-type controls were retained only in 250-and 300-μm aperture meshes while the mutant seeds were retained in a broader range, from 200 to 355 μm. Inheritance of the phenotype in candidate seed size mutants was tested by weighing seed from M3 plants. A parental group producing seeds larger than controls (Fig. 1A,B), and also containing larger embryos (Fig. 1C,D) was selected for further study; this line was later named *megaintegumenta* (*mnt*) to reflect increased size of the integuments (see below). Apart from the seed phenotype, *mnt* mutants have a variety of abnormalities in vegetative and reproductive development (see below), including failure of flowers to open. This trait was found to co-segregate with the large seed phenotype and was subsequently used for scoring mutant plants. The *mnt* floral phenotype segregates as a single gene recessive mutation (62 wild-type and 23 *mnt* mutant plants were scored in F2 populations following crosses between wild-type and mutant parents; for a 3:1 segregation χ^2=0.192, P>0.05).

Adult *mnt* mutants have a pleiotropic phenotype: inflorescence stems are thick and twisted; plants flower approximately 1 week late with more rosette leaves than wild-type plants grown simultaneously under long day conditions, and the leaves are larger (Fig. 1E; see also below). The mutants have a low degree of self-fertility associated with the failure of floral bud opening (Fig. 1F,G), but female fertility is normal following manual crosses with either *mnt* or wild-type pollen parents, indicating that self-sterility is due to mechanical failure of pollination. However, the last few flowers on a mutant plant self-pollinate and set seed (not shown).

The seed cavity in *mnt* seeds is larger throughout development but endosperm is not hypertrophic

Growth of *mnt* and wild-type seeds was compared by measuring cleared seeds at different stages (Fig. 2A-J; see Table S1 in the supplementary material). Seeds produced by homozygous *mnt* mutants were longer, wider and more pointed at the micropylar pole, with a larger seed cavity, than wild-type seeds at every stage examined. At 5 days after pollination (dap), wild-type seeds had reached the heart stage of embryogenesis, the chalazal endosperm formed a compact rounded cyst, and the peripheral endosperm was cellularizing from the micropylar pole (Fig. 2K, left). At the same

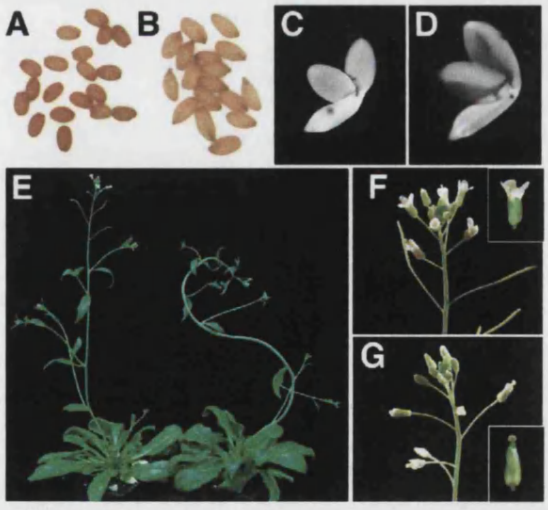

Fig. 1. Pleiotropic effects of the *mnt* mutation. (A-D) Mature seeds (**A**,**B**) and embryos (**C**,**D**) from self-pollinated wild-type Col-3 (A,C) and *mnt* mutant plants (B,D). (**E**) Wild-type (left) and *mnt* (right) plants, showing the *mnt* stem phenotype. (**F**,**G**) Inflorescences from wild-type (F) and *mnt* plants (G); insets show flowers at similar stages.

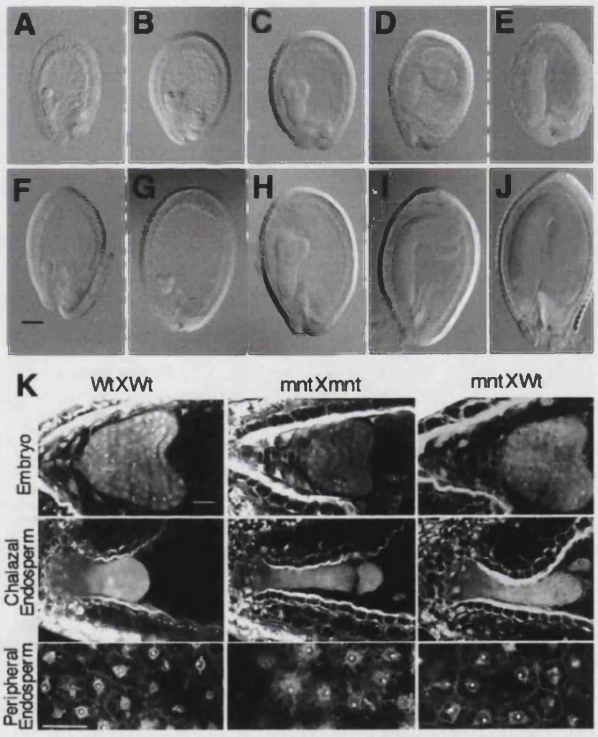

Fig. 2. Seed development in wild-type and *mnt* mutant plants. (**A-J**) Cleared seeds imaged with differential contrast optics; (A-E) wild-type and (F-J) *mnt* seeds at similar stages of embryogenesis. Scale bar: 100 μm. (**K**) CLSM images of Feulgen-stained seeds at 5 dap. Scale bars: 20 μm in embryo and chalazal endosperm; 25 μm in peripheral endosperm.

time point, *mnt* homozygous seeds had globular to early heart stage embryos, and the chalazal endosperm was long and thin, presumably due to the abnormal shape of the seed coat (Fig. 2K, middle). Peripheral endosperm did not appear substantially different from wild type. Heterozygous seeds from a cross between an *mnt* homozygous mutant seed parent and a wild-type pollen parent also had the *mnt* mutant phenotype (Fig. 2K, *right*), indicating a maternal effect on seed development.

In *Arabidopsis*, large seeds resulting from an increased ratio of paternal to maternal genomes in the seed ('paternalized'), or DNA hypomethylation of the seed parent, show characteristic endosperm phenotypes, including delayed cellularization of the peripheral endosperm and hypertrophy of the chalazal endosperm and associated nodules (Scott et al., 1998; Adams et al., 2000). There was not a strong trend of late endosperm cellularization in *mnt* mutants. We measured the maximum cross-sectional area of the chalazal cyst plus nodules at 6 dap, a stage at which differences are apparent between wild-type and paternalized endosperms (Scott et al., 1998). Mean areas were 2690 μm^2 (±s.e.m. 328) for wild-type seeds (n=4) and 2537 μm^2 (±416) for *mnt* seeds (n=5), and there was no significant difference between the mutant and wild-type endosperms (two-tailed Student's t-test, P=0.79). Therefore, we concluded that *mnt* endosperms do not have the overgrowth phenotype associated with paternal excess. However, it is possible that eventually more cells are formed in the peripheral endosperm of *mnt* seeds to fill the larger seed cavity.

The increased volume of *mnt* mutant ovules is due to extra cell division in the integuments

As *mnt* mutant seeds were larger than wild-type even at the earliest stage examined, we next compared ovule development in mutant and wild-type plants to investigate the origins of the size difference. Ovule development has been described in detail for *Arabidopsis* (Schneitz et al., 1995; Baker et al., 1997). Early in ovule formation three regions are defined along the proximal-distal axis: the funiculus, which connects the ovule to the mother plant; the chalaza; and the nucellus, which harbours the megaspore mother cell and later the embryo sac. The inner and outer integuments initiate on the flanks of the chalaza and elongate to enclose the nucellus. The integuments divide to a greater extent on the abaxial side, contributing to the curvature of the ovule.

Both *mnt* and wild type followed the pattern previously described for nearly the entire duration of ovule development (Fig. 3A-F; later stages not shown). Female gametophyte development in *mnt* mutants also appeared normal, culminating in a Stage 3-VI embryo sac [staging according to Schneitz et al. (Schneitz et al., 1995)] (Fig. 3G,H). However, at this stage *mnt* mutant ovules were larger and more curved than wild type and the integuments contained more cells in each layer, as well as a partial extra layer in some ovules (Fig. 3H, arrow).

Two layers of the abaxial integuments were examined in more detail: oi2, the outer layer of the outer integument; and ii1', a layer of the inner integument that spans part of the embryo sac (Schneitz et al., 1995; Beeckman et al., 2000). For both layers, *mnt* integuments were longer and contained significantly more cells than wild-type Col-3 (Fig. 3I,J; Table 1). We measured cell length along the proximal-distal axis; for layer ii1' the cell width (abaxial-adaxial axis) was also measured, as cell expansion in this layer coincides with seed growth after fertilization (Beeckman et al., 2000) (Fig. 3K, Table 1). There was no significant difference between wild type and mutant in cell lengths or widths (Table 1). The above evidence indicates that the greater size of integuments in *mnt* ovules is due to extra anticlinal cell divisions in both inner and outer integuments. We also observed extra cells in *mnt* mutant seed coats (data not shown). The pointed shape of *mnt* mutant seeds appears to be due to extension of the seed coat at the micropylar pole combined with overgrowth of the adaxial layers of the seed coat.

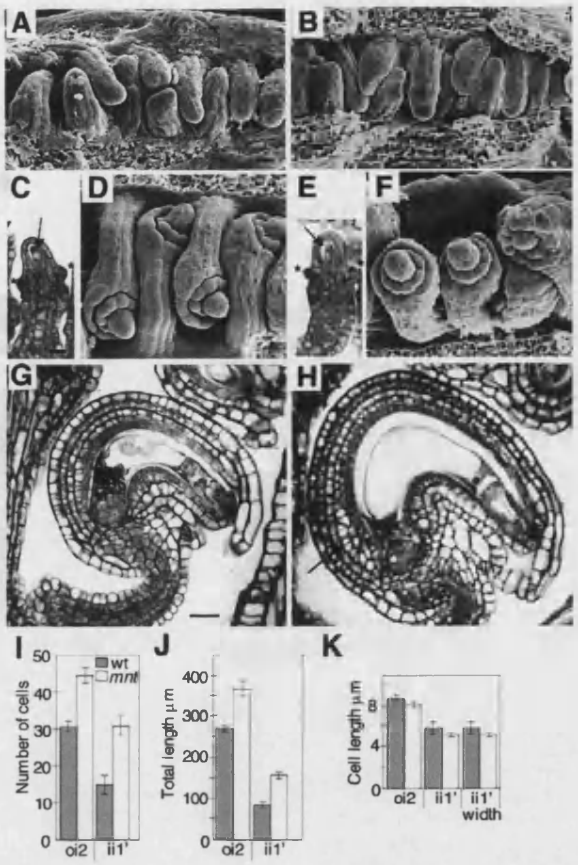

Fig. 3. Ovule development in wild-type and *mnt* mutant plants. (**A-F**) Early ovule development in wild type (A,C,D) and *mnt* (B,E,F). (A,B) SEMs of stage 1-II ovules. (C,E) Sections of stage 2-III ovules showing megaspore mother cell (arrow) and initiating inner integument (*). (D,F) SEMs of later stage 2 ovules showing integuments beginning to extend over nucellus. (**G,H**) Sections of mature wild-type (G) and *mnt* (H) ovules. The arrow in (H) shows an extra cell layer. Scale bars: 10 µm in A-F; 20 µm in G,H. (**I-K**) Comparison of number of cells (I), total length of integument (J) and mean size of cells (K) in the abaxial oi2 and ii1' layers of wild-type and *mnt* integuments. Error bars: s.e.m. n=4 wild type, 8 *mnt*.

Factors affecting seed size in *mnt* mutants

To investigate seed weight in *mnt* mutants, we carried out four sets of crosses – [wild type × wild type], [wild type × *mnt*], [*mnt* × *mnt*], [*mnt* × wild type] – using two treatments for each. In the first treatment, six flowers on each primary inflorescence of five plants were manually pollinated and all other flowers on the primary shoot were removed, although the secondary inflorescences were allowed to set self-seed. Due to the poor self-fertility of *mnt* mutants, wild-type seed parents formed many more siliques on secondary

Table 1. Number and size of cells in abaxial integuments of stage 3-VI ovules

	oi2	ii1	ii1′
Number of cells			
Wild type	30.5±1.4	21.5±2.5	15.0±2.0
mnt	44.4±2.2	40.6±2.6	30.8±1.9
P	0.0020	0.0009	0.0004
Total length (μm)			
Wild type	270.8±7.1	126.3±4.9	85.1±7.8
mnt	368.4±18.5	193.2±10.1	158.3±11.1
P	0.0049	0.0011	0.0014
Mean cell length (μm)			
Wild type	8.9±0.3	6.1±0.6	5.8±0.5
mnt	8.2±0.2	4.8±0.2	5.2±0.3
P	0.061	0.030	0.33
Mean cell width (μm)			
Wild type			4.3±0.3
mnt			4.7±0.2
P			0.30

Data represent mean±s.e.m.
n=4 ovules for wild type, *n*=8 ovules for *mnt*.
For Student's *t*-tests, H_0 wild type≠*mnt*.

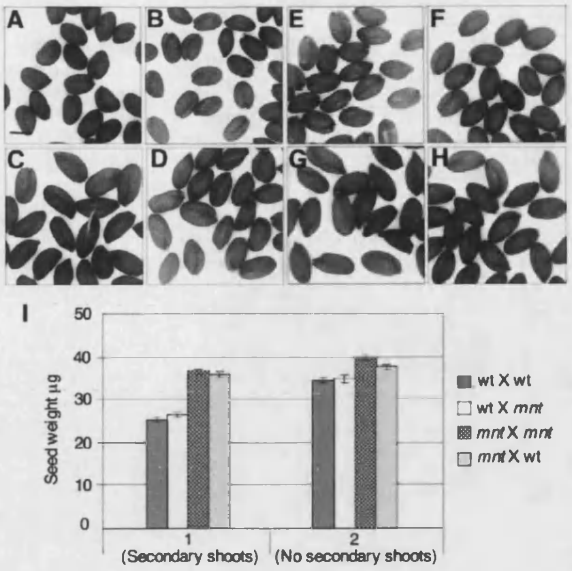

Fig. 4. Comparison of seeds generated by wild-type and *mnt* mutant plants. (**A-D**) Seeds from pollinations where all secondary shoots were allowed to set seed; (**E-H**) seeds from pollinations where secondary shoots were removed (see text). (A,E) [wild type × wild type]; (B,F) [wild type × *mnt*]; (C,G) [*mnt* × *mnt*]; (D,H) [*mnt* × wild type]. Scale bar: 250 μm. (**I**) Comparison of seed weights following the two treatments. Error bars: s.e.m.

inflorescences. Therefore, in order to control for the influence of seed number on seed weight, for the second treatment all secondary inflorescences were removed, so that wild-type and mutant seed parents set the same number of siliques overall.

We found that the genotype of the seed parent is a factor in the overall size, shape and weight of the seed. For both treatments, [*mnt* × *mnt*] and [*mnt* ×wild type] seeds were larger and more pointed than seeds from crosses using a wild-type mother (cf. Fig. 3A,B,E,F and Fig. 3C,D,G,H). [*mnt* × *mnt*] seeds generated by Treatment 1 ('Secondary shoots') were 46% heavier than [wild type × wild type], and [*mnt* × wild type] 35% heavier than [wild type × *mnt*]. However, the weight difference between the two classes decreased when seed set was restricted by removing secondary shoots (Fig. 4I; Table 2A); for example, Treatment 2 ('No secondary shoots') raised [*mnt* × *mnt*] seed weight by 9% while [wild type × wild type] seed weight increased by 36%. However, although increasingly restricted seed set narrowed the gap between them, [*mnt* × *mnt*] seed was still 16% heavier than [wild type × wild type], and this difference was significant (Student's *t*-test, H_0 *mnt*>wild type, *P*=0.0002). We subsequently identified another allele of *mnt*, the T-DNA insertion allele *arf2-8* (see below), and incorporated this allele in two repetitions of the seed weight assay using Treatment 2 and self-pollinations only (Table 2B,C). In each of these replicates both *mnt* and *arf2-8* mutant plants produced significantly heavier seeds (*P*<0.0005) than wild-type (Table 2B,C), with *arf2-8* seeds weighing up to 21% more than wild type even when seed set was severely restricted to control for the reduced fertility of the mutants. We concluded that the difference in seed weights observed between self-pollinated *arf2* mutants and wild-type plants is likely to have two components: direct effects of the mutations on seed development, and an indirect effect due to low self-fertility of the mutants. For both *arf2* alleles tested, in three separate experiments homozygous mutant plants produced significantly heavier seeds than wild-type controls even when the number of siliques on each plant was held constant.

Floral and vegetative development in *mnt* mutants

To investigate the failure of flower opening and self-pollination in *mnt* mutants, we compared floral buds from *mnt* and wild-type plants (Fig. 5A). Mutant inflorescences contain more buds at each stage. At stage 13 (Smyth et al., 1990), when wild-type flowers open, the petal blades have extended above the sepals and reflexed,

Table 2. Seed weights in wild-type and mutant plants

A					B			C		
	Wild type × wild type	Wild type × *mnt*	*mnt* × *mnt*	*mnt* × wild type	Wild type	*mnt*	*arf2-8*	Wild type	*mnt*	*arf2-8*
Secondary shoots	25.0±0.4 μg (*n*=1280)	26.3±0.4 (*n*=705)	36.4±0.6 (*n*=995)	35.4±0.9 (*n*=1171)						
No secondary shoots	34.0±0.6 (*n*=1085)	34.8±1.1 (*n*=978)	39.4±0.7 (*n*=1228, *P*=0.0002)	37.7±0.6 (*n*=1359)	33.4±0.6 (*n*=1287)	37.3±0.5 (*n*=1135, *P*=0.0004)	39.3±0.7 (*n*=1192, *P*=0.0001)	28.2±0.2 (*n*=1506)	32.6±0.6 (*n*=971, *P*=0.0000)	34.1±0.7 (*n*=1112, *P*=0.0000)

Mean weights represent the mean for five plants per cross within each treatment±s.e.m.
n=total number of seeds weighed. *P* represents the P-value obtained from using Student's *t*-test.
H_0 *mnt* or *arf2-8*>wild type.

stigmatic papillae are expanded, the anthers have dehisced, and long stamens are level with the stigma. In *mnt* mutant flowers with expanded stigmatic papillae and dehisced anthers, the gynoecia are longer than the stamens and pollen is shed on the side of the gynoecium in the unopened flower bud rather than on the stigma, explaining the failure of pollination (inset Fig. 5A).

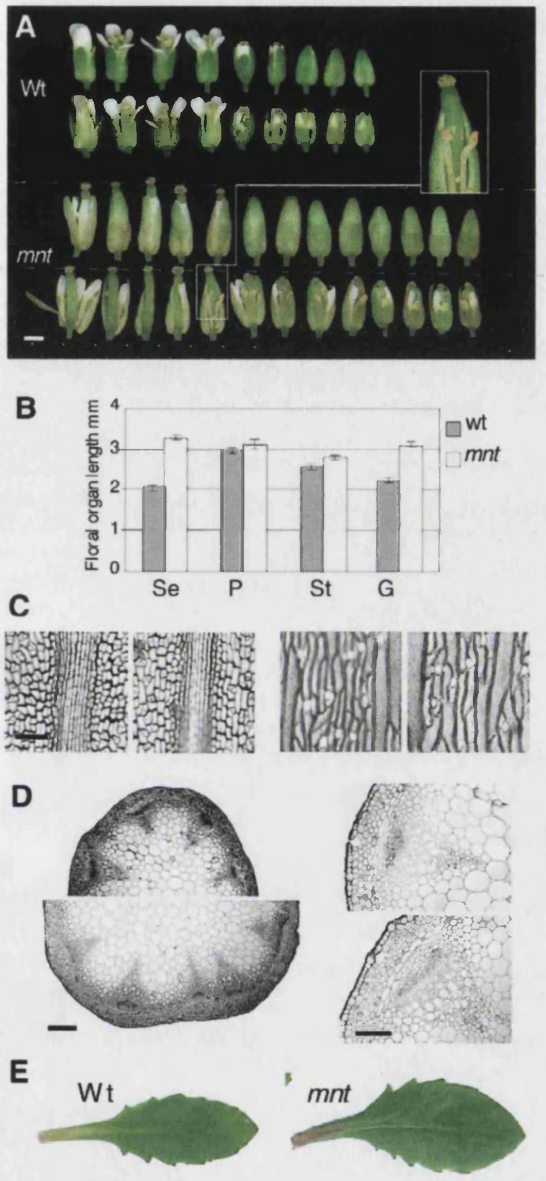

Fig. 5. Floral and vegetative phenotypes of *mnt*. (**A**) Alignment of buds from wild-type and *mnt* inflorescences, approximately stage 12–16. In each part of the figure the bottom row of buds shows the top row partially dissected. (**B**) Lengths of floral organs in stage 13 flowers. (**C**) Nail varnish casts of epidermis from carpel valve (left) and medial sepal (right) of wild-type and *mnt* stage 13 flowers. In each pair the wild type is on the left. (**D**) Transverse sections of inflorescence stem between nodes 2 and 3 from the base: (top) wild-type, (bottom) *mnt*. (**E**) Largest leaf from a wild-type (left) and *mnt* mutant (right) rosette. Scale bars: 1 mm in A; 50 μm in C; 200 μm in D, left; 100 μm in D, right. G, gynoecium (excluding stigma); P, petal; Se, medial sepal; St, long stamen.

We measured the lengths of floral organs in wild-type and *mnt* stage 13 flowers (Fig. 5B; Table 3). Sepals and gynoecia were both significantly longer in the mutant; the resulting disturbance to the petal:sepal and long stamen:gynoecium ratios in *mnt* flowers (Table 3) is consistent with failure of floral opening and pollination. Although the gynoecium length was a consistent factor in failure of self-pollination, in some plants the stamen filaments also failed to elongate fully.

Examination of the epidermal surface of sepals and carpel valves showed that the cells in *mnt* mutants were slightly larger in both organs (Fig. 5C); however, this could not account for the entire increase in size. *mnt* sepals were 60% longer than wild-type (Table 3), but pavement cells in the dorsal sepal epidermis were 32% longer (mean cell length, *mnt* 53.7 μm ± s.e.m. 1.8, n=122 cells in three sepals; wild type 40.8 μm ± 1.8, n=111 cells in three sepals); and *mnt* gynoecia were 42% longer (Table 3), while pavement cells were only 14% longer (*mnt* 26.9 μm ± s.e.m. 1.7, n=113 cells in three carpels; wild type 23.7 μm ± 1.3, n=126 cells in three carpels). We concluded that the increased length of gynoecia and sepals in *mnt* mutants is due to a combination of extra divisions and greater cell expansion.

The diameter of the primary inflorescence stem of wild-type and mutant plants was measured between the first and second nodes from the base when the stems were 15 to 22 cm in length. *mnt* mutant stems had a significantly greater diameter (mean diameter, *mnt* 1.55 mm ± s.e.m. 0.03, n=11; wild type 1.31 ± 0.02, n=10; two-tailed Student's t-test, P=0.0000). Transverse sections of the primary inflorescence stem (Fig. 5D) showed that stem morphology was normal in mutants but there were extra cells of many types. In addition, stem epidermal cells were longer in the mutant (not shown).

mnt mutants produced approximately 30% more rosette leaves than wild-type plants (mean number of leaves per rosette, *mnt* 15.1 ± s.e.m. 0.4, n=14; wild type 11.5 ± 0.5, n=13). In 5-week-old plants we found a significant difference in surface area of the largest leaf (Fig. 5E) (mean area, *mnt* 592.8 mm^2 ± s.e.m. 32, n=14; wild type 440.2 mm^2 ± 22, n=13; two-tailed Student's t-test, P=0.0007). Examination of leaf epidermal cells indicated that, as for sepals, the greater size of *mnt* leaves is most likely due to a combination of extra cell division and expansion (not shown).

mnt is an allele of ARF2

The *MNT* locus was mapped to a 60.9-kb interval on chromosome 5 containing 16 annotated genes on the MTG10 BAC (http://www.arabidopsis.org) (Fig. 6A). Genomic DNA corresponding to the coding region for each gene, along with 5′ and 3′ flanking regions, was transformed into *mnt* mutant plants, and progeny assayed for the wild-type phenotype. Simultaneously, lines with T-DNA insertions in these genes (http://signal.salk.edu) (Alonso et al., 2003) were investigated for similarity to the *mnt* mutant. Homozygous mutants from Salk_108995, which carries an insertion in gene At5g62000, resembled *mnt* mutants in stem, floral and seed phenotype (Fig. 6B; Table 2B,C). An allelism test between *mnt* and Salk_108995 mutants produced F1 plants with the mutant phenotype (Fig. 6B), and the complementation experiment showed that only a genomic fragment including At5g62000 rescued *mnt* mutants (Fig. 6C). Therefore *mnt* is an allele of At5g62000, which encodes ARF2 (Ulmasov et al., 1999a; Li et al., 2004; Okushima et

Table 3. Dimensions of floral organs in wild-type and *mnt* plants

	Medial sepal (mm)	Petal (mm)	Long stamen (mm)	Gynoecium (mm)	Petal/sepal ratio	Long stamen/gynoecium ratio
Wild type	2.06±0.05	2.95±0.08	2.58±0.09	2.20±0.05	1.43±0.03	1.17±0.02
mnt	3.29±0.09	3.12±0.12	2.80±0.09	3.12±0.09	0.95±0.02	0.90±0.01
P	0.0000	0.24	0.095	0.0000	0.0000	0.0000

Data represent mean±s.e.m.
n=10 flowers of each genotype.
P, the *P*-value obtained from using Student's *t*-test. H_0 wild type≠*mnt*.

al., 2005a; Okushima et al., 2005b; Ellis et al., 2005). The Salk_108995 allele was previously designated *arf2-8* (Okushima et al., 2005a); the *mni* allele is *arf2-9* (Fig. 6D).

We sequenced genomic DNA from *mnt/arf2-9* mutants for the predicted ARF2 coding region plus 4371 bases of the 5′ and 525 bases of the 3′ flanking regions. A single base change with respect to the wild-type Col-0 sequence (http://www.arabidopsis.org), from G to A, was identified at position 665 from translational start, at the end of intron 3. This was predicted to affect splicing by changing the 3′ splice site from the consensus AG sequence to AA. We sequenced the first 837 bases of the *mnt/arf2-9* cDNA from start of translation, and the same region from wild-type Col-3 cDNA, confirming that four bases are deleted from the beginning of exon 4 in the mutant cDNA (Fig. 6E). Based on the cDNA sequence, we predicted the mnt/arf2-9 mutant protein has a frameshift from amino acid position 123 and a premature stop codon at position 167 (Fig. 6F). These changes both occur in the DNA-binding domain of ARF2 (Fig. 6G) and probably cause a complete loss of function.

ARF2 expression in reproductive organs

RNA gel blot analysis has shown that *ARF2* is expressed in roots, leaves, flowers and siliques (Ulmasov et al., 1999b). To investigate the pattern of *ARF2* gene expression in reproductive organs we generated a reporter construct consisting of 2.5 kb of the *ARF2* 5′ flanking sequence fused to a nuclear-localized GFP gene (Choi et al., 2002). Consistent with the *mnt* mutant phenotype, GFP was expressed in floral organs and ovules (Fig. 7A,B). As the ovule matured, expression remained high in the funiculus and gradually declined in the integuments. In mature ovules there was strong signal in the small group of nucellar cells remaining at the chalazal pole (Beeckman et al., 2000) (Fig. 7A, arrow). After fertilization no expression was detected in the seed coat, although signal was seen in embryos dissected from mature seeds (not shown). In floral organs, GFP was observed in the gynoecium at floral stages 8–9 and 12 (Fig. 7B, left), and the signal continued in siliques after fertilization (not shown). GFP was also strongly expressed in other floral organs at stages 8–9, but had largely disappeared by stage 12 (Fig. 7B).

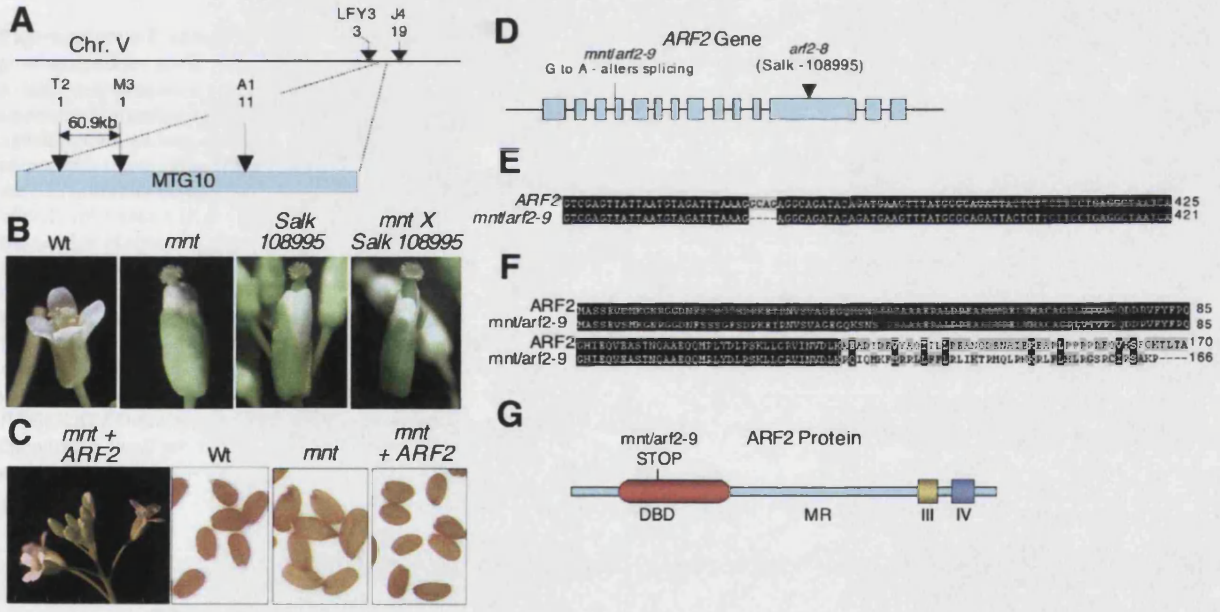

Fig. 6. Mapping and sequencing *MNT*. (**A**) *mnt* mutations were mapped to BAC MTG10 on chromosome V. Figures below the marker names show the number of recombination events in 1578 chromosomes scored. (**B**) Scoring of an allelism test between *mnt* mutants and Salk_108995 T-DNA insertion mutants by floral phenotype. (**C**) Scoring of complementation by floral and seed phenotype. *mnt* + *ARF2*=T1 progeny of an *mnt* mutant transformed with the wild-type *ARF2* gene and flanking genomic DNA. This construct restored wild-type floral (left) and seed phenotypes (right) to the mutant. (**D**) The *ARF2* gene with the positions of the *mnt/arf2-9* and Salk_108995/*arf2-8* mutations marked. (**E**) Alignment of a fragment of wild-type *ARF2* cDNA with the mutated region in *mnt/arf2-9* showing a 4-bp deletion. (**F**) Alignment of the N-terminal portion of the wild-type ARF2 and mutant mnt/arf2-9 proteins, showing an early frameshift and stop codon. (**G**) The ARF2 protein marked with the position of the stop codon generated by the mnt/arf2-9 lesion. DBD, DNA binding domain; MR, variable middle region; III and IV, domains involved in dimerization with other ARFs or with Aux/IAAs (Liscum and Reed, 2002).

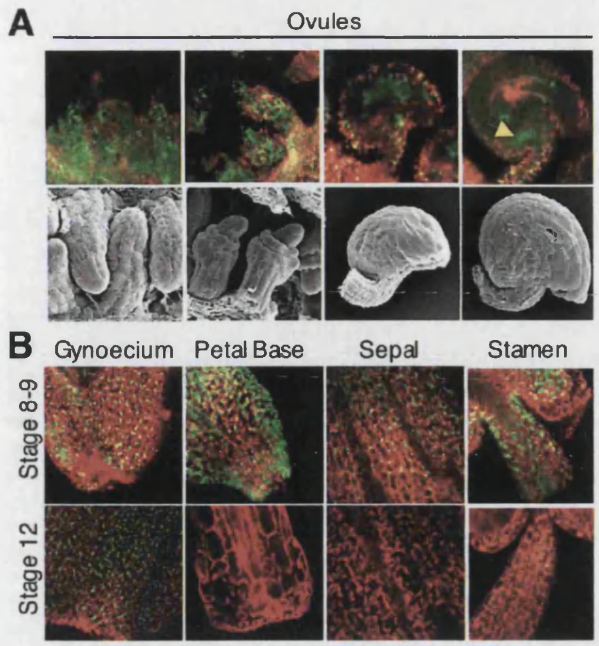

Fig. 7. Expression of nuclear-localized GFP under control of the *ARF2* promoter. (**A**) Expression in ovules; SEMs show ovules at similar stages. (**B**) Expression in floral organs.

Expression of genes promoting cell division is prolonged in *arf2* mutants

It has been proposed that *ANT* is necessary and sufficient to control cell number and growth of lateral organs during shoot development, as loss-of-function *ant* mutations result in small plants with fewer cells, while ectopic *ANT* expression directed by the *35S* promoter results in large organs due to an extended period of cell proliferation (Krizek, 1996; Mizukami and Fischer, 2000). Regulation of the cell cycle by *ANT* is mediated at least in part by prolonging expression of *CYCD3;1*, a D-type cyclin that integrates cell cycle entry with exogenous signals such as hormones, including auxin (Oakenfull et al., 2002): rosette leaves from 9-week-old *35S::ANT* plants continue to express *ANT* and *CYCD3;1*, while expression of both genes in wild-type plants has ceased by this stage (Mizukami and Fischer, 2000). *AUXIN-REGULATED GENE INVOLVED IN ORGAN SIZE* (*ARGOS*), encoding a small protein of unknown function, has similar loss- and gain-of-function phenotypes to those of *ANT*, and also appears to have a role in control of organ size and cell proliferation, acting downstream of auxin signalling and promoting *ANT* and *CYCD3;1* expression (Hu et al., 2003).

Like *35S::ANT* and *35S::ARGOS* plants, *arf2* mutants produce enlarged organs containing extra cells. To investigate whether *ARF2* affects *ARGOS*, *ANT* or *CYCD3;1* transcription, we assayed expression of these three genes in two organs that show increased cell division in *arf2* mutants, rosette leaves and inflorescence stems (Fig. 8). For young leaves and stems, we found that each gene had similar expression levels in wild-type and mutant plants; this is consistent with previous observations that overexpression of *ARGOS* or *ANT* does not increase expression of *CYCD3;1* in young, dividing tissues (Mizukami and Fischer, 2000; Hu et al., 2003). However, we detected both *ANT* and *CYCD3;1* expression in mature leaves of mutant but not wild-type plants, indicating that loss of *ARF2* function prolongs expression of these genes. In mature stems, these genes were still detectable in wild type but at a lower level than in the mutants. By contrast, *ARGOS* was expressed in mature leaf and stem at similar levels in mutants and wild type.

DISCUSSION

arf2 mutations increase seed size and weight through 'integument-led' seed growth

In a screen for *Arabidopsis* mutants producing large seeds we identified the *mnt* mutant, which contains a lesion in the *ARF2* gene likely to cause complete loss of function. We found that *arf2* mutants generate seeds up to 46% heavier than wild-type seed parents, regardless of the pollination partner. *mnt/arf2-9* seed coats contain more cells than wild type, due to the production of extra cells in the integuments before fertilization (Fig. 3; Table 1). These observations suggest that the *arf2* mutations have a maternal effect on seed size, primarily due to enlarged integuments. However, the reported trade-off between seed number and size in many species (Harper et al., 1970), including *Arabidopsis* (Alonso-Blanco et al., 1999; Meyer et al., 2004), led us to investigate this further by restricting pollination to allow equivalent seed set in wild-type and *arf2* mutant plants. This showed that a component of the difference initially found between *arf2* and wild-type seeds is explained by low seed set in self-pollinated *arf2* plants. Significantly, however, *arf2* mutant seeds were up to 21% heavier than wild type, even when seed set was held constant (Fig. 4; Table 2). Therefore reduced seed set in *arf2* mutants accounts for only part of the increased seed size. Similarly, recent reports show that *ap2* mutations increase seed size partly because of reduced fertility but also through a separate maternal effect on seed growth (Jofuku et al., 2005; Ohto et al., 2005).

Differences between wild-type and *mnt/arf2-9* mutant seeds are apparent before fertilization, and mutant endosperms lack the paternalized phenotype observed in large seeds in which the genetic

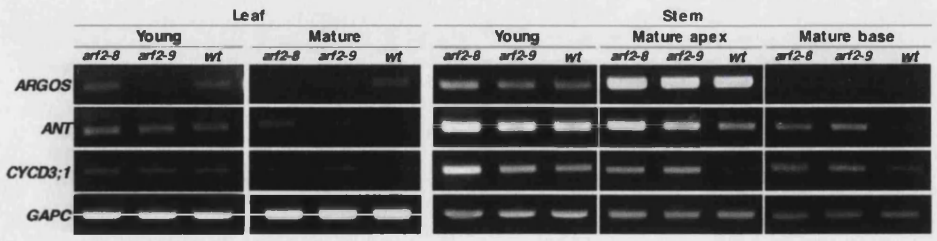

Fig. 8. Comparison of *ARGOS*, *ANT* and *CYCD3;1* transcript levels in young and mature organs of wild-type and mutant plants. See Materials and methods for explanation of developmental staging.

constitution of the endosperm has been altered (Scott et al., 1998; Adams et al., 2000). Therefore, the increased seed size in *arf2* mutants appears to be 'integument-led'. One explanation for integument-led growth is that the larger seed cavity in mutant seeds (Fig. 2) allows greater endosperm growth. Another possibility is that the larger seed cavity provides a greater area of contact for endosperm with the seed coat, leading to increased nutrient uptake.

Mutations affecting integument size often have pleiotropic effects, particularly on flower development (Skinner et al., 2004). *arf2* mutants fit this pattern but are otherwise unusual among integument mutants, as most others reduce female fertility. *aberrant testa shape* (*ats*) and *ap2* mutants are reported to have normal female fertility; however, in these mutants the seed coats are irregularly shaped and display loss of cell layers or structures (Léon-Kloosterziel et al., 1994; Jofuku et al., 1994; Debeaujon et al., 2000). By contrast, the seed coat in *mnt/arf2-9* mutants appears structurally normal, with only a minor effect on shape.

Alonso-Blanco et al. (Alonso-Blanco et al., 1999) reported that growth of the seed coat and endosperm accounted for the larger size of Cvi seeds compared with L*er*, and that as ovules were longer in L*er* than Cvi before fertilization, ovule size differences could not explain the final variation. However, a QTL for seed length was mapped to a region at the bottom of chromosome 5 that contains *ARF2*, and it would be interesting to determine whether *ARF2* corresponds to this locus. Weber et al. (Weber et al., 1996), investigating small- and large-seeded genotypes of broad bean, concluded that the number of cells in the integuments before fertilization could not explain the size differences. The maternal effect of *ap2* mutations on seed size may involve the seed coat (Ohto et al., 2005), but the mechanism for this is not known. Garcia et al. (Garcia et al., 2005) reported that overexpression of the cell cycle inhibitor *KRP2* decreased the number of cells in seed coat without decreasing seed size, and concluded that cell division and cell elongation in the seed coat compensate for each other. However, the effects of increasing cell number in the seed coat were not investigated. The results presented here reveal a mechanism not previously described for increasing seed size within a species, the production of extra cells in the integuments before fertilization.

ARF2 is a general repressor of cell division

The *mnt/arf2-9* mutation causes a variety of phenotypes in the adult plant, including thick stems, large rosette leaves and failure of floral bud opening (Figs 1, 5). These phenotypes were reported for other *arf2* mutant alleles by Li et al. (Li et al., 2004), Okushima et al. (Okushima et al., 2005b) and Ellis et al. (Ellis et al., 2005); here we show they are associated with extra cell division and expansion. Expression of *ARF2* throughout the plant (Ulmasov et al., 1999b) and, within reproductive organs, in floral buds and ovules (Fig. 7), is consistent with the pleiotropy of the mutant phenotype.

Auxin is involved in many processes, including pattern formation, cell division and cell expansion (Leyser, 2002; Vandenbussche and Van Der Straeten, 2004). Single and double mutant phenotypes for other *ARF*s include disturbances to organ patterning, cell expansion or division, response to light or gravity, auxin homeostasis or flower maturation (Berleth and Jürgens, 1993; Sessions and Zambryski, 1995; Liscum and Briggs, 1996; Przemeck et al., 1996; Sessions et al., 1997; Watahiki and Yamamoto, 1997; Hardtke and Berleth, 1998; Stowe-Evans et al., 1998; Harper et al., 2000; Hardtke et al., 2004; Tian et al., 2004; Nagpal et al., 2005; Okushima et al., 2005a; Wang et al., 2005; Wilmoth et al., 2005). We observed that the *mnt/arf2-9* mutation increases cell division in several organs without producing a major effect on morphology, and two mutant alleles of *arf2* had prolonged expression in stem and rosette leaf of *CYCD3;1*, a D-type cyclin involved in cell cycle entry, and *ANT*, a transcription factor involved in organ growth and cell division control. We conclude that ARF2 is a general repressor of cell division in many aerial organs of the plant.

Cell division is not the only process affected by *ARF2*. Li et al. (Li et al., 2004) reported that *ARF2* regulates differential cell elongation in seedlings, and our observations of stem, leaf and floral phenotypes in *mnt/arf2-9* mutants also indicate that *ARF2* plays a role in cell expansion. In addition it has been proposed that *ARF2* promotes developmental transitions such as flowering, floral organ abscission, silique ripening and leaf senescence (Okushima et al., 2005b; Ellis et al., 2005). In this context, extra cell division in *mnt/arf2-9* mutants could result from a delay in transition from the proliferative to the fully differentiated state. Our observations that integument cells in mutant ovules divide for a longer period rather than more rapidly, and that *ANT* and *CYCD3;1* expression is sustained in mature organs rather than increased in young ones, are consistent with this interpretation. However, the timing of cell division and expression of relevant genes need to be investigated in more organs to determine whether extra cell division in *arf2* mutants is generally due to extended proliferation.

Effects of *ARF2* on gene expression

The predominant view of ARFs is that they bind to auxin response elements (AuxREs) in the promoters of auxin-regulated genes, and mediate auxin signalling by activating or repressing gene transcription. It is proposed that auxin influences ARF function through its effects on gene expression and protein turnover of Aux/IAAs, short-lived nuclear proteins that contain AuxREs and are both induced and degraded in response to auxin. Aux/IAAs can dimerize with ARFs, and repress the ability of ARFs to activate gene expression in protoplast transfection assays (Abel and Theologis, 1996; Ulmasov et al., 1997; Leyser, 2002; Liscum and Reed, 2002; Hagen and Guilfoyle, 2002; Tiwari et al., 2003). We found that expression of *ANT* and *CYCD3;1* is prolonged in leaves and stems of *arf2* mutants (Fig. 8), but the mechanism by which this occurs remains to be discovered.

Expression of *ANT* and *CYCD3;1* is also sustained in mature leaves of plants overexpessing *ARGOS* (Hu et al., 2003). *ARGOS* is induced by auxin, and overexpression leads to enlargement of aerial plant organs due to increased cell division (Hu et al., 2003). However, we did not find that *arf2* mutations affected *ARGOS* expression in young or mature organs (Fig. 8), suggesting that *ARF2* does not mediate *ANT* or *CYCD3;1* expression through effects on *ARGOS* expression.

ARF2 represses transcription of reporter genes under the control of synthetic AuxREs both in vitro and in vivo (Tiwari et al., 2003; Li et al., 2004). Surprisingly, *arf2* mutations have not been found to affect global expression of auxin-regulated genes (e.g. *Aux/IAA*s) in seedlings, or expression of specific *IAA* genes in flowers (Okushima et al., 2005b; Ellis et al., 2005). However, there is increasing evidence that *ARF2* affects expression of other types of genes: in addition to prolonging expression of *ANT* and *CYCD3;1* in mature stems and leaves (Fig. 8), loss of *ARF2* function inhibits expression of three members of the *ACS* gene family (involved in ethylene biosynthesis) in flowers (Okushima et al., 2005b) and *SENESCENCE ASSOCIATED GENE 12* (*SAG12*) in senescing leaves (Ellis et al., 2005). It has been proposed that ARF2 does not conform to the canonical auxin response model but may, for example, bind promoters of genes not directly regulated by auxin (the AuxRE motif is highly

represented in the *Arabidopsis* genome), or interact with proteins not directly participating in auxin signalling (Okushima et al., 2005b; Ellis et al., 2005). Identification of the direct targets of ARF2 and its dimerization partners will clarify the mechanism of ARF2 function.

We are grateful to NASC for Col-0, Ler and Salk_108995 seed (also the Salk Institute for the latter); to Robert Fischer for the GFP_DME_NLS vector; to Bart Janssen (Hort+Research New Zealand) for the BJ36 and BJ40 vectors; to Michael Mogie for assistance with statistical analysis; to Ursula Potter for help with SEM; to Jason Reed for sharing unpublished data; and to Richard Hooley for helpful discussions. M.C.S., M.S., S.T. and N.F. were funded by Sulis Innovation; and S.A. by the BBSRC.

Supplementary material

Supplementary material for this article is available at http://dev.biologists.org/cgi/content/full/133/2/251/DC1

References

Abel, S. and Theologis, A. (1996). Early genes and auxin action. *Plant Physiol.* **111**, 9-17.

Adams, S., Vinkenoog, R., Spielman, M., Dickinson, H. G. and Scott, R. J. (2000). Parent-of-origin effects on seed development in *Arabidopsis thaliana* require methylation. *Development* **127**, 2493-2502.

Alonso, J. M., Stepanova, A. N., Leisse, T. J., Kim, C. J., Chen, H., Shinn, P., Stevenson, D. K., Zimmerman, J., Barajas, P., Cheuk, R. et al. (2003). Genome-wide insertional mutagenesis of Arabidopsis thaliana. *Science* **301**, 653-657.

Alonso-Blanco, C., Blankestijn-De Vries, H., Hanhart, C. J. and Koornneef, M. (1999). Natural allelic variation at seed size loci in relation to other life history traits of *Arabidopsis thaliana*. *Proc. Natl. Acad. Sci. USA* **96**, 4710-4717.

Baker, S. C., Robinson-Beers, K., Villanueva, J. M., Gaiser, J. C. and Gasser, C. S. (1997). Interactions among genes regulating ovule development in *Arabidopsis thaliana*. *Genetics* **145**, 1109-1124.

Beeckman, T., De Rycke, R., Viane, R. and Inzé, D. (2000). Histological study of seed coat development in *Arabidopsis thaliana*. *J. Plant Res.* **113**, 139-148.

Berleth, T. and Jürgens, G. (1993). The role of the *monopteros* gene in organising the basal body region of the *Arabidopsis* embryo. *Development* **118**, 575-587.

Bushell, C., Spielman, M. and Scott, R. J. (2003). The basis of natural and artificial postzygotic hybridization barriers in *Arabidopsis* species. *Plant Cell* **15**, 1-14.

Cheng, W.-H., Taliercio, E. W. and Chourey, P. S. (1996). The *Miniature1* seed locus of maize encodes a cell wall invertase required for normal development of endosperm and maternal cells in the pedicel. *Plant Cell* **8**, 971-983.

Choi, Y., Gehring, M., Johnson, L., Hannon, M., Harada, J. J., Goldberg, R. B., Jacobsen, S. E. and Fischer, R. L. (2002). DEMETER, a DNA glycosylase domain protein, is required for endosperm gene imprinting and seed viability in *Arabidopsis*. *Cell* **110**, 33-42.

Chojecki, A. J. S., Bayliss, M. W. and Gale, M. D. (1986). Cell production and DNA accumulation in the wheat endosperm, and their association with grain weight. *Ann. Bot.* **58**, 809-817.

Clough, S. J. and Bent, A. F. (1998). Floral dip: a simplified method for *Agrobacterium*-mediated transformation of *Arabidopsis thaliana*. *Plant J.* **16**, 735-743.

Cui, K.-H., Peng, S.-B., Xing, Y.-Z., Yu, S.-B. and Xu, C.-G. (2002). Molecular dissection of relationship between seedling characteristics and seed size in rice. *Acta Botanica Sinica* **44**, 702-707.

Davies, D. R. (1975). Studies of seed development in *Pisum sativum*. I. Seed size in reciprocal crosses. *Planta* **124**, 303-309.

Davies, D. R. (1977). DNA contents and cell number in relation to seed size in the genus *Vicia*. *Heredity* **39**, 153-163.

Debeaujon, I., Léon-Kloosterziel, K. M. and Koornneef, M. (2000). Influence of the testa on seed dormancy, germination, and longevity in Arabidopsis. *Plant Physiol.* **122**, 403-413.

Doganlar, S., Frary, A. and Tanksley, S. D. (2000). The genetic basis of seed-weight variation: tomato as a model system. *Theor. Appl. Genet.* **100**, 1267-1273.

Ellis, C. M., Nagpal, P., Young, J. C., Hagen, G., Guilfoyle, T. J. and Reed, J. W. (2005). *AXIN RESPONSE FACTOR1* and *AXIN RESPONSE FACTOR2* regulate senescence and floral abscission in *Arabidopsis thaliana*. *Development* **132**, 4563-4574.

Garcia, D., Saingery, V., Chambrier, P., Mayer, U., Jürgens, G. and Berger, F. (2003). Arabidopsis *haiku* mutants reveal new controls of seed size by endosperm. *Plant Physiol.* **131**, 1661-1670.

Garcia, D., Fitz Gerald, J. N. and Berger, F. (2005). Maternal control of integument cell elongation and zygotic control of endosperm growth are coordinated to determine seed size in Arabidopsis. *Plant Cell* **17**, 52-60.

Hagen, G. and Guilfoyle, T. (2002). Auxin-responsive gene expression: genes, promoters and regulatory factors. *Plant Mol. Biol.* **49**, 373-385.

Hardtke, C. S. and Berleth, T. (1998). The *Arabidopsis* gene *MONOPTEROS* encodes a transcription factor mediating embryo axis formation and vascular development. *EMBO J.* **19**, 4997-5006.

Harper, J. L., Lovell, P. H. and Moore, K. G. (1970). The shapes and sizes of seeds. *Annu. Rev. Ecol. Syst.* **1**, 327-356.

Harper, R. M., Stowe-Evans, E. L., Luesse, D. R., Muto, H., Tatematsu, K., Watahiki, M. K., Yamamoto, K. and Liscum, E. (2000). The *NPH4* locus encodes the auxin response factor ARF7, a conditional regulator of differential growth in aerial Arabidopsis tissue. *Plant Cell* **12**, 757-770.

Hu, Y., Xie, Q. and Chua, N.-H. (2003). The Arabidopsis auxin-inducible gene *ARGOS* controls lateral organ size. *Plant Cell* **15**, 1951-1961.

Hyten, D. L., Pantalone, V. R., Sams, C. E., Saxton, A. M., Landau-Ellis, D., Stefaniak, T. R. and Schmidt, M. E. (2004). Seed quality QTL in a prominent soybean population. *Theor. Appl. Genet.* **109**, 552-561.

Jofuku, K. D., den Boer, B. G. W., Van Montagu, M. and Okamuro, J. K. (1994). Control of Arabidopsis flower and seed development by the homeotic gene *APETALA2*. *Plant Cell* **6**, 1211-1225.

Jofuku, K. D., Omidyar, P. K., Gee, Z. and Okamuro, J. K. (2005). Control of seed mass and seed yield by the floral homeotic gene *APETALA2*. *Proc. Natl. Acad. Sci. USA* **102**, 3117-3122.

Krannitz, P. G., Aarssen, L. W. and Dow, J. M. (1991). The effect of genetically based differences in seed size on seedling survival in Arabidopsis thaliana (Brassicaceae). *Am. J. Bot.* **78**, 446-450.

Krizek, B. A. (1999). Ectopic expression of *AINTEGUMENTA* in *Arabidopsis* plants results in increased growth of floral organs. *Dev. Genet.* **25**, 224-236.

Léon-Kloosterziel, K. M., Keijzer, C. J. and Koornneef, M. (1994). A seed shape mutant of Arabidopsis that is affected in integument development. *Plant Cell* **6**, 385-392.

Leyser, O. (2002). Molecular genetics of auxin signaling. *Annu. Rev. Plant Biol.* **53**, 377-398.

Li, H., Johnson, P., Stepanova, A., Alonso, J. M. and Ecker, J. R. (2004). Convergence of signaling pathways in the control of differential cell growth in *Arabidopsis*. *Dev. Cell* **7**, 193-204.

Liscum, E. and Briggs, W. E. (1996). Mutations of Arabidopsis in potential transduction and response components of the phototropic signaling pathway. *Plant Physiol.* **112**, 291-296.

Liscum, E. and Reed, J. W. (2002). Genetics of Aux/IAA and ARF action in plant growth and development. *Plant Mol. Biol.* **49**, 387-400.

Lopes, M. A. and Larkins, B. A. (1993). Endosperm origin, development, and function. *Plant Cell* **5**, 1383-1399.

Meyer, R. C., Törjék, O., Becher, M. and Altmann, T. (2004). Heterosis of biomass production in Arabidopsis. Establishment during early development. *Plant Physiol.* **134**, 1813-1823.

Mizukami, Y. and Fischer, R. L. (2000). Plant organ size control: *AINTEGUMENTA* regulates growth and cell numbers during organogenesis. *Proc. Natl. Acad. Sci. USA* **97**, 942-947.

Nagpal, P., Ellis, C. M., Weber, H., Ploense, S. E., Barkawi, L. S., Guilfoyle, T. J., Hagen, G., Alonso, J. M., Cohen, J. D., Farmer, E. E. et al. (2005). Auxin response factors ARF6 and ARF8 promote jasmonic acid production and flower maturation. *Development* **132**, 4107-4118.

Oakenfull, E. A., Riou-Khamlichi, C. and Murray, J. A. H. (2002). Plant D-type cyclins and the control of G1 progression. *Phil. Trans. R. Soc. Lond. B* **357**, 749-760.

Ohto, M., Fischer, R. L., Goldberg, R. B., Nakamura, K. and Harada, J. J. (2005). Control of seed mass by *APETALA2*. *Proc. Natl. Acad. Sci. USA* **102**, 3123-3128.

Okushima, Y., Overvoorde, P. J., Arima, K., Alonso, J. M., Chan, A., Chang, C., Ecker, J. R., Hughes, B., Lui, A., Nguyen, D. et al. (2005a). Functional genomic analysis of the *AUXIN RESPONSE FACTOR* gene family members in *Arabidopsis thaliana*: unique and overlapping functions of *ARF7* and *ARF19*. *Plant Cell* **17**, 444-463.

Okushima, Y., Mitina, I., Quach, H. L. and Theologis, A. (2005b). AUXIN RESPONSE FACTOR 2 (ARF2): a pleiotropic developmental regulator. *Plant J.* **43**, 29-46.

Przemeck, G. K. H., Mattsson, J., Hardtke, C. S., Sung, Z. R. and Berleth, T. (1996). Studies on the role of the *Arabidopsis* gene *MONOPTEROS* in vascular development and plant cell axialization. *Planta* **200**, 229-237.

Reddy, V. M. and Daynard, T. B. (1983). Endosperm characteristics associated with rate of grain filling and kernel size in corn. *Maydica* **28**, 339-355.

Ruzin, S. E. (1999). *Plant Microtechnique and Microscopy*. Oxford: Oxford University Press.

Schneitz, K., Hülskamp, M. and Pruitt, R. E. (1995). Wild-type ovule development in *Arabidopsis thaliana*: a light microscope study of cleared whole-mount tissue. *Plant J.* **7**, 731-749.

Scott, R. J., Spielman, M., Bailey, J. and Dickinson, H. G. (1998). Parent-of-origin effects on seed development in *Arabidopsis thaliana*. *Development* **125**, 3329-3341.

Sessions, A., Nemhauser, J. L., McCall, A., Roe, J. L., Feldmann, K. A. and

Zambryski, P. C. (1997). *ETTIN* patterns the *Arabidopsis* floral meristem and reproductive organs. *Development* **124**, 4481-4491.
Sessions, R. A. and Zambryski, P. C. (1995). *Arabidopsis* gynoecium structure in the wild type and in *ettin* mutants. *Development* **121**, 1519-1532.
Skinner, D. J., Hill, T. A. and Gasser, C. S. (2004). Regulation of ovule development. *Plant Cell* **16**, S32-S45.
Smyth, D. R., Bowman, J. L. and Meyerowitz, E. M. (1990). Early flower development in *Arabidopsis*. *Plant Cell* **2**, 755-767.
Stowe-Evans, E. L., Harper, R. M., Motchoulski, A. V. and Liscum, E. (1998). NPH4, a conditional modulator of auxin-dependent differential growth responses in Arabidopsis. *Plant Physiol.* **118**, 1265-1275.
Tian, C., Muto, H., Higuchi, K., Matamura, T., Tatematsu, K., Koshiba, T. and Yamamoto, K. T. (2004). Disruption and overexpression of *auxin response factor 8* gene of *Arabidopsis* affect hypocotyl elongation and root growth habit, indicating its possible involvement in auxin homeostasis in light condition. *Plant J.* **40**, 333-343.
Tiwari, S. B., Hagen, G. and Guilfoyle, T. (2003). The roles of auxin response factor domains in auxin-responsive transcription. *Plant Cell* **15**, 533-543.
Ulmasov, T., Hagen, G. and Guilfoyle, T. (1997). ARF1, a transcription factor that binds to auxin response elements. *Science* **276**, 1865-1868.
Ulmasov, T., Hagen, G. and Guilfoyle, T. (1999a). Activation and repression of transcription by auxin-response factors. *Proc. Natl. Acad. Sci. USA* **96**, 5844-5849.
Ulmasov, T., Hagen, G. and Guilfoyle, T. (1999b). Dimerization and DNA binding of auxin response factors. *Plant J.* **19**, 309-319.
Vandenbussche, F. and Van Der Straeten, D. (2004). Shaping the shoot: a circuitry that integrates multiple signals. *Trends Plant Sci.* **9**, 499-506.
Wang, J.-W., Wang, L.-J., Mao, Y.-B., Cai, W.-J., Xue, H.-W. and Chen, X.-Y. (2005). Control of root cap formation by microRNA-targeted auxin response factors in Arabidopsis. *Plant Cell* **17**, 2204-2216.
Watahiki, M. K. and Yamamoto, K. T. (1997). The *massugu1* mutation of Arabidopsis identified with failure of auxin-induced growth curvature of hypocotyl confers auxin insensitivity to hypocotyl and leaf. *Plant Physiol.* **115**, 419-426.
Weber, H., Borisjuk, L. and Wobus, U. (1996). Controlling seed development and seed size in *Vicia faba*: a role for seed coat-associated invertases and carbohydrate state. *Plant J.* **10**, 823-834.
Wilmoth, J. C., Wang, S., Tiwari, S. B., Joshi, A. D., Hagen, G., Guilfoyle, T. J., Alonso, J. M., Ecker, J. R. and Reed, J. W. (2005). NPH4/ARF7 and ARF19 promote leaf expansion and auxin-induced lateral root formation. *Plant J.* **43**, 118-130.